

**Carbohydrate-based inhibitors and multivalent
probes for LOX-1 and DC-SIGN receptors**

Chadamas Sakonsinsiri

Submitted in accordance with the requirements for the degree of

Doctor of Philosophy

The University of Leeds

School of Chemistry

May 2016

The candidate confirms that the work submitted is her own, except where work which has formed part of jointly-authored publications has been included. The contribution of the candidate and the other authors to this work has been explicitly indicated below. The candidate confirms that appropriate credit has been given within the thesis where reference has been made to the work of others.

1. Chapter 5: Carbohydrate-functionalised polymers as multivalent inhibitors for targeting LOX-1, includes content from the following publication:

“Templating carbohydrate-functionalised polymer-scaffolded dynamic combinatorial libraries with lectins” Mahon, C. S.; Fascione, M. A.; Sakonsinsiri, C.; McAllister, T. E.; Turnbull, W. B.; Fulton, D. A. *Organic & Biomolecular Chemistry*, **2015**, *13*, 2756-2761.

The manuscript was composed by D. A. Fulton, C. S. Mahon and W. B. Turnbull. Carbohydrates were synthesised and characterised by the candidate and M.A. Fascione. LTB was produced by T. E. McAllister. All other experimental work was conducted by C. S. Mahon.

2. Chapter 6: Synthesis and biological evaluations of multivalent probes for DC-SIGN, includes content from the following publication:

“Compact, polyvalent mannose quantum dots as sensitive, ratiometric FRET probes for multivalent protein-ligand interactions” Guo, Y.; Sakonsinsiri, C.; Nehlmeier, I.; Fascione, M.A.; Zhang, H.; Wang, W.; Pöhlmann, S.; Turnbull, W.B.; Zhou, D. *Angewandte Chemie International Edition*, **2016**, *55*(15), 4738-4742.

The manuscript was composed by Y. Guo, D. Zhou and W. B. Turnbull. Carbohydrates were synthesised and characterised by the candidate. Glyco-quantum dots were prepared and characterised by Y. Guo and the candidate. Protein production and labelling were performed by Y. Guo. FRET experiments were performed by Y. Guo. DLS experiments were performed by Y. Guo and the candidate. Viral inhibition assays were conducted by I. Nehlmeier and S. Pöhlmann.

This copy has been supplied on the understanding that it is copyright material and that no quotation from the thesis may be published without proper acknowledgement.

Acknowledgements

First of all, I would like to thank my supervisor, Dr Bruce Turnbull, for his support, inspiration and endless encouragement. Bruce has always made time for discussions about my project. Without his advice and guidance, this thesis would not have been possible. He is also thanked for understanding and supporting my decision to suspend my study for a year to deal with my family problems back in Thailand and for kindly letting me leave my stuff at his house for a year!

For financial support, I am grateful to Khon Kaen University (KKU), Thailand and the Faculty of Medicine at KKU, the Royal Society and my supervisor Bruce. Special thanks to my colleagues at the Department of Biochemistry, Faculty of Medicine, KKU for support and help with the extra workload during my study leave.

I am grateful to my internal assessor, Dr Stuart Warriner, for his useful comments on my project. My sincere thanks also must go to the following collaborators who contributed their work to this thesis: Dr Sreenivasan Ponnambalam, Dr Katie Lacey, Izma Abdul Zani, Dr David Fulton, Dr Clare Mahon and Dr Yuan Guo. Great team work!

I also would like to acknowledge the assistance of technical and administrative staff in the School of Chemistry, including Martin Huscroft, Simon Barrett, Tanya Marinko-Covell, Anna Luty and Francis Billingham and his colleagues from Stores.

I would like to extend my gratitude to the past and current Lab 1.49 members: Pintu, Martin, Heather, Jeff, James R, Tom B, Tom Mc, Dan, Kat, Phil, Diana, Kristian, Ivona, Darren, Laura, Matt, Clare, Gemma, Zoe, Arthur, Ludwig, Dana and James W who made my time in the lab such an enjoyable experience. Particular thanks to Pintu and Martin for helping me get started in the lab; Dan, Kristian and Clare for constant support through the ups and downs of my research; Darren for saving my life when I was locked out of the garage! Appreciations are also given to Dr Mike Webb, Kat and Diana for kindly allowing me to stay at their places when needed.

My heartfelt thanks to all my best friends: Praew, Imm and P'Ake for friendship and moral support; Uma and Poy for taking care of me and my family during my absence. I am deeply indebted to my mother for her patience, support and belief in me throughout the years of my education in France and in the UK. Last but not least, huge thanks to my daughter Orm for always putting a smile on my face and providing me energy to pursue this PhD. Without their love and support, I would not be here where I am today.

Abstract

Lectin-like oxidized low-density lipoprotein receptor-1 (LOX-1) is a scavenger receptor that plays an important role in atherosclerosis development. The binding and internalisation of oxidized low-density lipoprotein (Ox-LDL) via LOX-1 induces endothelial dysfunction, leukocyte recruitment, foam cell formation, and thus atherosclerotic plaque development. Therefore, inhibiting the LOX-1/Ox-LDL interaction would be an attractive way to prevent and fight against this cardiovascular disease. However, the recognition mode of LOX-1 to Ox-LDL is still unclear. A trisaccharide was previously shown to inhibit LOX-1 binding to Ox-LDL in cells and mice. This thesis presents an improved synthetic strategy towards an analogue of the lead trisaccharide, and an approach to increase its binding affinity by attaching the trisaccharide units to a polymer scaffold to make multivalent carbohydrate structures. The α -selectivity of glycosylation reactions was significantly improved by the use of a thiophenyl glycoside having a 4-methoxybenzoyl group at the O-4 position, potentially due to the remote protecting group participation. Moreover, α -manno- and α -galactopyranoside bearing a 4-methoxycarbonylphenyl group were prepared and converted to the corresponding hydrazide for use in glycopolymer dynamic combinatorial libraries. Using the same strategy, the trisaccharide epitopes were successfully attached to a polymer scaffold.

Dendritic cell-specific intercellular adhesion molecule-3-grabbing non-intergrin (DC-SIGN) is a C-type lectin receptor that is implicated in several viral infections, e.g., HIV and Ebola viruses. This lectin and its related receptor DC-SIGNR bind to high-mannose glycan structures. However, these two receptors still have distinct functions and specificities for different glycans. More structural and functional data of DC-SIGN and DC-SIGNR still awaits investigations. This thesis outlines successful synthetic routes to azide-appended mannose epitopes in form of mono- and disaccharides and a newly established and efficient method to prepare dense and compact mannose-capped quantum dots (*i.e.*, mono-Man-QDs and di-Man-QDs) to be used as multivalent probes for carbohydrate-binding proteins, e.g., DC-SIGN and DC-SIGNR via FRET (Förster resonance energy transfer) technique. The interactions between the synthetic Man-QDs with DC-SIGN and DC-SIGNR were for the first time investigated by FRET. The results showed that the mannose-capped QDs exhibited higher binding affinities to DC-SIGN than its related receptor DC-SIGNR. This finding was confirmed by viral inhibition assays, indicating that the tested mono-Man QDs specifically inhibited DC-SIGN- but not DC-SIGNR-mediated *pseudo*-Ebola viral entry of target cells.

List of Abbreviations

Ac	Acetyl
AcLDL	Acetylated low density lipoprotein
AGEs	Advanced glycation end-products
All	Allyl
anhyd.	Anhydrous
Apo-E	Apolipoprotein E
aq.	Aqueous
Ar	Aromatic
ArC	Aromatic carbon atoms
ArH	Aromatic protons
Bn	Benzyl
BSA	Bovine serum albumin
BSP	1-Benzenesulfonyl piperidine
Bz	Benzoyl
col.vol.	Column volume
Con A	Concanavalin A
COX	Cyclooxygenase
CRD	Carbohydrate recognition domain
CRP	C-reactive protein
CSA	(+/-)-10-Camphorsulfonic acid
CTLD	C-type lectin like domain
D	Dextrorotatory
DAMP	Damage-associated molecular pattern
DBU	1,8-Diazobicyclo[5.4.0]undec-7-ene
DC	Dendritic cell
DCE	1,2-Dichloroethane

DCM	Dichloromethane
DC-SIGN	Dendritic cell-specific intercellular adhesion molecule-3-grabbing non-integrin
DC-SIGNR	DC-SIGN related receptor
DHLA	Dihydrolipoic acid
Dil	1,1'-Dioctadecyl-3,3,3'-tetra-methylindocarbocyanine perchlorate
DIPEA	<i>N,N</i> -Diisopropylethylamine
DLS	Dynamic light scattering
DMAP	4-Dimethylaminopyridine
DMF	<i>N,N</i> -Dimethylformamide
EBOV-GP	Ebola virus glycoprotein
ECD	Extracellular domain
ECM	Extracellular matrix
Eqiv.	Equivalent
ES	Electrospray
EtOAc	Ethyl acetate
EtOH	Ethanol
FRET	Förster resonance energy transfer
Fuc	Fucose
g	gram
Gal	Galactose
GalNac	<i>N</i> -Acetylgalactosamine
GlcNac	<i>N</i> -Acetylglucosamine
h	Hour(s)
H-bond	Hydrogen bond
HDL	High density lipoprotein
HIV	Human immunodeficiency virus
HMBC	Heteronuclear multiple bond correlation
HMG-CoA	3-Hydroxy-3-methylglutaryl coenzyme A

HMQC	Heteronuclear multiple-quantum correlation
HPLC	High performance liquid chromatography
HRMS	High resolution mass spectrometry
HSP	Heat shock protein
Hz	Hertz
ICAM	Intracellular adhesion molecule
IR	Infra-red
<i>J</i>	Coupling constant
LA	Lipoic acid
LC-MS	Liquid chromatography-mass spectrometry
LDL	Low density lipoprotein
LOX-1	Lectin-like oxidized low-density lipoprotein receptor-1
L-SIGN	Liver/lymph node-specific ICAM-3 grabbing non-integrin
LTB	Heat labile toxin B-subunit
m.p.	Melting point
Man	Mannose
MCP-1	Monocyte chemoattractant protein-1
Me	Methyl
mg	Milligram
min	Minute(s)
MLV	Murine leukemia virus
MS	Molecular sieves
NIS	<i>N</i> -Iodosuccinimide
NMO	<i>N</i> -Methylmorpholine- <i>N</i> -oxide
NMR	Nuclear magnetic resonance
OxLDL	Oxidized low density lipoprotein
<i>p</i>	Para
PAMP	Pathogen-associated molecular pattern
PBS	Phosphate-buffered saline

PEG	Polyethylene glycol
PMBz	<i>para</i> -Methoxybenzoyl
ppm	Parts per million
PRR	Pattern recognition receptor
PS-DCL	Polymer-scaffolded dynamic combinatorial library
<i>p</i> -Ts	<i>para</i> -Toluenesulfonyl
QD	Quantum dot
r.t.	Room temperature
ROS	Reactive oxygen species
sat.	Saturated
sLOX-1	Soluble LOX-1
TBAI	Tetrabutylammonium iodide
TBDMS	<i>tert</i> -Butyldimethylsilyl
Temp.	Temperature
Tf	Trifluoromethanesulfonyl
THF	Tetrahydrofuran
TLC	Thin layer chromatography
TMD	Transmembrane domain
TMSOTf	Trimethylsilyltrifluoromethanesulfonate
TNF	Tumour necrosis factor
TTBP	2,4,6-tri- <i>tert</i> -Butylpyrimidine
UV	Ultraviolet
VCAM-1	Vascular cell adhesion molecule 1
VOC	Vaso-occlusive crisis
VSV-G	Vesicular stomatitis virus glycoprotein
wt.	Weight

Tables of Contents

Acknowledgements	iii
Abstract.....	iv
List of Abbreviations	v
Tables of Contents	ix
List of Tables	xiii
List of Figures.....	xiv
List of Schemes	xxi
Chapter 1: Introduction	1
1.1 Cell surface carbohydrate-protein interactions	2
1.1 Multivalency	5
1.2 Glycomimetics and multivalent glycoconjugates.....	8
1.3 Cell surface receptors: lectins	12
1.4 LOX-1 and its implication in atherosclerosis	14
1.4.1 Atherosclerosis.....	14
1.4.2 Prevention and treatment of atherosclerosis.....	15
1.4.3 Roles of LOX-1 in atherosclerosis	15
1.4.4 Identification and structure of LOX-1	17
1.4.5 LOX-1 ligands.....	18
1.4.6 LOX-1 inhibitors.....	20
1.4.7 Previous studies on LOX-1 ligand bindings	24
1.5 DC-SIGN and its implication in viral infection	28
1.5.1 Structures of DC-SIGN and DC-SIGNR.....	28
1.5.2 Functions of DC-SIGN and DC-SIGNR.....	35
1.5.3 The roles of DC-SIGN and DC-SIGNR in viral infections	35
1.6 Project objectives	38
1.6.1 LOX-1.....	38
1.6.2 DC-SIGN and its related receptor DC-SIGNR.....	40

Chapter 2: Synthesis of a monovalent inhibitor for LOX-1	42
2.1 Introduction	43
2.2 Aims and objectives	43
2.3 Synthesis of a trisaccharide analogue containing an aromatic amine group	43
2.3.1 Synthesis of a glycosyl acceptor.....	43
2.3.2 Synthesis of a glycosyl donor	47
2.3.3 Glycosylation reactions.....	47
2.4 A model study for derivatising an aromatic amine glycoside.....	49
2.5 Conclusions	51
Chapter 3: Optimisation of the glycosylation reaction and replacement of the central galactose residue with a non-sugar moiety using 1,2-<i>cis</i>-cyclohexanediol	53
3.1 Introduction	54
3.2 Glycosylation reaction in general.....	54
3.3 Optimisation of the glycosylation reaction using 1,2- <i>cis</i> -cyclohexanediol.....	54
3.4 Variable temperature NMR experiment	64
3.5 Conclusions	65
Chapter 4: Reinvention of the synthesis of a trisaccharide.....	66
4.1 Introduction	67
4.2 Synthesis of a glycosyl acceptor containing a 4-methoxycarbonylphenyl group	67
4.2.1 Improved regioselectivity of allylation.....	68
4.3 Synthesis of a disaccharide intermediate	73
4.4 Selective deprotection: deallylation	74
4.5 Attaching another galactose residue to the disaccharide intermediate	75
4.6 Removal of the protecting groups.....	78
4.7 Conclusions	79
Chapter 5: Carbohydrate-functionalised polymers as multivalent inhibitors for targeting LOX-1.....	80
5.1 Introduction	81
5.2 Aims and objectives	83
5.3 Synthesis of α -mannosyl and α -galactosyl hydrazides for making carbohydrate-functionalised polymer-scaffolded dynamic combinatorial libraries (PS-DCLs).....	84

5.3.1 Synthesis of α -mannosyl and α -galactosyl hydrazides	84
5.3.2 Templating carbohydrate-functionalised polymer-scaffolded dynamic combinatorial libraries with lectins	86
5.4 Preparation of the polymers with the LOX-1 ligand trisaccharide	88
5.4.1 Derivatisation of the trisaccharide for attaching to a multivalent scaffold	89
5.4.2 Identification of the side-product formed in the reaction in D ₂ O using ¹ H NMR spectroscopy.....	91
5.4.3 Synthesis of carbohydrate-functionalised polymers.....	92
5.5 Conclusions	96
Chapter 6: Synthesis and biological evaluations of multivalent probes for DC-SIGN.....	98
6.1 Introduction	99
6.2 Aims and objectives	100
6.3 Synthesis of an azido-mannopyranoside.....	101
6.4 Multivalent mannose quantum dots for the study of carbohydrate and DC-SIGN and DC-SIGNR interactions	101
6.5 Biological evaluations.....	105
6.5.1 Binding studies using QD-FRET technique.....	105
6.5.2 Viral inhibition assays	107
6.6 Synthesis of the azido-disaccharide analogue.....	110
6.6.1 Attempted synthesis of the azido-disaccharide analogue starting from the azido-monosaccharide version.....	111
6.6.2 Successful synthesis of the azido-disaccharide analogue starting from D-mannose tetraacetate	115
6.7 Multivalent di-mannose quantum dots for the study of carbohydrate and DC-SIGN and DC-SIGNR interactions	119
6.8 Binding studies using QD-FRET technique	120
6.9 Conclusions	124
Chapter 7: Conclusions and future work	125
7.1 LOX-1 project.....	126
7.1.1 Summary.....	126
7.1.2 Achievements.....	128
7.1.3 Challenges and limitations.....	128
7.1.4 Future work	129

7.2 DC-SIGN project	131
7.2.1 Summary	131
7.2.2 Achievements	132
7.2.3 Challenges and limitations	132
7.2.4 Future work	132
Tables of compounds	134
Chapter 8: Experimental	146
8.1 General methods	146
8.2 Chemical synthesis	148
8.2.1 Synthesis of carbohydrates	148
8.2.2 Synthesis of carbohydrate-functionalised quantum dots	202
Chapter 9: Appendix	208
Chapter 10: References	210

List of Tables

Table 1-1. Examples of different types of lectins and their ligands.....	13
Table 3-1. Glycosylation of 1,2- <i>cis</i> -cyclohexanediol 49 with perbenzylated glycosyl donor 41 , giving pseudo-trisaccharides 50-51	56
Table 3-2. Literature data on galactosyl donors bearing different O-4 protecting groups	57
Table 3-3. Glycosylation of 1,2- <i>cis</i> -cyclohexanediol 49 with glycosyl donors 41 and 55 . Entries 1-4 are reiterated from Table 3-1 for convenience to the readers..	63
Table 5-1. Hydrazinolysis reactions of trisaccharide 27	90
Table 6-1. Glycosylation reactions of acceptor 101 with mannosyl imidate 95 under different conditions.	116
Table 6-2. The binding data for dimannose capped QDs binding to DC-SIGN and DC-SIGNR.....	123

List of Figures

- Figure 1-1.** An electron microscopic image of glycocalyx on the surface of a coronary artery, figure reproduced from reference 1. 2
- Figure 1-2.** Cell surfaces are decorated with different carbohydrate structures, which were exploited by several pathogens for the cell entry, figure reproduced from reference 9. 3
- Figure 1-3.** A schematic representation of the hydrogen bond network established between the extended binding site of Con A and the bound mannotriose Man- α -1,3-(Man- α -1,6)-Man (in red). Hydrogen bonds are represented as black dotted lines, reproduced from reference 13, model based on X-ray crystal structure. 4
- Figure 1-4.** Hydrophobic stacking between maltose (in red) and tryptophan and tyrosine residues on maltodextrin-binding protein, redrawn from reference 14, model based on X-ray crystal structure. 4
- Figure 1-5.** The binding site of E-selectin in complex with sLe^x (Nue5Ac α 2-3Gal β 1-4(Fuc α 1-3)GlcNAc β -O(CH₂)₈COOMe, in red), showing the amino acid residues involved in coordinating the calcium ion and binding the trisaccharide, reproduced from reference 20, model based on X-ray crystal structure. 5
- Figure 1-6.** Possible modes of multivalent ligand binding for an increase in the binding affinity: a) chelate effect; b) receptor cluster; c) subsite binding; d) statistical effects; e) steric stabilisation. 7
- Figure 1-7.** Selected multivalent carbohydrate structures using different scaffolds. 8
- Figure 1-8.** Chemical structures of the silyl Lewis^x (sLe^x) mimic GMI-1070 (**1**) and the physiological ligand sLe^x (**2**). 9
- Figure 1-9.** Structure of: Man₉ (**3**); DC-SIGN inhibitors: a trimannoside analogue **4**; a glycocluster **5** and a glycodendrimer **6**. 11
- Figure 1-10.** DC-SIGN inhibitors: a disaccharide analogue **7** with a cyclohexane-based aglycone; a disaccharide analogue **8** with a bis-benzylamide; a *pseudo*-disaccharide dendrimer **9**; a *pseudo*-disaccharide linked by a rod-like spacer **10**. 12
- Figure 1-11.** Carbohydrate binding domain of DC-SIGN having a prototype C-type lectin fold, figure reproduced from reference 45. 14

- Figure 1-12.** The roles of LOX-1 in atherosclerosis. Low density lipoprotein (LDL) particles diffuse into the arterial intima, followed by the conversion of LDL to oxidized LDL. The recognition of OxLDL by LOX-1 induces several effects including lipid uptake and formation of foam cells and atherosclerotic plaques, figure reproduced from reference 59. 16
- Figure 1-13.** a) Schematic representation of human LOX-1 in a dimeric form. Each individual protein contains 4 different domains: a short cytoplasmic N-terminal domain, a single transmembrane domain, a neck domain, and a C-terminal C-type lectin-like domain (CTLD); b) LOX-1 in dimeric form upon the binding to ligands, e.g., Ox-LDL..... 17
- Figure 1-14.** X-ray crystal structure of human LOX-1 ligand CTLD binding domain in: a) side view and b) top view. The central hydrophobic tunnel is outlined by dotted lines, figure reproduced from reference 68. 18
- Figure 1-15.** The percentage of LOX-1 transfected cells binding to labelled OxLDL which depends on interaction with protein moieties (A) or sugar moieties (B), figure reproduced from K. Lacey's Ph.D. thesis University of Leeds 2012, reference 81. LDL, Low-density lipoprotein; OxLDL, Oxidized low-density lipoprotein; PNGaseF, N-glycosidase F; Endo H, endoglycosidase H. 20
- Figure 1-16.** The result of different isomers of procyanidins in inhibiting OxLDL binding to LOX-1 expressing cells, figure reproduced from reference 82. 21
- Figure 1-17.** Chemical structures of epicatechin **11** and the trimer procyanidin isomers used for the binding assay (**12** and **13**)..... 21
- Figure 1-18.** Chemical structures of: ellagic acid (**14**) and EGCG (**15**)..... 22
- Figure 1-19.** Chemical structures of: simvastatin (**16**), atorvastatin (**17**), aspirin (**18**), and gliclazide (**19**). 23
- Figure 1-20.** Chemical structure of a potential inhibitor of LOX-1 called PLAzPC. 23
- Figure 1-21.** Chemical structures of potential small molecule inhibitors of LOX-1..... 24
- Figure 1-22.** Glycan array data of extracellular LOX-1 showing the two carbohydrate structures that could bind to LOX-1, K. Lacey's Ph.D. thesis University of Leeds 2012, reference 81..... 25
- Figure 1-23.** Chemical structures of three oligosaccharides used for the binding assays. 26
- Figure 1-24.** The tests of various carbohydrates in inhibiting OxLDL binding to LOX-1 expressing cells. (S2 = disaccharide **23**; S3 = trisaccharide **25**; S4 = tetrasaccharide **24**), figure reproduced from K. Lacey's Ph.D. thesis University of Leeds 2012, reference 81. 26

- Figure 1-25.** The effect of trisaccharide **25** (sugar 3) on plaque formation in ApoE-deficient transgenic mice. Control (saline), 0.1 mM and 1 mM of trisaccharide **25** administration was evaluated in ApoE-deficient mice after 10 weeks on a cholesterol- and fat-rich diet, figure reproduced from K. Lacey's Ph.D. thesis University of Leeds 2012, reference 81. 27
- Figure 1-26.** a) Schematic representation of the structures of DC-SIGN and DC-SIGNR; b) Arrangement of DC-SIGN and DC-SIGNR in a tetramer through the tandem-neck domains. 29
- Figure 1-27.** A) Neck sequences of DC-SIGN and DC-SIGNR; B) Effects of neck sequences on oligomerisation of DC-SIGN and DC-SIGNR, figure adapted from reference 102. 30
- Figure 1-28.** a) Structure of the DC-SIGNR four-bundle of 23-amino acid repeat motifs which are connected through a short non-helical segments, *i.e.*, a proline residue (Pro); b) Model of much of the extracellular domain of DC-SIGNR, including neck repeats 2 to 8 and the CRD, figure reproduced from reference 28. 31
- Figure 1-29.** Interactions of DC-SIGN and DC-SIGNR with GlcNAc₂Man₃. A) Interactions of the α 1-3-linked branch with DC-SIGNR. Only important sugars are shown. Ca²⁺ coordination is shown by solid black lines and hydrogen bonds as dashed lines; B) Interactions of the α 1-3-linked branch with DC-SIGN. The terminal GlcNAc1 forms a cross link by forming the typical C-type lectin interactions with the principal Ca²⁺ (grey) are shown, figure reproduced from reference 45. 32
- Figure 1-30.** Glycan array probed with fluorocein-labelled DC-SIGN and DC-SIGNR. a) DC-SIGN binds to fucose- and mannose-containing glycans; b) DC-SIGNR binds to mannose-containing glycans, figure reproduced from reference 99. 33
- Figure 1-31.** DC-SIGN in complex with: a) Man₄ structure and b) Le^x tetrasaccharide of NMFPIII. Cyan spheres are bound Ca²⁺ ions. Ca²⁺-coordination is shown by black lines, hydrogen bonds as dashed lines, figure reproduced from reference 105. 34
- Figure 1-32.** The roles of DC-SIGN in HIV-1 infection and transmission: *trans*-infection mediated by DCs can occur by two pathways (a,b) and *cis*-infection mediated by DCs involves one pathway (c), figure reproduced from reference 121. 37
- Figure 1-33.** Lead compound **25** and its analogous compounds **26** and **27**. 38
- Figure 1-34.** Designed sugar derivative **28**. 39

Figure 1-35.	Cartoon representation of a trisaccharide analogue containing a reactive hydrazine group attached to a multivalent polymer.....	39
Figure 1-36.	Target azido-mannopyranoside 29 and schematic representation of monomannoside bearing quantum-dots 30 ; QD = quantum dots.....	40
Figure 1-37.	Target azido-mannopyranoside 31 and schematic representation of dimannoside bearing quantum-dots 32 ; QD = quantum dots.....	41
Figure 2-1.	Chemical structure of lead trisaccharide 25 , which was identified as an inhibitor of LOX-1.	43
Figure 2-2.	¹ H NMR spectrum of trisaccharide 44 (500 MHz, D ₂ O). Highlighted in red shows peaks corresponding to minor compounds presented in the sample.	49
Figure 2-3.	Chemical structure of 4-methoxycarbonylphenyl trisaccharide 27	50
Figure 3-1.	Chemical structure of lead compound 25	55
Figure 3-2.	Synthetic route to <i>pseudo</i> -trisaccharide 51	64
Figure 3-3.	Stacked plot of ¹ H NMR spectra of <i>pseudo</i> -trisaccharide 51 at variable temperature (from 26 °C to 90 °C, D ₂ O and 500 MHz).	65
Figure 4-1.	Formation of dibutyl stannylene acetal and dimerisation.	68
Figure 4-2.	Possible explanations for non-regioselective and regioselective allylation via stannylene acetal intermediates.....	69
Figure 4-3.	Confirmation of the presence of an allyl groups occupying at the O-3 position by acetylation at the O-2 position (<i>cf.</i> proton numbering in Figure 8-1). ¹ H NMR spectra of a) galactopyranoside 85 and b) its acetylated product (500 MHz, CDCl ₃).	71
Figure 4-4.	Overlay of the HMQC (red) and HMBC (purple) spectra of galactopyranoside 79 (75 MHz, CDCl ₃) showed a correlation of C-allyl group to H-3 indicating the attachment of an allyl group at the C-3 position.	73
Figure 4-5.	A stacked plot of ¹ H NMR spectra of a) allylated compound 80 and b) deallylated compound 81 (500 MHz, CDCl ₃).	75
Figure 4-6.	Stacked plot of the entire ¹ H NMR spectra and the expanded area of trisaccharide 82 (500 MHz, CDCl ₃) a) at higher temperature (328 K) and b) at room temperature (301 K). The expanded area showed distinct proton signals, <i>i.e.</i> , two signals for H-4 next to each C-4 ester group and three anomeric protons (2 × H-1 α and H-1 β).	77

- Figure 4-7.** Overlay of HMBC (red) and HMQC (blue) spectra of trisaccharide **82** (75 MHz, CDCl₃, 331 K) showed that the C-1 signals of the adjacent galactose units correlated with the signals of each H-3 and H-4 of the central galactose residue..... 78
- Figure 5-1.** Representative examples of polymer scaffolds..... 81
- Figure 5-2.** Preparation of a polymer scaffold dynamic combinatorial library by reaction of acylhydrazines (represented as open purple squares and open blue circles) with a polymer bearing aldehyde functionalities. Changes of the residual composition within the PS-DCL was induced upon addition of a molecular template, figure reproduced from reference 124..... 83
- Figure 5-3.** α -Mannosyl hydrazide **86** (also called **MAN**) and α -galactosyl hydrazide **89** (also called **GAL**) used for the synthesis of carbohydrate-functionalised polymer-scaffold dynamic combinatorial libraries (PS-DCLs). 86
- Figure 5-4.** Preparation of a carbohydrate-functionalised polymer-scaffold dynamic combinatorial library by conjugation of acylhydrazide functionalised carbohydrate residues onto an aldehyde-functionalised polymer scaffold. Compositional changes within PS-DCL were induced upon addition of a lectin, resulting in polymers of improved affinity for the lectin added, figure reproduced from reference 125. 86
- Figure 5-5.** a) ¹H NMR spectroscopic analysis (500 MHz, D₂O, pH 4.5) of PS-DCL before (t = 0 h) and after (t = 16 h) addition of Con A, highlighting the changes in intensity of the diagnostic anomeric resonances of **GAL** and **MAN** 16 h after addition of template. b) Effect of addition of lectin templates to PS-DCLs upon relative concentrations of **GAL** and **MAN** as a function of time, suggesting preferential incorporation of the carbohydrate residue preferred by the lectin added. There is no observed change in the relative concentrations of **GAL** and **MAN** in the absence of a lectin template, figure reproduced from reference 125. 88
- Figure 5-6.** Chemical structure of trisaccharide **27**..... 89
- Figure 5-7.** Comparison of the aromatic regions of the ¹H NMR spectra of: a) the trisaccharide with an aryl ester group (starting material), b) the attempted hydrazinolysis in D₂O which still contains the starting material, c) the hydrolysed products of a mixture from previous attempted reaction and d) the desired hydrazinolytic product which was formed by the hydrazinolysis in MeOH. All ¹H NMR spectra were acquired at 500 MHz in D₂O. 92
- Figure 5-8.** Cartoon presentation of the attachment of target trisaccharide residues **90** onto an aldehyde-functionalised polymer. 94

- Figure 5-9.** Cartoon presentation of the attachment of α -galactopyranoside residues **89** onto an aldehyde-functionalised polymer..... 95
- Figure 6-1.** (A) Structures of DHLA-appended PEG ligands functionalised with mannose (*i.e.*, DHLA-EG₃-Man and DHLA-PEG₁₃-Man); Preparation of mannose-capped QDs (B) QD-PEG₁₃-Man (C) QD-EG₃-Man (D) QDs capped with mannose and DHLA-zwitterion (DHLA-ZW) spacer ligand, figure reproduced from reference 156. 104
- Figure 6-2.** Size distribution histograms of: (A) QD-PEG₁₃-Man and (B) and QD-EG₃-Man, measured by DLS, figure reproduced from reference 156. 105
- Figure 6-3.** Schematic representation of the FRET technique used to investigate multivalent interactions between carbohydrate-recognition domain (CRD) of labelled DC-SIGN and DC-SIGNR and PEG terminated mannose-capped QDs, figure reproduced from reference 156..... 106
- Figure 6-4.** Fluorescence spectra of the donor-acceptor pair: (A) DC-SIGN + QD-PEG₁₃-Man; (B) DC-SIGN + QD-EG₃-Man; (C) DC-SIGNR + QD-PEG₁₃-Man; (D) DC-SIGNR + QD-EG₃-Man; (E) DC-SIGN CRD monomer + QD-EG₃-Man. (F) Correlation between the FRET ratio and the protein concentrations, figure reproduced from reference 156. 107
- Figure 6-5.** Impact of QD-EG₃-Man on viral inhibition. Human 293T cells expressing DC-SIGN, DC-SIGNR or empty plasmid (pcDNA) were treated with QD-EG₃-Man (at 0, 62.5 and 250 nM). Cells were transfected with: (A) murine leukaemia virus (MLV) vectors bearing Ebola virus glycoprotein (MLV-EBOV-GP) or (B) the control vesicular stomatitis virus glyco-protein (MLV-VSV-G) for delivering luciferase gene. Luciferase activities in the lysates were determined. In the case of MLV-EBOV-GP, the difference between untreated and treated with 250 nM QD-EG₃-Man is statistically significant ($p = 0.024$, from two-tailed students t-test), figure reproduced from reference 156. 109
- Figure 6-6.** (A) Schematic representation of the structure of DC-SIGN and DC-SIGNR monomer; proposed ligand-receptor binding modes between the QDs and: (B) DC-SIGN or (C) DC-SIGNR due to their different orientations of tetrameric CRDs, figure reproduced from reference 156. 110
- Figure 6-7.** Structure of target dimannosyl azide **31**. 111

- Figure 6-8.** ^1H NMR spectra of a) mannopyranoside **94** and b) its acetylated product (500 MHz, CDCl_3), confirming that an acetyl protecting group was attached at the O-2 position and a *tert*-butyldimethylsilyl (TBDMS) ether protecting group was at the O-6-position (*cf.* proton numbering in Figure 8-1). 112
- Figure 6-9.** ^1H NMR spectra of a) mannopyranoside **97** and b) its acetylated product (500 MHz, CDCl_3), confirming that an acetyl protecting group was attached at the O-2 position and a *tert*-butyldiphenylsilyl (TBDPS) ether protecting group was at the O-6-position (*cf.* proton numbering in Figure 8-1). 114
- Figure 6-10.** Gated decoupled ^{13}C spectrum of dimannose **102** (500 MHz, CDCl_3) showing a doublet of doublets with a large and a small coupling constants (174 Hz and 6 Hz), resonating at 98.3 ppm and a double with a coupling constant of 162 Hz resonating at 91.0 ppm. α -, β -Configurations were determined according to their coupling constants. 117
- Figure 6-11.** The ^1H - ^{13}C HMQC spectrum of acetylated manno- and galactose **102** (500 MHz, CDCl_3), showing the correlation between anomeric carbon and anomeric proton of each mannose residue. 118
- Figure 6-12.** (A-H) Preliminary data on fluorescence spectra of QD-PEG_n-Man α -1,2-Man ($\lambda_{\text{EM}} = 554$ nm, final QD concentration, CQD = 40 nM) after binding to Atto-594 labelled proteins: (A) DC-SIGN + QD-PEG₁₀-Man α -1,2-Man (73%) + ZW (27%); (B) DC-SIGN + QD-EG₃-Man α -1,2-Man (25%) + ZW (75%); (C) DC-SIGN + QD-PEG₁₀-Man α -1,2-Man (100%); (D) DC-SIGN + QD-EG₃-Man α -1,2-Man (25%) + ZW (75%); (E) DC-SIGNR + QD-PEG₁₀-Man α -1,2-Man (73%) + ZW (27%) ; (F) DC-SIGNR + QD-PEG₁₀-Man α -1,2-Man (25%) + ZW (75%); (G) DC-SIGNR + QD-EG₃-Man α -1,2-Man (100%); (H) DC-SIGNR + QD-EG₃-Man α -1,2-Man (25%) + ZW (75%). 122
- Figure 6-13.** FRET ratio (I_{626}/I_{554}) between di-mannose capped QDs donors and dye-labelled DC-SIGN and DC-SIGNR acceptors (collectively called DC-SIGN/R). 123
- Figure 8-1.** Proton numbering in ^1H NMR for a) galacto-configured mono- and di- and trisaccharides b) manno-configured mono- and disaccharides. 147

List of Schemes

Scheme 2-1. Synthetic route to 4-nitrophenyl galactopyranoside 36 .	44
Scheme 2-2. The necessity of protecting group arrangements for the synthesis of the target trisaccharide analogue.	45
Scheme 2-3. Synthetic route to compounds 38a , 38b , and 38c .	46
Scheme 2-4. Synthetic route to galactopyranoside 39 , which would be used as a glycosyl acceptor for further glycosylation reactions. N.B. Starting material contains 60% of 38b and 40% of 38c . Yield was calculated based on the amount of 38b present in the starting material.	47
Scheme 2-5. Synthetic route to glycosyl donor 41 .	47
Scheme 2-6. Synthetic route to deprotected trisaccharide 44 .	48
Scheme 2-7. Attempted synthesis of galactopyranoside 48 .	50
Scheme 2-8. Entire synthesis of 4-aminophenyl galactopyranoside 44 with two key challenges to be improved: 1) the regioselectivity of the protecting group (blue box) and 2) the α -selectivity of glycosylation (red box).	52
Scheme 3-1. General mechanism of a glycosylation reaction.	54
Scheme 3-2. A possible mechanism for remote participating group participation at O-4 position.	58
Scheme 3-3. An isotopic labelling probe designed by Crich and co-workers.	59
Scheme 3-4. Synthetic route to glycosyl donors 68 and 55 .	61
Scheme 4-1. Synthetic route to galactopyranoside 73 .	67
Scheme 4-2. A non-regioselective allylation, giving a mixture of three products.	69
Scheme 4-3. Attempted synthesis of compound 74 and synthetic route to compound 75 .	70
Scheme 4-4. Synthetic route to galactopyranoside 79 .	72
Scheme 4-5. Synthetic route to disaccharide 80 .	74
Scheme 4-6. Synthetic route to compound 81 .	74
Scheme 4-7. Synthetic route to trisaccharide 82 .	75
Scheme 4-8. Synthetic route to fully-deprotected trisaccharide 27 .	79
Scheme 5-1. Preparation of galacto-functionalised polymers by a tandem post-polymerisation modification. 1) amine (variable amounts)/triethylamine (TEA; 1 equiv.)/ DMF, 5 h.; 2) GaIn ₃ (1.5 equiv./CuBr/TBTA, DMSO).	82
Scheme 5-2. Synthetic route to mannosyl hydrazide 86 .	85
Scheme 5-3. Synthetic route to galactosyl hydrazide 89 .	85

Scheme 5-4. Synthetic route to α -galatopyranoside 91	91
Scheme 5-5. Synthesis of an aldehyde-functionalised polymer with variation of numbers of monomers.	93
Scheme 5-6. Synthesis of a control polymer having ethylene glycol units instead of carbohydrate residues.....	96
Scheme 6-1. Synthetic route to azido-mannopyranoside 29	101
Scheme 6-2. Preparation of: a) Dihydrolipoic acid-poly(ethylene glycol)-mannose (DHHLA-PEG _n -Man, where n = 3 or ~13) and b) Dihydrolipoic acid-zwitterionic ligand (DHHLA-ZW). N.B. Both LA-EG ₃ -cyclooctyne and LA-PEG ₁₃ -cyclooctyne were used as a mixture of stereoisomers. Both LA-EG ₃ -Man and LA-PEG ₁₃ -Man were formed as a mixture of regioisomers, only the predominant stereoisomer is shown.	103
Scheme 6-3. Synthetic route to azido-mannopyranoside 94	111
Scheme 6-4. Attempted synthesis to azido-disaccharide analogue 96	113
Scheme 6-5. Synthetic route to azido-mannopyranoside 97	113
Scheme 6-6. Attempted synthesis of azido-mannopyranoside 99	115
Scheme 6-7. Synthetic route to mannopyranosyl acetate 101	115
Scheme 6-8. Synthetic route to fully deprotected azido-mannopyranoside 31	119
Scheme 6-9. Preparation of dihydrolipoic acid-poly(ethylene glycol)-dimannose (DHHLA-PEG _n -Man- α -1,2-Man, where n = 3 or ~10). N.B. Both LA-EG ₃ -cyclooctyne and LA-PEG ₁₀ -cyclooctyne were used as a mixture of stereoisomers. Both LA-EG ₃ -Man and LA-PEG ₁₀ -Man were formed as a mixture of regioisomers, only the predominant stereoisomer is shown.	120

Chapter 1: Introduction

1.1 Cell surface carbohydrate-protein interactions

Mammalian cell surfaces are covered with a glycan-rich layer, referred to as glycocalyx (Figure 1-1), which comprises glycans of glycoproteins or glycolipids.¹ Cell surface glycans form complex and highly branched structures, as their monosaccharide units can form glycosidic linkages via hydroxyl groups at different positions on the sugar ring. The broad range of structures can also arise from different types of glycosidic linkages which have either an α - or β -configuration.

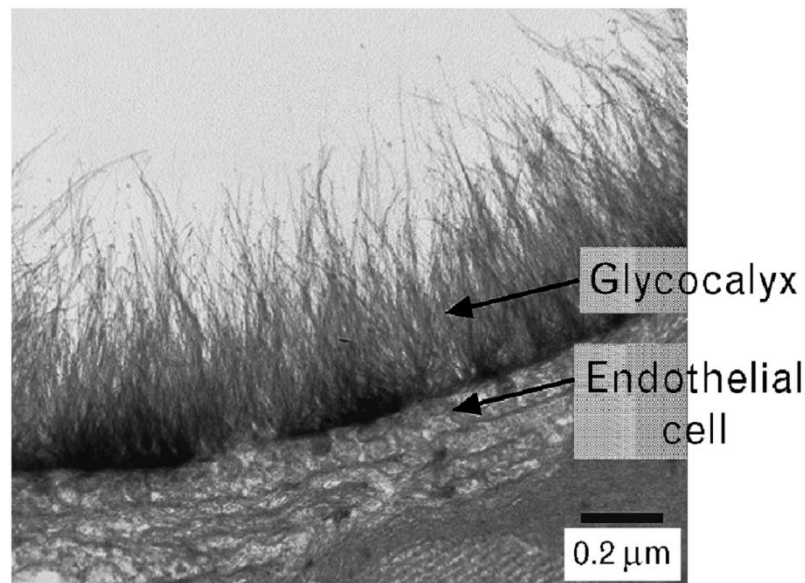


Figure 1-1.¹ An electron microscopic image of glycocalyx on the surface of a coronary artery, figure reproduced from reference 1.

The sugar-based information on cells can be decoded by carbohydrate binding proteins, e.g., lectins, which recognise specific carbohydrate structures. These protein-carbohydrate interactions play crucial roles in many important biological processes, e.g., fertilisation,^{2,3} inflammation,⁴ signal transduction.⁵ On the other hand, carbohydrate recognition in biological systems is also associated with various pathologic conditions and diseases, e.g., inflammation-associated cancer,⁶ cancer metastasis,^{7,8} viral and bacterial infections.⁹ Several pathogenic bacteria and viruses exploit specific glycan structures to adhere to and infect host cells (Figure 1-2). For instance, *Staphylococcus aureus* specifically binds to sialyl-Lewis^x structures, influenza virus recognises sialic acid residues of glycoproteins and bacterial toxins from *Vibrio cholera* bind selectively to blood group O antigens.^{10,11}

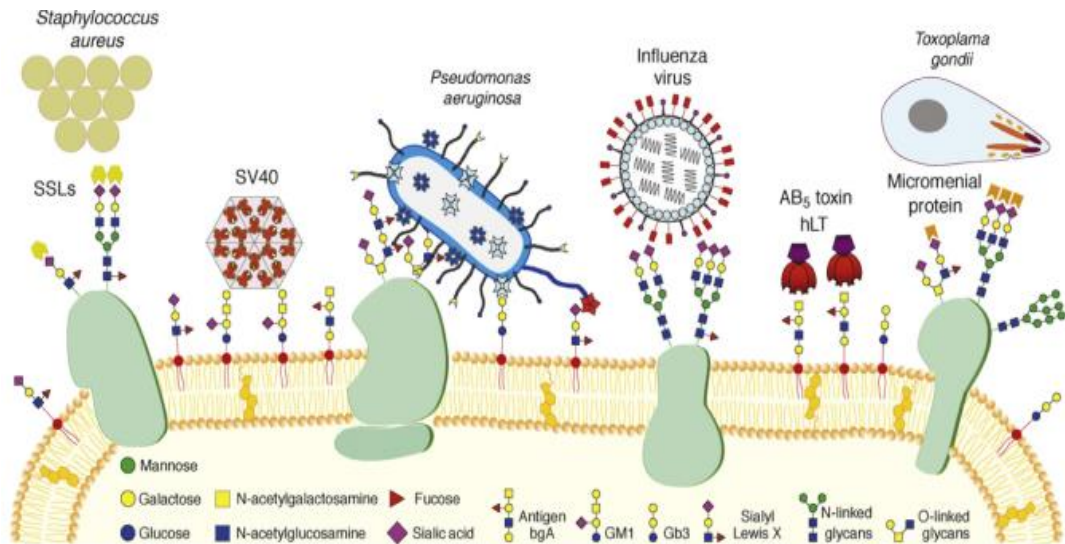


Figure 1-2.⁹ Cell surfaces are decorated with different carbohydrate structures, which were exploited by several pathogens for the cell entry, figure reproduced from reference 9.

Generally, interactions between proteins and carbohydrates can occur through different types of interactions, e.g., hydrogen bonds (H-bonds), hydrophobic stacking, electrostatic interactions and interactions with water and calcium ions.¹² Hydroxyl groups on carbohydrates can facilitate the formation of H-bonds with polar moieties of proteins that are considered the most important interaction of protein with carbohydrates. Also, water-mediated interactions play an important role in protein-carbohydrate complexation. Water molecules often facilitate the interactions between sugar hydroxyl groups and amino acid residues in the protein binding site. One example of protein-carbohydrate complex that exemplifies the hydrogen bond network is the trimannose binding site of Concanavalin A (Con A) in complex with trisaccharide $\text{Man-}\alpha\text{-1,3-(Man-}\alpha\text{-1,6)-Man}$ (Figure 1-3).¹³

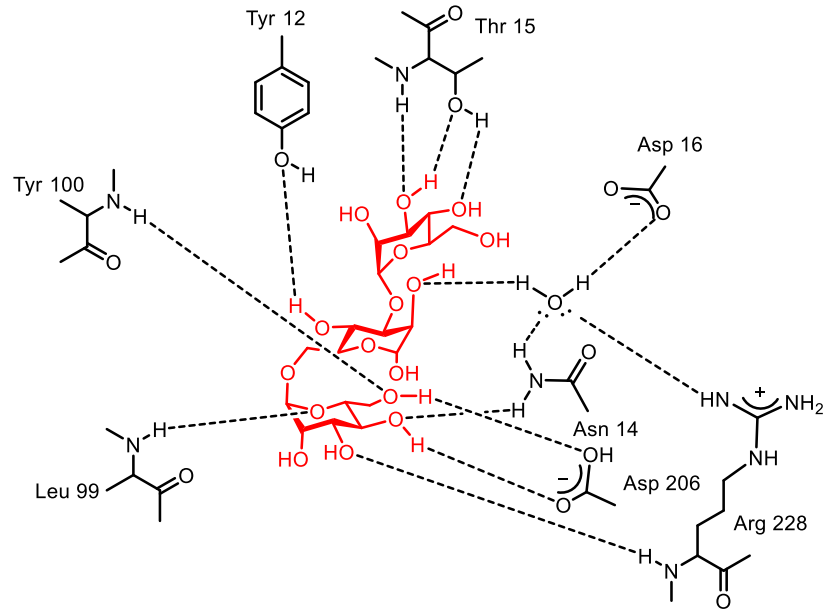


Figure 1-3.¹³ A schematic representation of the hydrogen bond network established between the extended binding site of Con A and the bound mannotriose Man- α -1,3-(Man- α -1,6)-Man (in red). Hydrogen bonds are represented as black dotted lines, reproduced from reference 13, model based on X-ray crystal structure.

Hydrophobic stacking can also take part in protein-carbohydrate interactions. Although carbohydrates are hydrophilic molecules, they also possess hydrophobic faces (α and β faces) of the sugar ring, exhibiting C-H patches. The hydrophobic faces of the carbohydrates can interact with electron-rich aromatic side chains of proteins (e.g., tryptophan, phenylalanine, tyrosine), contributing to hydrophobic CH- π interactions (Figure 1-4).^{14,15}

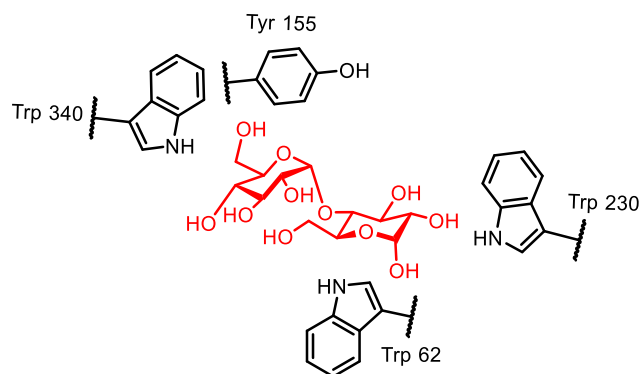


Figure 1-4.¹⁴ Hydrophobic stacking between maltose (in red) and tryptophan and tyrosine residues on maltodextrin-binding protein, redrawn from reference 14, model based on X-ray crystal structure.

Other groups present on the sugar scaffold, *e.g.*, the methyl moiety of acetamido groups, can be involved in non-polar contacts with the interacting partners.¹⁶ Moreover, aromatic aglycones (*i.e.*, non-sugar moieties) introduced to carbohydrates have been reported to exhibit a higher affinity than glycosides without such hydrophobic substituent as a result of additional hydrophobic effects and/or π - π interactions.¹⁷ Some sugars or modified sugars (*e.g.*, sialic acids, glucosamines, phosphorylated and sulfated sugars) are positively or negatively charged, and can interact with charged residues on lectins through ionic electrostatic interactions.¹⁸

Calcium ions (Ca^{2+}) are essential for the formation of lectin-carbohydrate complexes, either by direct co-ordination with the carbohydrate itself or maintaining the geometry of the binding site. Such an interaction is found in lectins belonging to the C-type family, which are Ca^{2+} -dependent upon binding to their carbohydrate ligands. For example, the carbohydrate recognition domain of E-selectin coordinates with a calcium ion and partakes in multiple H-bonds with the amino acid residues (Figure 1-5).¹⁹ Dendritic cell-specific intercellular adhesion molecule-3-grabbing non-integrin (DC-SIGN), a C-type lectin, also requires calcium ions for carbohydrate binding. The structure of this type of lectin will be discussed in Section 1.3.

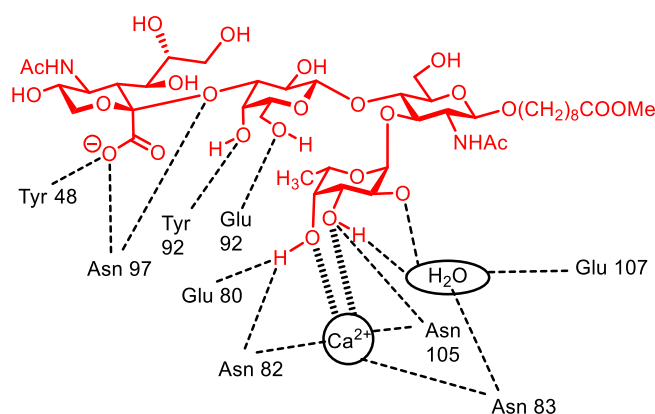


Figure 1-5.¹⁹⁻²⁰ The binding site of E-selectin in complex with sLe^x (Nue5Ac α 2-3Gal β 1-4(Fuc α 1-3)GlcNAc β -O(CH $_2$) $_8$ COOMe, in red), showing the amino acid residues involved in coordinating the calcium ion and binding the trisaccharide, reproduced from reference 20, model based on X-ray crystal structure.

1.1 Multivalency

Individual protein-carbohydrate interactions are typically weak with typical dissociation constant in the mM range. The binding is enthalpy-driven and via the contribution of multiple hydrogen bonding and hydrophobic interactions. Water-mediated interactions can influence the binding thermodynamics comprising the entropic gain of displacing

highly ordered water molecules and the enthalpy decrease of breaking water-protein H-bonds. However, this process is counteracted by unfavorable entropy which may result from reduced flexibility of carbohydrates.²¹

Nature has therefore means to enhance the binding affinity involving multivalency, *i.e.*, the use of multiple copies of binding epitopes to promote clustering events.²² Advantages of multivalent binding are not only for having a greater contact between the surfaces but also magnifying the overall binding affinity. The multivalent effect was originally observed by Lee and Lee and termed the “glycoside cluster effect”, wherein the relatively small di- and trivalent cluster glycosides provided almost an exponential enhancement of the binding potency to the corresponding lectin.²³

According to Bertozzi and Kiessling,²⁴ this enhanced binding could occur through several possible mechanisms (Figure 1-6), including:

- a) Chelate effect (chelation) involves the simultaneous binding of a multivalent ligand to a multivalent receptor. An increase in binding affinity can occur when the carbohydrate ligand spacing matches the inter-binding-site distances.
- b) Receptor clustering induced by the multivalent ligands enhances the binding affinity by increasing proximity of the receptors.
- c) Subsite binding describes the occupation of the carbohydrate ligand to the primary site and the secondary site of the same receptor.
- d) Statistical effects result from the increased probability of rebinding by a high local concentration of carbohydrate epitopes.
- e) Steric stabilisation can be explained by steric hindrance of a bulky ligand that blocks further ligand interaction.

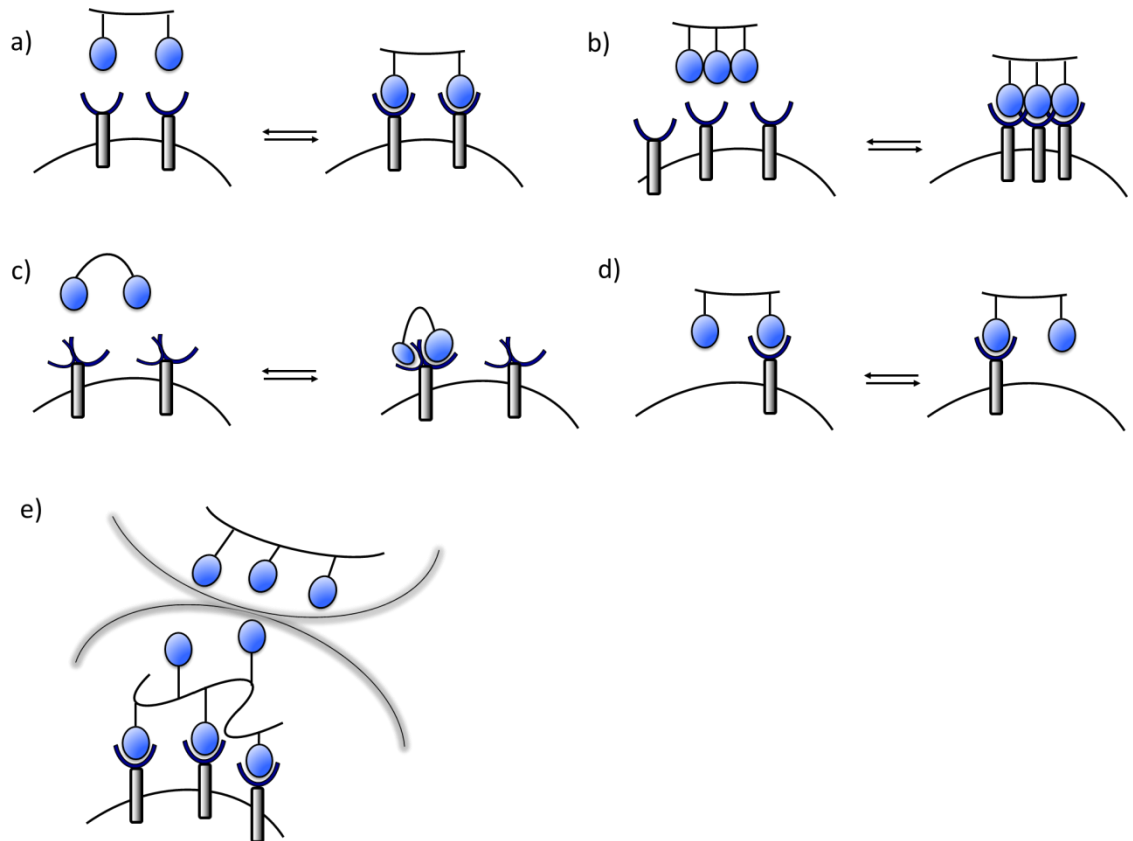


Figure 1-6. Possible modes of multivalent ligand binding for an increase in the binding affinity: a) chelate effect; b) receptor cluster; c) subsite binding; d) statistical effects; e) steric stabilisation.

Multivalency is involved in many biological processes, such as cellular adhesion, viral entry, and host-pathogen interactions. Some bacterial toxins bind and gain entry to cells by the use of multivalent interactions. A typical example is Shiga toxin, which is produced by *Shigella dysenteriae*. Infection of this toxin can cause diarrhea, hemorrhagic colitis or hemolytic uremic syndrome. Shiga toxin comprises two subunits; a toxic A subunit and a pentameric B subunit which delivers the A subunit into the host cell. The recognition of globotriaosylceramide (Gb₃) glycolipids on the host cell surface by the B subunit permits the internalisation of the A-subunit by receptor-mediated endocytosis.²⁵ Each of the individual B subunits contains three binding sites. The organization of the B subunits in a pentameric form provides a total of 15 carbohydrate binding sites, which allows multivalent interactions with the Gb₃ and thus increases the binding avidity.²⁶

Also, several lectin receptors, e.g., DC-SIGN, occur as a tetramer and form clusters on the cell surfaces to increase the probability of multivalent bindings to viral glycoproteins.^{27,28}

1.2 Glycomimetics and multivalent glycoconjugates

The involvement of carbohydrate-protein interactions, as well as their multivalency, in numerous biological and pathological processes, directed research into the rational design and synthesis of glycomimetics and multivalent glycoconjugates to understand and mediate such interactions. Many different glycomimetics (molecules that mimic the key bioactive structural motifs of carbohydrates) have been developed as probes or inhibitors, which may be beneficial for treating diseases, *e.g.*, inflammatory diseases, viral and bacterial infections. Furthermore, the attachment of glycomimetics onto multivalent scaffolds, forming multivalent glycoconjugates, could augment their affinity to target proteins. Various multivalent scaffolds have been developed to present multiple copies of carbohydrate ligands. Examples of the multivalent scaffolds include peptides, lipids, polymers, nanoparticles, cyclodextrins, calixarenes, fullerenes, dendrimers, liposomes, viruses (Figure 1-7).²⁹

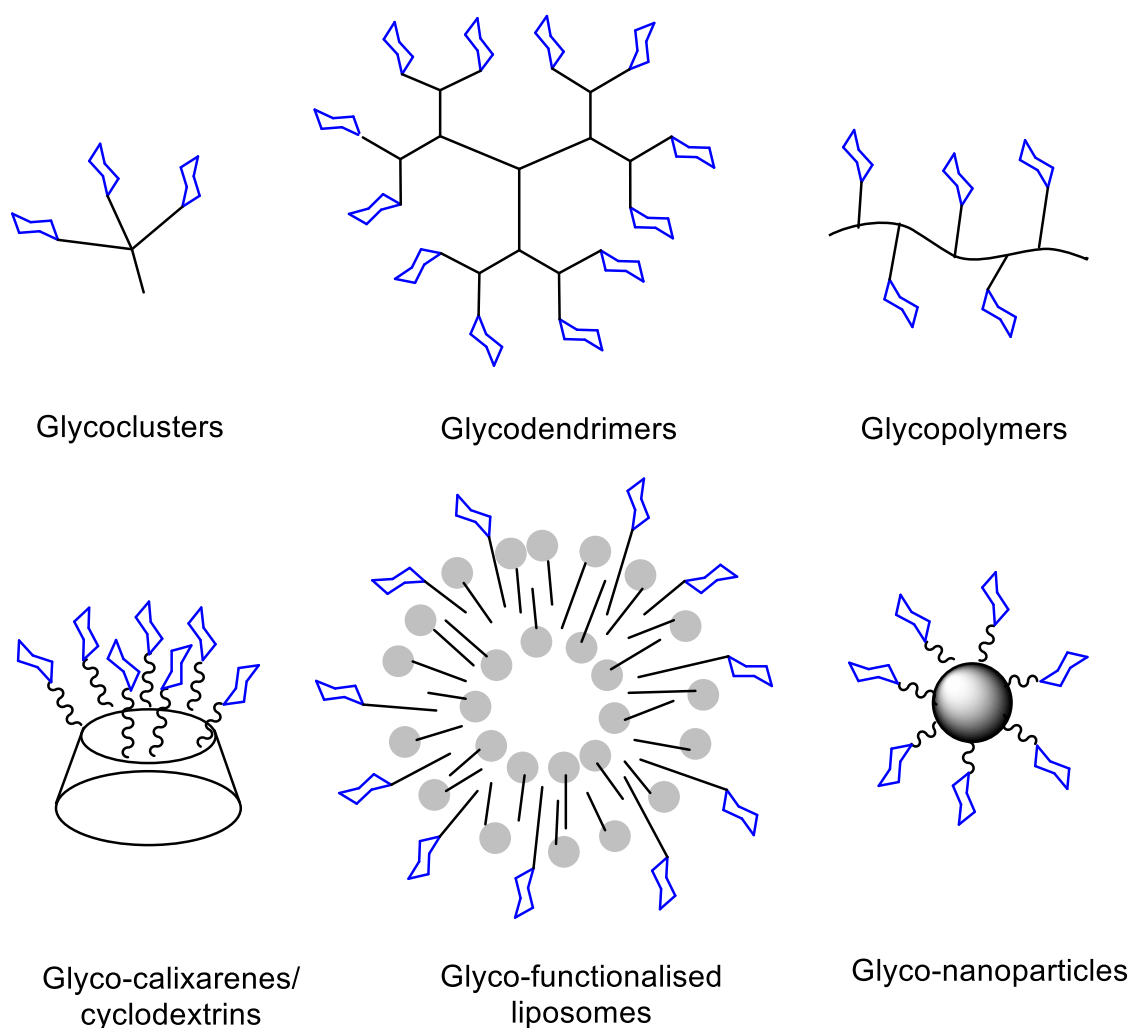


Figure 1-7. Selected multivalent carbohydrate structures using different scaffolds.

In the following, selected carbohydrate-based therapeutics for lectin targeting (e.g., selectins and DC-SIGN) will be discussed.

Selectins, a family of three adhesion molecules (*i.e.*, E-selectin, L-selectin and P-selectin), mediate the initial steps of the inflammatory response, *i.e.*, the tethering and rolling of leukocytes on endothelial cells. These adhesion molecules contribute to vaso-occlusive crisis (VOC) of sickle cell disease patients.³⁰ VOC is caused by the obstruction of capillaries by sickle-shaped erythrocytes, leukocytes and platelets leading to reduced blood flow, ischemia, and tissue damage. These adhesion processes were mediated by adhesive molecules, *i.e.*, selectins. Inhibiting these selectins would therefore be beneficial for preventing or reversing VOC. For instance, rivipansel (also called GMI-1070; compound **1**, Figure 1-8) have been shown to be a potent pan-selectin antagonist and could reverse vaso-occlusion in mice.³¹ This compound is currently in Phase III clinical trial for sickle cell disease. This antagonist was rationally designed to mimic the biologically active conformation of the sialyl-Lewis^x (sLe^x, compound **2**) carbohydrate core in the binding domain of E-selectin. NMR methods had shown close contacts of the asterisked atoms (Figure 1-8) with the protein.^{32,33} Another important feature incorporated in the structure was an extended sulfated domain, which was required for binding to L- and P-selectins.³¹

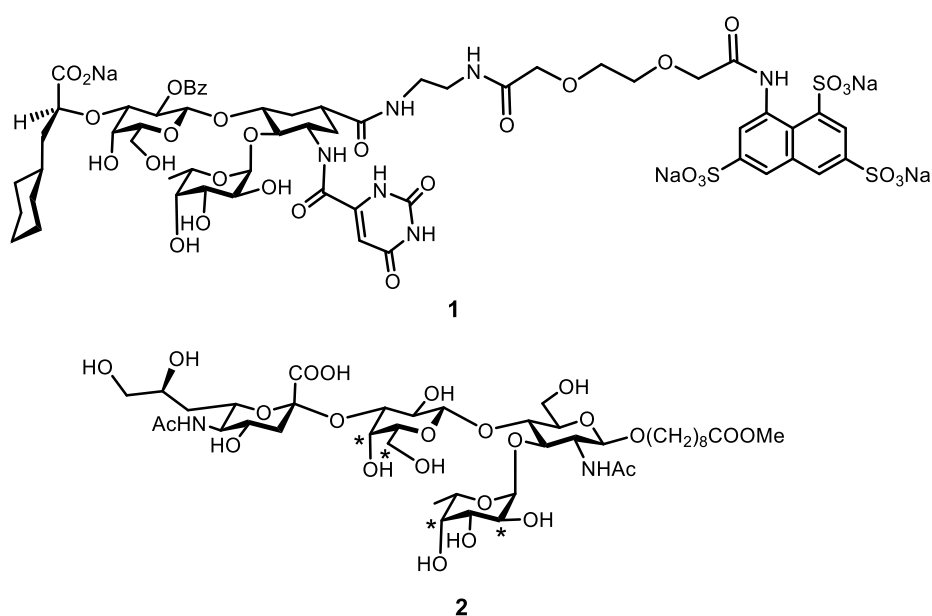


Figure 1-8. Chemical structures of the silyl Lewis^x (sLe^x) mimic GMI-1070 (**1**) and the physiological ligand sLe^x (**2**).

Several glycomimetics and multivalent ligands have been developed to target DC-SIGN, which is a C-type lectin involved in the recognition of viruses, such as human immunodeficiency virus type 1 (HIV-1) and Ebola virus.³⁴ An approach to design high affinity ligands for DC-SIGN is to mimic the two or three determinant mannose residues of the oligomannoside $(\text{Man})_9(\text{GlcNAc})_2$ natural ligand (**3**, Figure 1-9).³⁵ A linear trimannose analogue (**4**) exhibited anti-HIV activity in a cell-based assay.³⁶ The presentation of this linear trimannoside mimic in a tetravalent glycoclusters (**5**) also enhanced the binding properties and provided more efficient inhibition of HIV transinfection of T-cells both in cellular and human cervical explant models.^{36,37} The same trimannoside glycomimetic was conjugated to Boltorn™ dendrimer to form a glycodendrimer (**6**) containing multiple copies of the synthetic epitopes. The *pseudo*-mannosylated glycodendrimers effectively inhibited DC-SIGN-mediated Ebola or HIV viral infections.^{38,39}

Furthermore, as $\text{Man}\alpha\text{-1,2-Man}$ disaccharide was the minimal carbohydrate epitope for DC-SIGN recognition, the $\text{Man}\alpha\text{-1,2-Man}$ mimic (**7**, Figure 1-10) containing a cyclohexane-based aglycone showed anti-Ebola viral activity *in vitro*.⁴⁰ Further DC-SIGN inhibitors development by Varga *et al.* led to the bis-benzylamide (**8**), which binds DC-SIGN with an improved selectivity.⁴¹ They also demonstrated that a hexavalent bis-benzamide *pseudo*-disaccharide dendrimer (**9**) could inhibit HIV transinfection of T-cells, as well as DC-SIGN mediated uptake of Dengue virus.⁴² Recently, Ordanini *et al.* showed that trimers of the same bis-benzamide *pseudo*-disaccharide linked by a rod-like spacer (**10**) even more potentially block HIV transinfection, possibly because of chelate effect and statistical rebinding.⁴³

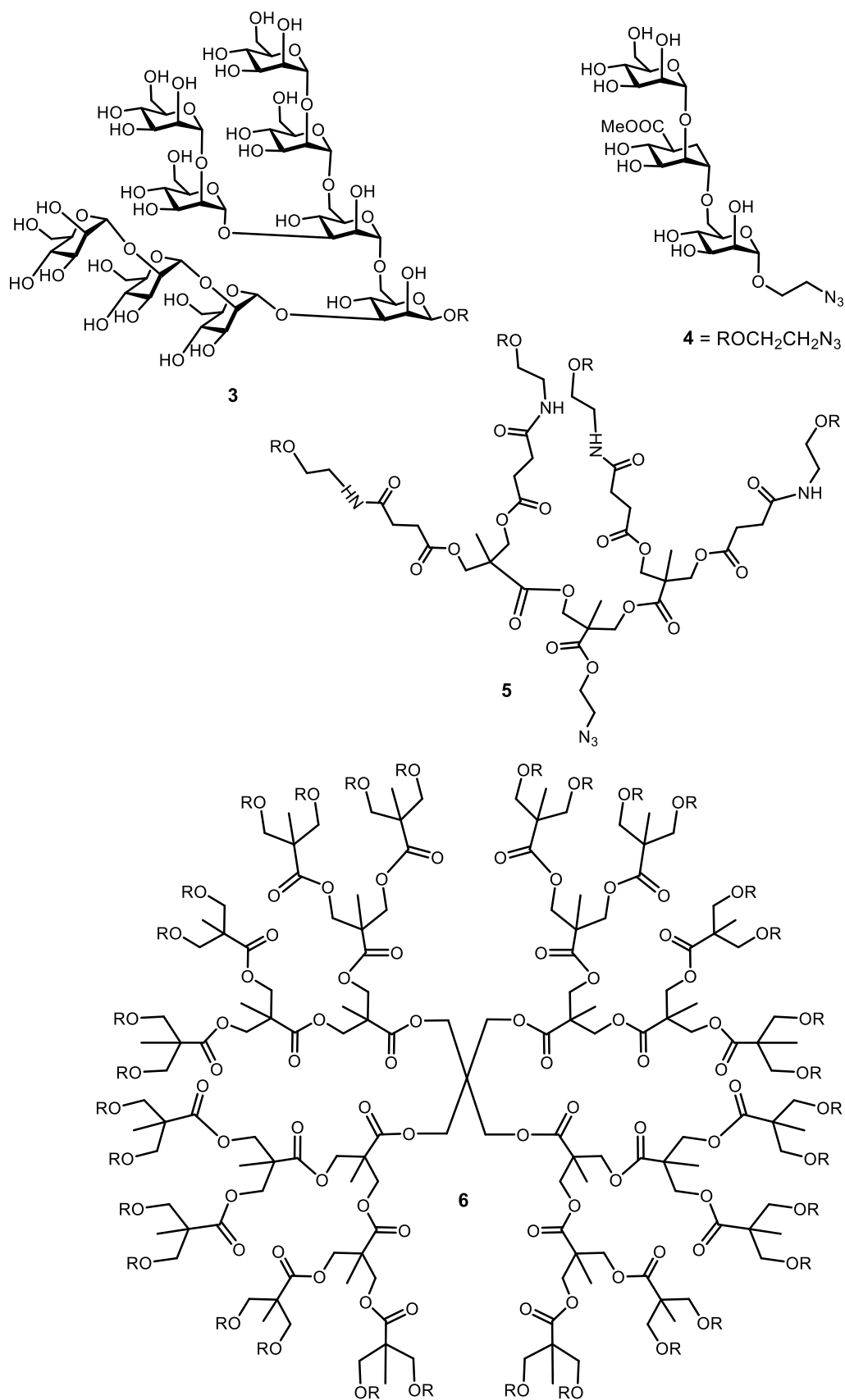


Figure 1-9. Structure of: Man_9 (**3**); DC-SIGN inhibitors: a trimannoside analogue **4**; a glyocluster **5** and a glycodendrimer **6**.

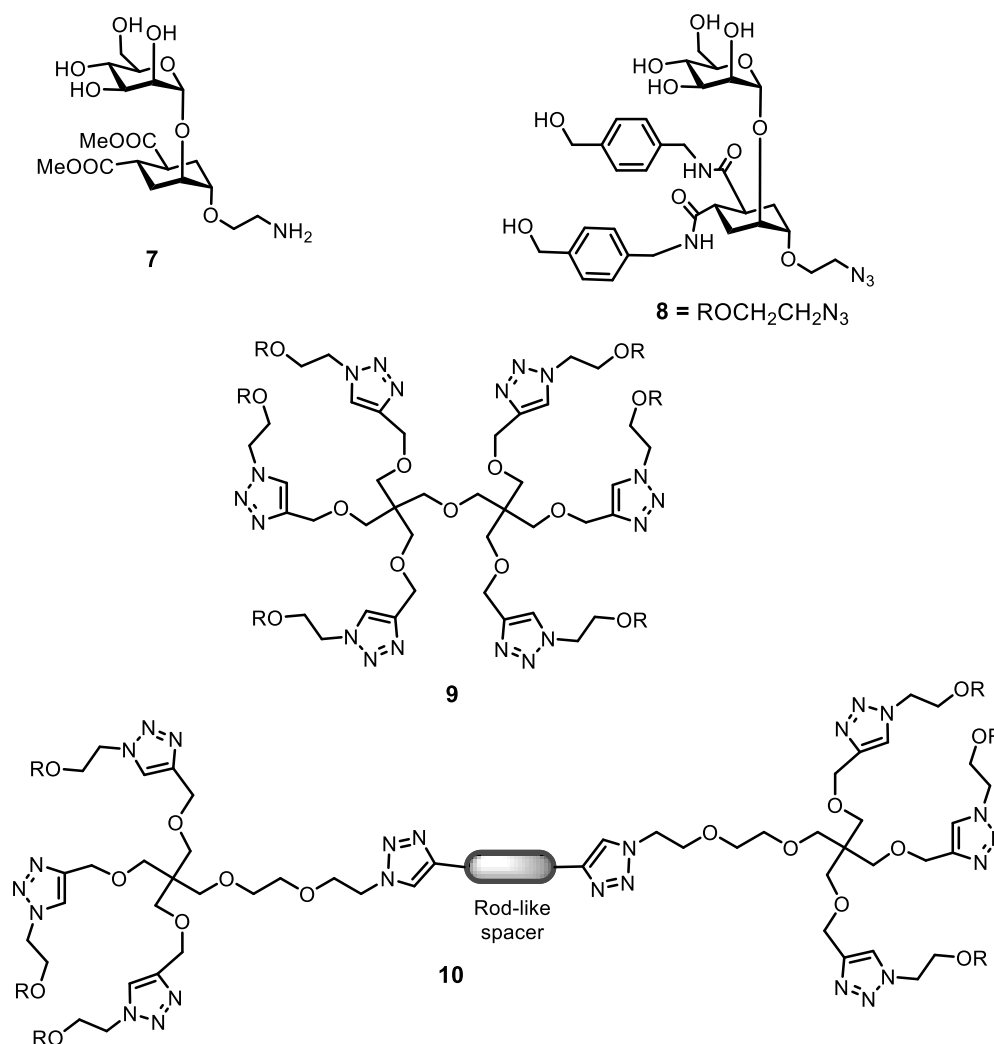


Figure 1-10. DC-SIGN inhibitors: a disaccharide analogue **7** with a cyclohexane-based aglycone; a disaccharide analogue **8** with a bis-benzylamide; a *pseudo*-disaccharide dendrimer **9**; a *pseudo*-disaccharide linked by a rod-like spacer **10**.

1.3 Cell surface receptors: lectins

Cell surface receptors are responsible for binding of extracellular ligands and induction of signal transduction pathways. Among various types of cell surface receptors, lectins are of particular interest because of the ability to bind to specific carbohydrates, their important roles in cell-to-cell communication and their involvement in diseases. Lectins are classified according to the domain architecture and folding patterns of their carbohydrate recognition domains (CRDs) into different types, e.g., C-type, I-type, P-type. Examples of type of lectins, ligands and folding patterns are present in Table 1-1.⁴⁴

Table 1-1.⁴⁴ Examples of different types of lectins and their ligands.

Type of fold	Example of lectin	Example of ligand
C-Type (Unique mixed α/β structure)	Asialoglycoprotein receptor, selectins, DC-SIGN, DC-SIGNR	Fuc, Gal, GalNAc, Man, heparin tetrasaccharide
I-type (Immunoglobulin super family)	N-CAM, TIM-3, siglecs	Man ₆ GlcNAc ₂ , NHK-1 epitope, α 2,3/6-sialylated glycans
P-type (Unique β -rich structure)	Mannose-6-phosphate receptors	Man-6-phosphate, Man _{5,8} GlcNAc ₂
β -sandwich (jelly-roll)	L-type (ERGIC-53, VIP36)	Man _x GlcNAc ₂
	Galectins	β -galactosides
	Calnexin, calreticulin	Glc ₁ Man ₉ GlcNAc ₂

However, some types of lectins, *e.g.*, L-type lectins, C-type lectins, calnexin, and calreticulin, share a similar Ca²⁺ dependent binding property. In other words, not only C-type lectins require Ca²⁺ for ligand binding. In this section, C-type lectins and C-type lectin like receptors will be briefly outlined.

C-types lectins have the ability to recognise carbohydrate epitopes in a Ca²⁺ dependent manner through their carbohydrate recognition domains (CRDs). These lectins have a C-type lectin fold (Figure 1-11) which is characterised by two-stranded antiparallel β -sheets formed by a conserved series of amino acids connected by two α -helices and a three-stranded antiparallel β -sheet.⁴⁵ The CRD has two highly conserved amino acids for disulfide bonds and up to four sites for calcium binding. Examples of these C-type lectins include asialoglycoprotein receptor, selectins, rat serum mannose-binding protein (MBP-A), DC-SIGN and DC-SIGN related receptor (DC-SIGNR).

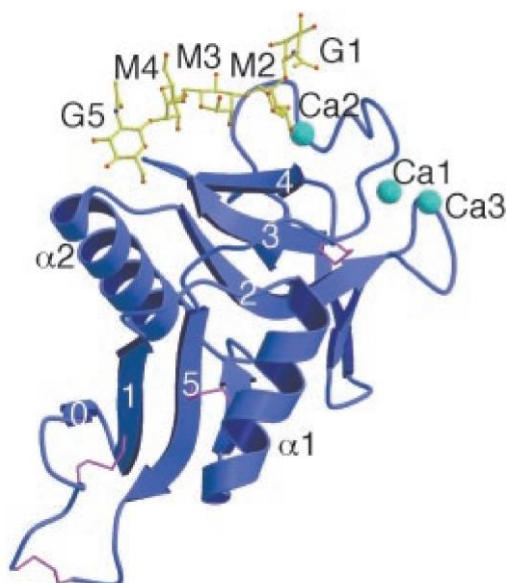


Figure 1-11.⁴⁵ Carbohydrate binding domain of DC-SIGN having a prototype C-type lectin fold, figure reproduced from reference 45.

Several proteins (e.g., natural killer (NK) cell receptors) have a C-type lectin fold but are not known to bind carbohydrates due to the lack of some or all amino acids responsible for Ca^{2+} and/or glycan interactions. They contain a C-type lectin-like domain (CTLD) which is homologous to the C-type lectin CRDs of C-type lectins by sharing the same fold.⁴⁶

In this thesis, two main families of receptor will be explored: one is lectin-like oxidized low density lipoprotein receptor 1 (LOX-1) which is implicated in atherosclerosis and the other is DC-SIGN which is involved in recognition of viruses via the immune system. LOX-1 functions with a CTLD as a scavenger receptor, while DC-SIGN is a C-type lectin that acts as a pattern recognition receptor (PRR).

1.4 LOX-1 and its implication in atherosclerosis

1.4.1 Atherosclerosis

Atherosclerosis is a chronic inflammatory disease, characterised by the accumulation of cholesterol-rich lipids within blood vessel walls. Various risk factors can provoke atherosclerosis including inflammation, smoking, dyslipidemia, hypertension, diabetes mellitus, and genetic factors.⁴⁷ It has been hypothesised that early atherosclerotic lesions are caused by endothelial dysfunction which often results from oxidized low density lipoprotein (OxLDL).⁴⁸

1.4.2 Prevention and treatment of atherosclerosis

Life style improvements, such as smoking cessation, exercise, and low fat diet consumption, are important for the primary prevention of atherosclerosis. Low dose of aspirin has also been used in the secondary prevention of atherosclerosis in patients with type 2 diabetes mellitus.⁴⁹ Aspirin can prevent blood clots and platelet aggregation by inhibiting cyclooxygenase (COX), which in turn blocks the formation of thromboxane A₂, reducing platelet aggregation. Statins are one drug choice that can be used to reduce cholesterol levels and retard the progression of atherosclerotic plaques by inhibiting 3-hydroxy-3-methylglutaryl coenzyme A (HMG-CoA) reductase. Statins inhibit the rate limiting step in cholesterol synthesis, lowering cholesterol in LDL particles.⁵⁰ However, patients treated with statins still retained significant residual risk of cardiovascular disease and even receiving high dose medication, more than 20% of patients have the recurrent disease.⁵¹ Furthermore, atherosclerosis can be treated by surgical techniques such as balloon dilation, angioplasty with stenting, and bypass operation. Nonetheless, more effective prevention and treatment of atherosclerosis are still required. Exploring new biological targets either for reducing LDL or inhibiting the binding of OxLDL to receptors, *i.e.*, LOX-1, would be one of the best strategies to fight against this multifactor cardiovascular disease.

1.4.3 Roles of LOX-1 in atherosclerosis

LOX-1 plays a critical role in the initiation and development of atherosclerosis, notably in endothelial dysfunction.⁵² Under normal conditions, the expression of LOX-1 is low. However, the upregulation of LOX-1 is induced by several processes, both *in vivo* and *in vitro*, which are related to atherosclerosis including hypertension, diabetes mellitus and dyslipidemia.⁵³ Several studies showed the augmented expression of LOX-1 around the atherosclerotic lesion in hypercholesterolemic rabbits⁵⁴ and in human carotid arteries.⁵⁵ Hayashida *et al.* reported that soluble LOX-1 (sLOX-1) in serum is increased in acute coronary syndrome.⁵⁶ Moreover, it was found that the deletion of the LOX-1 gene can reduce the formation of atherosclerotic plaques in LDL-receptor deficient mice.⁵⁷ These findings showed the link between LOX-1 and atherosclerosis progression. Thus, LOX-1 would be one of the attractive targets for cardiovascular disease therapy.

LOX-1 is classified as a scavenger receptor which is a group of proteins that identify and remove unwanted entities (*e.g.*, apoptotic cells, Ox-LDLs). The roles of LOX-1 include binding, internalisation, formation of foam cells, and degradation of OxLDL.⁵⁸ LDL particles enter the intima layer of the artery wall and undergo oxidation to form

OxLDL (Figure 1-12). The binding of OxLDL to LOX-1 promotes the expression of adhesion molecules and leads to endothelial cell dysfunction and the recruitment of monocytes into the arterial blood cell wall. Monocytes are differentiated to macrophages and take up OxLDL via LOX-1, leading to the formation of foam cells and plaques, which are vulnerable to rupture and can lead to thrombosis and myocardial infarction.^{59,60} The recognition of OxLDL by LOX-1 also mediates pro-atherogenic cellular responses many of which can induce endothelial dysfunction including a reduction of nitric oxide (NO) release, increased production of reactive oxygen species (ROS), secretion of monocyte chemoattractant protein-1 (MCP-1), expression of matrix metalloproteinases-1 and -3, adhesion molecules and apoptosis.⁶¹

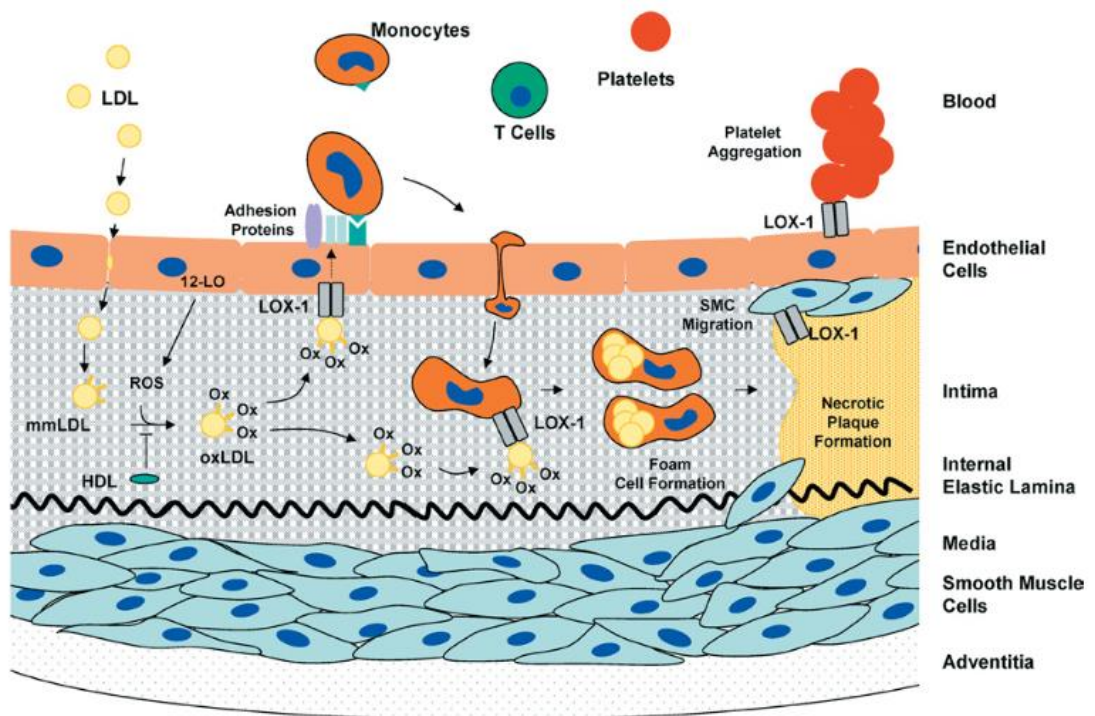


Figure 1-12.⁵⁹ The roles of LOX-1 in atherosclerosis. Low density lipoprotein (LDL) particles diffuse into the arterial intima, followed by the conversion of LDL to oxidized LDL. The recognition of OxLDL by LOX-1 induces several effects including lipid uptake and formation of foam cells and atherosclerotic plaques, figure reproduced from reference 59.

High levels of soluble forms of membrane proteins secreting into the blood stream can reflect abnormally expressed proteins in the presence of some disease states. LOX-1 also exists in a soluble form (sLOX-1) and may be used as a prognostic biomarker for acute coronary syndrome.^{56,62}

1.4.4 Identification and structure of LOX-1

LOX-1 was originally identified in 1997 by Sawamura *et al.* as a receptor for OxLDL in endothelial cells.⁵² Subsequently, this protein was also detected in macrophages,⁶³ platelets,⁶⁴ smooth muscle cells, monocytes, and cardiac fibroblasts.⁶⁵ LOX-1 is a type II membrane glycoprotein, which belongs to the C-type lectin-like protein superfamily. This receptor does not share structural homology with any others scavenger receptors but it is likely to resemble natural killer (NK) cell receptors, *e.g.*, CD94 (KLRD1) and NKR-P1 (KLRB1) because they possess a C-type lectin-like domain (CTLD).⁵² LOX-1 comprises 4 domains (Figure 1-13): a short cytoplasmic N-terminal domain, a single transmembrane domain (TMD), an extracellular connecting neck domain, and a C-terminal C-type lectin like domain.⁵⁹ Chen and colleagues have demonstrated that the CTLD is essential and conserved for ligand binding of LOX-1.^{66,67}

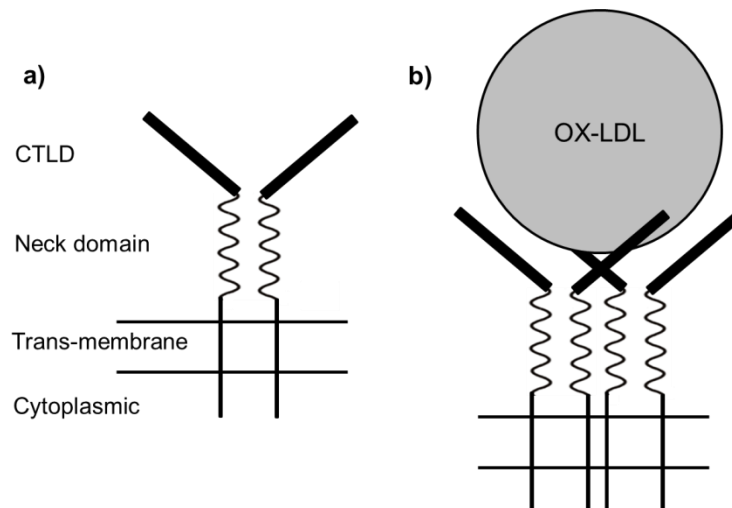


Figure 1-13. a) Schematic representation of human LOX-1 in a dimeric form. Each individual protein contains 4 different domains: a short cytoplasmic N-terminal domain, a single transmembrane domain, a neck domain, and a C-terminal C-type lectin-like domain (CTLD); b) LOX-1 in dimeric form upon the binding to ligands, *e.g.*, Ox-LDL.

The X-ray crystal structure of LOX-1 has revealed to be a heart-shaped homodimer connected by a disulfide linkage (Figure 1-14).^{68,69}

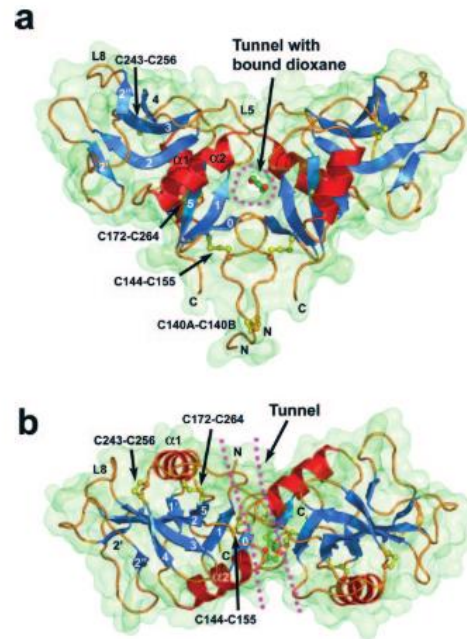


Figure 1-14.⁶⁸ X-ray crystal structure of human LOX-1 ligand CTLD binding domain in: a) side view and b) top view. The central hydrophobic tunnel is outlined by dotted lines, figure reproduced from reference 68.

On the top of the CTLD dimer of LOX-1, there is a linear arrangement of positively charged residues, spanning over the dimer surface, called basic spine which is responsible for the ligand binding.^{68,69} Studies also showed that the central hydrophobic tunnel extending through the entire LOX-1 molecule is essential for Ox-LDL recognition and binding.⁷⁰ However, the components of Ox-LDL that are recognised by LOX-1 are still unknown.

1.4.5 LOX-1 ligands

Similar to other scavenger receptors, LOX-1 does not bind only to OxLDL, but also to various other ligands. A previous study reported that LOX-1 recognises other forms of modified lipoproteins such as hypochlorite-modified high density lipoprotein (HDL) in human umbilical venous endothelial cells (HUVECs).⁷¹ HDL can be modified by hypochlorous acid (HOCl) and hypochlorite (OCl⁻), which are oxidants produced by the myeloperoxidase-H₂O₂-chloride system of activated phagocytes, forming an atherogenic lipoprotein particle.

Jono and co-workers have shown that advanced glycation end-products (AGEs), formed by the non-enzymatic reaction of sugars with free amino groups on proteins, exhibit binding activity to LOX-1 and serves as a ligand for LOX-1.⁷²

Cellular ligands, e.g., aged/apoptotic cells, activated platelets, and bacteria can also be recognised by LOX-1. There is evidence that LOX-1 could bind to aged red blood cells and apoptotic cells in bovine aortic endothelial cells (BAE) and Chinese hamster ovary (CHO) cells expressing bovine LOX-1. Due to the fact that these interactions can be inhibited by phosphatidylserine (PS) liposomes, it was proposed that PS was the ligand recognised by LOX-1 on surface of the apoptotic cell.^{73,74}

In addition, activated platelets can also bind to LOX-1.⁶⁴ The binding activities of aged/apoptotic cells and activated platelets support the role of LOX-1 in the process of phagocytosis and the induction of endothelial dysfunction. It has been reported that LOX-1 can serve as a receptor for Gram-positive and Gram-negative bacteria including *Staphylococcus aureus* and *E. coli* in both cultured vascular endothelial cells and Chinese hamster ovary-K1 (CHO-K1) cells stably expressing LOX-1.⁷⁵

C-reactive protein (CRP), an acute phase protein expressed by hepatocytes in response to inflammation and tissue damage, has been shown to be recognised by LOX-1 in cells expressing LOX-1.⁷⁶ Another study also showed that LOX-1 binds to CPR and the ligand-receptor interaction promotes endothelial inflammation.⁷⁷

Heat shock proteins (HSPs) were originally discovered as molecular chaperones that interfere in inflammation and protect proteins from environmental stress. Recently, evidence has indicated that HSPs are ligands for LOX-1. The receptor could bind and internalise HSP60 and HSP70 in dendritic cells.^{78,79}

Moriwaki and colleagues have suggested that LOX-1 recognises the protein moiety of OxLDL and the lipid part of the ligand is unlikely to be important for the binding activity.⁸⁰ However which part of the major ligand OxLDL binds to LOX-1 remains obscure as no conclusion can be drawn from the published crystal structure.

To identify whether the carbohydrate or protein moieties of OxLDL is more important for being recognised by LOX-1, Dr. K. Lacey and Dr. S. Ponnambalam (School of Molecular and Cellular Biology, University of Leeds), our collaborators, digested OxLDL particles with either protein kinase K or N-glycosidase F (also known as PNGase F) and endoglycosidase H (Endo H).⁸¹ Their results revealed that only removal of the carbohydrate part showed significant reduction in binding to LOX-1 expressing cells (Figure 1-15). This observation thus raised a question: does a carbohydrate compound bind to LOX-1 and inhibit the Ox-LDL/LOX-1 interaction? As a consequence, a glycan array screening was performed and will be discussed in Section 1.4.7.

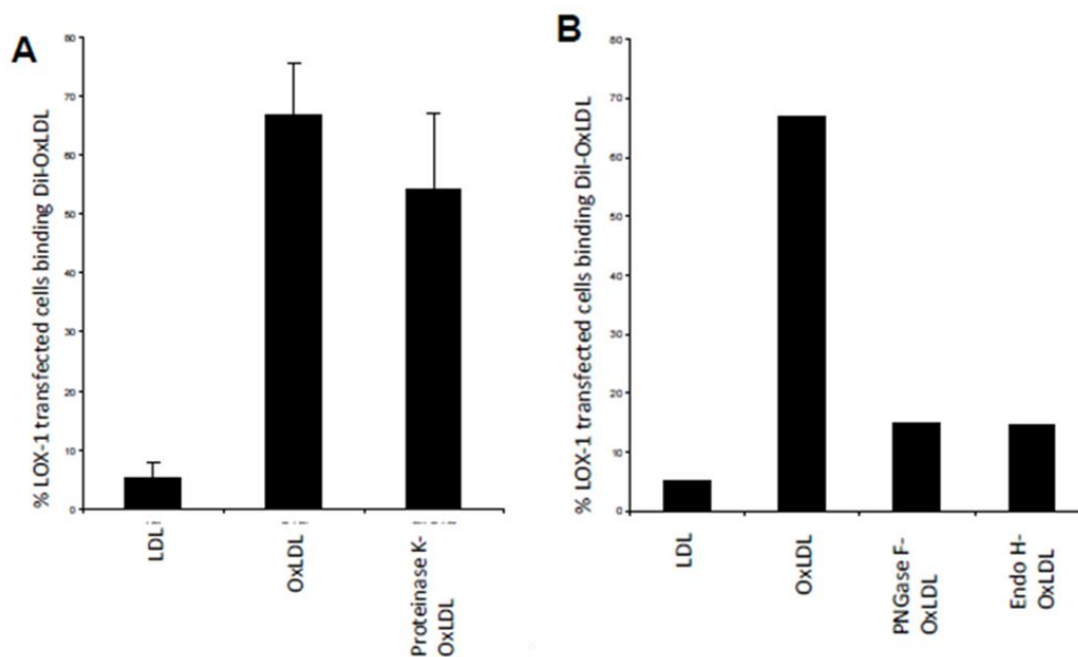


Figure 1-15.⁸¹ The percentage of LOX-1 transfected cells binding to labelled OxLDL which depends on interaction with protein moieties (A) or sugar moieties (B), figure reproduced from K. Lacey's Ph.D. thesis University of Leeds 2012, reference 81. LDL, Low-density lipoprotein; OxLDL, Oxidized low-density lipoprotein; PNGase F, N-glycosidase F; Endo H, endoglycosidase H.

1.4.6 LOX-1 inhibitors

In general, there are two ways to inhibit the activity and function of LOX-1 that are 1) blocking LOX-1 from binding to OxLDL and 2) suppressing LOX-1 expression. Sawamura and co-workers identified procyanidins, polyphenolic compounds abundantly found in apples and red wine, as potent inhibitors for LOX-1.⁸² A total of 472 food extract samples were tested to identify materials that had inhibitory effect for LOX-1 using an enzyme-linked immunosorbent assay (ELISA) and 1,1'-dioctadecyl-3,3,3',3'-tetramethylindocarbocyanine perchlorate (DiI)-labeled OxLDL uptake assay. Their results indicated that procyanidins are potent inhibitors of LOX-1. Purified procyanidins in form of a dimer, a trimer, and a tetramer could also inhibit OxLDL uptake (Figure 1-16), whereas monomeric epicatechin (**11**, Figure 1-17) did not show an inhibitory effect. The chemical structures of the trimer procyanidin isomers (**12** and **13**) used in their study are present in Figure 1-17. Moreover, the chronic administration of oligomeric procyanidins in stroke-prone spontaneously hypertensive rats (SHR-SP) showed suppression of lipid accumulation in arteries.

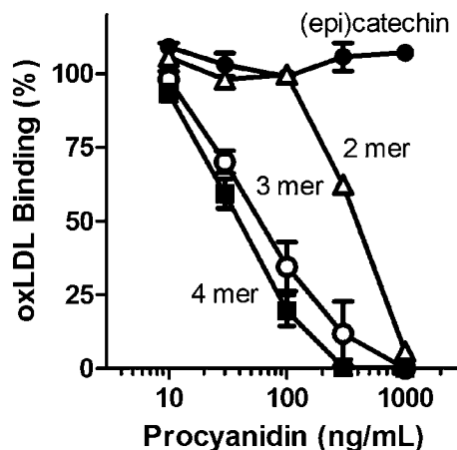


Figure 1-16.⁸² The result of different isomers of procyanidins in inhibiting OxLDL binding to LOX-1 expressing cells, figure reproduced from reference 82.

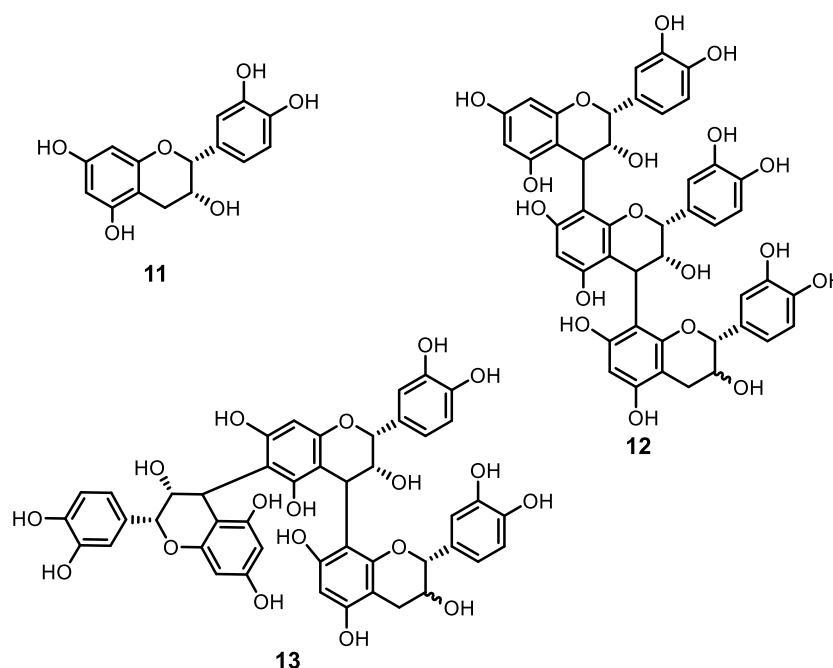


Figure 1-17. Chemical structures of epicatechin **11** and the trimer procyanidin isomers used for the binding assay (**12** and **13**).

There is also evidence showing that polyinosinic acid (*i.e.*, a homopolymer of inosine which is a nucleotide that is composed of hypoxanthine and ribose) and carrageenans (*i.e.*, a class of sulfated polysaccharides), significantly reduced OxLDL binding to LOX-1 by 62% and 60%, respectively in Chinese hamster ovary K1 (CHO-K1) cells stably expressing LOX-1.⁸⁰ These findings demonstrate that polyinosinic acid and carrageenan are chemical inhibitors of LOX-1.

On the other hand, some polyphenolic antioxidants and drugs have shown to exert inhibitory effects on LOX-1 expression. Lee and co-workers have reported that ellagic acid (**14**, Figure 1-18), present in numerous fruits and vegetables, inhibits OxLDL-mediated LOX-1 expression, ROS production, and inflammation in human endothelial cells.⁸³ Likewise, epigallocatechin-3-gallate (EGCG, **15**), the most abundant antioxidant found in green tea, has been shown to inhibit OxLDL-induced LOX-1-mediated signaling pathway. This antioxidant compound is involved in the anti-atherosclerotic processes by inhibiting NADPH oxidase and consequent ROS-enhanced LOX-1 expression (Figure 1-12).⁸⁴ Moreover, mulberry (*Morus Alba* L., family Moraceae) leaf aqueous fractions have proved to reduce oxidative modification of LDL by inhibiting TNF- α -induced-NF- κ B activation and LOX-1 expression in vascular endothelial cells.⁸⁵

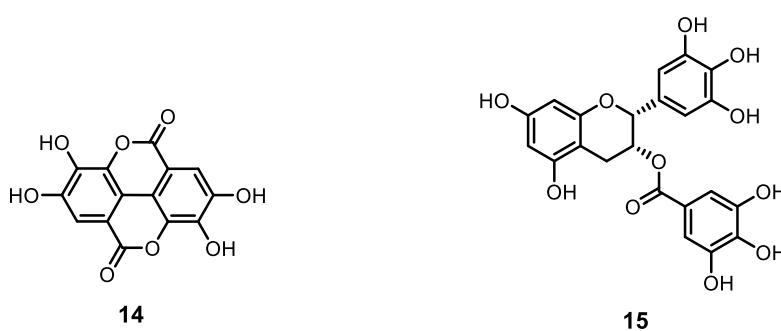


Figure 1-18. Chemical structures of: ellagic acid (**14**) and EGCG (**15**).

Furthermore, several drugs with antioxidant effects, e.g., simvastatin (**16**, Figure 1-19) atorvastatin (**17**), aspirin (**18**), gliclazide (**19**) have been shown to inhibit OxLDL-mediated LOX-1 expression in endothelial cells. It is known that OxLDL upregulates the expression of LOX-1 and endothelial nitric oxide synthase (eNOS) in human coronary artery endothelial cells (HCAECs).^{86,87} Pre-treatment of such cells with simvastatin or atorvastatin showed the reduction on OxLDL-induced up-regulation of LOX-1 and down-regulation of eNOS. These results suggest that besides acting as HMG-CoA inhibitors, statins have an additional advantage on LOX-1 activity.⁸⁸ Moreover, the inhibitory effect of aspirin, an anti-platelet drug, on LOX-1 expression has been studied in HCAECs. The results indicate that aspirin suppressed OxLDL-mediated LOX-1 expression.⁸⁹ Another example of a drug with antioxidant effect against LOX-1 is an oral anti-diabetic drug, gliclazide.⁹⁰ The incubation of human aortic endothelial cells (HAECs) with OxLDL showed an increase in LOX-1 expression, and induced apoptosis. The treatment of gliclazide thus abolished these effects.

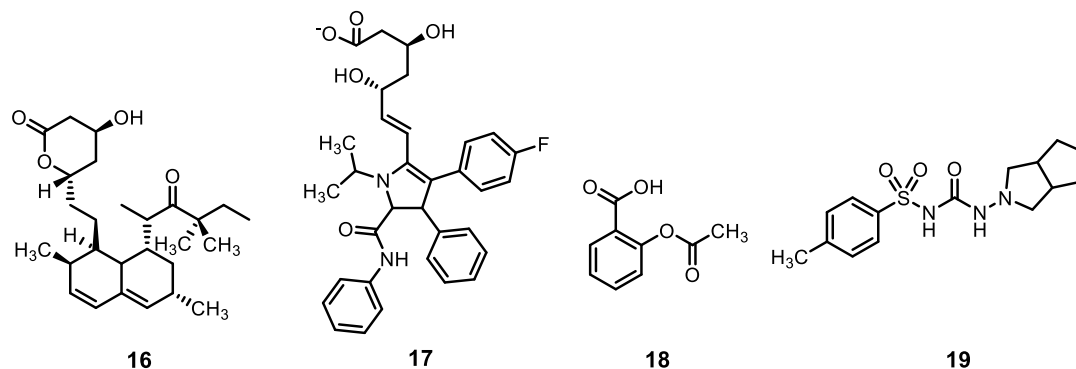


Figure 1-19. Chemical structures of: simvastatin (**16**), atorvastatin (**17**), aspirin (**18**), and gliclazide (**19**).

Biocca and colleagues reported that lovastatin disrupted LOX-1 receptor cluster distribution in plasma membranes, disturbing LOX-1 function.⁹¹ They further demonstrated that statins could inhibit LOX-1 from binding to Ox-LDL by direct interaction with the CTLD of LOX-1 in a cell-based assay.⁹²

A synthetic phospholipid-based compound called PLAzPC (**20**, Figure 1-20) developed by Falconi *et al.* was shown to fill the hydrophobic tunnel in the LOX-1 CTLD dimer surface and is also stabilised by electrostatic interactions with water and other residues.⁹³ Cell-based assays showed that this modified phospholipid could inhibit Ox-LDL from binding to LOX-1 in COS fibroblasts transiently transfected with full length human LOX-1. Their finding could lead to the development of selective inhibitors for LOX-1.

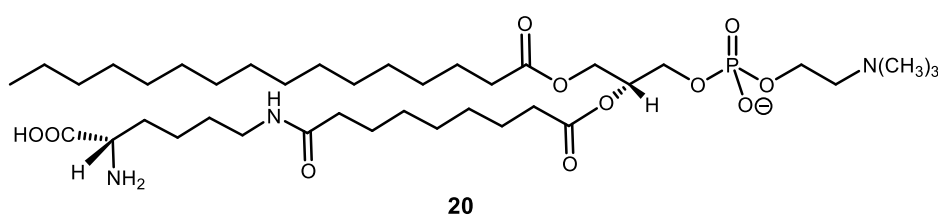


Figure 1-20. Chemical structure of a potential inhibitor of LOX-1 called PLAzPC.

More recently, Thakkar *et al.* has identified two small molecules (**21** and **22**, Figure 1-21) as inhibitors of LOX-1. Using cell-based assays, these compounds significantly decreased the uptake of ox-LDL by human endothelial cells (HUVECs). It should be noted that compound **22** was also confirmed the efficacy in HUVECs as well as in CHO cells expressing LOX-1. Moreover, both small molecules reduced the LOX-1 transcription and the downstream effects like MAPKs activation as well as the

expression of adhesion molecules on endothelial cells and subsequent monocyte adhesion.⁹⁴

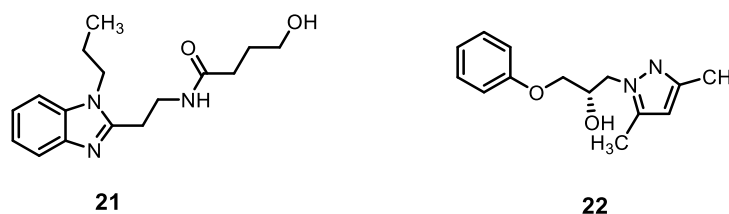


Figure 1-21. Chemical structures of potential small molecule inhibitors of LOX-1.

1.4.7 Previous studies on LOX-1 ligand bindings

This section briefly describes the studies on LOX-1 ligand bindings which were previously performed by Dr. K. Lacey (Dr. S. Ponnambalam, School of Molecular and Cellular Biology, University of Leeds).⁸¹

As previously mentioned, Dr. K. Lacey demonstrated that the carbohydrate portion of Ox-LDL was important for LOX-1 binding than the protein composition. Further, soluble recombinant LOX-1 (sLOX-1) was used to screen against a carbohydrate array of more than 300 natural occurring and synthetic sugars in the presence of calcium ions.* Bound sLOX-1 was detected by fluorescent-labelled anti-HexaHis monoclonal antibody. The glycan array revealed two sugars molecules, GalNAc α 1-3Gal β (**23**) and Gal α 1-3(Gal α 1-4)Gal β 1-4GlcNAc β (**24**), that were capable of binding to LOX-1 (Figure 1-22). These findings supported the hypothesis that carbohydrate molecules are involved in the interaction between OxLDL and LOX-1.

* Recombinant LOX-1 was produced by Dr. R.Vohra, University of Leeds, U.K. and the glycan array data were obtained by Dr. R.Vohra working with the Consortium for Functional Glycomics, Atlanta, USA.

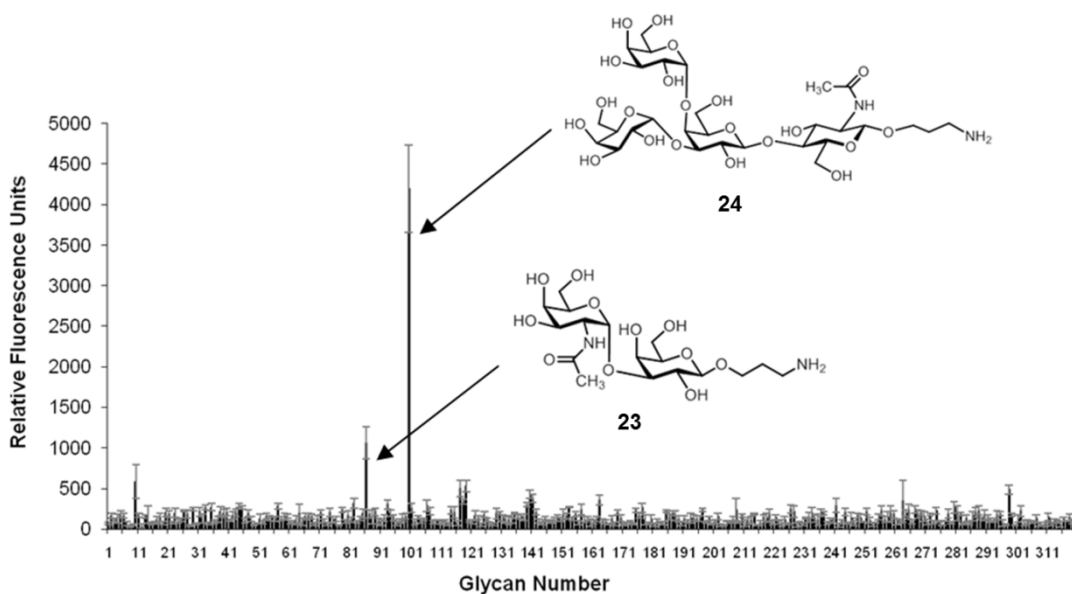


Figure 1-22.⁸¹ Glycan array data of extracellular LOX-1 showing the two carbohydrate structures that could bind to LOX-1, K. Lacey's Ph.D. thesis University of Leeds 2012, reference 81.

A hypothesis was then formulated that a specific carbohydrate structure would inhibit the binding of OxLDL to LOX-1, leading to a reduced accumulation of lipids in cells expressing LOX-1. To test this hypothesis, three different synthetic oligosaccharides **23-25** (Figure 1-23) were synthesised[†] and tested for their ability to inhibit OxLDL binding to LOX-1 expressed on immortalised epithelial (HeLa) cells. The biological testings of the carbohydrates were performed by Dr. K. Lacey (Figure 1-24). The DiI-labelled-OxLDL uptake assay showed that disaccharide **23** was unable to block the OxLDL-LOX-1 interaction but tetrasaccharide **24** almost completely blocked the OxLDL binding at 10 mM. Surprisingly, a more simple carbohydrate structure **25**, which is an intermediate for the synthesis of tetrasaccharide **24** showed an improved inhibitory effect.

[†] Carbohydrate compounds were synthesised by Dr. P. Mandal, a former postdoc in the Turnbull research group.

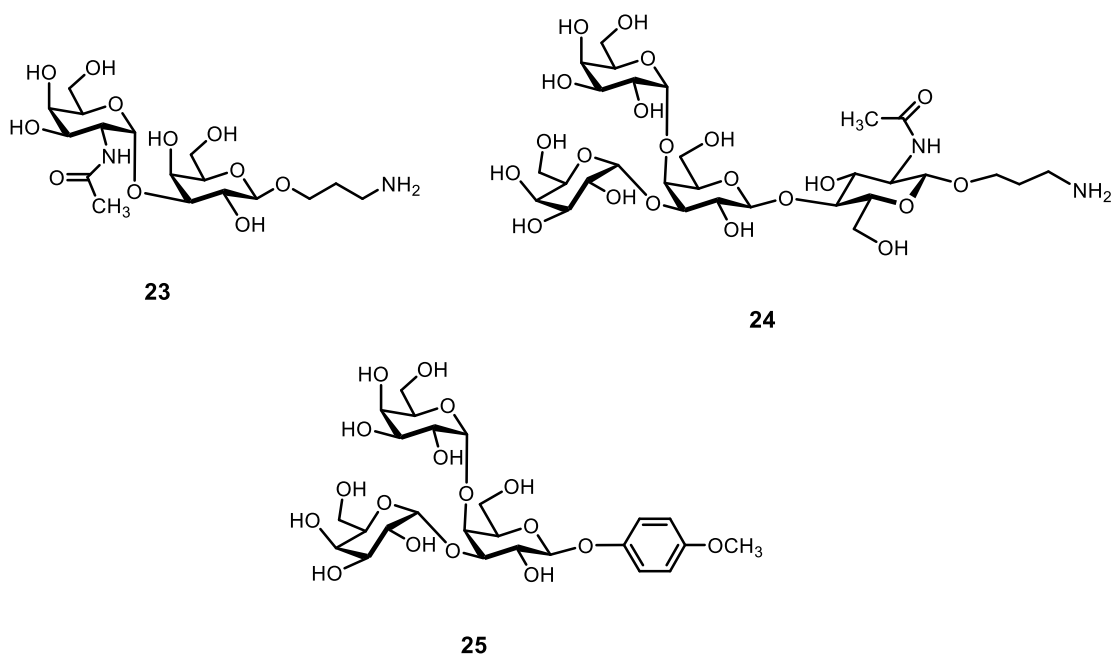


Figure 1-23. Chemical structures of three oligosaccharides used for the binding assays.

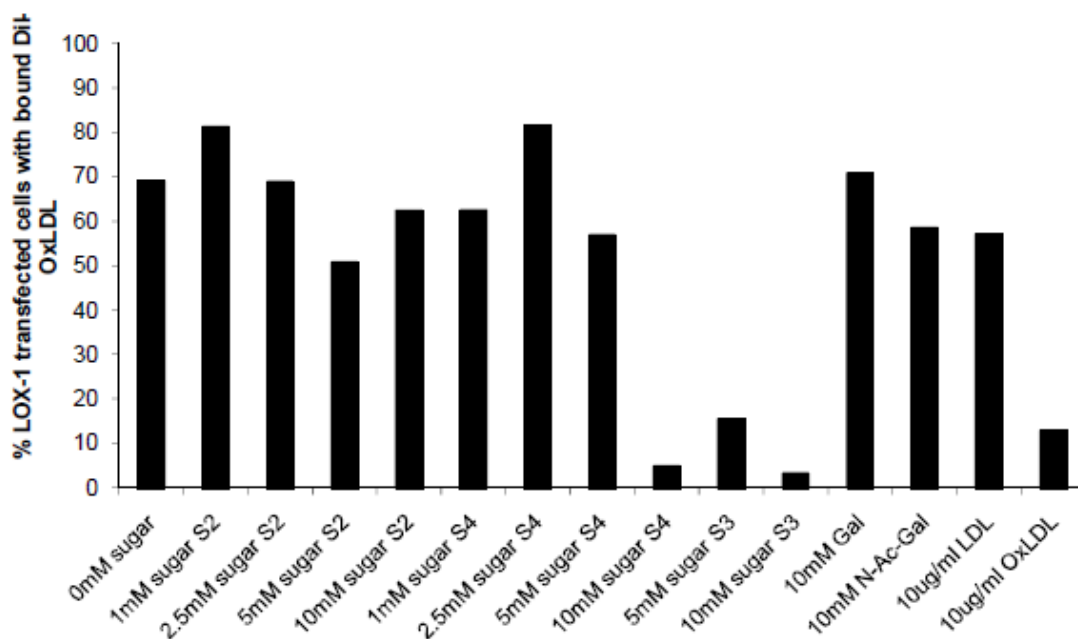
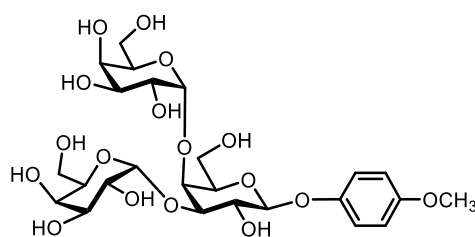


Figure 1-24.⁸¹ The tests of various carbohydrates in inhibiting OxLDL binding to LOX-1 expressing cells. (S2 = disaccharide **23**; S3 = trisaccharide **25**; S4 = tetrasaccharide **24**), figure reproduced from K. Lacey's Ph.D. thesis University of Leeds 2012, reference 81.

Trisaccharide **25** was used for further tests in an animal model because of its high specificity to LOX-1, relative to another scavenger receptor (CD 36).⁸¹ Apolipoprotein E

(Apo-E)-deficient mice fed a fat-rich diet were used as an animal model of atherosclerosis. In the absence of Apo-E, lipoprotein remnants are not transported to the liver and the mice develop hypercholesterolemia, which leads to atherosclerotic lesions after 10-12 weeks on a fat-rich diet. The results showed that trisaccharide **25** can reduce the formation of atherosclerotic plaques in the mouse aorta in comparison to controls (Figure 1-25).



25
(Sugar 3)

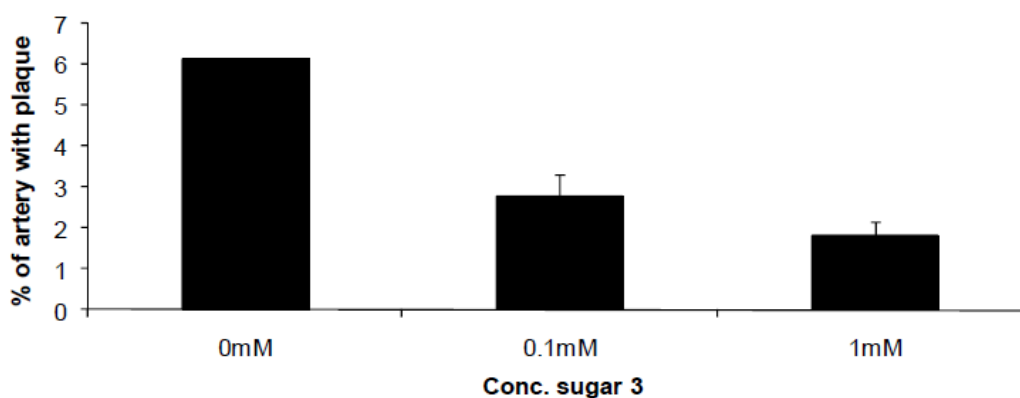


Figure 1-25.⁸¹ The effect of trisaccharide **25** (sugar 3) on plaque formation in ApoE-deficient transgenic mice. Control (saline), 0.1 mM and 1 mM of trisaccharide **25** administration was evaluated in ApoE-deficient mice after 10 weeks on a cholesterol- and fat-rich diet, figure reproduced from K. Lacey's Ph.D. thesis University of Leeds 2012, reference 81.

Therefore, trisaccharide **25** could serve as a starting point for the development of a more potent inhibitor of LOX-1. A potential strategy for the enhancement of the binding affinity and inhibitory effect is to synthesise a trisaccharide analogue and present the synthetic carbohydrate compounds on a multivalent scaffold.

1.5 DC-SIGN and its implication in viral infection

DC-SIGN (Dendritic cell-specific Intercellular adhesion molecule-3-grabbing non-integrin; also known as CD209) was originally cloned and identified from human placenta as a receptor for the HIV envelope glycoprotein gp120 by Curtis *et al.*⁹⁵ and was discovered later as an intercellular adhesion molecule (ICAM-3) receptor that supports DC-mediated T-cell clustering by Geijtenbeek *et al.*^{34,96,97} DC-SIGN and the related receptor DC-SIGNR (also known as L-SIGN, Liver/lymph node-specific ICAM-3 grabbing non-integrin or CD209L) share 73% identity at nucleic acid level²⁷ and 77% at amino acid level with DC-SIGN.⁹⁸ The two receptors are trans-membrane proteins that belong to C-type calcium-dependent lectin family. They involved in the innate immune system by acting as cell adhesion and pathogen recognition receptors of various pathogens through pattern recognition process. These receptors thus were classified to be in a group of receptors called pattern recognition receptors (PRRs), which recognise pathogen-associated molecular patterns (PAMPs) by binding to conserved motifs present on pathogens and also have the ability to bind to endogenous stress signals called damage-associated molecular patterns (DAMPs). These interactions result in the triggering of signals associated with immune response.

This section outlines the similarities and differences of DC-SIGN and its homologue DC-SIGNR, notably on their structural and functional aspects.

1.5.1 Structures of DC-SIGN and DC-SIGNR

DC-SIGN and DC-SIGNR share similar overall structural organisation, comprising four domains: an N-terminal cytoplasmic domain, a trans-membrane domain, a tandem-repeat neck domain and a carbohydrate recognition domain (CRD) (Figure 1-26). Despite their structural similarity, biochemical and structural investigations revealed that they exhibit distinct binding properties and different physiological functions,^{96,99} which are discussed in Section 1.1.5.1 and Section 1.5.2.

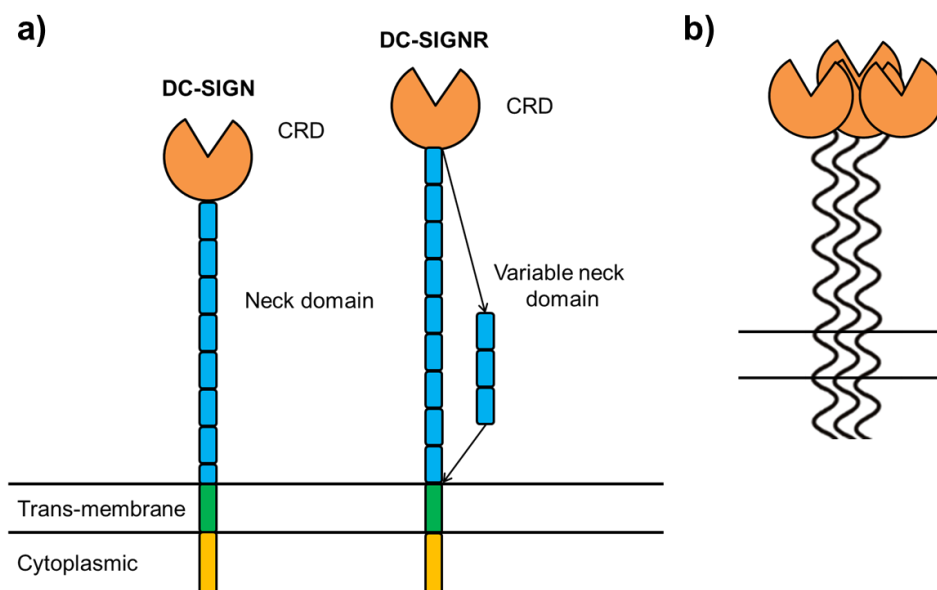


Figure 1-26. a) Schematic representation of the structures of DC-SIGN and DC-SIGNR; b) Arrangement of DC-SIGN and DC-SIGNR in a tetramer through the tandem-neck domains.

1.5.1.1 Extracellular region

The extra-cellular region of DC-SIGN and DC-SIGNR comprises the CRD and neck domains. As a single CRD interacts with low affinity to carbohydrate ligands, homo-oligomerisation into a tetramer through the α -helical neck regions is essential to provide a high affinity for ligand binding through multivalency.¹⁰⁰ Moreover, DC-SIGN tetramers can organise into nanoclusters, which can further increase the multivalent binding effect.²⁷

A remarkable difference of DC-SIGN and DC-SIGNR is found in the neck region. The neck region of DC-SIGN always consists of seven complete and one incomplete 23-residue tandem repeats, whereas that of DC-SIGNR varies from three to nine repeats.¹⁰¹ The variation of the length is thought to affect how CRDs are projected from the plasma membrane and therefore influencing ligand-binding properties. Feinberg *et al.* demonstrated that differences in oligomeric states of DC-SIGN and DC-SIGNR are caused by the number of repeats in the neck domain.¹⁰² They found that the lack of two repeats resulted in partial dissociation of the final tetramer, while the absence of more than five repeats leads to a reduced overall stability of the protein (Figure 1-27). The authors also showed that the neck and CRDs of DC-SIGN and DC-SIGNR are independently folded domains and the portion of the neck protein adjacent to the CRD is sufficient to mediate the formation of the dimers, whereas regions near the N-terminus are needed to stabilise the tetramers.¹⁰² Yu *et al.* also suggested that the

Tabarani and co-workers.¹⁰³ The neck region adjacent to the CDRs of DC-SIGNR was thought to slightly splay apart of the final neck repeat, placing the CRDs to the side of, rather than at the ends of, the helices compared with DC-SIGN. However, more details on ECD regions of the receptors were still required.

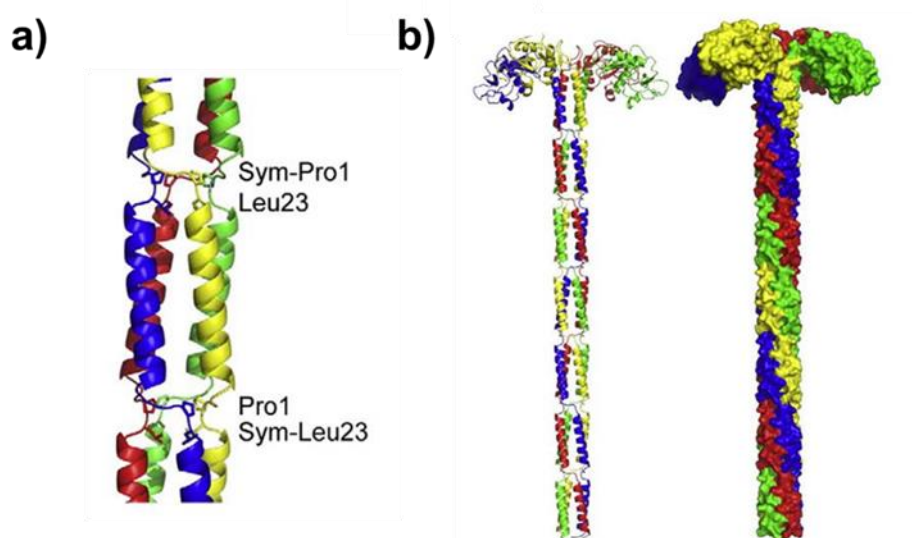


Figure 1-28.²⁸ a) Structure of the DC-SIGNR four-bundle of 23-amino acid repeat motifs which are connected through a short non-helical segments, *i.e.*, a proline residue (Pro); b) Model of much of the extracellular domain of DC-SIGNR, including neck repeats 2 to 8 and the CRD, figure reproduced from reference 28.

The Ca^{2+} dependent CRDs of DC-SIGN and DC-SIGNR, located at the C-terminus of the proteins, are projected from the membrane surface by neck domains. CRDs of DC-SIGN and DC-SIGNR play an essential roles in the ligand recognition by specifically bind high mannose glycan structures.^{45,100} The CRDs of DC-SIGN and DC-SIGNR bind $\text{Man}_9\text{GlcNAc}_2$ oligosaccharide 130- and 17-fold more tightly than mannose, and affinity for a glycopeptide bearing two such oligosaccharides is increased by a further factor of 5- to 25-fold.¹⁰⁴ The CRDs of DC-SIGN are thought to have a flexible arrangement, which is required for optimal adaptation upon binding to carbohydrate ligands.¹⁰⁵

Crystal structures of CRDs of DC-SIGN and DC-SIGNR in complex with a pentasaccharide, in combination with binding studies, showed that they selectively recognise high mannose oligosaccharides (Figure 1-29A&B).⁴⁵ The CRD in DC-SIGN adopts a typical long-form C-type lectin fold and selectively recognises high mannose glycans by ligation to bound Ca^{2+} site conserved in C-type lectin family. The CRD of DC-SIGN has two Ca^{2+} binding sites: one is important for the CRD conformation and the other is for direct ligation with carbohydrate ligands.

The CRDs of DC-SIGN and DC-SIGNR bind the central mannose residue (Man2) through equatorial 3-OH and 4-OH groups coordinating with the Ca^{2+} site, and the hydrogen bond network between distinct sugar residues of the ligand and the amino acid residues in the protein. The terminal GlcNAc (GlcNAc1) residues also form a number of contacts with DC-SIGN and DC-SIGNR. However, in the DC-SIGN complex, GlcNAc1 interacts with the partner CRD as it interacted with another Ca^{2+} site.

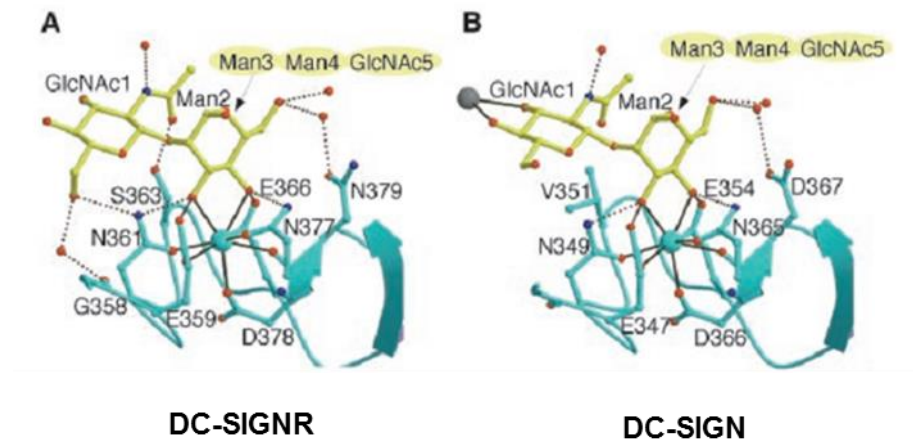


Figure 1-29.⁴⁵ Interactions of DC-SIGN and DC-SIGNR with $\text{GlcNAc}_2\text{Man}_3$ A) Interactions of the $\alpha 1$ -3-linked branch with DC-SIGNR. Only important sugars are shown. Ca^{2+} coordination is shown by solid black lines and hydrogen bonds as dashed lines; B) Interactions of the $\alpha 1$ -3-linked branch with DC-SIGN. The terminal GlcNAc1 forms a cross link by forming the typical C-type lectin interactions with the principal Ca^{2+} (grey) are shown, figure reproduced from reference 45.

Moreover, Guo and colleagues performed glycan array analysis to show that DC-SIGN and DC-SIGNR have different ligand-binding properties (Figure 1-30).⁹⁹ Both receptors recognise *N*-linked high-mannose structures, among which $\text{Man}_9\text{GlcAsn}$ glycopeptide had a highest binding affinity. DC-SIGN recognises a broader set of ligands than DC-SIGNR; that is DC-SIGN but not DC-SIGNR binds to a selected set of fucosylated oligosaccharides, including Lewis^a and Lewis^x blood group epitopes found on some pathogens.^{45,99}

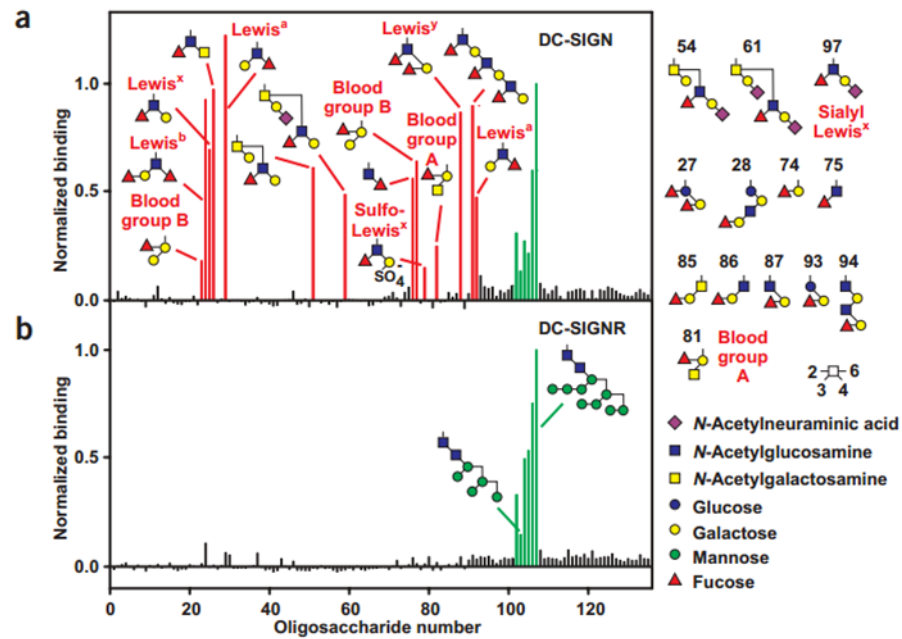


Figure 1-30.⁹⁹ Glycan array probed with fluorocein-labelled DC-SIGN and DC-SIGNR. a) DC-SIGN binds to fucose- and mannose-containing glycans; b) DC-SIGNR binds to mannose-containing glycans, figure reproduced from reference 99.

Guo *et al.* also investigated the ability of DC-SIGN to bind fucosylated ligands and a high mannose glycan (Figure 1-31).⁹⁹ In the case of a high mannose glycan binding, the α 1,3-linked mannose residue interacts with the primary Ca^{2+} binding site of the DC-SIGN CRD and the α 1,6-linked mannose residue fills in the secondary binding site. Interestingly, the primary binding site of DC-SIGN may not be necessary to bind to the terminal mannose residues of the ligand. However, $\text{Man}\alpha$ -1,2-Man, which is unusually found in high mannose glycan structures, is in contact with the DC-SIGN CRD. On the other hand, DC-SIGN binds to fucose-containing glycans (e.g., Le^x tetrasaccharide); a fucose residue interacts with the DC-SIGN primary binding site in a different geometry compared to the mannose residues bound to the protein. The branched oligosaccharides with terminal fucose residues are oriented with the central GlcNAc residue pointing away from the protein while the terminal galactose residue making additional contacts with the protein.

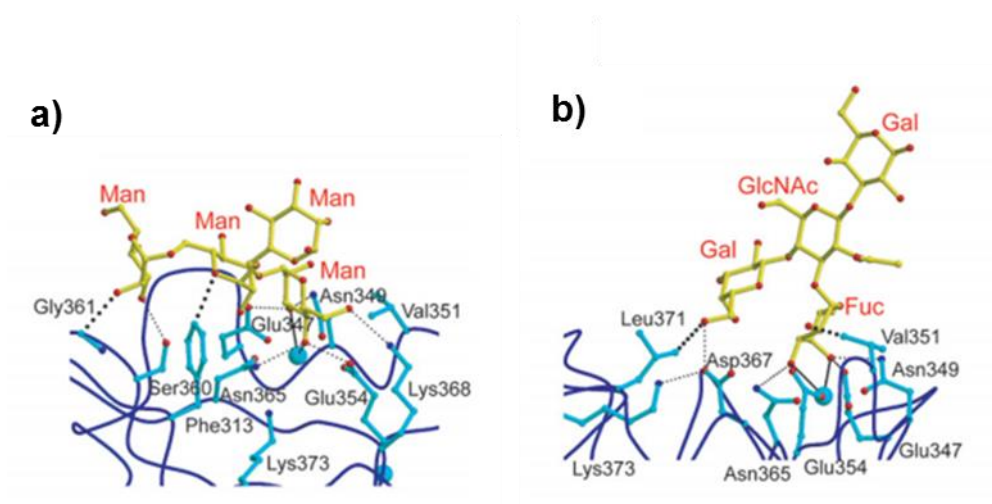


Figure 1-31.⁹⁹ DC-SIGN in complex with: a) Man_4 structure and b) Le^x tetrasaccharide of NMFPIII. Cyan spheres are bound Ca^{2+} ions. Ca^{2+} -coordination is shown by black lines, hydrogen bonds as dashed lines, figure reproduced from reference 105.

Furthermore, structural characteristics of the interaction of the DC-SIGN and DC-SIGNR with oligosaccharides containing mannose or Lewis^x by NMR methods show that in certain cases crystallography may reveal only one of multiple modes of ligand binding.^{96,106} More details on the binding of DC-SIGN CRD to their relevant ligands still await investigation.

1.5.1.2 Trans-membrane and cytoplasmic domains

Trans-membrane domains of DC-SIGN and DC-SIGNR contain approximately 18 and 22 amino acids that anchor the proteins to the cytoplasmic membrane.²⁷

The cytoplasmic N-terminal region of DC-SIGN and DC-SIGNR contains several internalisation motifs: DC-SIGN contains a di-leucine (LL) motif, a triacidic (EEE) cluster, an incomplete immunoreceptor tyrosine-based activation motif (ITAM), whereas the related receptor DC-SIGNR contains an LL motif and an EEE cluster, but no tyrosine motif.¹⁰⁷⁻¹⁰⁹

1.5.1.3 Tissue distribution of DC-SIGN and DC-SIGNR

DC-SIGN and DC-SIGNR are expressed in different tissues. DC-SIGN is expressed on the surface of dendritic cells, macrophages and placenta, whereas DC-SIGNR is present on sinusoidal endothelial cells in the liver and on endothelial cells in lymph node sinuses and placental villi but not on dendritic cells.^{27,110,111}

1.5.2 Functions of DC-SIGN and DC-SIGNR

Comparison of DC-SIGN and DC-SIGNR showed that they have different ligand binding properties and physiologic functions.⁹⁹ The natural ligands of DC-SIGN are high-mannose glycans and fucose-Lewis type determinants.^{96,99,112} DC-SIGNR has a more restricted set of ligands recognising only high-mannose oligosaccharides but not fucose-containing oligosaccharides. Both C-type lectins play essential roles in the immune system; they share the ability to bind to ICAM-3 (the endogenous adhesion molecule of T-cells) and enhance several pathogens infection of T-cells and other cells of the immune system.^{97,101} Both receptors functions as cell adhesion receptor by recognising glycoproteins on HIV, Ebola virus, hepatitis C virus (HCV), Dengue virus and many other pathogens.^{34,103,113-115} However, only DC-SIGNR can recognise the West Nile Virus (WNV) and facilitates infection.¹¹⁶ Moreover, DC-SIGN binds to ICAM-2 and facilitates the rolling and trans-endothelial migration of DCs.²⁸ Besides having a function in the role of adhesion receptor and DC-T-cell interaction, DC-SIGN has also been shown to mediate endocytosis, trafficking as a recycling receptor and releasing ligand at endosomal pH, whereas DC-SIGNR only acts as an adhesion receptor and does not release ligand at low pH or mediate endocytosis.^{99,107,108,117} However, the roles and mechanism of DC-SIGN and DC-SIGNR in pathogen recognition and uptake are still unclear.

DC-SIGN was utilised by several pathogens for host cell entry. One of the most studied and currently accepted models of DC-SIGN-mediated pathogen infection is the case of HIV infection, which is briefly discussed in Section 1.5.3.

1.5.3 The roles of DC-SIGN and DC-SIGNR in viral infections

The first step of viral entry is the attachment of the virus to the host cell surface. In the case of human immunodeficiency virus type 1 (HIV-1), which is the most widespread type, the interaction of gp120 viral envelop with CD4⁺ target cells is important for this process, permitting fusion of the virus to the host cell membrane and transfer of the viral genome to the target cells. Apart from CD4, other HIV-1 co-receptors (*e.g.*, CXCR4, CCR5, Figure 1-32) also mediate the viral entry and productive infection.¹¹⁸ Although CD4⁺ T-cells are major targets that are infected by HIV-1 viruses,¹¹⁹ accumulating evidence showed that dendritic cells (DCs) are among the first cell types confronted by HIV-1. DCs are antigen presenting cells that express various PPRs, *e.g.*, DC-SIGN which is involved in antigen capture and internalisation. DC-SIGN functions in HIV infection can be summarised as follows: 1) DC-SIGN acts as an antigen uptake receptor to recognise HIV-1 viral envelope protein gp120, allowing immature DCs to

capture pathogens and migrate to lymphoid tissues to present the antigen to T-cell 2) DC-SIGN enables cell-cell interactions by binding to receptors on CD4⁺ T-cells creating infectious synapse.

The dual functions of DC-SIGN enhance HIV-1 infection of T-cells and contribute to *trans*- and *cis*-infection pathways (Figure 1-32).^{120,121} *Trans*-infection – direct infection of HIV into CD4⁺ T-cells across the infectious synapse (pathway a) or DC-SIGN mediated capture of HIV which cycles through the DC creating exosomes bearing HIV which infect CD4⁺ T-cells (pathway b). *Cis*-infection – virus becomes integrated into DC genome and new virus particles are released to infect CD4⁺ T-cells (pathway c).

All functional data of DC-SIGN were obtained from *in vitro* studies, nevertheless, the roles of DC-SIGN in HIV infection *in vivo* is not fully understood and remains to be evaluated.

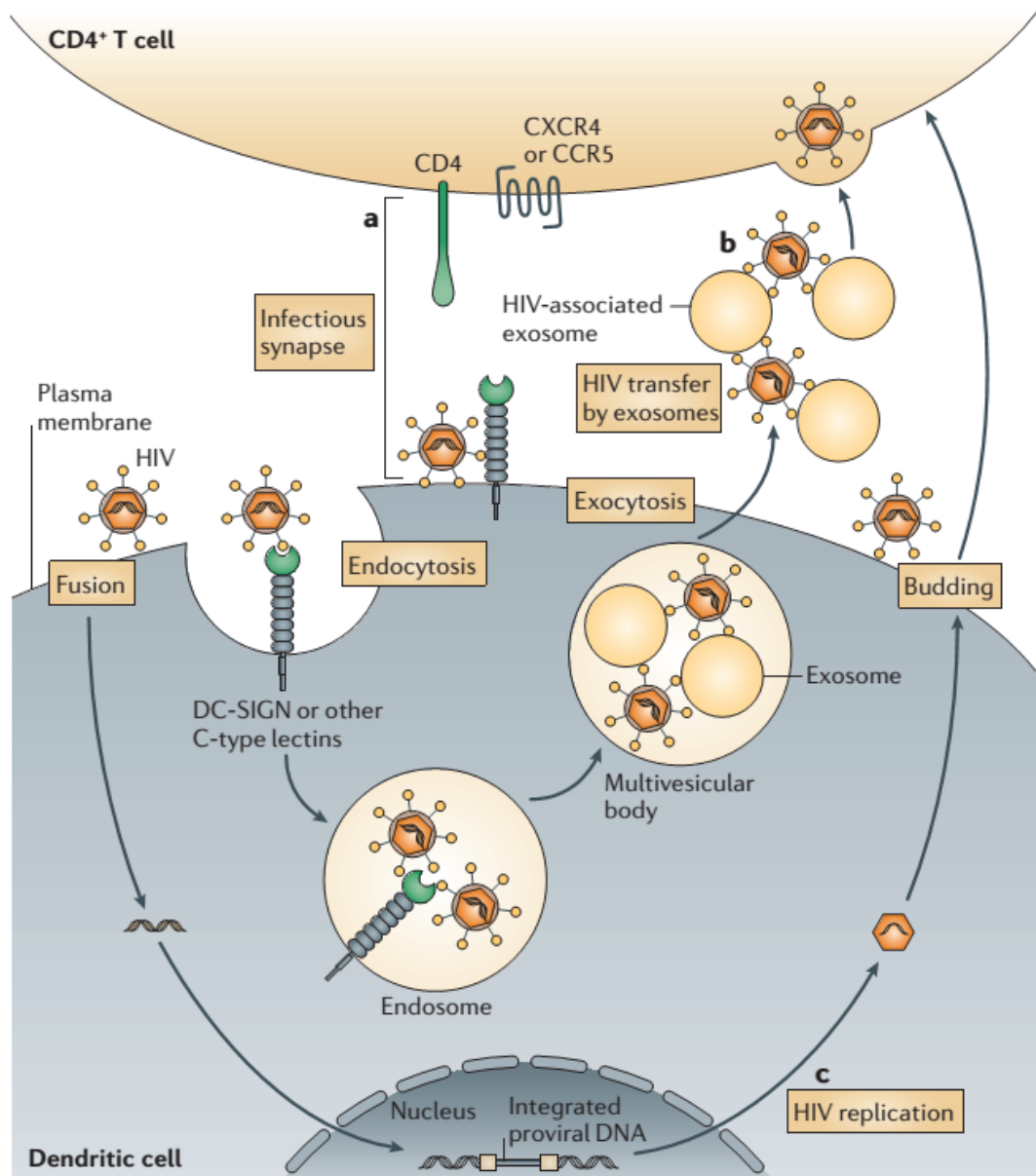


Figure 1-32.¹²¹ The roles of DC-SIGN in HIV-1 infection and transmission: *trans*-infection mediated by DCs can occur by two pathways (a,b) and *cis*-infection mediated by DCs involves one pathway (c), figure reproduced from reference 121.

DC-SIGNR functions as an HIV-receptor in *trans*-infection, but in this case it is expressed on the surface of endothelial cells in the liver lymph node sinuses, and placental villi but not on DCs. Boily-Larouche *et al.* also demonstrated that DC-SIGNR might be essential for mother-to-child transmission of HIV-1.¹²²

Ebola virus exploits DC-SIGN and DC-SIGNR in *trans*- and *cis*-infection and transmits the captured infective particles to susceptible cells.¹²³

A better understanding of DC-SIGN and DC-SIGNR activities in viral infection and protein-ligands interactions would give an insight into the basis of structural information for the development of probes or therapeutic agents.

1.6 Project objectives

1.6.1 LOX-1

1.6.1.1 Synthesis of a monovalent carbohydrate-based inhibitor for LOX-1

As described in Section 1.4.7, lead compound **25** was previously synthesised and identified as an inhibitor of LOX-1 (Figure 1-33). One of the main objectives of this thesis is to synthesise analogous compounds **26** and **27** by replacing a methoxy group of the lead trisaccharide with an amine or a methoxycarbonyl group. These lead trisaccharide derivatives would be used to construct multivalent carbohydrate structures, which were anticipated to have an increased binding affinity to LOX-1.

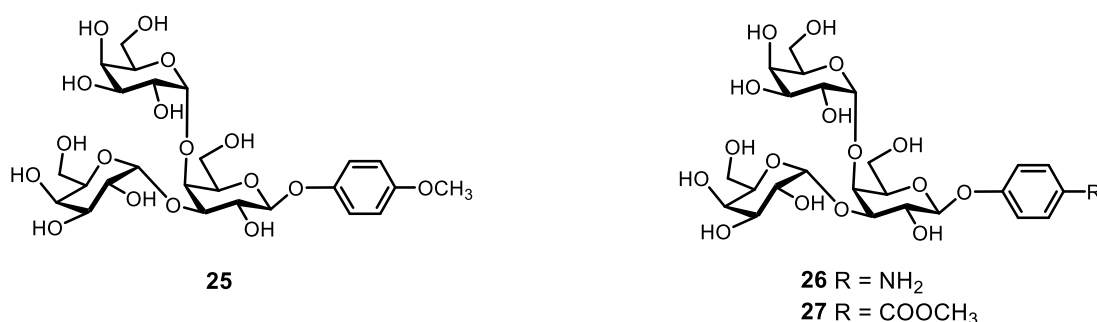


Figure 1-33. Lead compound **25** and its analogous compounds **26** and **27**.

1.6.1.2 Simplification of the lead compound structure and optimisation of the glycosylation reactions

The central galactose residue of the lead compound was chosen to be replaced with 1,2-*cis*-cyclohexanediol to form compound **28** (Figure 1-34). This simplified compound would allow determining of the significance of central galactose residue for the binding activity with LOX-1.

Replacing the central sugar with 1,2-*cis*-cyclohexanediol would not only allow the production of a simplified analogue **28** of the lead compound **25**, but also the optimisation of glycosylation reactions.

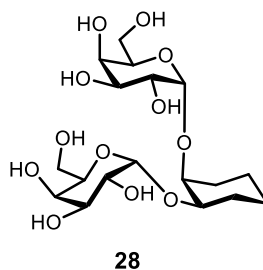


Figure 1-34. Designed sugar derivative **28**.

1.6.1.3 Synthesis of multivalent carbohydrate structures

Since the individual binding interaction of the lead trisaccharide and LOX-1 was relatively weak, attaching carbohydrate compounds to a multivalent scaffold could be a way to increase the binding affinity to LOX-1. To achieve this aim, a trisaccharide analogue containing a reactive hydrazide group would be synthesised and used to attach to a polymer bearing aldehyde functions (Figure 1-35).¹²⁴

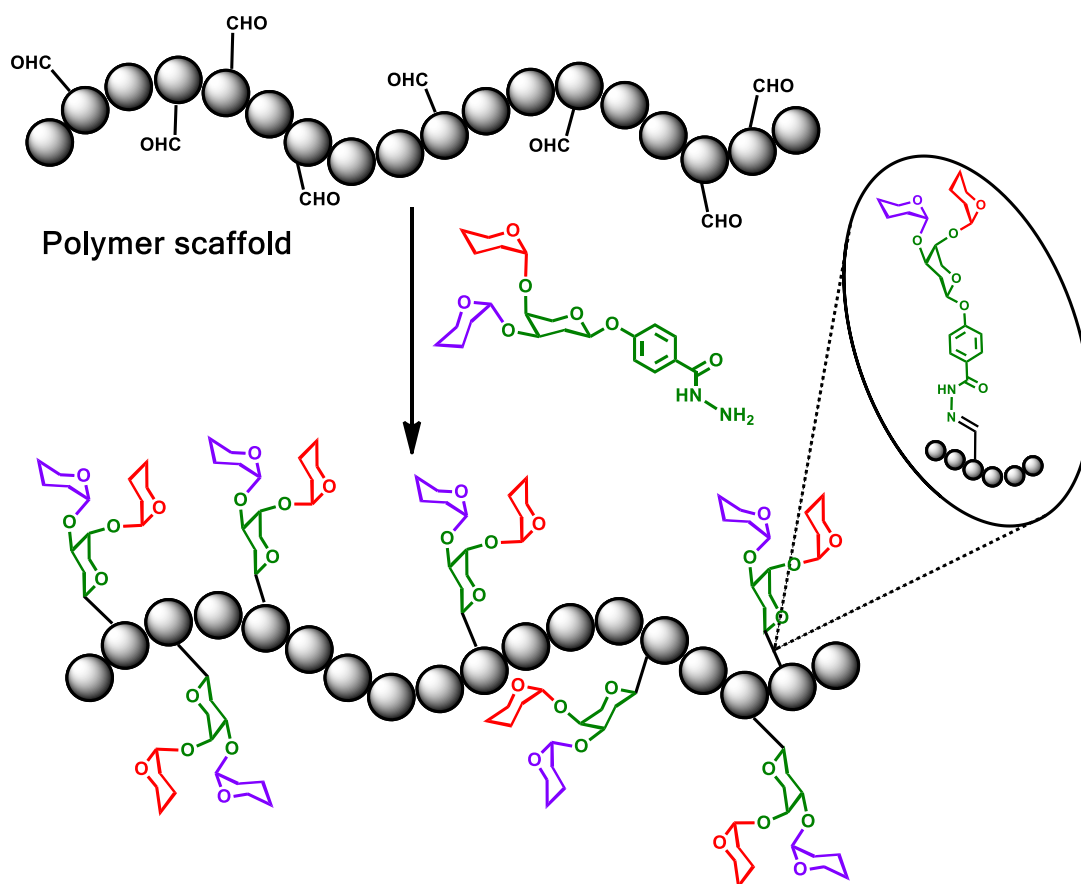


Figure 1-35. Cartoon representation of a trisaccharide analogue containing a reactive hydrazine group attached to a multivalent polymer.

1.6.1.4 Evaluation for the inhibitory effects

Synthesised trisaccharide analogues would be evaluated for their inhibitory effects in cells expressing LOX-1. This should ultimately provide an effective novel inhibitor for LOX-1.

1.6.2 DC-SIGN and its related receptor DC-SIGNR

1.6.2.1 Synthesis of a monomannoside-bearing multivalent probe

Azido-mannopyranoside **29** (Figure 1-36) was to be synthesised and conjugated to quantum dots by strain-promoted alkyne-azide cycloaddition, to form a monomannoside-bearing multivalent probe **30**. This monomannosylated-probe would be used to investigate the differences in multivalent binding by the closely related receptors DC-SIGN and DC-SIGNR, employing Förster resonance energy transfer (FRET) technique.

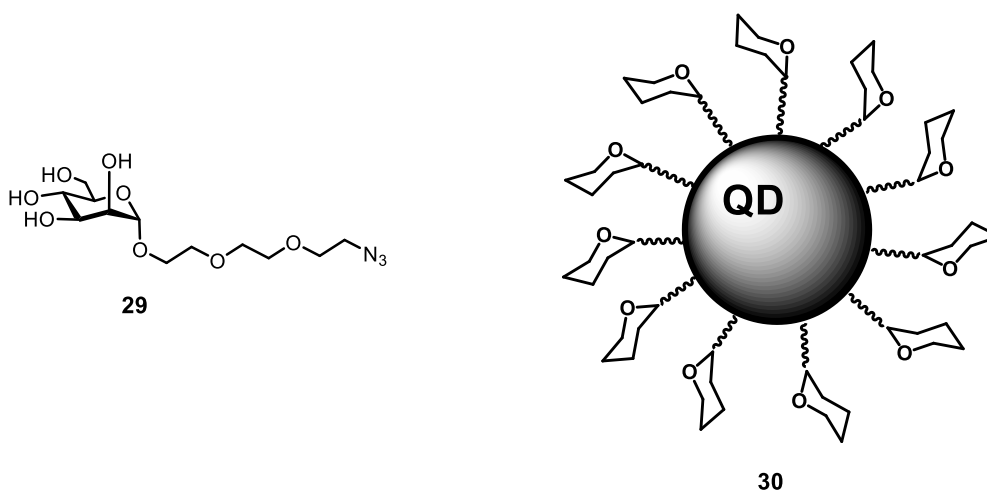


Figure 1-36. Target azido-mannopyranoside **29** and schematic representation of mono-mannoside bearing quantum-dots **30**; QD = quantum dots.

1.6.2.2 Synthesis of a dimannoside-bearing multivalent probe

As $\text{Man}\alpha 1\text{-2Man}$ dimannoside was expected to be of improved binding affinity, azido-mannopyranoside **31** (Figure 1-37) was to be prepared and attached to quantum dots, to make a dimannoside-bearing multivalent probe **32** also for DC-SIGN and DC-SIGNR.

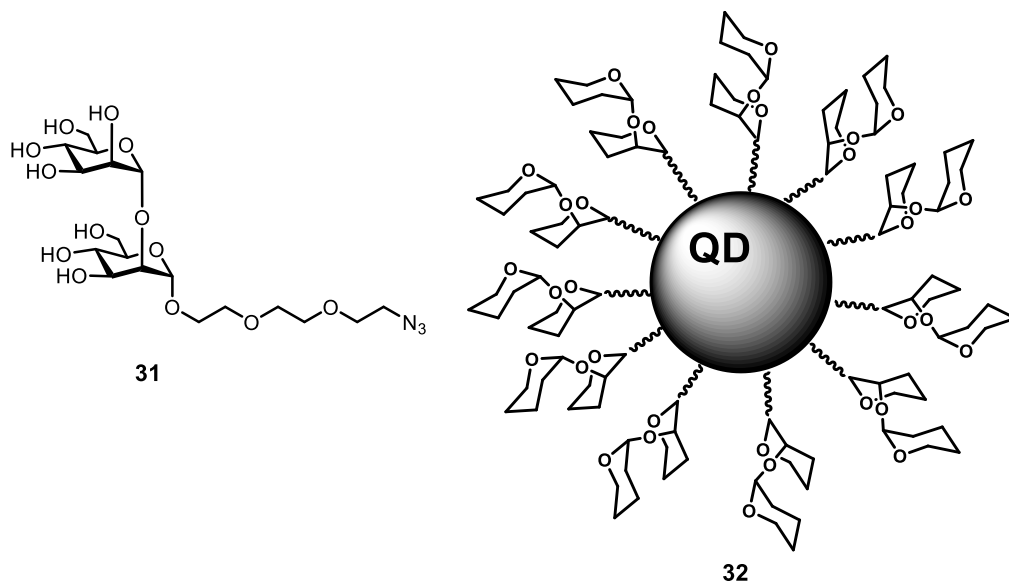


Figure 1-37. Target azido-mannopyranoside **31** and schematic representation of di-mannoside bearing quantum-dots **32**; QD = quantum dots.

Chapter 2: Synthesis of a monovalent inhibitor for LOX-1

2.1 Introduction

As discussed in Section 1.4.7, lead trisaccharide **25** (Figure 2-1), which was synthesised in the Turnbull research group by Dr. P. Mandal, has been previously identified as an inhibitor of LOX-1 because it could inhibit LOX-1-oxLDL binding to cells and reduce atherosclerosis in mice.⁸¹ However, the binding affinity between the trisaccharide and LOX-1 was relatively weak; constructing multivalent carbohydrate structures would be a way to enhance the binding affinity of this interaction.

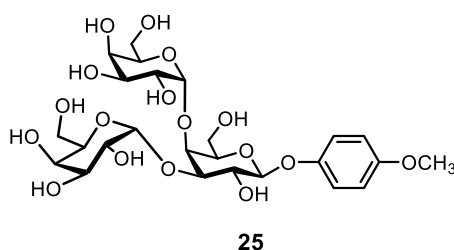


Figure 2-1. Chemical structure of lead trisaccharide **25**, which was identified as an inhibitor of LOX-1.

2.2 Aims and objectives

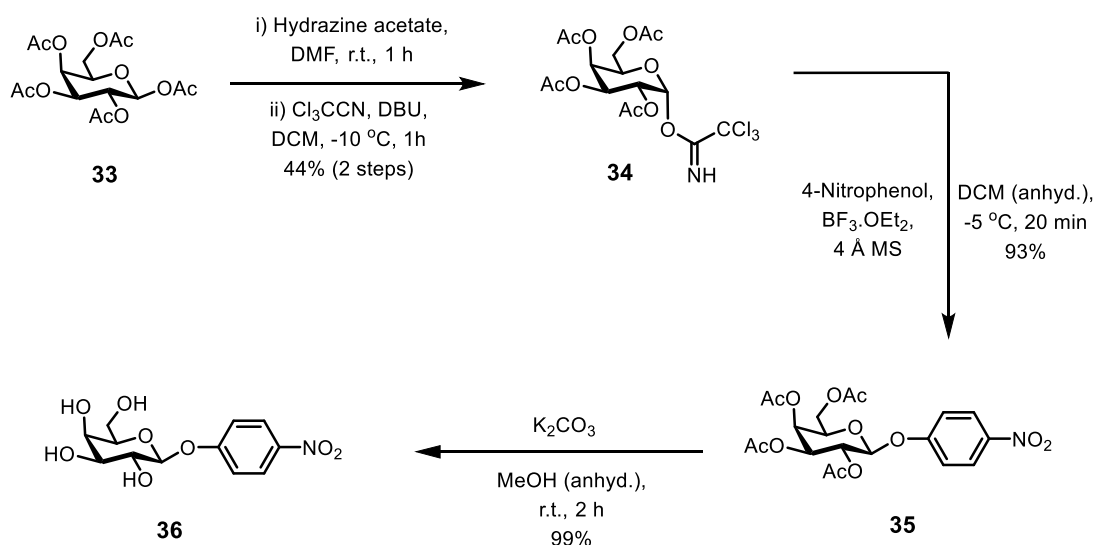
The objective of this chapter was to synthesise a lead compound analogue, containing an aromatic nitro group at one end. This nitro group was to be reduced to an amine for attachment to a polymer scaffold to make a glycopolymer bearing multiple copies of trisaccharide analogues.

2.3 Synthesis of a trisaccharide analogue containing an aromatic amine group

2.3.1 Synthesis of a glycosyl acceptor

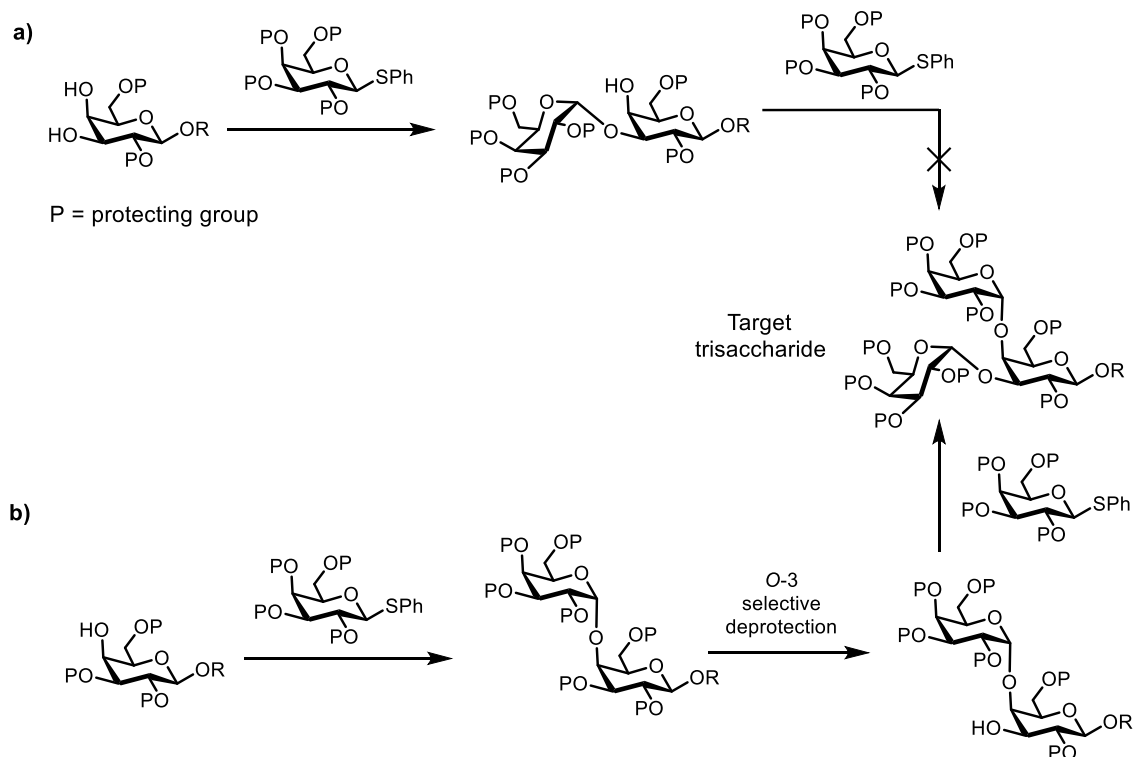
The first step in the synthesis was the removal of the anomeric acetyl group from galactose pentaacetate **33** to form a hemiacetal (Scheme 2-1). Treatment of the alcohol with trichloroacetonitrile and a base gave α -anomeric trichloroacetimidate **34**, which has the ability to act as a glycosyl donor under mild acidic conditions such as provided by a Lewis acid. Formation of the α - or β -trichloroacetimidate depends on the type of base used to deprotonate the free hydroxyl group. With a weak base, mutarotation occurs faster than the nucleophilic attack; therefore the β -alcohol reacts preferentially. With a strong base, such as DBU, the product can anomerise therefore the α -anomeric trichloroacetimidate is preferred because it is more thermodynamically stable than the β -form. α -Trichloroacetimidate **34** was reacted with 4-nitrophenol, in the

presence of $\text{BF}_3 \cdot \text{OEt}_2$, to give β -galactopyranoside **35**, which was deacetylated by treatment with potassium carbonate in anhydrous MeOH to yield galactopyranoside **36**.



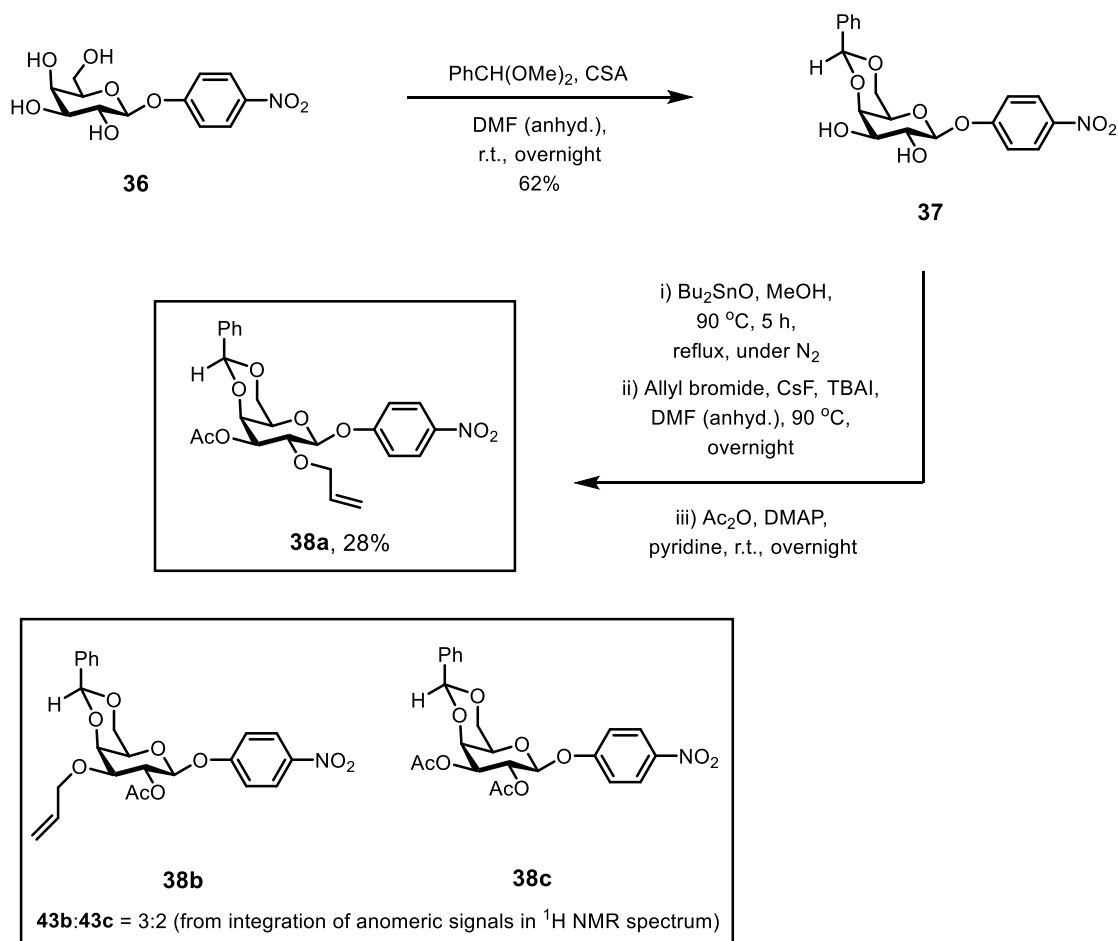
Scheme 2-1. Synthetic route to 4-nitrophenyl galactopyranoside **36**.

Although, the same galactosyl donor was to be used twice to glycosylate the central galactose residue, it was necessary to perform one glycosylation reaction at a time. A previous attempt was made by Dr. P. Mandal to attach the same galactosyl donor at the O-3 and O-4 positions simultaneously, but the glycosylation did not work. It was assumed that if the two sugars were attached at the same time, the less hindered equatorial position would be glycosylated in preference to the axial position. Hence, it would become more difficult to react the axial alcohol with the galactosyl donor to form the target trisaccharide (Scheme 2-2a). A way to avoid this problem was to first of all selectively protect the O-3 equatorial position and then attach the first sugar onto the O-4 axial position. Thereafter, a selective deprotection to reveal the O-3 hydroxyl group would allow attachment to the next sugar residue, producing the target trisaccharide (Scheme 2-2b).



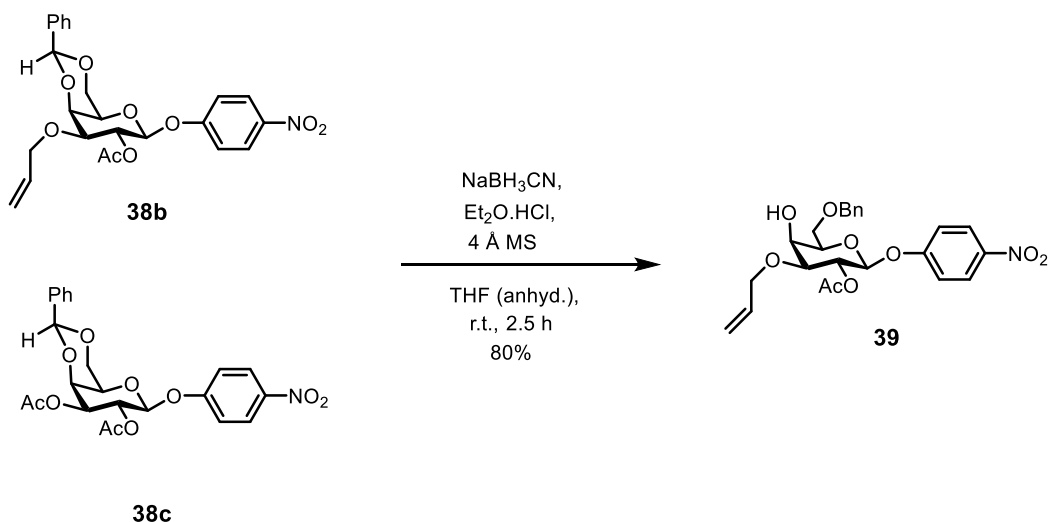
Scheme 2-2. The necessity of protecting group arrangements for the synthesis of the target trisaccharide analogue.

A benzylidene acetal was employed to selectively protect both O-4 and O-6 positions of galactopyranoside **36** by the reaction with benzaldehyde dimethylacetal and camphor sulfonic acid (CSA) (Scheme 2-3). The reaction was selective for the O-4, O-6 positions because formation of a compound containing a six-membered ring is thermodynamically preferred. 4,6-O-Benzylidene protected galactopyranoside **37** was treated with dibutyl tin oxide in MeOH at 90 °C and subsequently reacted with allyl bromide in the presence of cesium fluoride and tetrabutylammonium iodide (TBAI) at 90 °C, followed by acetyl protection using acetic anhydride and 4-dimethylaminopyridine (DMAP) in pyridine. The aim of this three-step synthesis was to selectively introduce an allyl group at the O-3 position of compound **37**. However, this process was not regiostereoselective, furnishing a mixture of three different compounds (**38a**, **38b** and **38c**). Compounds **38b** and **38c** were inseparable by flash column chromatography and were therefore used for the next step without further purification.



Scheme 2-3. Synthetic route to compounds **38a**, **38b**, and **38c**.

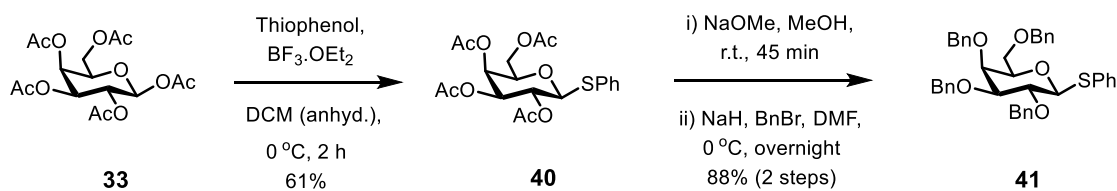
A mixture of compounds **38b** and **38c** was obtained in a ratio of 3:2, which was determined by integration of anomeric signals in ¹H NMR spectrum. The total of 4.84 g of the product mixture was obtained, which contained 6.15 mmol of **38b** (calculated from a relative mass of 472.25). The product mixture was subjected to reduction with sodium cyanoborohydride under acidic conditions (Scheme 2-4). After the ring-opening reaction, a pure galactopyranoside **39** was successfully isolated in a yield of 80%, which was calculated from 6.15 mmol of **38b** as starting material. This process selectively revealed a free hydroxyl group at the O-4 position on galactopyranoside **39**, which would be used as a glycosyl donor for further glycosylation reactions.



Scheme 2-4. Synthetic route to galactopyranoside **39**, which would be used as a glycosyl acceptor for further glycosylation reactions. N.B. Starting material contains 60% of **38b** and 40% of **38c**. Yield was calculated based on the amount of **38b** present in the starting material.

2.3.2 Synthesis of a glycosyl donor

Reaction of galactose pentacetate **33** with thiophenol in the presence of Lewis acid ($\text{BF}_3\cdot\text{OEt}_2$) yielded β -galactopyranoside **40** (Scheme 2-5). The β -galactopyranoside was formed preferentially as a result of the neighbouring group participation by the acetate protecting group at the O-2 position which could stabilise the intermediate by forming a cyclic oxacarbenium ion. Fully-benzylated glycosyl donor **41** was obtained by removal of the acetate protecting groups, followed by benzylation using benzyl bromide and sodium hydride.



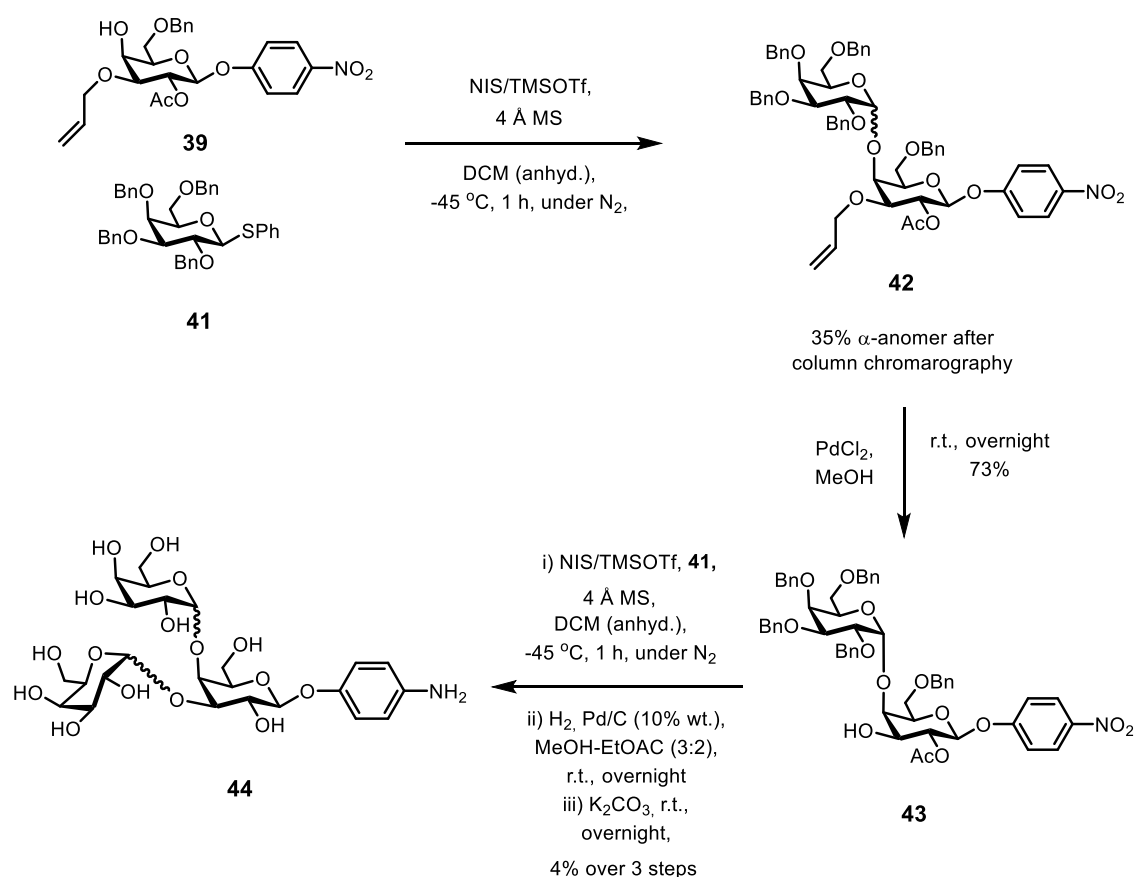
Scheme 2-5. Synthetic route to glycosyl donor **41**.

2.3.3 Glycosylation reactions

The glycosylation reaction was performed by coupling glycosyl acceptor **39** and glycosyl donor **41** using *N*-iodosuccinimide (NIS) and trimethylsilyltrifluoromethanesulfonate (TMSOTf) as a promoter system, producing disaccharide **42** (Scheme 2-6). It should be noted that this glycosylation provided both

α - and β -galactopyrananosides. However, the α -anomer could be isolated by flash column chromatography.

The allyl group at the O-3 position was then removed with PdCl₂ in MeOH to reveal a free hydroxyl group on disaccharide **43**, which was used as a glycosyl acceptor for the next reaction. Subsequent glycosylation of disaccharide **43** with glycosyl donor **41** under the same conditions as described above, followed by removal of protecting groups, afforded trisaccharide **44** in a low yield. Liquid chromatography-mass spectrometry (LC-MS) and high resolution mass spectrometry (HRMS) showed a mass to charge ratio (*m/z*) corresponding to the desired trisaccharide **44**.



Scheme 2-6. Synthetic route to deprotected trisaccharide **44**.

¹H NMR spectrum of fully-deprotected trisaccharide **44** showed three possible compounds present in the mixture, which could be the trisaccharide with different configurations of glycosidic linkages, *i.e.*, α,α,β or α,β,β or β,α,β (Figure 2-2). The major compound was the desired product bearing two α -linkages and a β -linkage according to the coupling constants of the three anomeric proton NMR signals (4.1 Hz, 3.7 Hz, and 7.3 Hz). However, on the account of the small amount of product obtained, this

sample was not amenable to ^{13}C NMR spectroscopic analysis. Thus, there was a need for an improved synthesis of the trisaccharide.

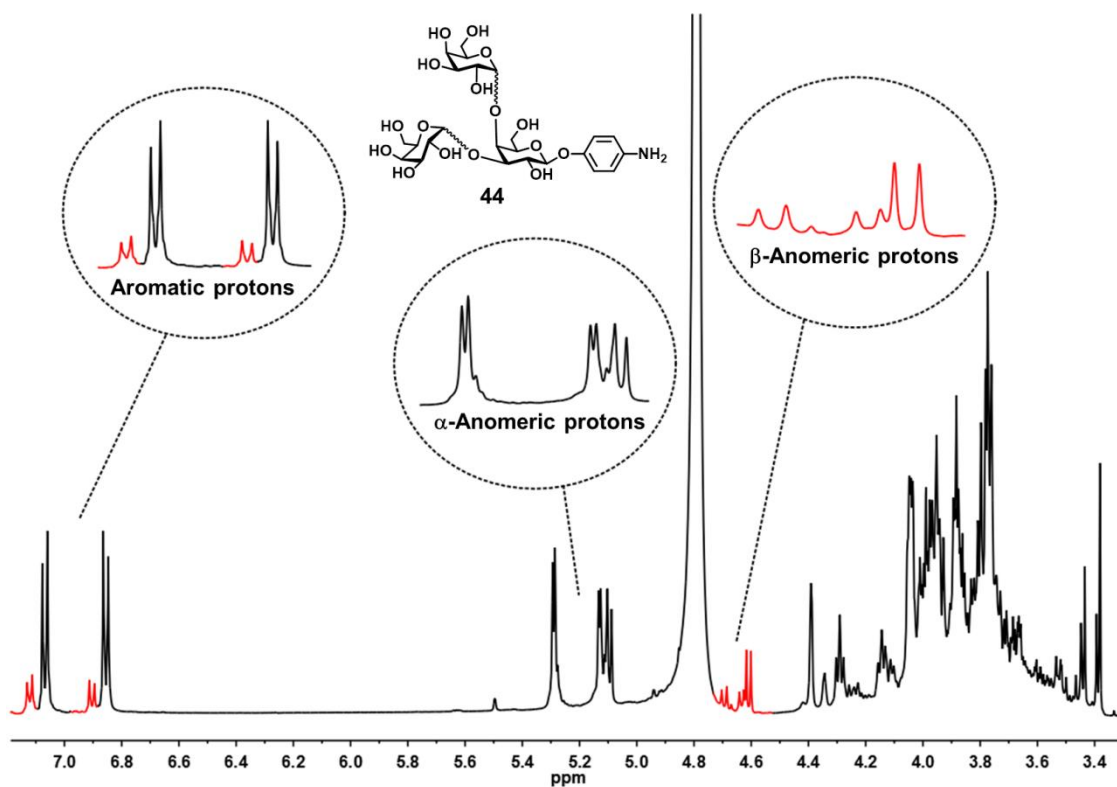
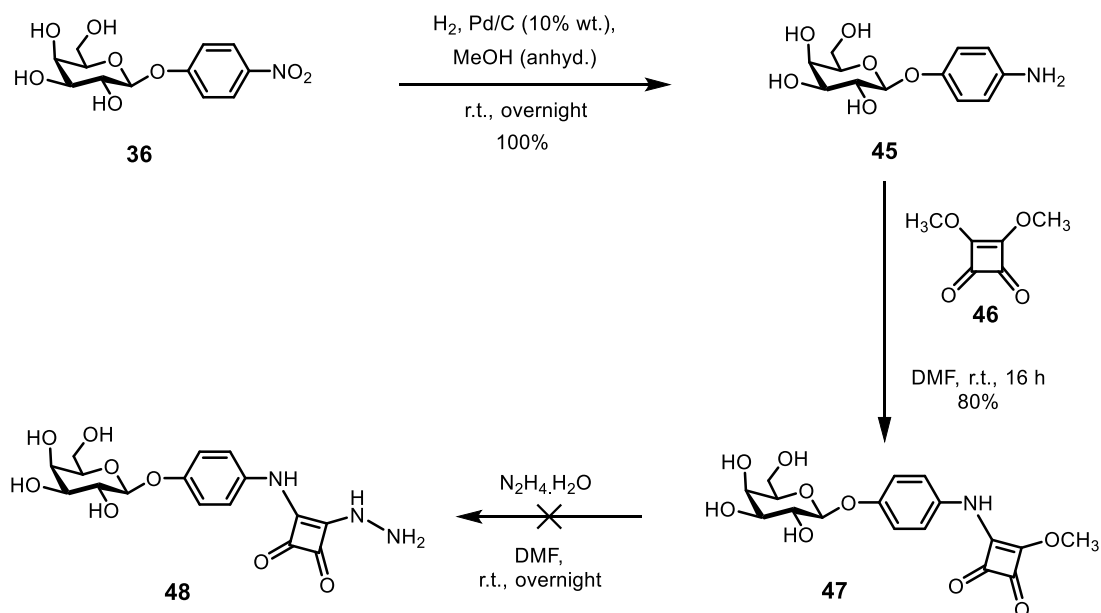


Figure 2-2. ^1H NMR spectrum of trisaccharide **44** (500 MHz, D_2O). Highlighted in red shows peaks corresponding to minor compounds presented in the sample.

2.4 A model study for derivatising an aromatic amine glycoside

Fully-deprotected trisaccharide **44** was to be further derivatised and used to attach to a multivalent scaffold to make multivalent carbohydrates. A model study for derivatising an aromatic amine glycoside was therefore conducted using a monosaccharide version of the target trisaccharide. 4-Nitrophenyl galactopyranoside **36**, an intermediate in the synthesis, was reduced by hydrogenation to give the corresponding amine **45** (Scheme 2-7). Dimethyl squarate **46** was successfully introduced on to the reactive amine group in a good yield. The reaction of the galactopyranoside **47** with hydrazine monohydrate was attempted but gave undesired product with impurities instead of hydrazide **48**. This might be because either hydrazine was too reactive and could result in dimer formation or it also could cleave the initial amide group of dimethyl squarate. It was thus impractical to employ ester squarate as a linker to join 4-aminophenyl galactopyranoside to a polymer containing aldehyde functions.



Scheme 2-7. Attempted synthesis of galactopyranoside **48**.

An alternative approach was to synthesise a trisaccharide containing other functionalities, e.g., aromatic ester **27** (Figure 2-3), which would be more practical because only a one-step derivatisation to a hydrazide was required. Moreover, trisaccharide **27** has the same aglycone structure present in the sugar compounds previously attached to the multivalent polymer scaffolds.¹²⁵ The detailed synthesis of trisaccharide **27** is further discussed in Chapter 4.

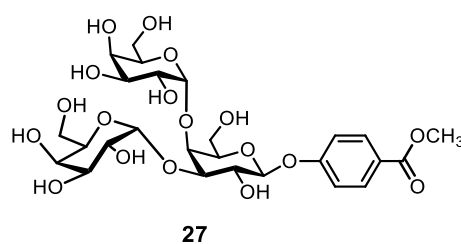
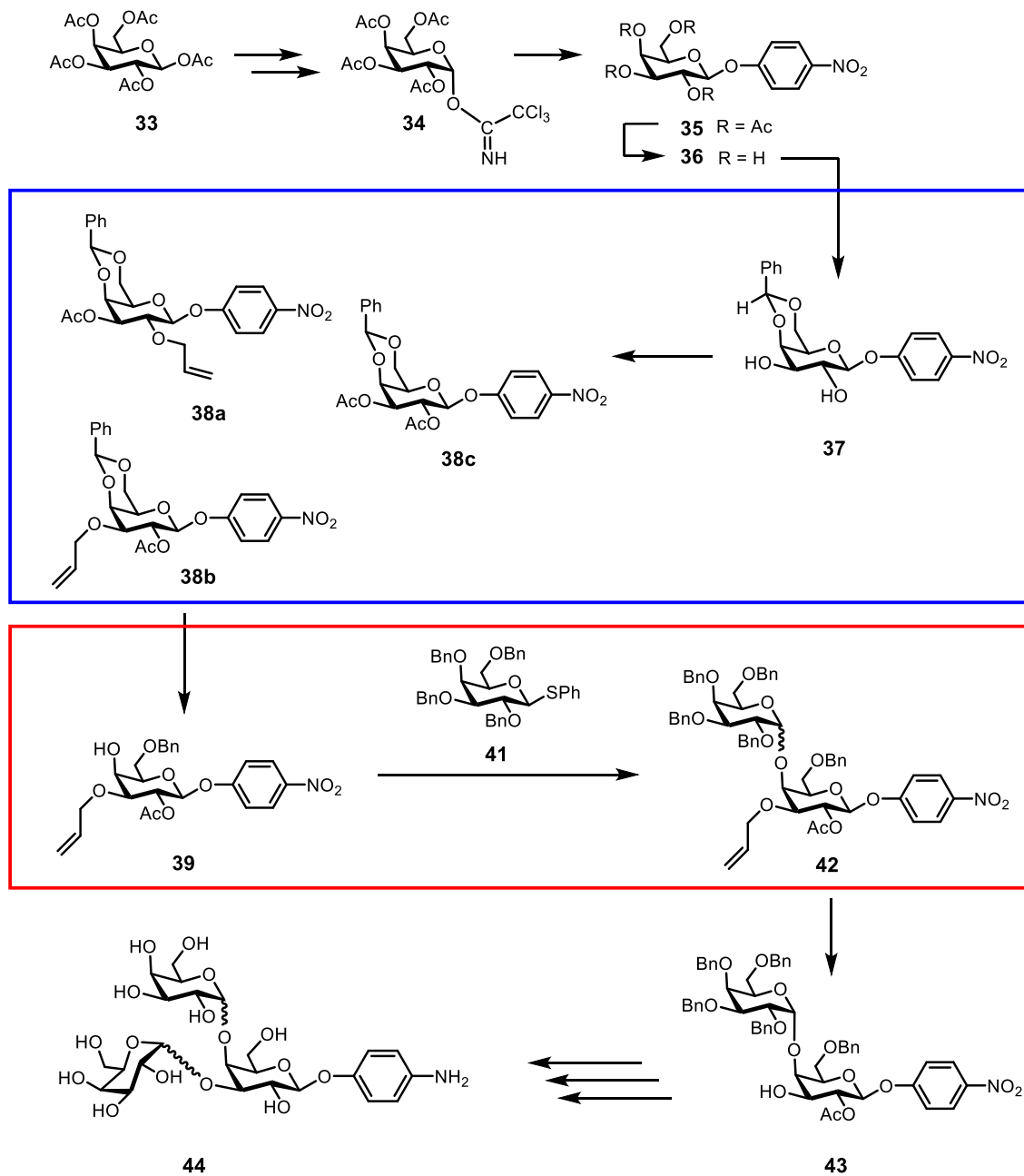


Figure 2-3. Chemical structure of 4-methoxycarbonylphenyl trisaccharide **27**.

2.5 Conclusions

The synthesis of 4-aminophenyl trisaccharide resulted in a relatively low yield and α -selectivity. The development of an improved synthesis of the lead trisaccharide derivatives was therefore necessary. The two key challenges to augment the overall yield were 1) improving the regioselectivity of the protecting group chemistry and 2) increasing the α -selectivity of glycosylation reactions (Scheme 2-8). Furthermore, a model derivatisation system to link 4-aminophenyl monosaccharide with a squarate ester was unsuccessful. The linkage of trisaccharide through a squarate ester was therefore impractical. Another possibility was to alter the aromatic amine to an aromatic ester, which was to be derivatised and then attached to a polymer scaffold, producing multivalent carbohydrates.



Scheme 2-8. Entire synthesis of 4-aminophenyl galactopyranoside **44** with two key challenges to be improved: 1) the regioselectivity of the protecting group (blue box) and 2) the α -selectivity of glycosylation (red box).

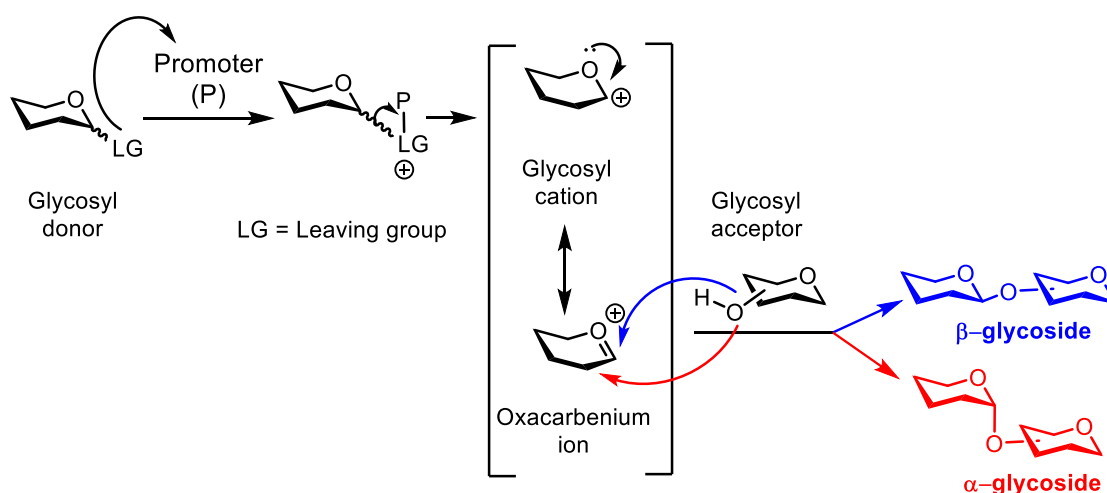
**Chapter 3: Optimisation of the
glycosylation reaction and
replacement of the central galactose
residue with a non-sugar moiety using
1,2-*cis*-cyclohexanediol**

3.1 Introduction

Before attempting to improve both stereoselectivity and regioselectivity of the trisaccharide synthesis, the coupling chemistry on a model system using cyclic diols was evaluated. One of the objectives of this evaluation was to simplify the molecular structure of the lead compound by replacing the central sugar residue with a non-sugar residue (*i.e.*, 1,2-*cis*-cyclohexanediol). The other, which could be done at the same time, was to use this simplified system as a means to optimise the glycosylation reaction using two different types of glycosyl donors.

3.2 Glycosylation reaction in general

In general, a glycosylation involves a reaction between a glycosyl acceptor and a glycosyl donor in the presence of a promoter, establishing a glycosidic linkage (Scheme 3-1). Upon activation, the promoter assists the departure of the leaving group at the anomeric centre of the donor and forms a glycosyl cation, which is further stabilised by resonance with the endocyclic oxygen and thus forms an oxacarbenium ion. Nucleophilic attack of a glycosyl acceptor is possible from either the top or the bottom face of the sugar, enabling the production of a β -glycoside and an α -glycoside, respectively.

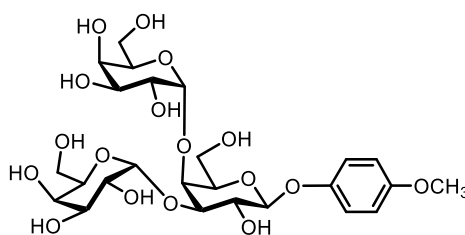


Scheme 3-1. General mechanism of a glycosylation reaction.

3.3 Optimisation of the glycosylation reaction using 1,2-*cis*-cyclohexanediol

In the initial synthesis (*cf.* Section 2.3.1, Scheme 2-6), on activation of the fully-benzylated glycosyl donor **41** with NIS/TMSOTf, the disaccharide **42** was formed as an anomeric mixture. Because in the lead compound **25** (Figure 3-1), two galactose

residues were bonded by α -linkages, controlling α -selectivity of glycosylation reaction is required to increase the overall of yield of the synthesis.

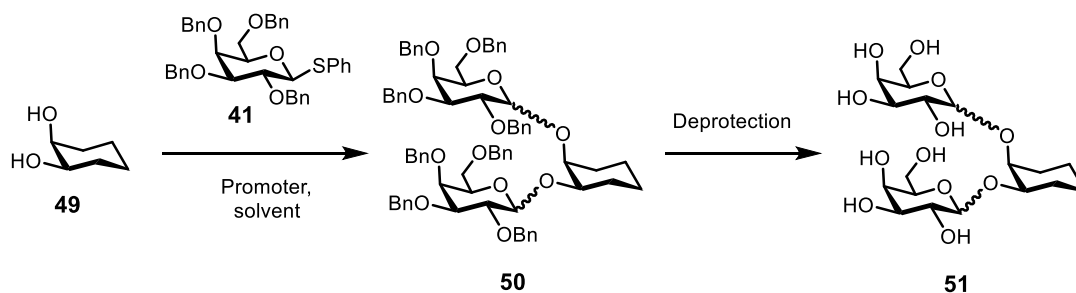


25

Figure 3-1. Chemical structure of lead compound **25**.

To investigate if it would be possible to achieve higher α -selectivity, glycosylation reactions of 1,2-*cis*-cyclohexanediol **49** (1 equiv.) with fully-benzylated glycosyl donor **41** (2.6 equiv.) was performed attempting to attach both galactopyranosyl groups in one-pot (Table 3-1). After each attempt, the crude product mixture was purified by either flash column chromatography (silica; hexane–EtOAc; Table 3-1, entries 1-3) or size exclusion chromatography (SX-1 Bio-Beads, toluene; Table 3-1, entry 4). Following purification, a hydrogenolysis of the benzyl ether protecting groups was necessary to avoid the overlapping ^1H NMR signals of the protecting groups and the sugar ring protons, notably the anomeric protons. Thus, the isolated yields present in the Table 3-1 correspond to the debenzylated products. It should be noted that these glycosylation reactions gave a mixture of anomers. The α/β ratios were determined by integration of anomeric signals in ^1H NMR spectra. The NIS/TMSOTf-promoted glycosylation reaction in DCM returned mostly unreacted glycosyl donor and the stereoselectivity was poor with α/β ratio of 1:3 (Table 3-1, entry 1). Ethereal solvents has been reported to enhance the α -selectivity by a participating electron donating effect which stabilises oxacarbenium ion intermediate, favouring the nucleophilic attack from the α -face of the sugar.¹²⁶ Consequently, another two glycosylation reactions were attempted in diethyl ether. However, they still resulted in low reactivity (Table 3-1, entries 2-3). It is also noteworthy that the use of 1-benzenesulfinyl piperidine/trifluoromethanesulfonic anhydride/2,4,6-*tert*-butylpyrimidine (BSP/Tf₂O/TTBP) as a promoter system led to a higher yield and less unreacted donor remained, when compared with NIS/TMSOTf system. The BSP/Tf₂O/TTBP-activated-glycosylation in DCM afforded *pseudo*-trisaccharide **51** in a relatively better yield compared to the glycosylation using the same promoter system in diethyl ether (Table 3-1, entry 4).

Table 3-1. Glycosylation of 1,2-*cis*-cyclohexanediol **49** with perbenzylated glycosyl donor **41**, giving pseudo-trisaccharides **50-51**.



Entry	Promoter system	Solvent	Returning unreacted donor	Ratio α/β^*	Yield**
1	NIS/TMSOTf	DCM	✓	1:3	29%
2	NIS/TMSOTf	Diethyl ether	✓	-	Trace
3	BSP/TTBP/Tf ₂ O	Diethyl ether	✓	-	Trace
4	BSP/TTBP/Tf ₂ O	DCM	*	2:1	87%

BSP

TTBP

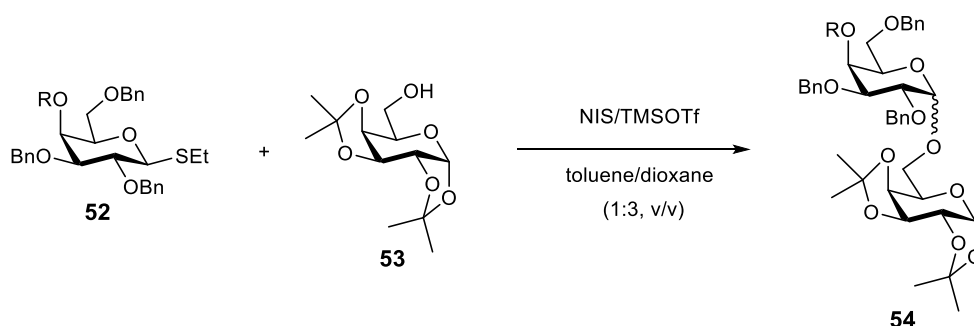
* α/β ratio was determined by integration of anomeric signals in the ¹H NMR spectrum of the reaction mixture purified by flash column chromatography (entries 1-3) or size exclusion chromatography (entry 4).

Isolated yields of debenzylated products **51.

From the above results, the BSP/Tf₂O/TTBP-promoted glycosylation reaction of 1,2-*cis*-cyclohexanediol with fully-benzylated donor **41** provided an improved yield and reasonable α -selectivity ($\alpha:\beta = 2:1$). However, the anomeric ratio was still not satisfactory for ensuring a high stereoselective glycosylation. Alternatively, the Boons group described a glycosyl donor with O-4 ester participating group which could increase α -selectivity of galactosylation.¹²⁷ For comparison, a series of O-4-acyl galactosyl donors were generated. By variation of the O-4 protecting group, the authors found that α -selectivity of galactosylation could be affected, as shown in Table 3-2. On exchanging O-4 benzyl for O-4 acetyl protecting group, the α -selectivity increased by 3-fold (Table 3-2, entry 2). Similarly, replacing O-4 acetyl with O-4 benzoyl protecting group increased the α/β ratio to 17:1 (Table 3-2, entry 3). Additional donors with

electron-donating ester functionality at O-4 position were also evaluated for α -selectivity (Table 3-2, entries 4-7). An ethyl thioglycoside bearing a 4-methoxybenzoyl group (PMBz) exhibited very promising results (Table 3-2, entry 7). The authors proposed that the α -directing effect of selected galactosyl donors was due to a remote neighbouring group participation at O-4 position. This finding is generally in agreement with the computational investigations of Miljkovic *et al.* who have introduced a general mechanism that involves electron donation from the electronegative substituent at the O-4 position of the galactopyranoside ring to the oxacarbenium intermediate.¹²⁸

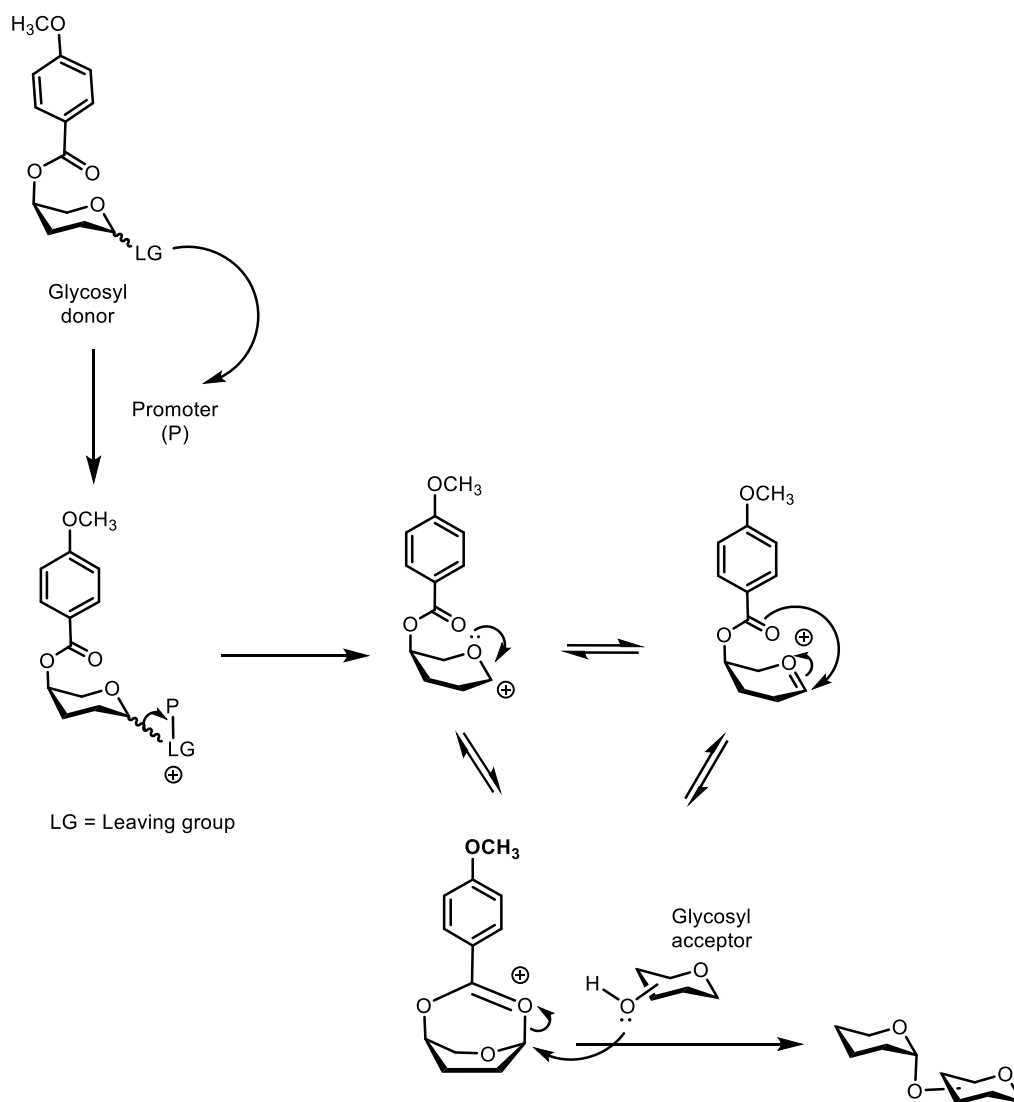
Table 3-2.¹²⁷ Literature data on galactosyl donors bearing different O-4 protecting groups



Entry	R	Ratio α/β	Yield (%) ¹²⁷
1	Benzyl	2.2:1	91
2	Acetyl	7.2:1	76
3	Benzoyl	17:1	72
4		14:1	87
5		16:1	74
6		18:1	82
7		33:1	85

A possible mechanism for remote neighbouring group participation at O-4 position is described in detail in Scheme 3-2. Upon activation, the promoter reacts with the

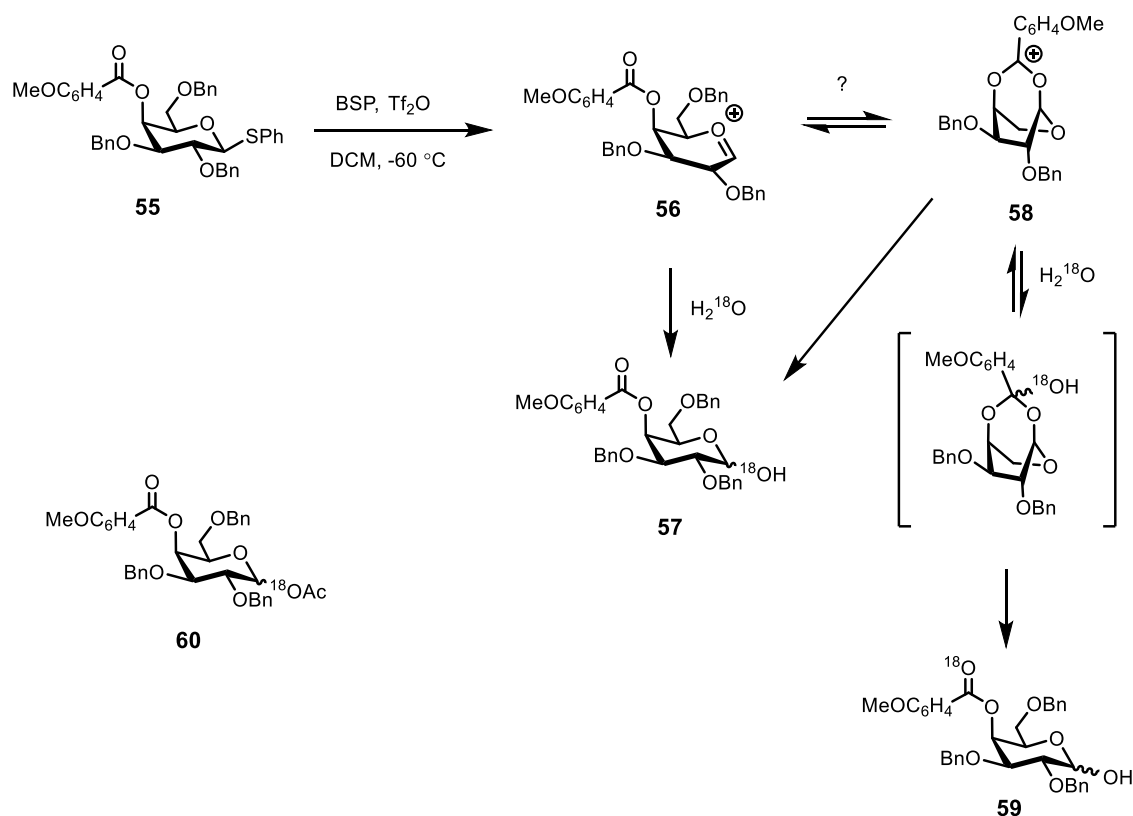
glycosyl donor leading to the departure of the leaving group and the formation of an oxacarbenium ion. The remote participating group at the *O*-4 position helps to stabilise the intermediate produced, blocking the β face of the sugar. Therefore, the nucleophilic attack of the acceptor takes place preferentially on the bottom face, favouring mostly α -glycoside.



Scheme 3-2. A possible mechanism for remote participating group participation at *O*-4 position.

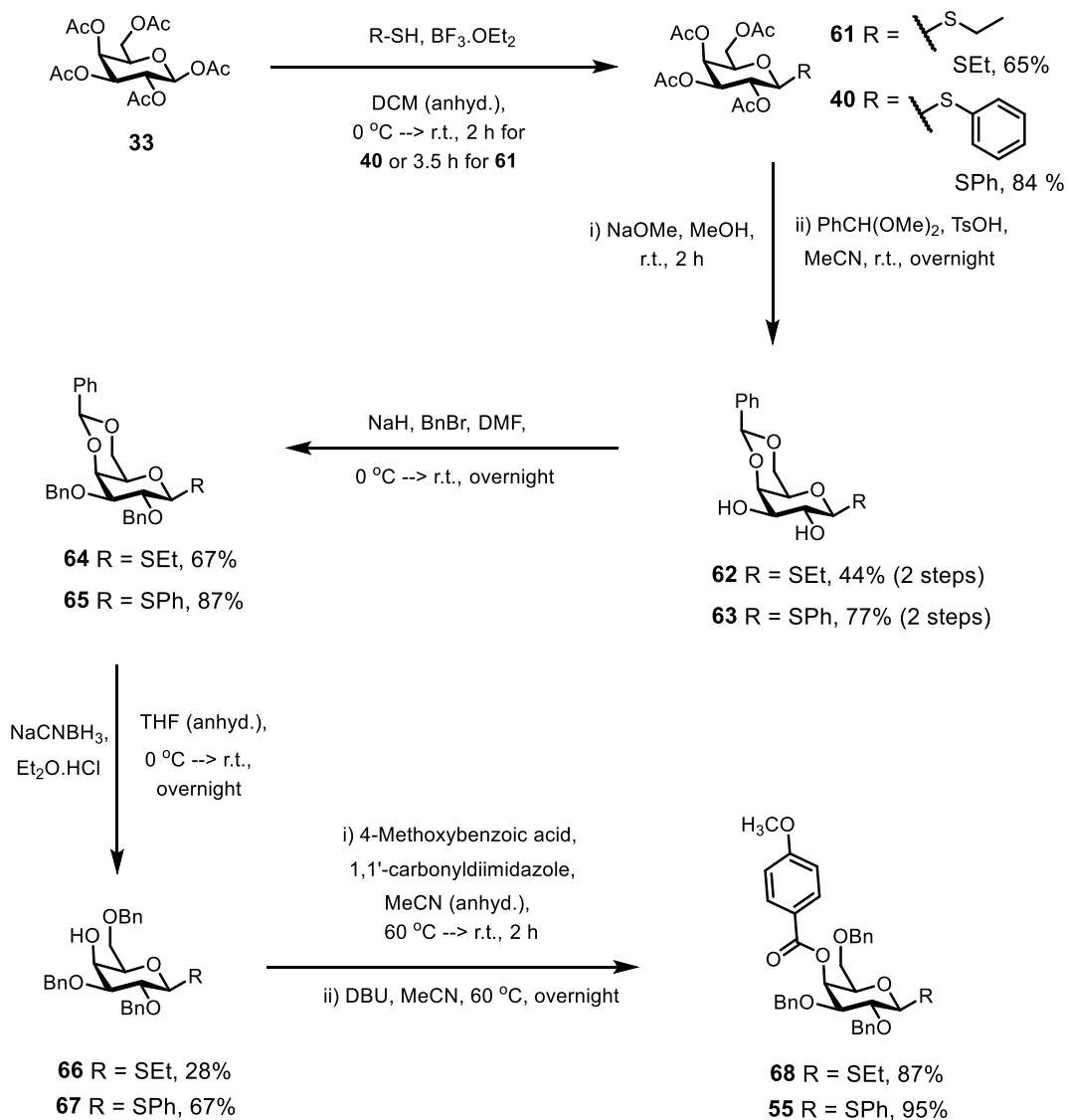
On the other hand, neighbouring group participation from the *O*-4 position has also been called into question by Crich *et al.*¹²⁹ A specific probe was developed for the detection of a bridging intermediate for neighbouring group participation by benzoate-type esters. The idea was to detect the existence of the bridging intermediate by quenching the reaction with ¹⁸O-enriched water to determine the position where the label would be incorporated. It was anticipated that upon low-temperature activation of

O-4 PMBz substituted phenyl thioglycosyl donor **55** with BSP/Tf₂O/TTBP in the absence of acceptors, glycosyl cation **56** would be formed, in equilibrium with cyclic cation **58** if the remote neighbouring group participation takes place (Scheme 3-3). ¹⁸O labelled water would be expected to be incorporated to the intermediate, forming either hydrolysis product **57** or **59**. Their experiment led to isolation of **57/59** mostly as the α -anomer; unfortunately, it was not possible to perform mass spectrometric analysis without first converting the products to the corresponding acetate **60**. They eventually confirmed that there was no evidence of the ¹⁸O-label attached to either C-4 or the benzoyl carbonyl group, implying that the stereochemical control did not appear to be the result of participation by the C-4 substituted ester, in contrast to the previous study of Boons and co-workers. However, the authors noted that alternative explanation for such α -selective effect of this type of benzoate-ester is still needed to be found. It should be noted that the evidence for and against the existence of the α -directing effect arising from remote neighbouring group participation at the O-4 position is still weak. The conclusion from the model study established by Crich *et al.* is still not widely accepted as the experiment assumes that the formation of product **59** via the hemiorthoester intermediate occurs at an appreciable rate compared to formation of **57** from either intermediates **56** or **58**. Moreover, the use of ¹⁸O-labelled water as an acceptor may not represent the reactivity of actual sugar acceptors.



Scheme 3-3.¹²⁹ An isotopic labelling probe designed by Crich and co-workers.

Regardless of the mechanism, experiments to investigate whether the use of a glycosyl donor in which the benzyl ether protecting group at the O-4 position was replaced with PMBz group could help increase the α -selectivity for the glycosylation with 1,2-*cis*-cyclohexanediol. Therefore, two related glycosyl donors were synthesised (Scheme 3-4): ethyl thioglycoside **68** as used previously by Boons and thiophenyl glycoside **55** to allow direct comparison with the fully-benzylated phenyl glycosyl donor. Acetylated ethyl and phenyl thioglycosides **61** and **40** were synthesised via the reaction of peracetylated galactose **33** with thiophenol/ethanethiol in the presence of boron trifluoride etherate. Zemplén deacetylation and subsequent benzylidene acetal protection at the O-4, O-6 positions of resulting galactopyranosides gave 4,6-O-benzylidene acetals **62** and **63**. The remaining hydroxyl groups were thereafter protected as benzyl ethers to provide compounds **64** and **65**. Selective reduction with sodium cyanoborohydride under acidic conditions resulted in alcohols **66** and **67**. The PMBz protecting group was introduced at the O-4 position by treatment with 4-methoxybenzoic acid and 1,1'-carbonyldiimidazole in MeCN in the presence of DBU, leading to formation of ethyl and phenyl thioglycosides **68** and **55**. However, under the same conditions, the preparation of ethyl thioglycoside was more challenging than that of the phenyl glycoside leading to lower yields of ethyl thioglycoside **68**; therefore it was decided to focus on donor **55**.



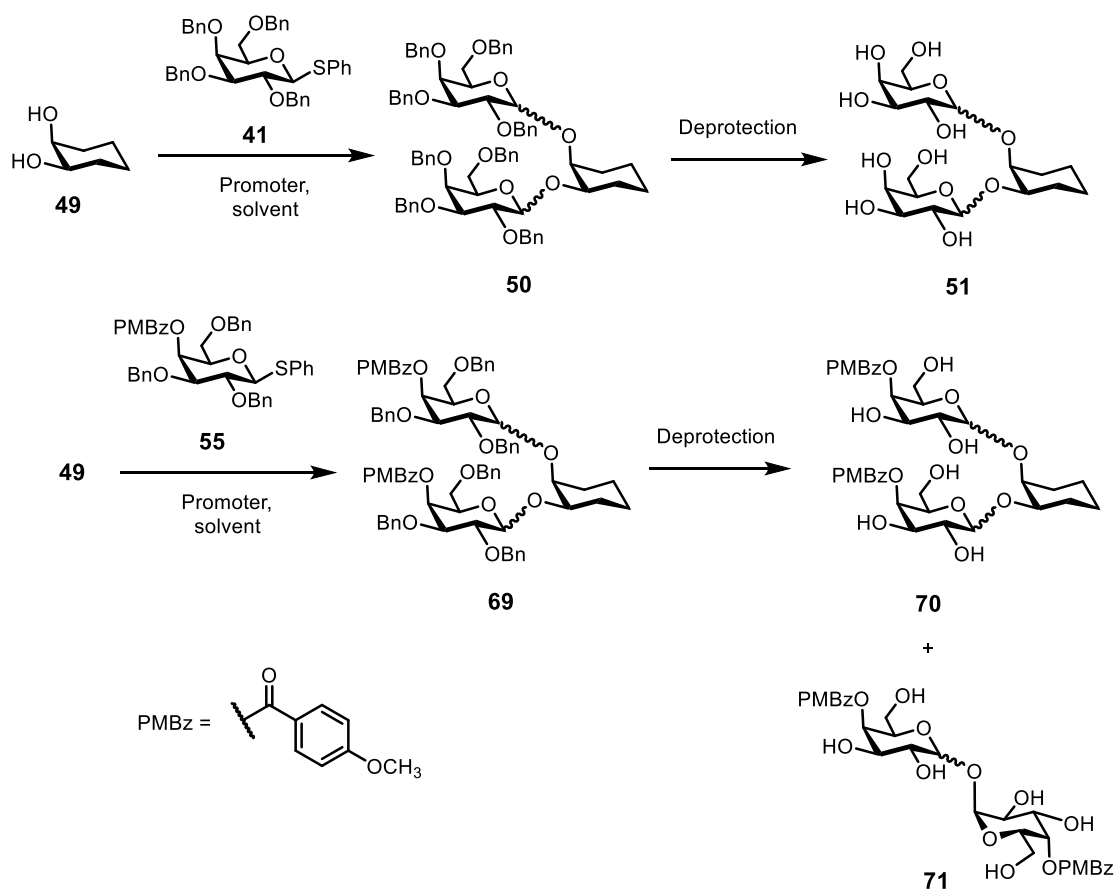
Scheme 3-4. Synthetic route to glycosyl donors **68** and **55**.

Thus, glycosylation reactions of 1,2-*cis*-cyclohexanediol **49** were repeated using phenyl thioglycoside **55** employing BSP/Tf₂O/TTBP as a promoter system in two different solvent systems, *i.e.*, DCM and DCM–diethyl ether (1:1, v/v; Table 3-3, entries 5-6). The crude products were purified by size exclusion chromatography (SX-1 Bio-Beads, toluene).

The use of this benzoate-ester type of glycosyl donor **55** exhibited improved α -selectivity with an α : β ratio of 5:1 (Table 3-3, entry 5) relative to the completely benzylated galactosyl donor **41** with an α : β of 2:1 (Table 3-3, entry 4). However, performing a glycosylation reaction in ethereal solvent (1:1, DCM–diethyl ether) still did not improve the stereoselectivity of the product because of the low reactivity (Table 3-3, entry 6). It is noteworthy that the product mixture obtained from reactions using

substituted benzoate-ester thioglycoside **55** also included a trehalose-like compound **71** that also part of the quoted yield in the table. It is noteworthy that the product mixture obtained from reactions using substituted benzoate-ester thioglycoside **55** also included traces of a trehalose-like compound **71** that could not be separated from product **70** without employing HPLC methods which would have risked leading to changes in α/β ratios. Therefore, while yields of **70** in the table are based on the molar ratio of products estimated from NMR spectra, the α/β ratios are for the mixture of all glycosides present in the mixture.

Table 3-3. Glycosylation of 1,2-*cis*-cyclohexanediol **49** with glycosyl donors **41** and **55**. Entries 1-4 are reiterated from Table 3-1 for convenience to the readers.



Entry	Donor (2.6 equiv.)	Promoter system	Solvent	Returning unreacted donor	Ratio α/β^*	Yields of 51/70**
1	41	NIS/TMSOTf	DCM	✓	1:3	29%
2			Diethyl ether	✓	-	Trace
3		BSP/TTBP/ Tf ₂ O	Diethyl ether	✓	-	Trace
4			DCM	✗	2:1	87%
5	55	BSP/TTBP/ Tf ₂ O	DCM	✗	5:1	21%
6			DCM: diethyl ether (1:1, v/v)	✗	5:1	30%

* α/β ratio was determined by integration of anomeric signals in the ¹H NMR spectrum of the reaction mixture purified by flash column chromatography (entries 1-3) or size exclusion chromatography (entries 4-6).

Isolated yields of debenzylated products **51 (entries 1-4) and **70** (entries 5-6). N.B. Only approximate yields are given for entries 5-6 as the products also contained small amounts of trehalose-like compound **71**.

The use of thioglycosyl donor **55** with a 4-methoxybenzoyl group, instead of perbenzylated glycoside, resulted in a great improvement in α -selectivity (α : β ratio of 5:1), probably as a result of remote protecting group participation. Furthermore, a mixture of compounds **70** and **71** was subjected to de-esterification to remove the O-4 PMBz protecting group using sodium hydroxide in MeOH (Figure 3-2). The product mixture was purified by mass-directed HPLC to provide compound **51** as a mixture of anomers (7 mg, α / β ratio of 8:1). Despite the relatively low yield, these optimal conditions were selected to perform further glycosylation reactions.

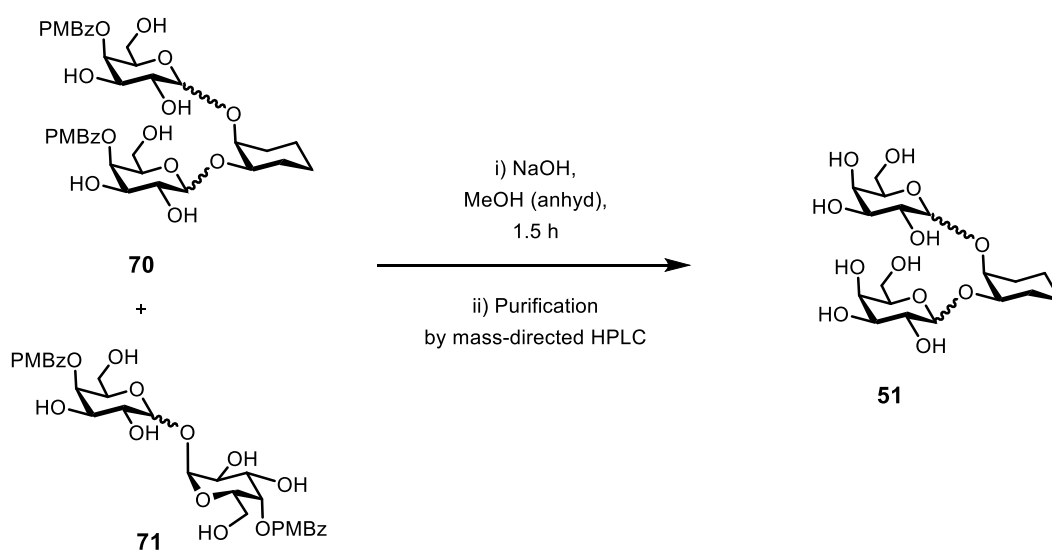


Figure 3-2. Synthetic route to *pseudo*-trisaccharide **51**.

3.4 Variable temperature NMR experiment

Fully-deprotected *pseudo*-trisaccharide **51** exhibited two α -anomeric proton signals in its NMR spectrum. A variable temperature NMR experiment (Figure 3-3) was used to investigate whether upon heating the anomeric protons peaks at 5.27 ppm and 5.18 ppm of the two galactose residues would coalesce, which could be the result of cyclohexane ring inversion, undergoing axial/equatorial exchange. However, upon varying from room temperature to 90 °C, coalescence of the two peaks did not occur; suggesting that a cyclohexane ring inversion might be a slow process. It should be noted that the coupling constants of the anomeric proton peak at 5.27 ppm were not influenced by the temperature change (3.9 Hz at 26 °C and 4.0 Hz at 90 °C), whereas the coupling constants of the peak at 5.18 ppm decreased from 4.1 Hz to 3.5 Hz. However, it is still challenging to assign proton peaks, especially for anomeric protons.

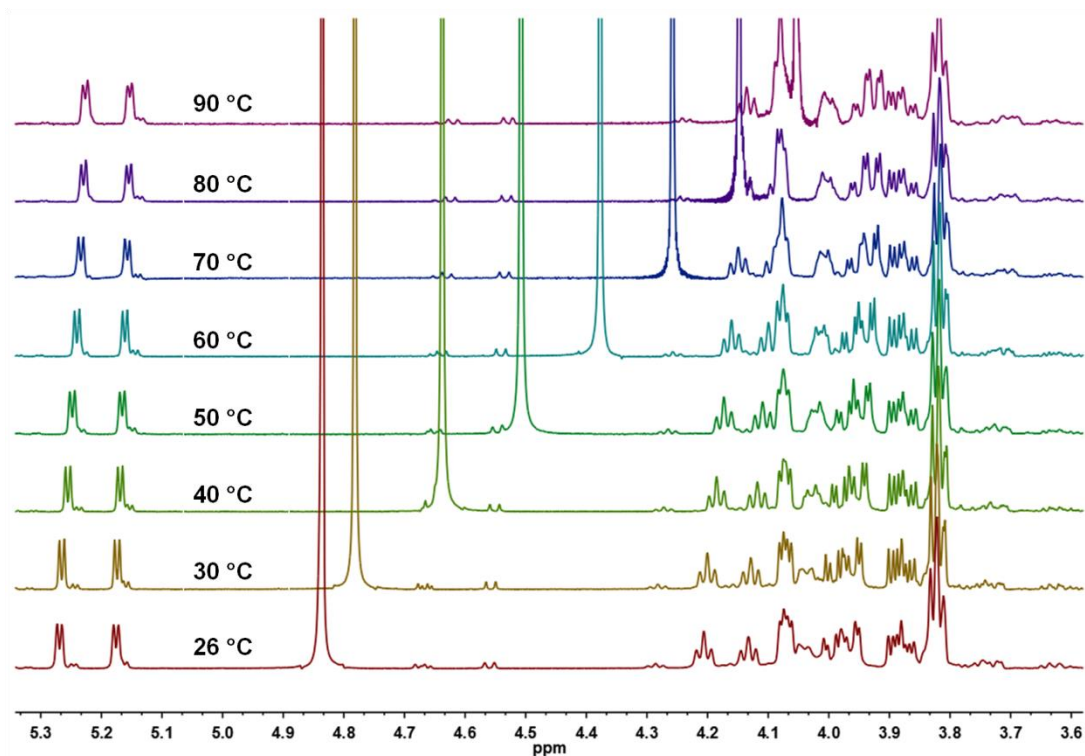
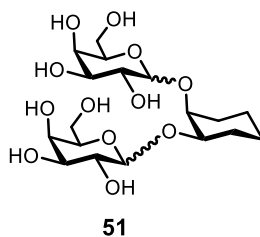


Figure 3-3. Stacked plot of ^1H NMR spectra of *pseudo*-trisaccharide **51** at variable temperature (from 26 °C to 90 °C, D_2O and 500 MHz).

3.5 Conclusions

Optimisation of the glycosylation reaction led to the conclusion that the use of thioglycosyl donor with a PMBz group instead of a benzyl ether at O-4 position, results in a great improvement in α -selectivity ($\alpha:\beta = 5:1$) which was possibly due to the remote protecting group participation. Unexpectedly, glycosylation reaction of 1,2-*cis*-cyclohexanediol to make a more simple analogue of trisaccharide **25** proved to be more difficult than manipulating sugars and their protecting groups. As a consequence, the synthesis of a trisaccharide had to be reinvented.

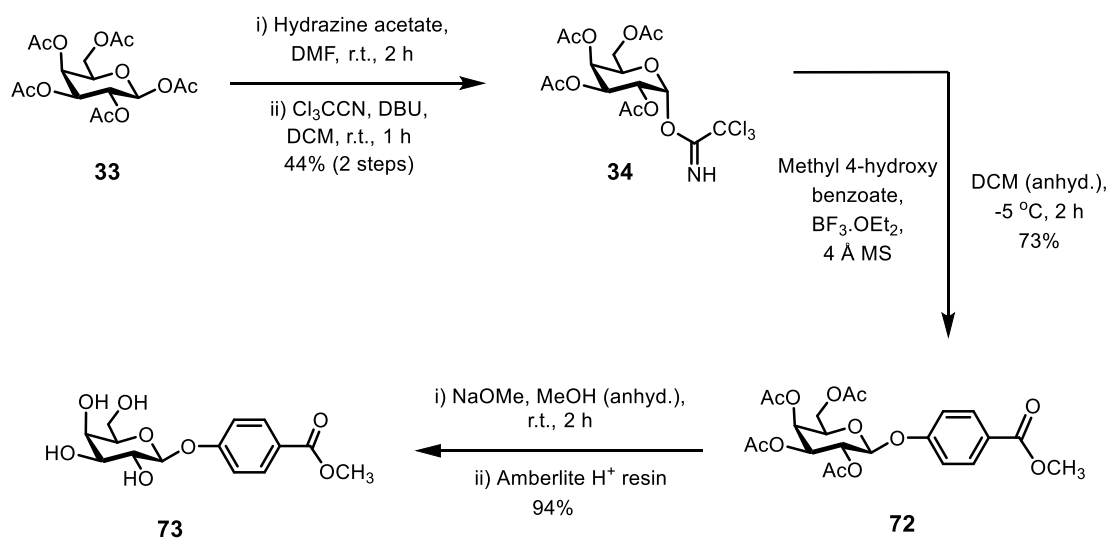
Chapter 4: Reinvention of the synthesis of a trisaccharide

4.1 Introduction

Working with 1,2-*cis*-cyclohexanediol appeared to be more problematic than performing experiments with sugars and manipulating their protecting groups (*cf.* Section 3.3); therefore, synthesis of the trisaccharide had to be redeveloped. According to Chapter 3, an improved glycosylation reaction had been identified. The remaining challenge to address was to enhance the regioselectivity of the protecting group chemistry and to allow stepwise glycosylation at the O-3 and O-4 positions. Moreover, as the trisaccharide will be further derivatised and used to attach to a multivalent scaffold to make multivalent carbohydrates, it was desirable to change the aglycone. A synthetic route to a trisaccharide with a carboxyphenyl aglycone was thus developed, starting with the synthesis of a glycosyl acceptor having an ester group.

4.2 Synthesis of a glycosyl acceptor containing a 4-methoxycarbonylphenyl group

The same synthetic procedures were employed as described in Chapter 2 for the preparation of a trisaccharide containing a 4-nitrophenyl group; in this case however, a 4-methoxycarbonylphenyl group was attached to the galactopyranoside instead. α -Trichloroacetimidate **34** was synthesised from galactose pentaacetate **33** by removal of the anomeric acetyl group, followed by treatment of the alcohol with trichloroacetonitrile under basic conditions (Scheme 4-1). The reaction of imidate **34** with methyl 4-hydroxy benzoate in the presence of $\text{BF}_3 \cdot \text{OEt}_2$ yielded β -galactopyranoside **72**, which was further subjected to Zemplén deacetylation in the presence of sodium methoxide in anhydrous MeOH, to give galactopyranoside **73**.



Scheme 4-1. Synthetic route to galactopyranoside **73**.

As mentioned in Section 2.3.1, the arrangement of the protecting group chemistry is required for attachment of the sugars one at a time. The next step was to protect galactopyranoside **73** at all of the hydroxyl groups except that at O-4 position, which would be available to partake in the next coupling reaction. According to the original synthesis, the regioselectivity of allylation needed to be improved.

4.2.1 Improved regioselectivity of allylation

Reaction of sugar hydroxyl groups with organotin reagents, e.g., dibutyltin oxide produces dibutyl stannylene acetals as intermediates that, after the treatment with an alkyl halide, give rise to corresponding monosubstituted products. However, the structure of the stannylene intermediate is not completely understood but it has been suggested that in non-polar solvents, such intermediates are predominantly in dimeric forms (Figure 4-1).¹³⁰

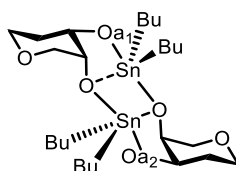
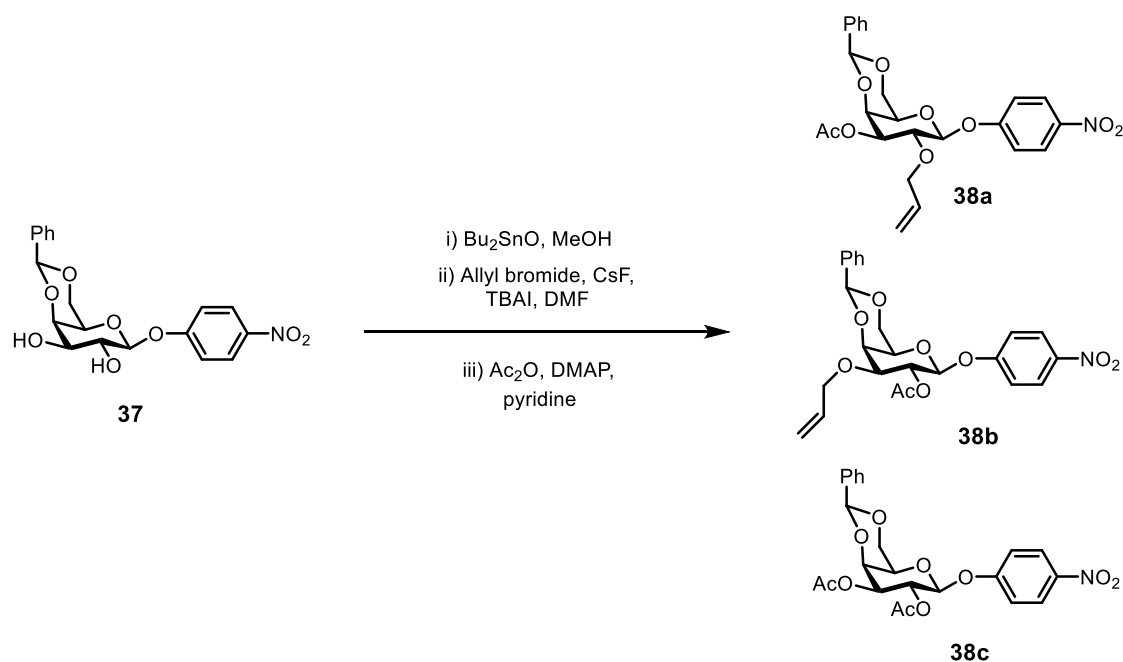


Figure 4-1. Formation of dibutyl stannylene acetal and dimerisation.

In a stannylene acetal monomer, the tin atom adopts a trigonal bipyramidal geometry. The apically bound oxygen atoms (Oa_1 and Oa_2) are more nucleophilic than the others; potentially the result of electron channelling from the tin atom and different effects of coordination.^{130,131} This activation is thought to lead to preferential Sn-O bond cleavage and bond formation of the apical oxygen atom with an electrophile, explaining the regioselectivity via dibutylstannylene acetals. Several studies showed that a dibutylstannylene acetal derived from a *cis*-diol on a pyranose ring generally gives a major product with an alkyl substituent at the equatorial position, whereas regioselectivities are usually poor in the case of *trans*-diols.¹³²

In the original synthesis in Section 2.3.1, a mixture of three compounds was obtained, demonstrating that the allylation of this *trans*-diol was not regioselective (Scheme 4-2). This observation is in the agreement with the hypothesis that the tin complex intermediate forming across the two equatorial positions will have similar reactivity. It might be more discriminating to use the tin acetal method with a 3,4-diol rather than a 2,3-diol (Figure 4-2). A method for the selective allylation was thus required to improve the trisaccharide synthesis.



Scheme 4-2. A non-regioselective allylation, giving a mixture of three products.

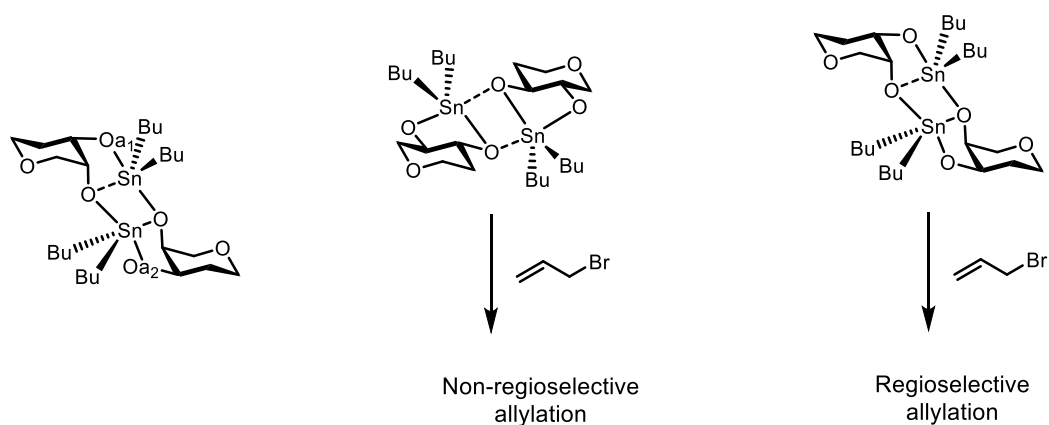
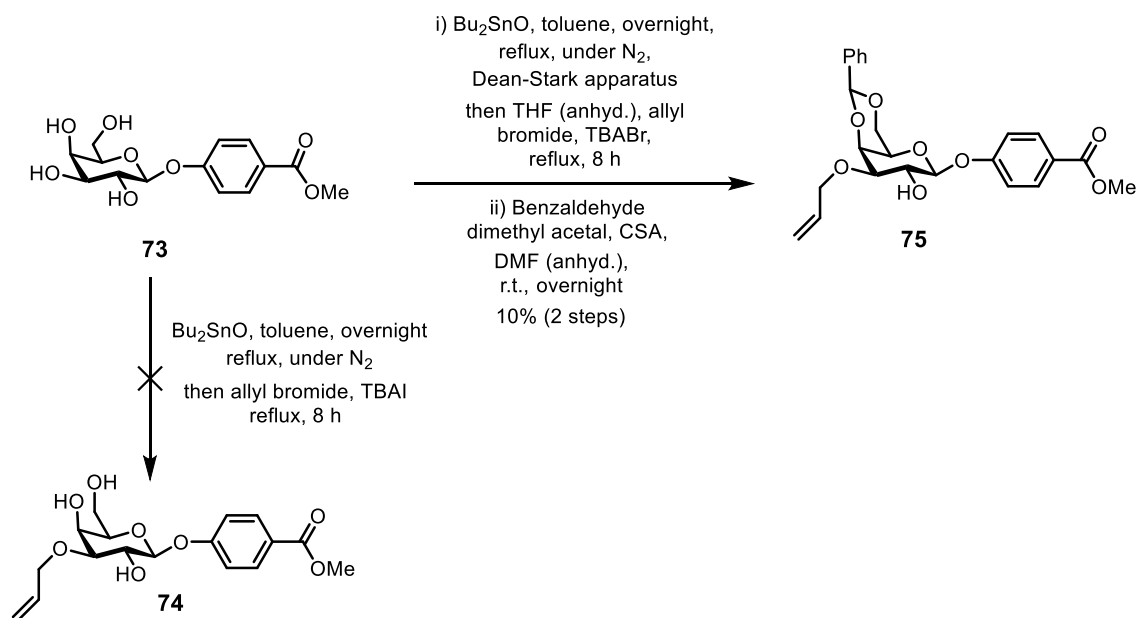


Figure 4-2. Possible explanations for non-regioselective and regioselective allylation via stannylenes acetals.

Peters and co-workers have reported a successful selective O-3 allylation by reacting unprotected 4-methoxyphenyl galactopyranoside with dibutyltin oxide in toluene, then with $\text{AlIBr}/\text{Bu}_4\text{NBr}$ in THF.¹³³ To simplify the literature process,¹³³ an attempt was made to conduct both tin acetal formation and allylation in toluene only for unprotected galactopyranoside **73** containing 4-methoxycarbonylphenyl (Scheme 4-3). However, TLC analysis showed multiple products formed, which rendered it difficult to separate by flash column chromatography. This unsuccessful reaction gave mostly di-substitution products, which was confirmed by mass spectrometric analysis. Following acetylation, ^1H NMR analysis showed that an allyl group was not substituted on the O-4

position but the other position, which could be the O-2, O-3 or O-6 positions, was less conclusive. Hence, in an attempt to achieve better regioselectivity, another allylation of galactopyranoside **73** was carried out by formation of the tin acetal in toluene, and subsequently allylation in THF as described in the literature procedures.¹³³ However, TLC analysis still showed formation of various products. After partial chromatographic purification, the sample was further subjected to 4,6-O-benzylidene protection to yield compound **75**. The position of the allyl group on galactopyranoside **75** was determined by acetylation with pyridine-acetic anhydride catalysed by DMAP. According to ¹H NMR analysis, the downfield shift of the O-2 acetyl group confirmed that the allyl group was successfully attached to the O-3 position (Figure 4-3). Nevertheless, compound **75** was obtained in a very low isolated yield, as a result of difficulties in purification and non-regioselective allylation.



Scheme 4-3. Attempted synthesis of compound **74** and synthetic route to compound **75**.

Unfortunately, the above tin-mediated allylation reactions on unprotected galactopyranoside **73** were not sufficiently selective. This would be because of the similar reactivity of the hydroxyl groups on the molecules. An alternative route to a better regioselectivity of allylation was still needed.

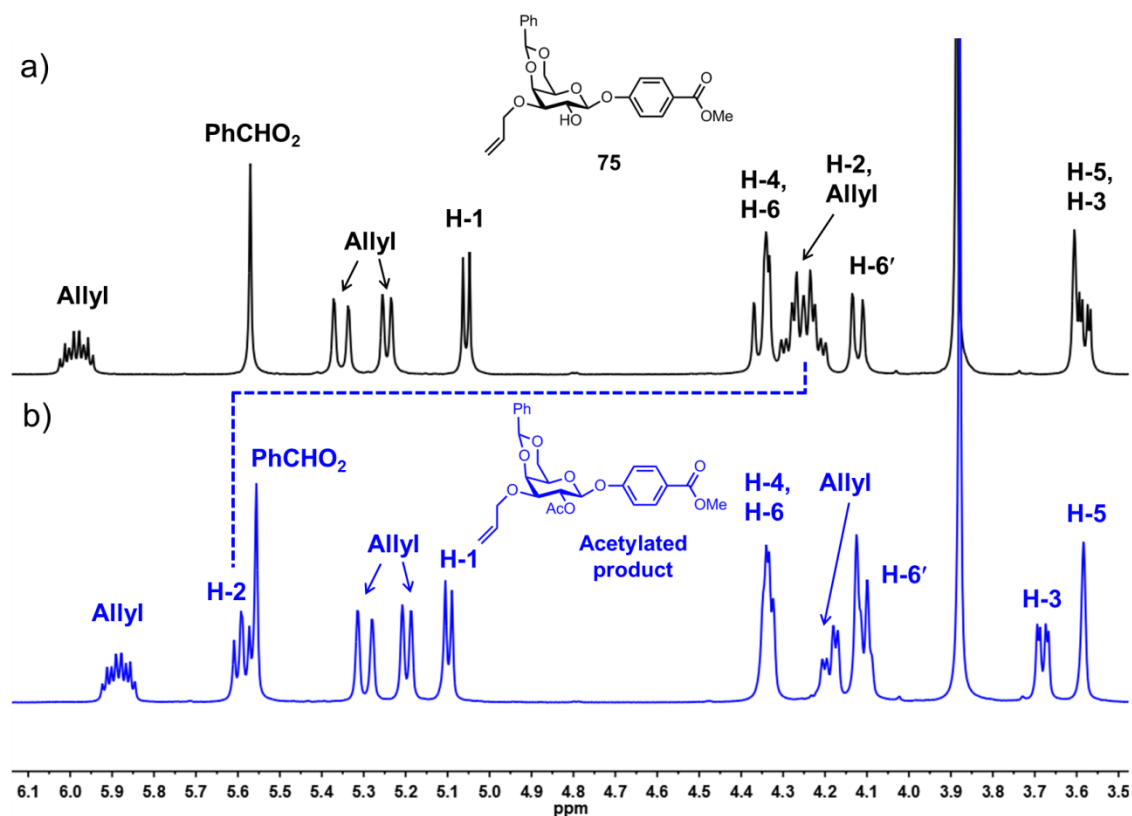
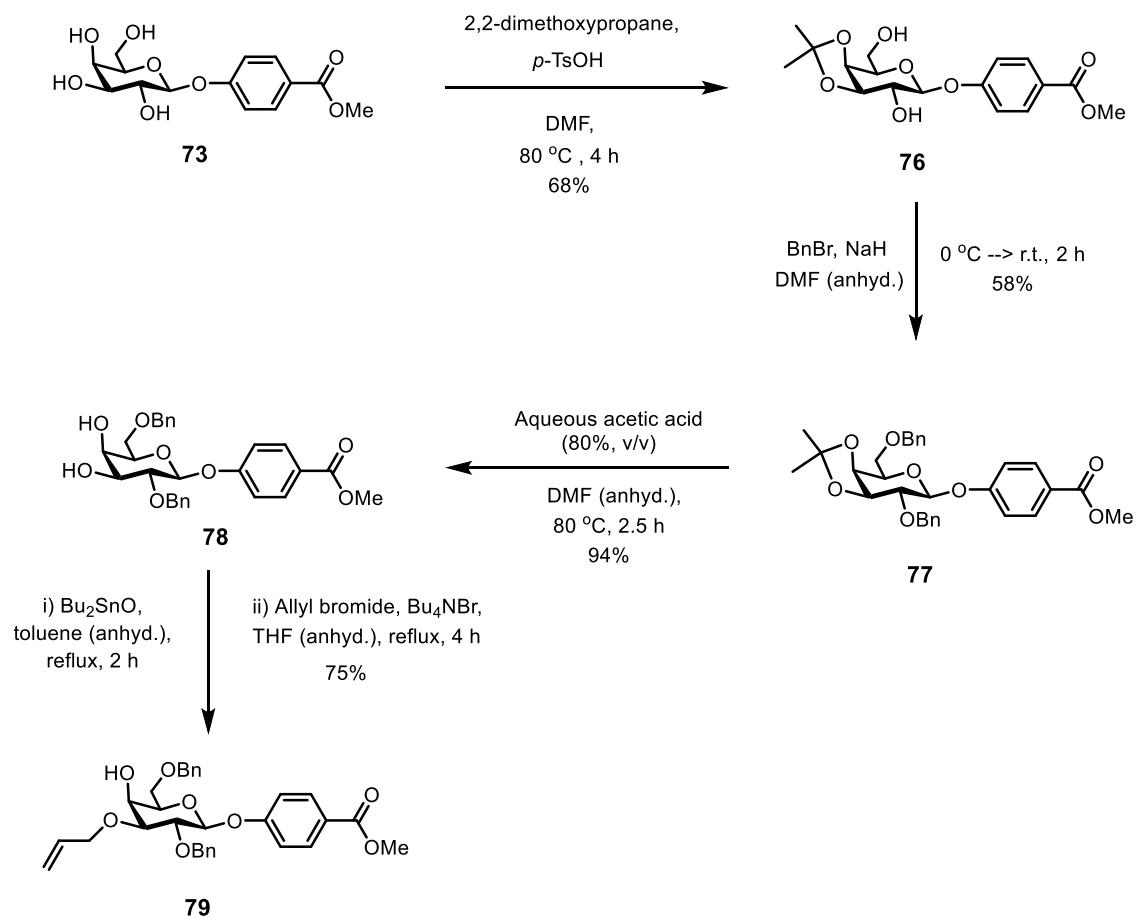


Figure 4-3. Confirmation of the presence of an allyl groups occupying at the O-3 position by acetylation at the O-2 position (cf. proton numbering in Figure 8-1). ^1H NMR spectra of a) galactopyranoside **75** and b) its acetylated product (500 MHz, CDCl_3).

Therefore, isopropylidene of galactopyranoside **73** with 2,2-dimethoxypropane in the presence of *p*-toluenesulfonic acid was carried out and gave 3,4-acetal **76** (Scheme 4-4). Benzoylation of the remaining hydroxyl groups, followed by removal of the isopropylidene group, revealed the O-3 and O-4 hydroxyl groups of galactopyranoside **77**. Subsequent stannylene acetal-mediated 3-O-allylation provided galactopyranoside **79** in a good yield with high regioselectivity. In this case, trying to distinguish between one equatorial and one axial hydroxyl groups worked successfully with tin chemistry because of their different reactivities. The presence of an allyl group at the O-3 position was confirmed by HMBC and HMQC experiments showing a correlation of the allyl group to H-3 (Figure 4-4). This result demonstrates a significant improvement in the synthesis of the glycosyl acceptor **79**, for use in glycosylation reactions.



Scheme 4-4. Synthetic route to galactopyranoside **79**.

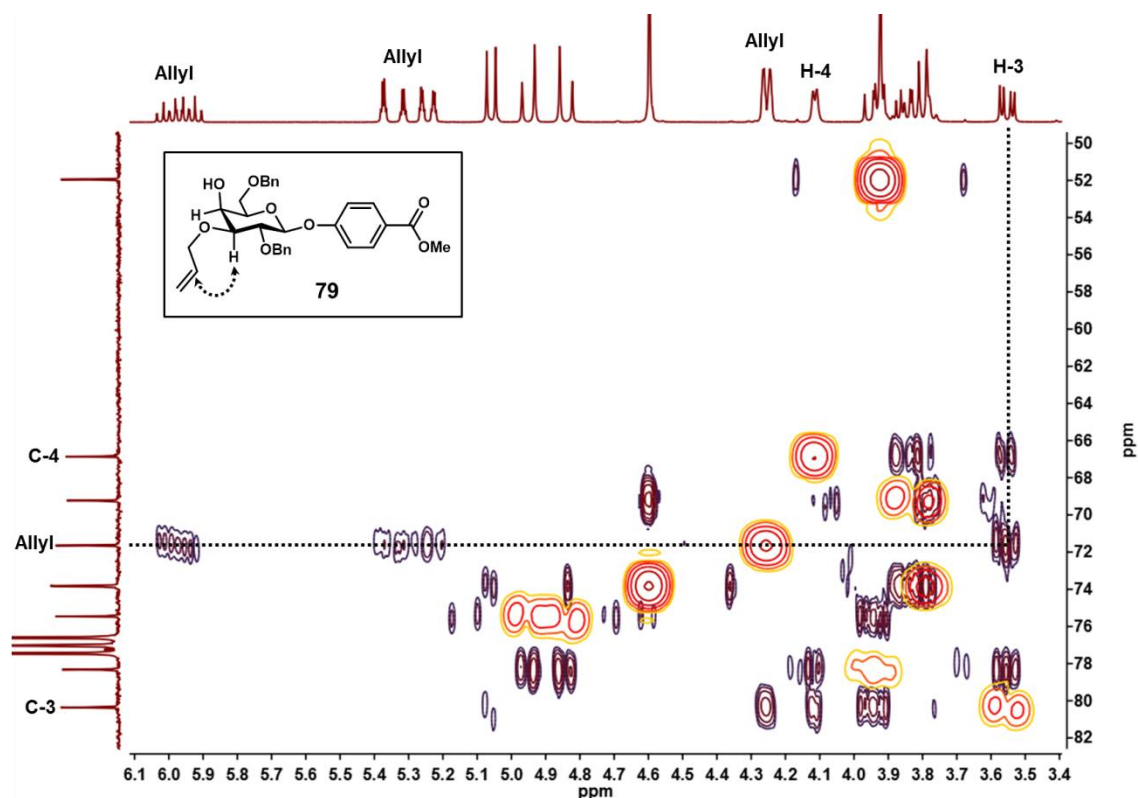
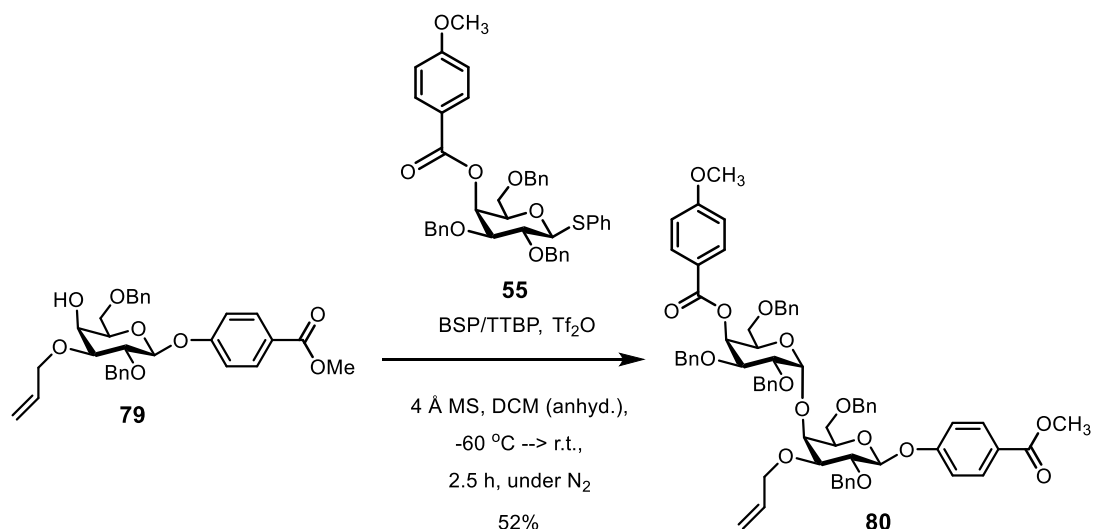


Figure 4-4. Overlay of the HMQC (red) and HMBC (purple) spectra of galactopyranoside **79** (75 MHz, CDCl₃) showed a correlation of C-allyl group to H-3 indicating the attachment of an allyl group at the C-3 position.

4.3 Synthesis of a disaccharide intermediate

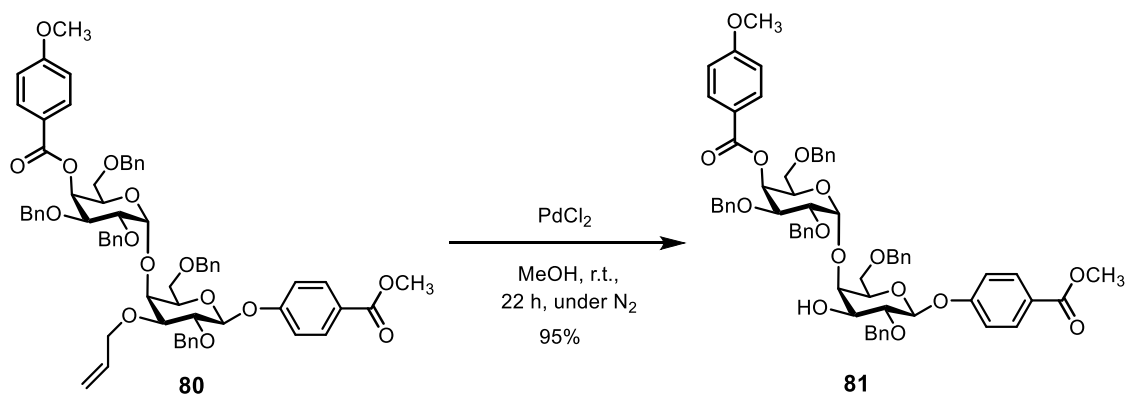
A gram-scale coupling reaction between glycosyl acceptor **79** (1.3 g) and 4-methoxybenzoyl thioglycosyl donor **55** (1.7 g) was performed, which provided disaccharide **80** in 52% yield (Scheme 4-5). ¹H NMR signals corresponding to a disaccharide with a β-linkage was not found, suggesting an α-selectivity greater than 99% for the glycosylation reaction.



Scheme 4-5. Synthetic route to disaccharide **80**.

4.4 Selective deprotection: deallylation

Deallylation of disaccharide **80** provided disaccharide **81** with a free O-3 hydroxyl group in a good yield (Scheme 4-6). Comparison of ^1H NMR spectra showed the disappearance of the allyl group peaks that were present for compound **80**, confirming the selective deprotection was successful (Figure 4-5), and ready to be used as a glycosyl acceptor for the synthesis of the target trisaccharide.



Scheme 4-6. Synthetic route to compound **81**.

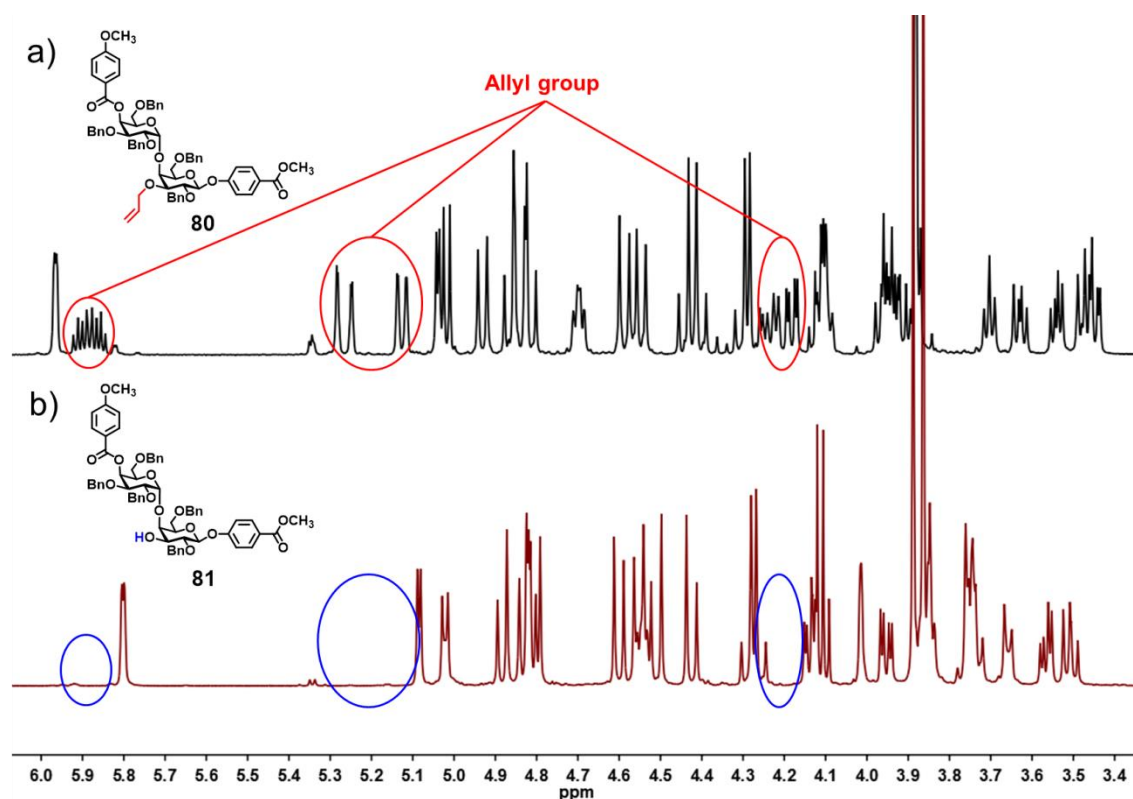
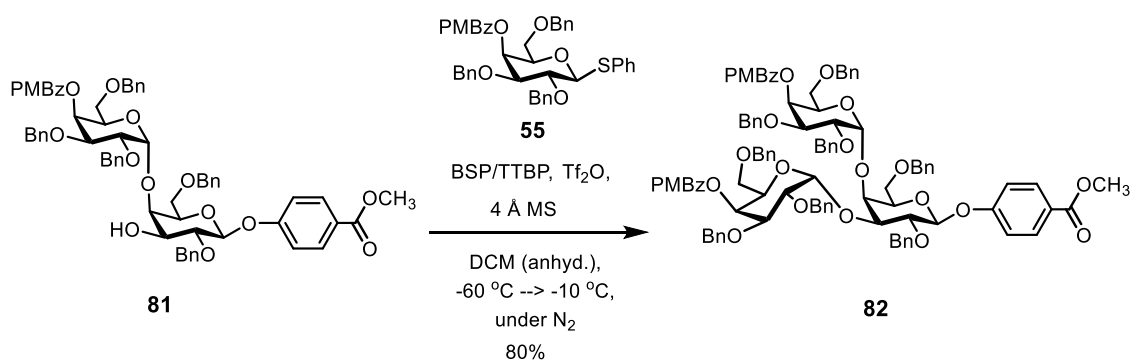


Figure 4-5. A stacked plot of ^1H NMR spectra of a) allylated compound **80** and b) deallylated compound **81** (500 MHz, CDCl_3).

4.5 Attaching another galactose residue to the disaccharide intermediate

Glycosylation of disaccharide **81** with glycosyl donor **55** was carried out under the same conditions as used in the synthesis of the disaccharide intermediate, providing fully-protected trisaccharide **82** (Scheme 4-7).



Scheme 4-7. Synthetic route to trisaccharide **82**.

^1H NMR experiments of trisaccharide **82** at 301 and 328 K in CDCl_3 were conducted to assess the molecular dynamics of the molecule. The spectrum at 301 K showed

broadened signals for some atoms, but the resonance peaks sharpened upon warming to 328 K (Figure 4-6). The expanded area displayed distinct proton signals, *i.e.*, two signals for H-4 next to each PMBz ester group and three anomeric protons; one for each monosaccharide unit. The broadening of their anomeric signals was probably due to the rate of conformational exchange occurring on a similar time scale to that of the NMR experiment. Upon warming to 328 K, the rate of conformational exchange was increased and an average signal for two different conformational states was observed.

The ^1H NMR spectrum at a higher temperature also revealed the coupling constants of three anomeric protons, which were 2.3 Hz, 3.3 Hz, 6.7 Hz, corresponding to the two α -configurations, and one with β -configuration, respectively. It is noteworthy that the proton-proton coupling constant of H-1 β was slightly lower than the value obtained for disaccharide **81** (7.0 Hz) as well as for the deprotected trisaccharide (7.5 Hz).[‡] The attachment of another galactose residue at the adjacent position was likely to affect the structural arrangement of the central galactose residue, which may have deviated from a perfect $^4\text{C}_1$ chair conformation. The distortion of the bond angle between the coupled H-1 β and H-2 β protons might therefore cause a decrease in their coupling constants. However, other proton signals of trisaccharide **82**, acquired at 301 and 328 K, were difficult to assign but they did not seem to broaden as for the anomeric proton signals, suggesting that the NMR signals broadening were not associated with the tumbling of the molecule.

[‡] For a detailed assignment of trisaccharides, see experimental.

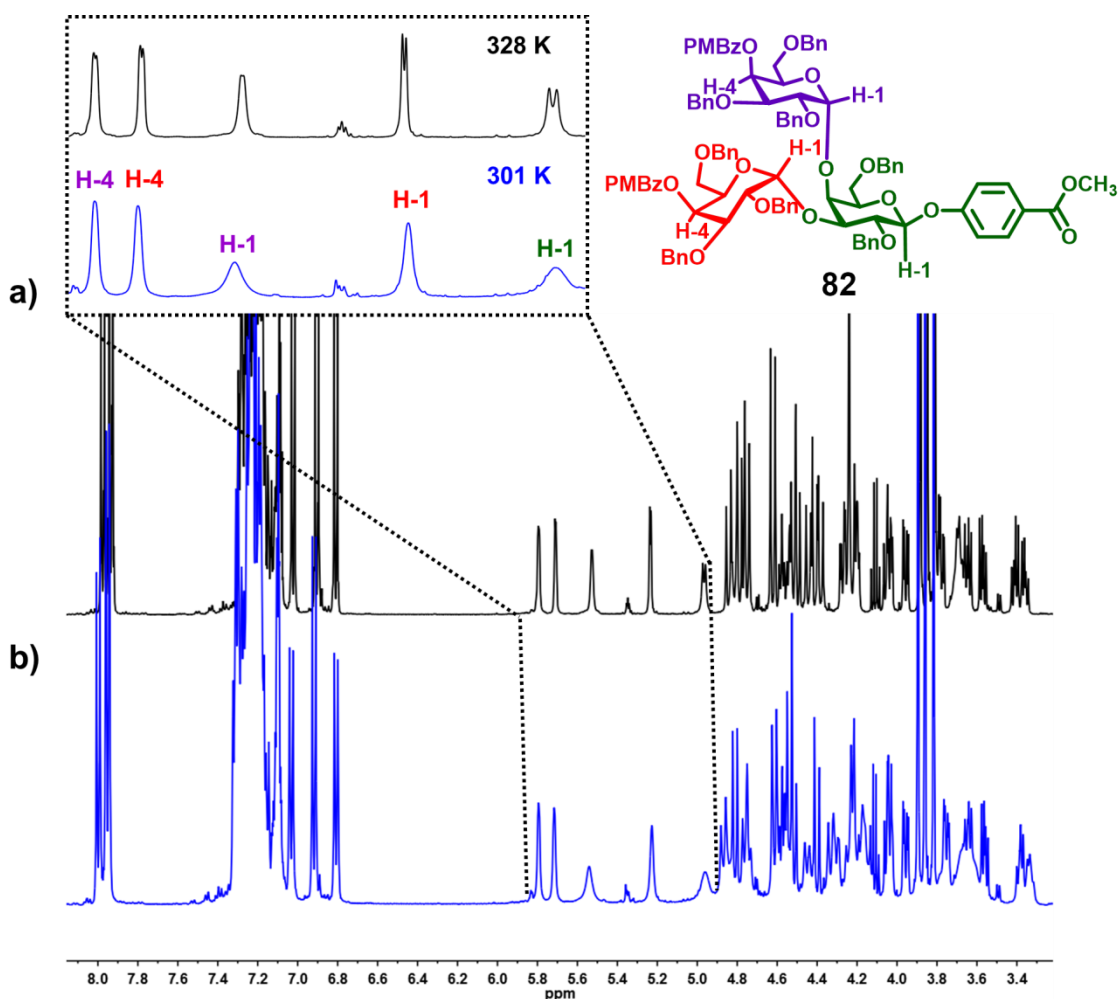


Figure 4-6. Stacked plot of the entire ^1H NMR spectra and the expanded area of trisaccharide **82** (500 MHz, CDCl_3) a) at higher temperature (328 K) and b) at room temperature (301 K). The expanded area showed distinct proton signals, *i.e.*, two signals for H-4 next to each C-4 ester group and three anomeric protons (2 \times H-1 α and H-1 β).

Two dimensional NMR experiments (*i.e.*, COSY, TOCSY, HMQC, HMBC) acquired at 331 K of trisaccharide **82** were also acquired in order to obtain sharpened peaks and to analyse the correlations between galactose residues. The overlaid HMBC and HMQC spectra of the trisaccharide **82** showed a correlation between one of the C-1 signals of the adjacent galactose units and the H-3 signal of the central galactose residue; the other C-1 signal coupled to the H-4 signal of the central galactose residue (Figure 4-7). Observation of these correlations enabled unambiguous assignment of the signals to each of the terminal galactose residues. ^1H - ^1H COSY and TOCSY spectra of trisaccharide **82** with the complete assignments of sugar proton resonances are shown in Chapter 9: Appendix.

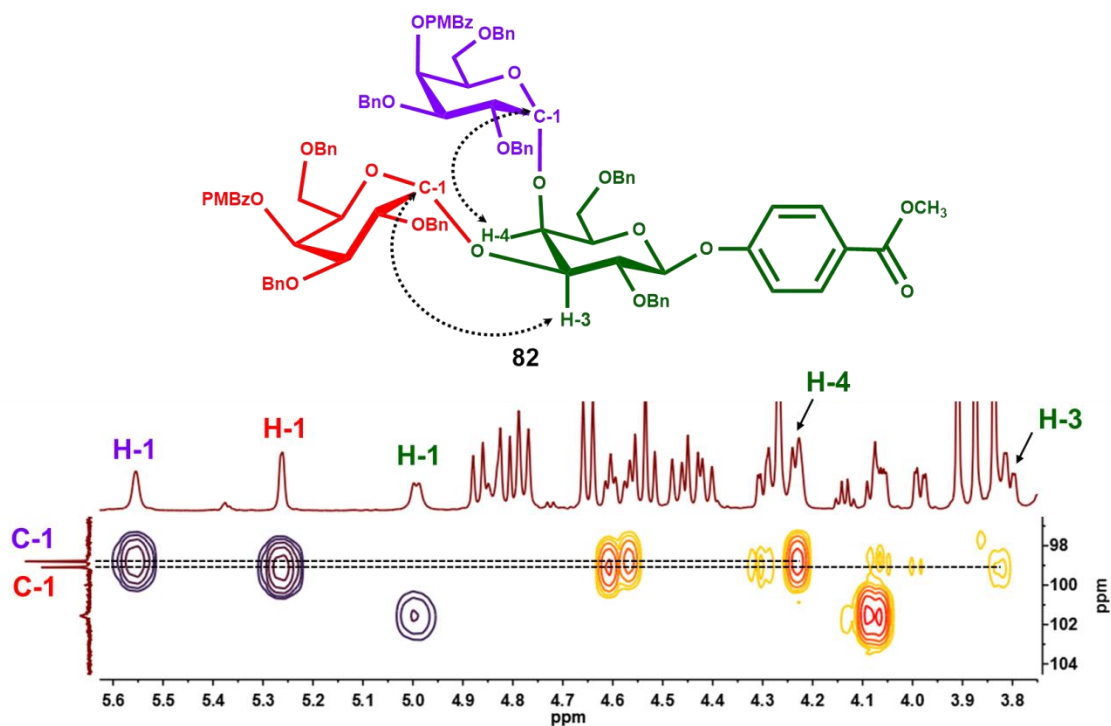
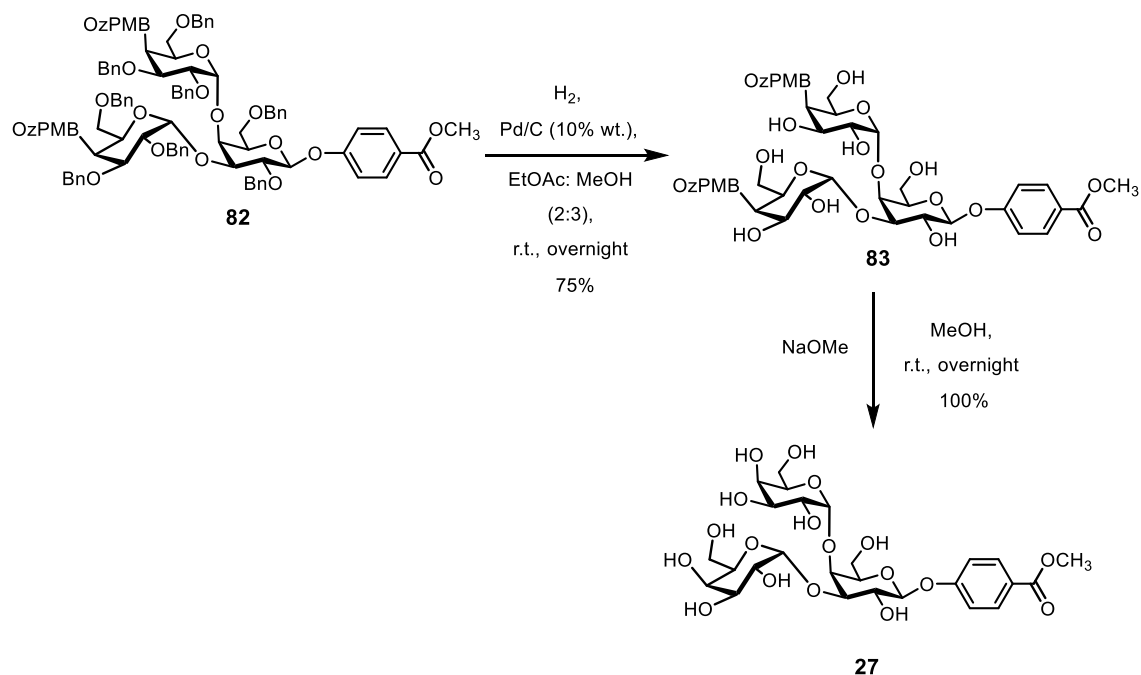


Figure 4-7. Overlay of HMBC (red) and HMQC (blue) spectra of trisaccharide **82** (75 MHz, CDCl_3 , 331 K) showed that the C-1 signals of the adjacent galactose units correlated with the signals of each H-3 and H-4 of the central galactose residue.

4.6 Removal of the protecting groups

Benzyl ether protecting groups were removed by hydrogenolysis of trisaccharide **82** to give trisaccharide **83**, which was subjected to de-esterification to give fully-protected trisaccharide **27** containing a 4-methoxycarbonylphenyl group (Scheme 4-8). This compound will be used as a monovalent compound for the testing for inhibitory effect on LOX-1 and for further converting its ester group to a hydrazide group and attaching to a multivalent scaffold.



Scheme 4-8. Synthetic route to fully-deprotected trisaccharide **27**.

4.7 Conclusions

The synthesis of an analogue of the lead trisaccharide containing a carboxyphenyl aglycone has been reinvented. After several attempts, the overall yield and the regioselectivity of the synthesis of a glycosyl acceptor precursor was significantly improved. This precursor was used for coupling with a thioglycosyl donor having a 4-methoxybenzoyl group at the O-4 position, which resulted in a great improvement in α -selectivity. Subsequent deallylation and another glycosylation reaction, with the same glycosyl donor under the optimised conditions, were successful, leading to the formation of a protected trisaccharide. After deprotection, the analogous trisaccharide was ready to be further derivatised and used to attach to a multivalent scaffold. Evaluation of the novel analogues for their inhibitory activity against LOX-1 expressing cells will be further performed.

Chapter 5: Carbohydrate-functionalised polymers as multivalent inhibitors for targeting LOX-1

A part of this chapter has been discussed in the following article: "Templating carbohydrate-functionalised polymer-scaffolded dynamic combinatorial libraries with lectins" Mahon, C. S.; Fascione, M. A.; Sakonsinsiri, C.; McAllister, T. E.; Turnbull, W. B.; Fulton, D. A. *Organic & Biomolecular Chemistry*, **2015**, *13*, 2756-2761.

5.1 Introduction

Carbohydrate-protein interactions are typically of low affinity. Multivalency enhances the binding affinities by having multiple interactions that reinforce one another. The multivalency effect in synthetic systems can be reproduced through the attachment of multiple carbohydrate residues to multivalent scaffolds, e.g., nanoparticles, polymers and dendrimers.

Among the synthetic multivalent forms of carbohydrate structures, glycopolymers have attracted much interest as tools to study the multivalent effects of carbohydrates to lectins (carbohydrate-binding proteins that are highly specific for carbohydrate moieties), cells and pathogens.^{134,135} Glycopolymers can be prepared either by the polymerisation of carbohydrate-bearing monomers or by the post-polymerisation glycosylation of synthetic polymers.¹³⁶ Various polymer backbone monomers, e.g., polyacrylamides, poly(*p*-phenylene ethynylene), have been incorporated in the glycopolymers (Figure 5-1).

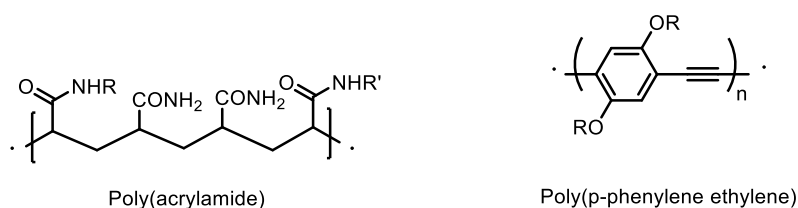


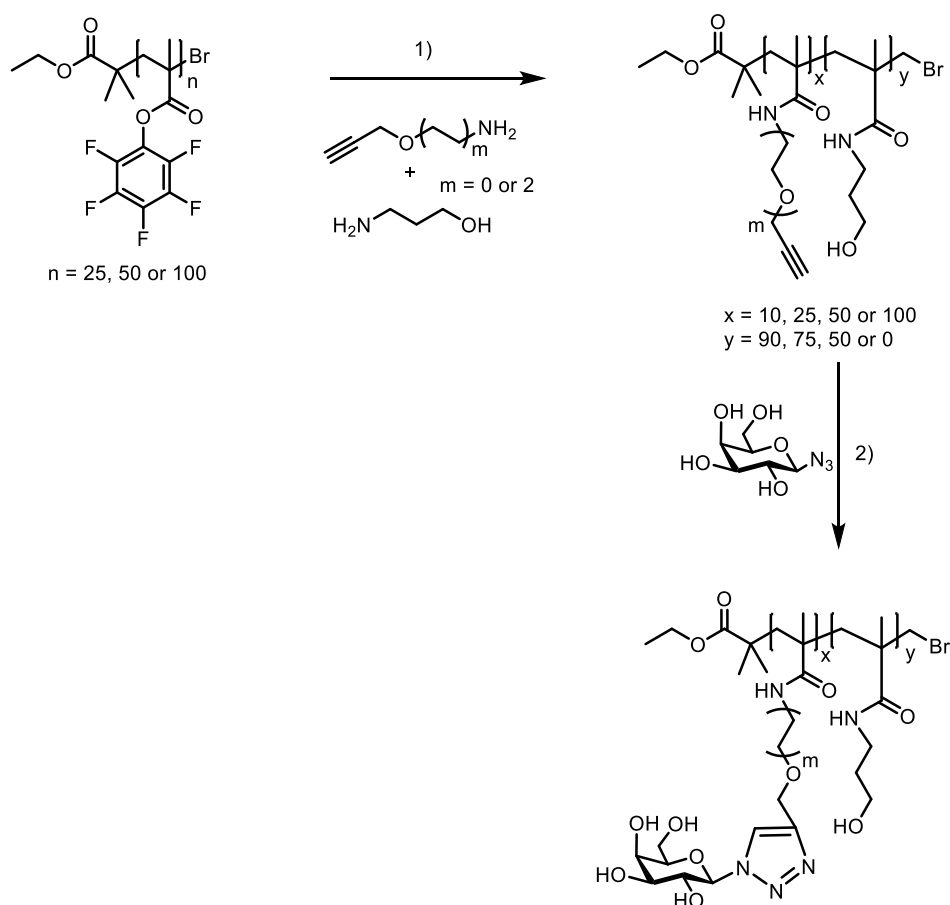
Figure 5-1. Representative examples of polymer scaffolds.

Selected examples of carbohydrate-functionalised polymers will be highlighted here. Whitesides and co-workers first successfully synthesised polyacrylamides bearing pendant α -sialoside groups which could inhibit the haemagglutination of influenza viruses. The authors suggested that the inhibitory potency depends on the polymerisation conditions and the sialic acid content of the polymers, demonstrating that multivalent polymers have amplified inhibitory effects.¹³⁷

Another example was the use of a fluorescent-labelled carbohydrate-functionalised poly(*p*-phenylene ethynylene) to detect multivalent pathogens, e.g. *E. coli*.¹³⁸ Multivalent interactions between mannose receptors on the bacterial pili and the mannosylated polymer could result in cell aggregation and allowed bacterial detection.

More recently, the Gibson group successfully prepared galacto-functional polymers by a tandem post-polymerisation modification methodology for use as cholera toxin inhibitors.¹³⁹ They used poly(pentafluorophenyl methacrylate) as the template scaffold

to react with two amino-functional alkynes and 2-hydroxypropylamine (Scheme 5-1). β -D-Galactose residues were subsequently 'clicked' on to pendant alkyne moieties to form galacto-functional polymers with varying sugar density, linker length and chain length. The series of glycopolymers was used to study the effect of carbohydrate-binding site accessibility with their target lectins, *i.e.*, the B-subunit of cholera toxin and peanut agglutinin. The latter lectin was used as a control because it binds to β -galactose. Their results showed that the polymer with longer linkers exhibited increased inhibition of B subunit of cholera toxin, which was related to the depth of the binding pocket.



Scheme 5-1. Preparation of galacto-functionalised polymers by a tandem post-polymerisation modification. 1) amine (variable amounts)/triethylamine (TEA; 1 equiv.)/ DMF, 5 h.; 2) GalN₃ (1.5 equiv./CuBr/TBTA, DMSO).

The Fulton group have developed the so called "polymer-scaffolded dynamic combinatorial library" (PS-DCL) concept which presents a new strategy to discover macromolecular receptors. Functionalised polymers were prepared by coupling different acylhydrazide residues onto an aldehyde-bearing polymer scaffold via acylhydrazone linkages (Figure 5-2).¹²⁴

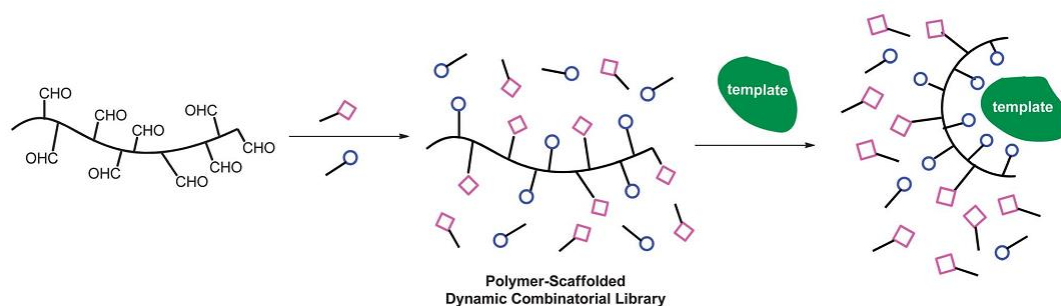


Figure 5-2.¹²⁴ Preparation of a polymer scaffold dynamic combinatorial library by reaction of acylhydrazines (represented as open purple squares and open blue circles) with a polymer bearing aldehyde functionalities. Changes of the residual composition within the PS-DCL was induced upon addition of a molecular template, figure reproduced from reference 124.

The reversible aspect of these linkages permits compositional changes on the polymer scaffold to favour products that bind to the target. Synthetic polymers and proteins, which were a 70 kDa poly(sodium-4-styrene sulfonate), bovine serum albumin (BSA) and bovine trypsin, were used as molecular templates. Upon the addition of different templates, the PS-DCL was shown to re-equilibrate and adapt its composition favouring binding to the specific template added, resulting in macromolecules with enhanced capabilities for molecular recognition. This approach could be used to generate synthetic recognition receptors for selected proteins and inexpensive antibody mimics. Moreover, using the same strategy, carbohydrate residues possessing a hydrazide group can be incorporated onto the same type of polymer scaffolds to form carbohydrate-functionalised polymer-scaffolded dynamic combinatorial libraries which will be further discussed in this chapter.

5.2 Aims and objectives

One of the aims of this chapter was to synthesise multivalent carbohydrate-based polymers presenting multiple copies of the target trisaccharide. These multivalent structures could aid in the development of more effective inhibitors with higher inhibitory potency towards LOX-1, a major receptor for Ox-LDLs involved in atherosclerosis initiation and progression. The inhibition by tri-galactoside polymers would be expected to block the binding of Ox-LDLs to its receptor, leading to a decrease in atherosclerotic plaque formation. One approach was to append carbohydrate compounds possessing reactive hydrazine groups to a multivalent polymer bearing aldehyde functions. In this chapter, the synthetic route to α -mannosyl and α -galactosyl hydrazides and the development of glycopolymer dynamic combinatorial libraries will first be presented. The derivatisation of the trisaccharide

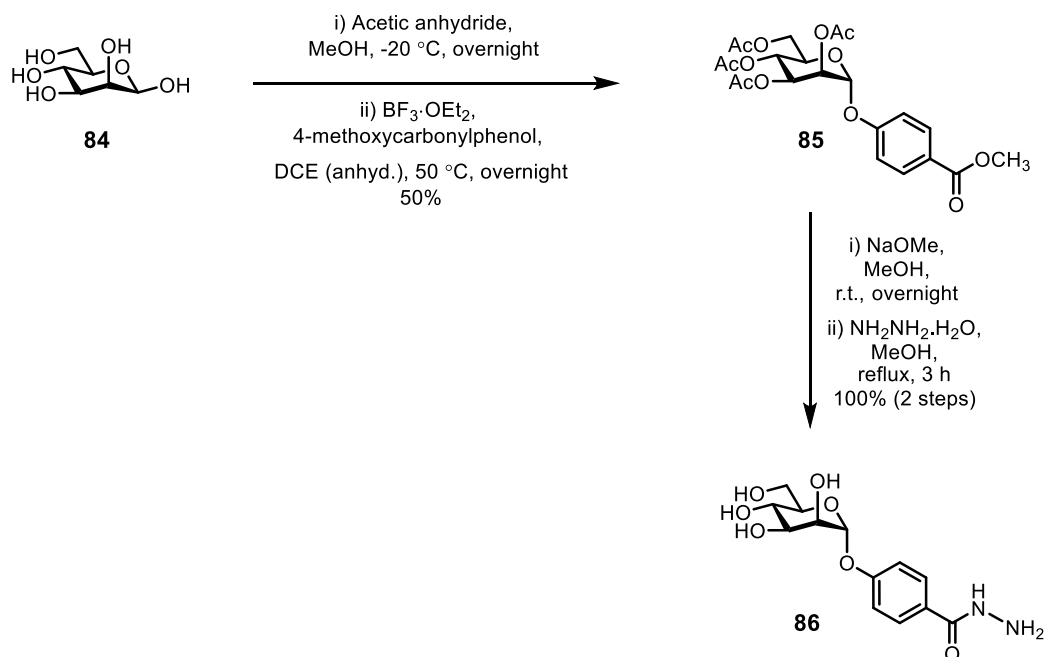
ligand for LOX-1 with a hydrazine to the corresponding hydrazide will subsequently be discussed. Preparation of carbohydrate-functionalised polymers and a polymer without carbohydrate moieties, which would serve as inhibitors for LOX-1 and a control polymer respectively, will also be outlined.

5.3 Synthesis of α -mannosyl and α -galactosyl hydrazides for making carbohydrate-functionalised polymer-scaffolded dynamic combinatorial libraries (PS-DCLs)

In collaboration with Dr. C. Mahon and Dr. D. Fulton (School of Chemistry, University of Newcastle), α -galactosyl and α -mannosyl hydrazides were used to generate carbohydrate-functionalised polymer-scaffolded dynamic combinatorial libraries (PS-DCLs), which were investigated further as macromolecular receptors for lectin templates.¹²⁵

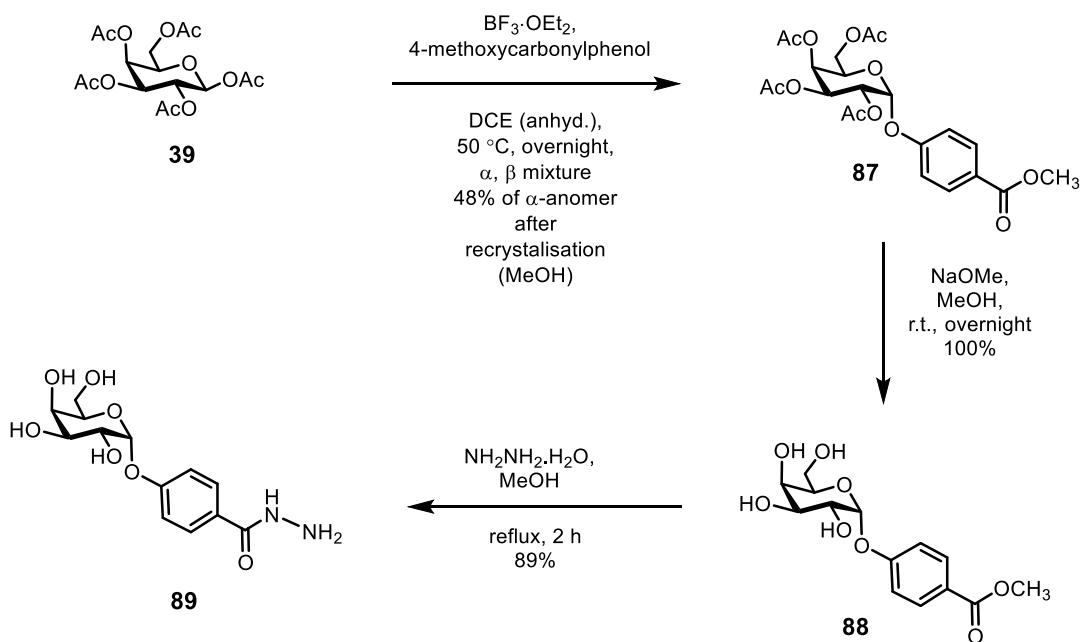
5.3.1 Synthesis of α -mannosyl and α -galactosyl hydrazides

α -Galactosyl and α -mannosyl hydrazides **86** and **89** were synthesised both by Dr. M. Fascione and C. Sakonsinsiri. The synthesis of mannosyl hydrazide **86** was achieved starting from acetylation of β -D-mannose **84**, followed by glycosylation of 4-methoxycarbonylphenol. Following recrystallization from MeOH, α -D-mannopyranoside **85** was obtained (Scheme 5-2). The resulting compound was deacetylated under Zemplén conditions and was subsequently reacted with hydrazine monohydrate in refluxing MeOH to afford α -D-mannopyranoside **86** having a hydrazide group at one end.



Scheme 5-2. Synthetic route to mannosyl hydrazide **86**.

Similarly, galactose pentaacetate **33** was reacted with 4-methoxycarbonylphenol to form α -galactopyranoside **87**, which was deacetylated under Zemplén conditions (Scheme 5-3). The resulting compound **88** was subjected to hydrazinolysis, providing α -D-galactopyranoside **89** possessing a hydrazide group.



Scheme 5-3. Synthetic route to galactosyl hydrazide **89**.

5.3.2 Templating carbohydrate-functionalised polymer-scaffolded dynamic combinatorial libraries with lectins

This part of the work was performed by Dr. C. Mahon. The α -mannosyl hydrazide **86** and α -galactosyl hydrazide **89** (Figure 5-3) were reversibly conjugated to an aldehyde-functionalised polymer using acylhydrazone exchange chemistry (Figure 5-4), generating carbohydrate-functionalised polymer-scaffold dynamic combinatorial libraries (PS-DCLs).¹²⁵ The PS-DCLs were prepared at pH 4.5.

PS-DCLs exhibited compositional changes upon the addition of lectin templates. Two very different lectins used as molecular templates in the study were Con A, and the B-subunit of *E.coli* heat labile toxin (LTB) with specificity for mannose-containing molecules and galactose-containing molecules, respectively.

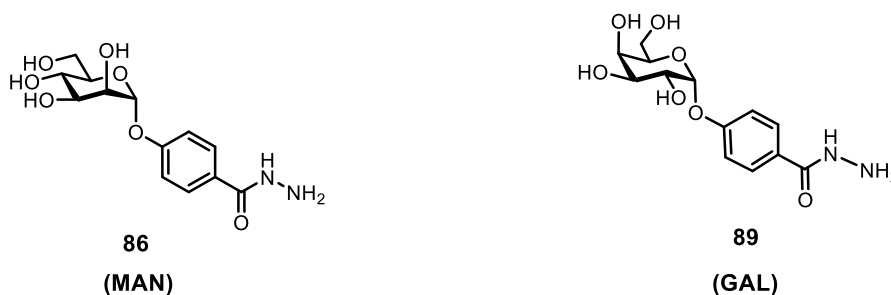


Figure 5-3. α -Mannosyl hydrazide **86** (also called **MAN**) and α -galactosyl hydrazide **89** (also called **GAL**) used for the synthesis of carbohydrate-functionalised polymer-scaffold dynamic combinatorial libraries (PS-DCLs).

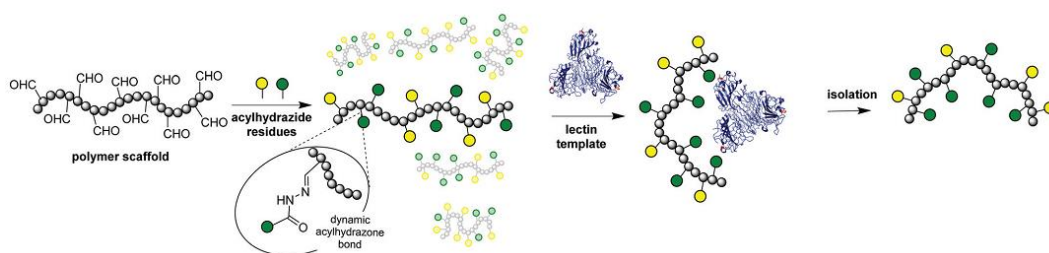


Figure 5-4.¹²⁵ Preparation of a carbohydrate-functionalised polymer-scaffold dynamic combinatorial library by conjugation of acylhydrazone functionalised carbohydrate residues onto an aldehyde-functionalised polymer scaffold. Compositional changes within PS-DCL were induced upon addition of a lectin, resulting in polymers of improved affinity for the lectin added, figure reproduced from reference 125.

The initial residue composition of the polymer scaffold containing **86** and **89** was determined by ¹H NMR spectroscopy as a ratio of 1.0:1.0. Upon addition of Con A, an

increase in the relative concentrations of mannose residues **86** and galactose residues **89** was in a 1.2:1.0 ratio, indicating the polymer scaffolds have adapted their composition by preferentially incorporating the mannose residues with the loss of galactose residues (Figure 5-5). Upon addition of LTB a decrease occurred in the relative concentration of mannose and galactose residues to 0.8:1.0, suggesting that the polymer scaffolds have also incorporated galactose residues in preference to mannose residues. These carbohydrate-functionalised PD-DCLs were shown to undergo compositional changes upon the addition of lectin templates, with the polymer backbone incorporating residues that are preferentially recognised by the target lectin. Furthermore, templating carbohydrate-functionalised PS-DCLs with lectins proved to provide polymeric macromolecular receptors of enhanced affinities for the lectin templates.

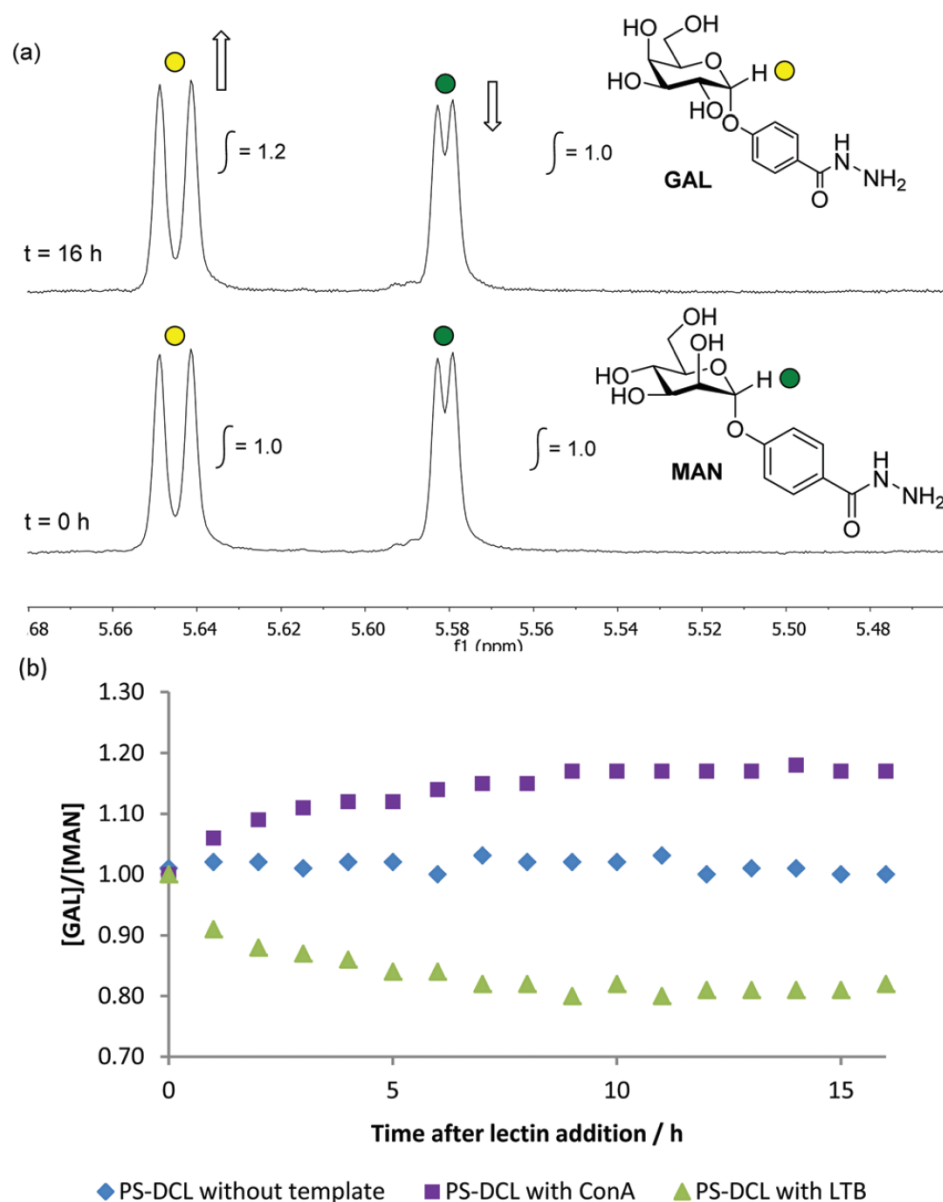


Figure 5-5.¹²⁵ a) ^1H NMR spectroscopic analysis (500 MHz, D_2O , pH 4.5) of PS-DCL before ($t = 0$ h) and after ($t = 16$ h) addition of Con A, highlighting the changes in intensity of the diagnostic anomeric resonances of **GAL** and **MAN** 16 h after addition of template. b) Effect of addition of lectin templates to PS-DCLs upon relative concentrations of **GAL** and **MAN** as a function of time, suggesting preferential incorporation of the carbohydrate residue preferred by the lectin added. There is no observed change in the relative concentrations of **GAL** and **MAN** in the absence of a lectin template, figure reproduced from reference 125.

5.4 Preparation of the polymers with the LOX-1 ligand trisaccharide

According to the PS-DCL method, the exchange process only happens when the system is at pH 4.5, and at pH 7 is no longer dynamic. Therefore, it is also possible to use these polymer scaffolds to prepare glycopolymers without necessarily exploiting the PS-DCL method.

Since the interaction of individual trisaccharide epitope with LOX-1 was weak, it was anticipated to increase the binding affinity to LOX-1 by attachment of trisaccharide **27** (Figure 5-6) with the above described polymer scaffold. However, prior to the attachment, there is a need to derivatise the trisaccharide to the corresponding hydrazide.

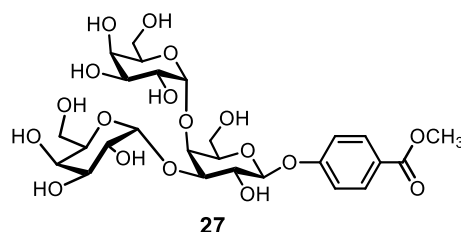
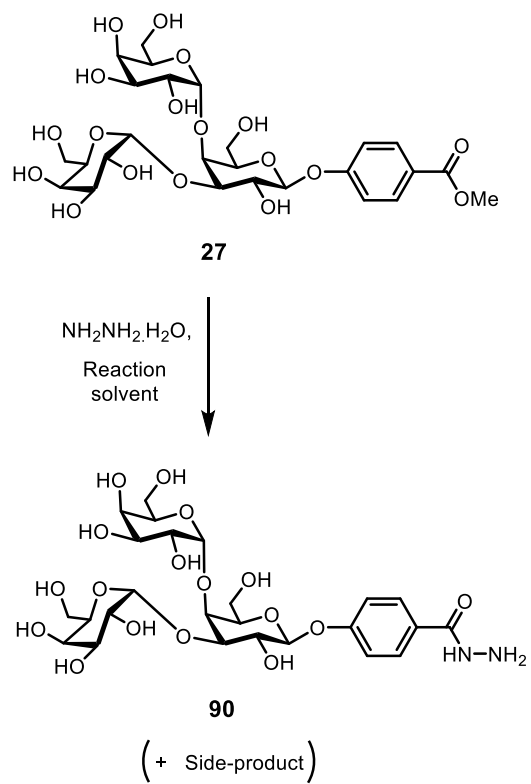


Figure 5-6. Chemical structure of trisaccharide **27**.

5.4.1 Derivatisation of the trisaccharide for attaching to a multivalent scaffold

To derivatise the previously synthesised trisaccharide **27** (*cf.* Chapter 4), hydrazinolysis reactions of trisaccharide **27** were conducted under different conditions to produce a trisaccharide **90** having an aryl hydrazide (Table 5-1). The progress of the reactions was monitored by ^1H NMR chemical shift changes in the aromatic proton signals. The aromatic proton NMR spectrum of the starting material **27** is shown in entry 1 of Table 5-1. Due to the limited solubility of trisaccharide **27** in MeOH, which had been used for previous hydrazide syntheses, hydrazinolysis reactions of trisaccharide **27** were first attempted in deuterium oxide (D_2O), while varying molar equivalents of hydrazine and reaction times. ^1H NMR spectrum of the overnight reaction using one equivalent of hydrazine showed aromatic signals corresponding to a mixture of two products; however, some the starting material also remained in the solution. After adding additional hydrazine and heating at 70 °C for further 16 h, the starting material was completely consumed (Table 5-1, entry 2); but this reaction still provided a mixture of two compounds, which would render the isolation and purification laborious. On the assumption that the side reaction might be suppressed by increasing the amount of hydrazine, another hydrazinolysis was attempted with an excess of hydrazine in water. The reaction was monitored by ^1H NMR spectroscopy at 2 h, 3 h and 4 h. In spite of 20-equivalent addition and 80 °C-heating, this hydrazinolysis did not proceed to completion and a mixture of two products still formed (Table 5-1, entry 3). These observations demonstrated that water might not be the best solvent for performing hydrazinolysis of the target trisaccharide.

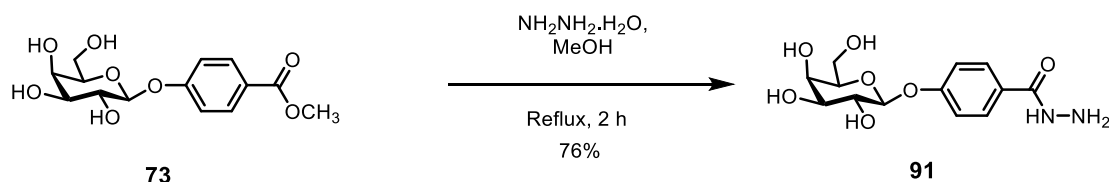
Table 5-1. Hydrazinolysis reactions of trisaccharide **27**.



Entry	Solvent	Hydrazine	Temp.	Time	¹ H NMR (500 MHz, 8.1-7.1 ppm, D ₂ O)
1	D ₂ O	Starting material 27			
2		1 equiv.	70 °C	16 h	
		2 equiv.		32 h	
3		10 equiv.	70 °C	2 h	
		20 equiv.		3 h	
		20 equiv.	80 °C	4 h	
4	MeOH	20 equiv.	Reflux	4 h	

8.1 8.0 7.9 7.8 7.7 7.6 7.5 7.4 7.3 7.2

All previous hydrazinolysis reactions had been performed in methanol; for example, hydrazinolysis of β -galactopyranside **73** with hydrazine monohydrate was successful in methanol as the solvent; giving rise to β -galactosyl hydrazide **91** (Scheme 5-4). However, because of the poor solubility of the trisaccharide **27** in methanol, performing hydrazinolysis in methanol was initially avoided.



Scheme 5-4. Synthetic route to β -galactopyranside **91**.

After several attempts in D₂O, hydrazinolysis of trisaccharide **27** was eventually successful in refluxing MeOH, despite its incomplete solubility, giving trisaccharide **90** as a sole product (Table 5-1, entry 4). Aromatic proton signals of the product having an aryl hydrazide appeared at 7.75 ppm and at 7.32 ppm, whereas those of the starting material were at 8.04 ppm and 7.34 ppm. Disappearance of the methoxyl group peak that was present for the starting material was also observed, indicating the hydrazinolysis had been achieved. In addition, ¹³C NMR spectrum of the product did not show any signal corresponding to the methoxyl functional group that was present for the starting material.[§]

5.4.2 Identification of the side-product formed in the reaction in D₂O using ¹H NMR spectroscopy

As LC-MS and HRMS analyses did not provide satisfactory results either by employing negative- or positive ion mode, ¹H NMR spectroscopy was used to identify the side-product formed when performed hydrazinolysis in D₂O (Figure 5-7). The product mixture from entry 3 of Table 5-1 was lyophilised to remove the excess hydrazine. The sample was then treated with sodium hydroxide (2 equiv., D₂O, 2 h) and neutralised with H⁺ ion exchange resin. Aromatic regions of the ¹H NMR spectra of the starting material and different samples were compared. Aromatic proton signals of the attempted hydrazinolysis (Figure 5-7b) showed a mixture of three compounds, which was comparable with the starting trisaccharide (Figure 5-7a), the desired hydrazide

[§] For a detailed assessment of compound **90**, see experimental.

product (Figure 5-7d), and the hydrolysed product after the treatment with sodium hydroxide and ion exchange H^+ resin (Figure 5-7c). This experiment with sodium hydroxide proves that the side-product formed from hydrazinolysis in D_2O was a trisaccharide containing a carboxyl group. This might be because there was more water than hydrazine present in the solution to react with the ester functionality on the trisaccharide. Methanol was thus the solvent of choice for hydrazinolysis of carbohydrates. Despite the poor solubility in MeOH, the hydrazinolysis could be carried out in suspension.

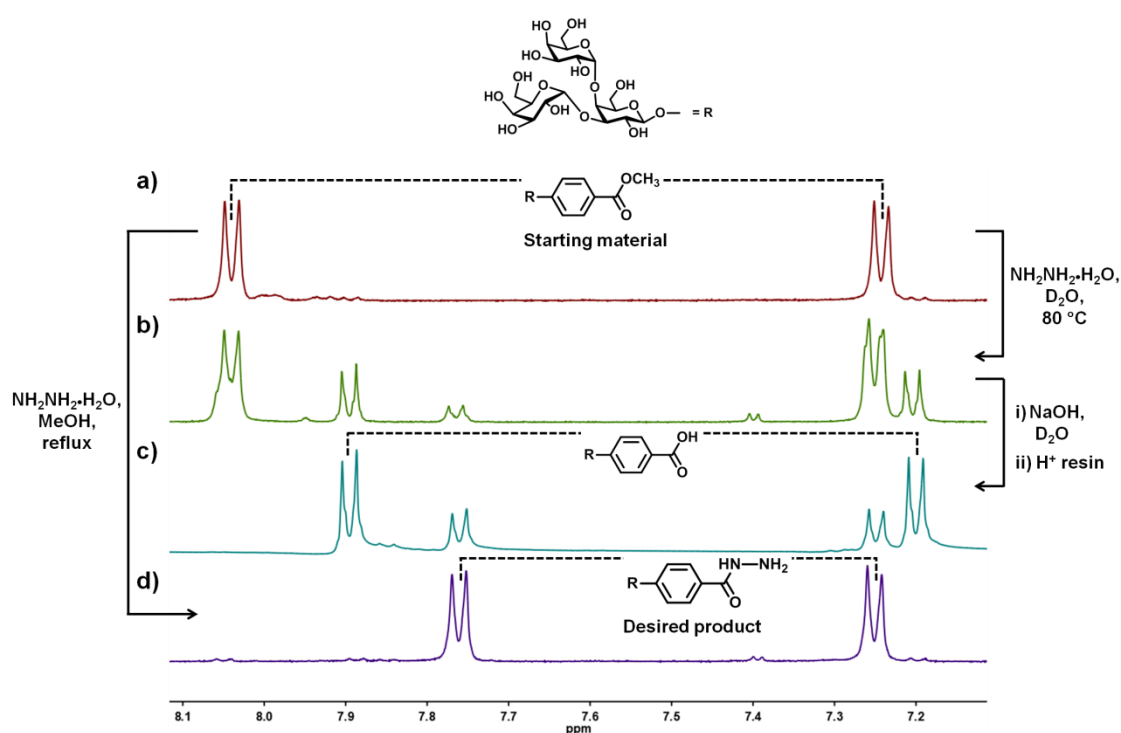


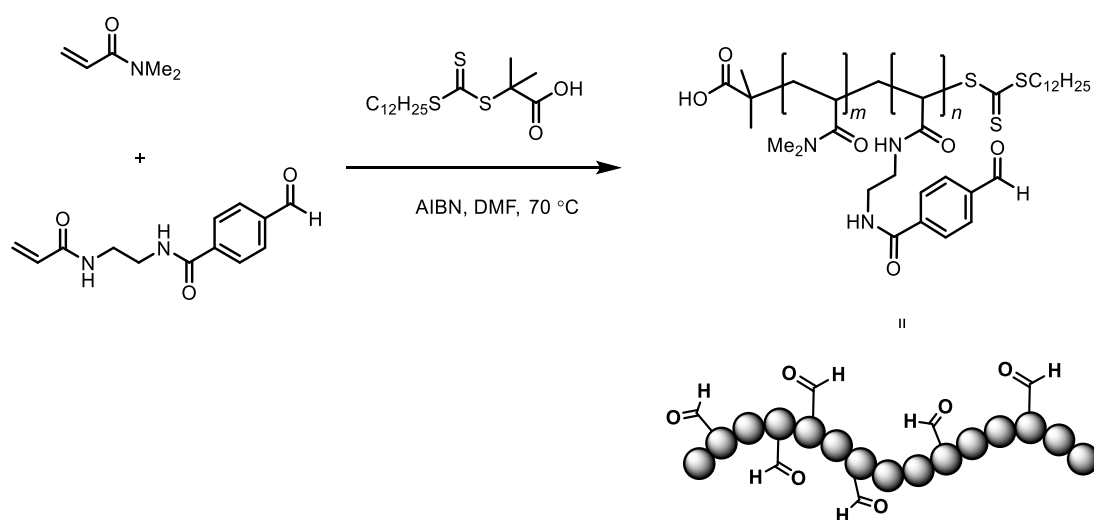
Figure 5-7. Comparison of the aromatic regions of the 1H NMR spectra of: a) the trisaccharide with an aryl ester group (starting material), b) the attempted hydrazinolysis in D_2O which still contains the starting material, c) the hydrolysed products of a mixture from previous attempted reaction and d) the desired hydrazinolysis product which was formed by the hydrazinolysis in MeOH. All 1H NMR spectra were acquired at 500 MHz in D_2O .

5.4.3 Synthesis of carbohydrate-functionalised polymers

Protein-carbohydrate interactions are generally weak; presenting multiple carbohydrate moieties on a multivalent scaffold could be a means to improve the binding affinity. As mentioned in Section 5.3.2, the collaborative work with Dr. C. Mahon and Dr. D. Fulton showed that an aldehyde-functionalised polymer could be used as a multivalent scaffold to conjugate with mannose- and galactose-functionalised arylhydrazide residues.¹²⁵ It was therefore anticipated that employing the same strategy

would allow the preparation of a target trisaccharide-functionalised polymer for the increased inhibition of the trisaccharide with LOX-1 receptor.

All of the following polymer preparations were performed by Dr. C. Mahon. An aldehyde functionalised polymer containing approximately 24 aldehyde units was prepared following a general reported procedure of Jackson and Fulton (Scheme 5-5).^{124,140} This aldehyde functionalised polymer was then used to conjugate with the target trisaccharide **90**, using the same procedure as used for conjugating mannose- and galactose-functionalised arylhydrazide residues, to form a glycopolymer containing approximately 24 units of trisaccharide epitopes (Figure 5-8).¹²⁵



Scheme 5-5. Synthesis of an aldehyde-functionalised polymer with variation of numbers of monomers.

Also, a monogalactoside polymer, which contains approximately 24 units of α -galactopyranoside residues, was prepared (Figure 5-9) and would be used to assay as an inhibitor of LOX-1. α -Galactopyranoside **89** was selected to be tested because α -glycosidic linkages were thought to be important for the binding of carbohydrates to LOX-1 receptor as present in the trisaccharide version.

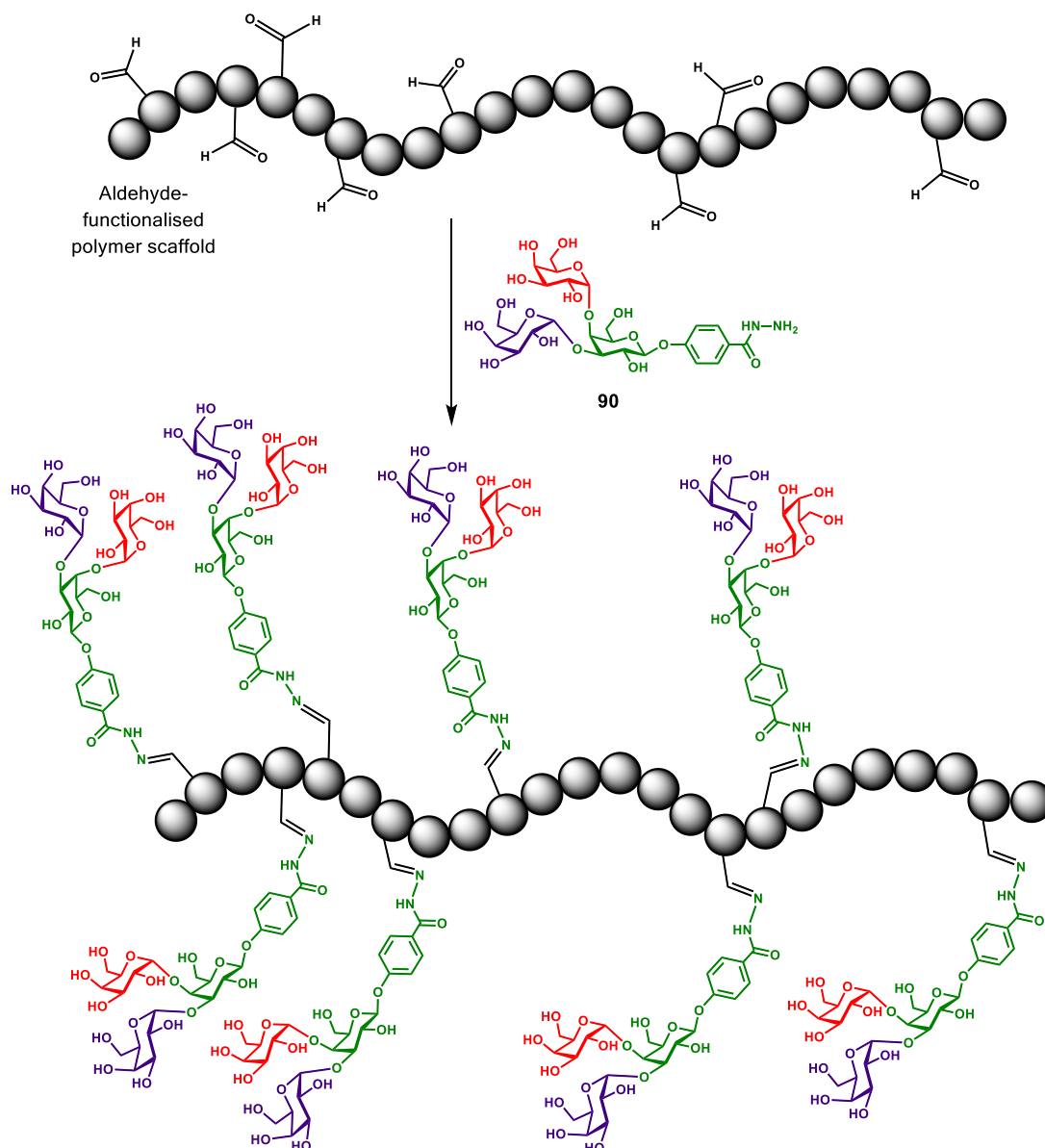


Figure 5-8. Cartoon presentation of the attachment of target trisaccharide residues **90** onto an aldehyde-functionalised polymer.

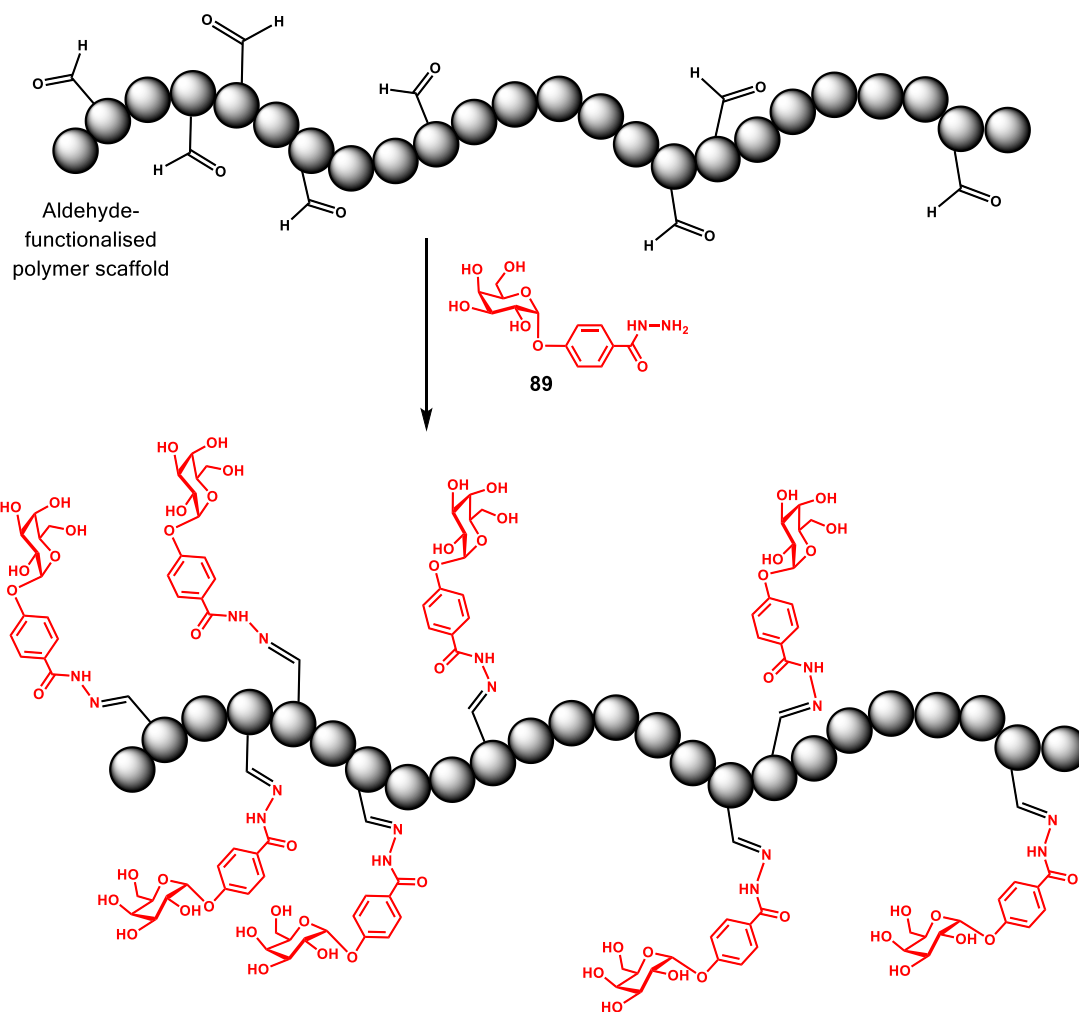
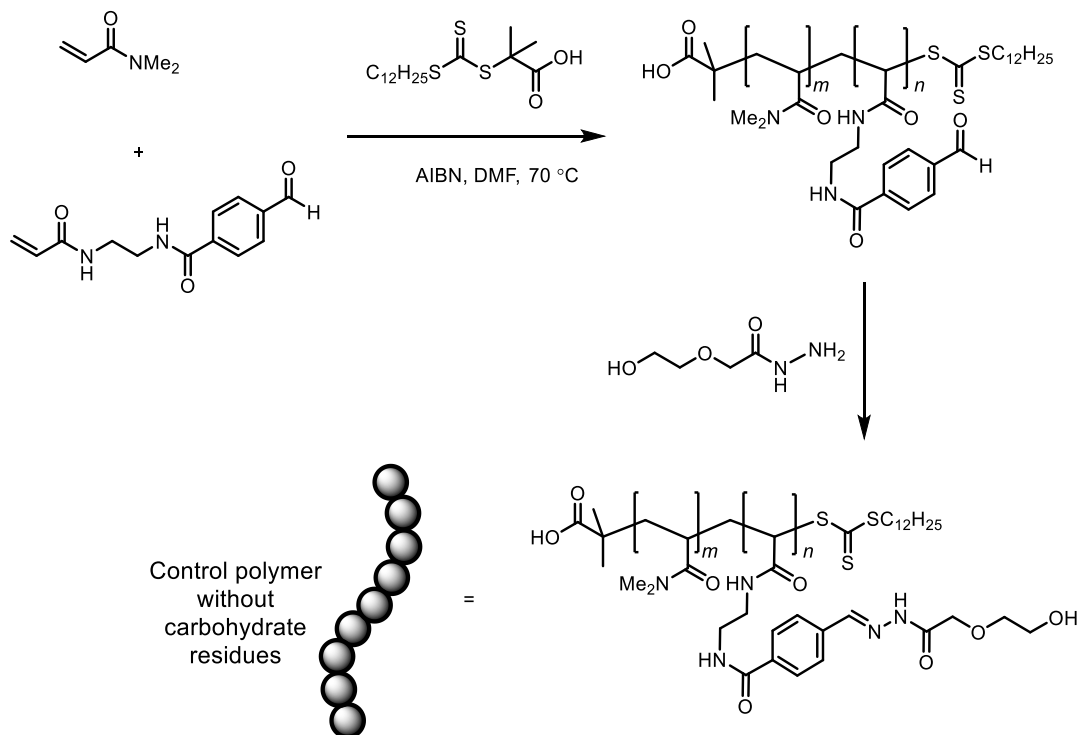


Figure 5-9. Cartoon presentation of the attachment of α -galactopyranoside residues **89** onto an aldehyde-functionalised polymer.

Another polymer containing ethylene glycol units instead of carbohydrate residues (Scheme 5-6) was also synthesised by Dr. C. Mahon and would be used as a control polymer for LOX-1 binding assays.



Scheme 5-6. Synthesis of a control polymer having ethylene glycol units instead of carbohydrate residues.

The generated mono- and tri-galactoside glycopolymers as well as the control polymer without sugar moieties appeared to be completely soluble in phosphate-buffered saline (PBS) pH 7.4. These synthesised glycopolymers in PBS buffer will be assayed for LOX-1 inhibitory effects.

5.5 Conclusions

α -Galactosyl and α -mannosyl hydrazides were synthesised and used for the generation of carbohydrate-functionalised polymer-scaffold dynamic combinatorial libraries (PS-DCLs) by hydrazine exchange under acidic conditions. These polymers induced compositional changes in response to addition of the lectin templates, thus producing polymers of enhanced binding affinities towards the lectin template.

The compositional exchange process in the PS-DCLs only occurs at pH 4.5, but not at pH 7. However, these polymers can be used to prepare non-dynamic glycopolymers for other purposes, e.g., for preparation LOX-1 polymeric carbohydrate based inhibitors. A trisaccharide was therefore derivatised and attached to these polymers for further study.

Derivatisation of the trisaccharide with hydrazine monohydrate in D_2O was problematic, giving a hydrolysed trisaccharide with a carboxylic group. This side-product was

identified by the treatment of an attempted reaction with sodium hydroxide and analysed by ^1H NMR spectroscopy. Hydrazinolysis of the trisaccharide was eventually achieved in refluxing MeOH despite its insolubility in MeOH.

Preparation of glycopolymers was performed by Dr. C. Mahon. As expected, the derivatised trisaccharide containing a reactive hydrazide group was successfully attached to an aldehyde-functionalised polymer using the same procedures as for the preparation of polymers conjugated with α -mannosyl and α -galactosyl hydrazides. In addition, a polymer containing approximately 24 of α -galactopyranoside residues was also synthesised and was to be used to compare the inhibitory effects on LOX-1 with the synthesised polymer bearing trisaccharide residues. Another polymer containing ethylene glycols instead of sugar residues was prepared to use as a control polymer for LOX-1 inhibition assays. Polymeric multivalent carbohydrate structures incorporating with mono-and trisaccharide residues as well as the control polymer were successfully developed and will be evaluated for their inhibitory effects with LOX-1 receptor. Multivalency would be expected to enhance the binding affinity of the inhibitors to LOX-1, which in turn would efficiently block the binding of OxLDL to its receptor and ultimately provide an effective novel inhibitor for LOX-1.

Chapter 6: Synthesis and biological evaluations of multivalent probes for DC-SIGN

This chapter is based upon the following article: "Compact, polyvalent mannose quantum dots as sensitive, ratiometric FRET probes for multivalent protein-ligand interactions" Guo, Y.; Sakonsinsiri, C.; Nehlmeier, I.; Fascione, M.A.; Zhang, H.; Wang, W.; Pöhlmann, S.; Turnbull, W.B.; Zhou, D. *Angewandte Chemie International Edition*, 2016, 55(15), 4738-4742.

6.1 Introduction

DC-SIGN and its homologue DC-SIGNR are C-type (*i.e.*, calcium-dependent) lectins that play important roles in HIV/Ebola infection by recognising the viral surface glycoproteins via their clustered carbohydrate recognition domains (CRDs). Evidence showed that notwithstanding of the 77% shared amino acid identity and similar tetrameric structure, they possess different glycan binding affinity, specificity and viral transmission. For instance, DC-SIGN recognises and transmits some HIV strains more efficiently than DC-SIGNR,¹⁴¹ while DC-SIGNR but not DC-SIGN has the ability to recognise the West Nile Virus.¹¹⁶ DC-SIGN and DC-SIGNR are specific to high mannose glycan structures; however, only DC-SIGN recognises fucose glycans including Lewis-type blood group antigens.^{99,117} The two homologous proteins are differently expressed on different cell types. DC-SIGN is expressed on the surface of dendritic cells, macrophages and placenta whereas DC-SIGNR is present on sinusoidal endothelial cells in the liver and on endothelial cells in lymph node sinuses and placental villi but not on dendritic cells.^{34,45,98} However, the biological functions and ligand binding properties of DC-SIGN and DC-SIGNR are still not yet thoroughly understood.

Nanomaterials could be used as scaffolds to display multiple copies of carbohydrates and to increase the binding strength for multivalent interactions. Several studies have been directed towards targeting DC-SIGN using multivalent carbohydrate structures, *e.g.*, glycomimetics, glycoclusters, glycodendrimers, glycodendrinanoparticles, glycodendrofullerenes.^{36,41,42,142-148} Quantum dots (QDs) recently attracted increasing interest because of their particular photoluminescence properties, which can be manipulated to a specific wavelength depending on their size. Generally, carbohydrate-functionalised quantum dots have been used as a useful tool to investigate multivalent carbohydrate-protein interactions, binding specificity, detection of lectins and bacteria, cellular monitoring and imaging, and as nanosensors.¹⁴⁹⁻¹⁵³ The first *in vitro* application of glyco-QDs as fluorescent bio-labels was successfully performed by Robinson *et al.*¹⁴⁹ CdSe/ZnS core/shell QDs were functionalised with mannose (Man) and β -*N*-acetyl glucosamine (GlcNAc) and used to stain pig, mouse, and sea-urchin sperm. The optical properties of glycan-functionalised QDs were detected by confocal scanning microscope imaging. The results demonstrated that GlcNAc-QDs distinctively accumulated only at the sperm heads while Man-QDs were spread over the whole sperm body due to specific distribution of the Man and GlcNAc receptors.

Seeberger *et al.* have succeeded in preparing carbohydrate-capped CdSe/ZnS core/shell QDs not only for *in vitro* imaging but also *in vivo* liver targeting in mice. They demonstrated that QDs capped with D-galactose were preferentially bound to asialoglycoprotein receptor-mediated endocytosis *in vitro*. Fluorescence microscopy also revealed that QDs capped with D-mannose and D-galactose sequestered in the liver.¹⁵² Furthermore, QDs conjugated to carbohydrates or viral coat proteins specific to DC-SIGN, *e.g.*, LewisX and the HIV-1 envelope protein gp120 have also been utilised as a means to visualise the binding and internalisation of antigens mediated by DC-SIGN in living cells.¹⁵³ Galan and co-workers also successfully applied QDs functionalised with different types of sugar for intercellular localisation in HeLa and SV40 epithelial cells. The glycan type on QDs surface could affect cellular uptake and lactose-QDs could serve as a 'Trojan horse' to help internalisation of QDs with other non-internalisable sugar moieties into the cell.¹⁵⁰ Another example was the use of CdSe/ZnS QDs functionalised with lactose, melibiose, and maltotriose for detection of lectins, *i.e.*, soybean agglutinin (SBA), jacalin, and Concanavalin A (Con A) through agglutination assay and monitored by light scattering.¹⁵¹ According to the results, melibiose-QDs selectively bound to SBA and were specifically de-agglutinated using α -D-galactose, confirming the specific and multivalent carbohydrate-protein interaction.

Despite all recent progress made for the use of QD in glycobiology, carbohydrate-capped QDs have not yet been applied to probe multivalent protein-ligand interactions via Förster resonance energy transfer (FRET), which is a technique of fluorescence resonance energy transfer, from a donor fluorophore to an acceptor fluorophore, allowing investigation of molecular interactions. Possessing fluorescent properties enables QDs to serve as energy donors for FRET, but there is still a need to develop a more efficient method to attach many sugar residues on the surface without influencing the optical properties of QDs to form dense and compact QDs which are required for multivalent binding and detectable FRET signals.¹⁵⁴ Therefore, the design and preparation of compact and dense carbohydrate-capped QDs to serve as multivalent probes for carbohydrate-binding proteins, *e.g.*, DC-SIGN and DC-SIGNRR via FRET would provide a better understanding of the roles of proteins in host-pathogen interactions.

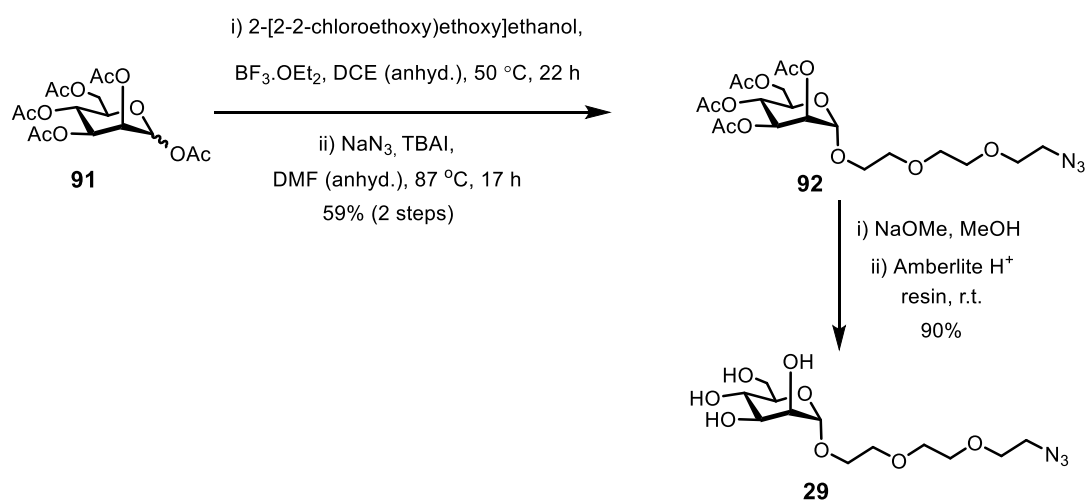
6.2 Aims and objectives

This chapter describes successful synthetic routes to azide-appended mannose residues in form of mono- and disaccharides and an efficient and convenient method to prepare mannose-capped CdSe/ZnS core/shell quantum dots by cap-exchange using

functional ligands appending a deprotonated dihydrolipoic acid (DHLA) moiety. A series of mannose-functionalised QDs were prepared and evaluated, for the first time, for the binding properties with dye-labelled DC-SIGN and DC-SIGNR using FRET and viral inhibition assays. These should provide an insight into how DC-SIGN interacts with viral ligands and a better understanding of the structural/functional parameters influencing the ligand-receptor binding of DC-SIGN and DC-SIGNR.

6.3 Synthesis of an azido-mannopyranoside

Acetylated azido-mannopyranoside **92** was prepared by reaction of mannose pentaacetate **91** with 2-[2-(2-chloroethoxy)ethoxy]ethanol in the presence of $\text{BF}_3 \cdot \text{OEt}_2$ in dichloroethane and subsequent treatment with sodium azide and tetrabutylammonium iodide in DMF (Scheme 6-1). Zemplén deacetylation of the resulting compound **92** gave azido-mannopyranoside **29** in a good yield. A proton-undecoupled NMR experiment revealed a one bond $^{13}\text{C} - ^1\text{H}$ coupling constant of 169 Hz, corresponding to α -configuration.¹⁵⁵



Scheme 6-1. Synthetic route to azido-mannopyranoside **29**.

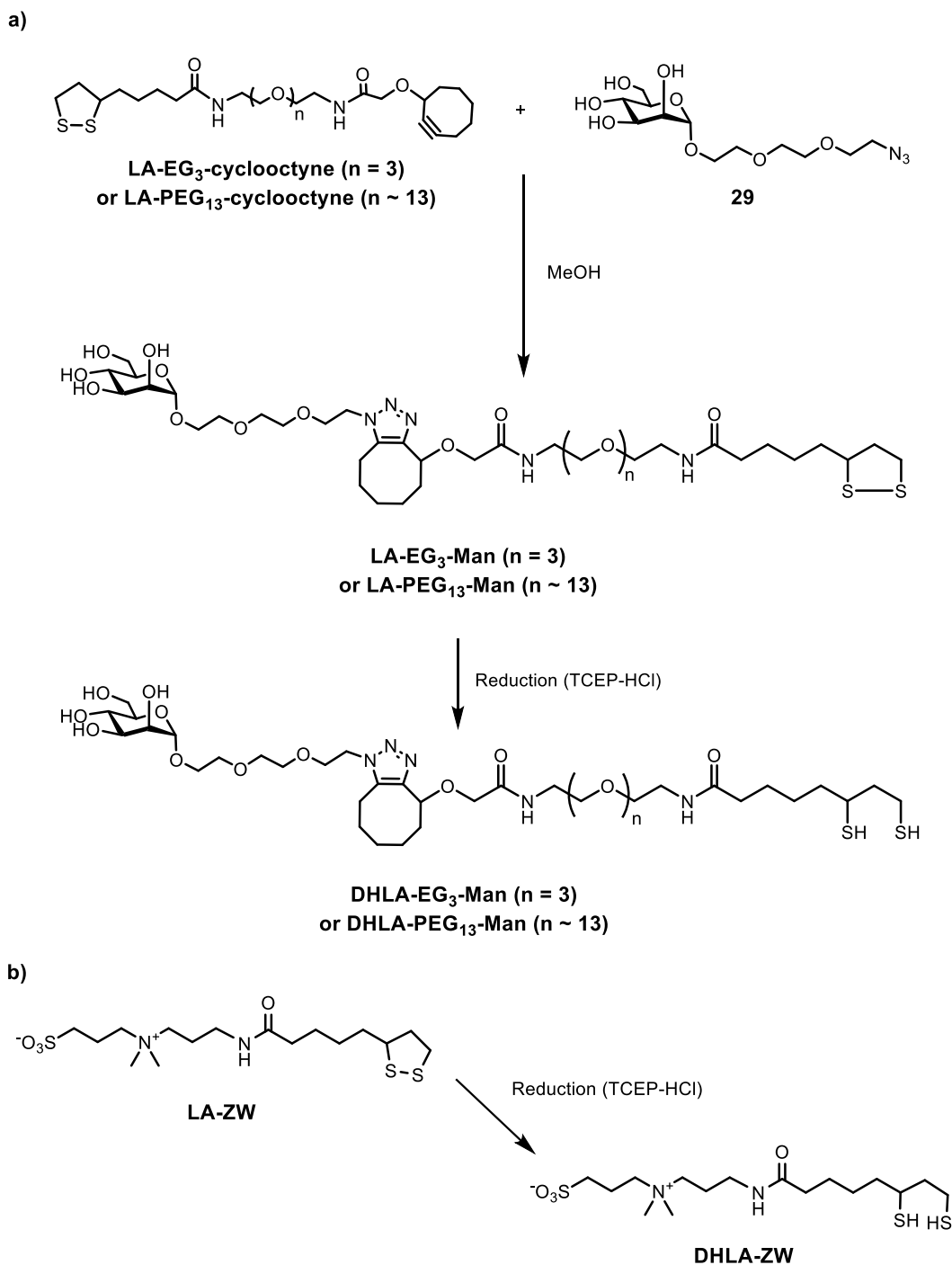
6.4 Multivalent mannose quantum dots for the study of carbohydrate and DC-SIGN and DC-SIGNR interactions

In collaboration with Dr. Y. Guo and Dr. D. Zhou (School of Chemistry, University of Leeds), synthetic azido-mannopyranoside **29** was attached to lipoic acid-poly (ethylene glycol)-cyclooctyne linkers**, *i.e.*, LA-EG₃-cyclooctyne and LA-PEG₁₃-cyclooctyne, by strain-promoted alkyne-azide cycloaddition (Scheme 6-2a). This process provided

** Linkers were supplied by Dr. D. Zhou, School of Chemistry, University of Leeds.

lipoic acid-poly(ethylene glycol)-mannose, which were referred to as LA-EG₃-Man and LA-PEG₁₃-Man. Following reduction, the corresponding dihydrolipoic forms (DHHLA-PEG₁₃-Man and DHHLA-EG₃-Man) were obtained. Lipoic acid-negatively charged (zwitterionic) ligand (LA-ZW)^{††} as also prepared (Scheme 6-2b). The requisite reduced form DHHLA-ZW was used as a diluent.

^{††} Linkers were supplied by Dr. D. Zhou, School of Chemistry, University of Leeds.



Scheme 6-2. Preparation of: a) Dihydrolipoic acid-poly(ethylene glycol)-mannose (DHLA-PEG_n-Man, where n = 3 or ~13) and b) Dihydrolipoic acid-zwitterionic ligand (DHLA-ZW). N.B. Both LA-EG₃-cyclooctyne and LA-PEG₁₃-cyclooctyne were used as a mixture of stereoisomers. Both LA-EG₃-Man and LA-PEG₁₃-Man were formed as a mixture of regioisomers, only the predominant stereoisomer is shown.

The ligands were designed to each comprise a DHLA moiety for strong chelative QD binding; a PEG linker for resisting non-specific adsorption and imposing high stability and biocompatibility; and a mannose residue for specific protein binding. The DHLA-appended PEG ligands functionalised with mannose could therefore provide an

effective cap-exchange of commercially available CdSeS/ZnS quantum dots (QDs, ~ 4.2 nm diameter, $\lambda_{EM} \sim 560$ nm) in the presence of sodium hydroxide using MeOH and chloroform as a solvent mixture. This highly efficient cap-exchange approach leads to preparation of compact, dense polyvalent mannose-QDs with varying PEG chain length and mannose density (Figure 6-1).¹⁵⁶ The estimation of carbohydrate loading on the QDs was performed using the phenol sulfuric acid method¹⁵⁷ by measuring the separated DHLA-PEG_n-Man ligands and comparing the concentration to the starting material. The concentration of mannose was determined by comparison to a standardised curve. The levels of glycan polyvalency were found to be 330 ± 80 and 170 ± 30 for QD-EG₃-Man and QD-PEG₁₃-Man respectively, which were considered as unprecedented high levels of sugar loading per dot. Dynamic light scattering (DLS) analysis also showed hydrodynamic diameters (D_h) of 8.9 for QD-EG₃-Man and of 9.6 nm for QD-PEG₁₃-Man, confirming the formation of compact sub-10 nm QDs (Figure 6-2).

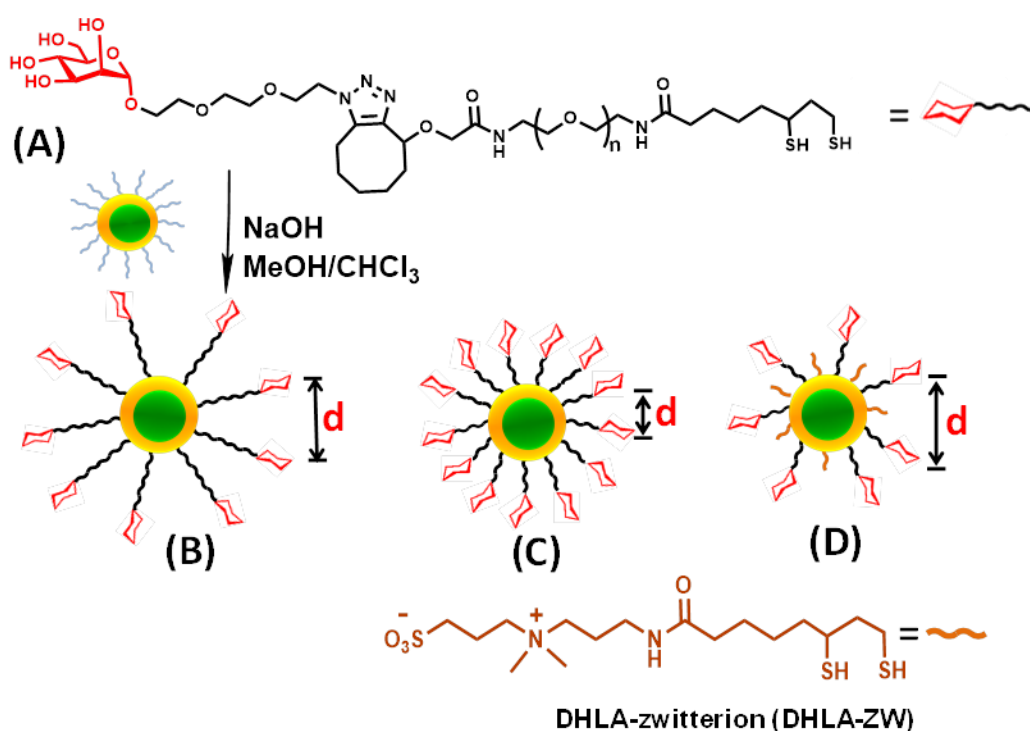


Figure 6-1.¹⁵⁶ (A) Structures of DHLA-appended PEG ligands functionalised with mannose (*i.e.*, DHLA-EG₃-Man and DHLA-PEG₁₃-Man); Preparation of mannose-capped QDs (B) QD-PEG₁₃-Man (C) QD-EG₃-Man (D) QDs capped with mannose and DHLA-zwitterion (DHLA-ZW) spacer ligand, figure reproduced from reference 156.

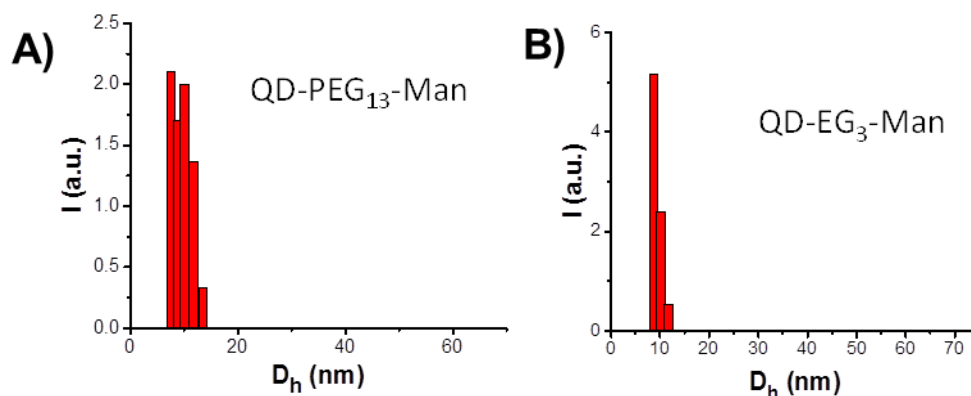


Figure 6-2.¹⁵⁶ Size distribution histograms of: (A) QD-PEG₁₃-Man and (B) and QD-EG₃-Man, measured by DLS, figure reproduced from reference 156.

It should be noted that the preparation of mannose-capped QDs, starting from LA-PEG₁₃-cyclooctyne or LA-EG₃-cyclooctyne, and the DLS analysis were performed by C. Sakonsinsiri and Dr. Y. Guo. Prepared QDs, including QD-EG₃-Man, QD-PEG₁₃-Man and QDs diluted with a DHLA-ZW spacer ligand were used for biological evaluations, which are discussed in Section 6.5.

6.5 Biological evaluations

6.5.1 Binding studies using QD-FRET technique

This part of the work was performed by Dr. Y. Guo. Previously-prepared QD-EG₃-Man and QD-PEG₁₃-Man (collectively referred to as QD-PEG_n-Man) were tested for the binding with dye-labelled DC-SIGN and DC-SIGNR, two closely related receptors of HIV/Ebola virus, using a sensitive, ratiometric FRET assay. DHLA-ZW capped QD was also used as a control. FRET interactions between QD-PEG_n-Man (donors) and two proteins DC-SIGN and DC-SIGNR (acceptors) that were labelled with fluorescent dye Atto-594 on a specifically introduced cysteine residue were investigated (Figure 6-3).

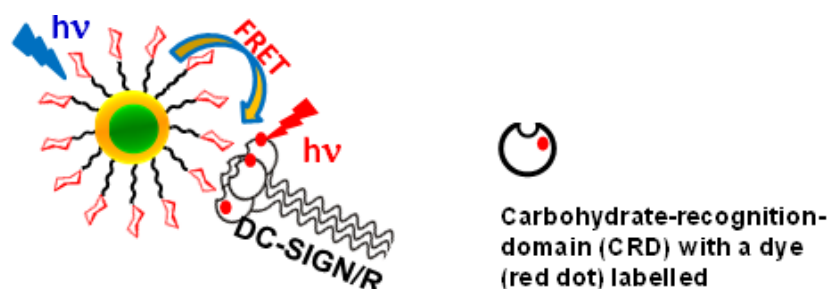


Figure 6-3.¹⁵⁶ Schematic representation of the FRET technique used to investigate multivalent interactions between carbohydrate-recognition domain (CRD) of labelled DC-SIGN and DC-SIGNR and PEG terminated mannose-capped QDs, figure reproduced from reference 156.

It was found that both QD-EG₃-Man and QD-PEG₁₃-Man specifically bound to DC-SIGN, but not to its closely related receptor DC-SIGNR (Figure 6-4). Stronger FRET signals and more severely quenched QD fluorescence were observed for DC-SIGN binding to QD-EG₃-Man over QD-PEG₁₃-Man, indicating more efficient FRET in the former pair with a shorter PEG chain (Figure 6-4A&B). Presumably, this might be because shorter linker in the QD-EG₃-Man brings the QD and fluorophore into closer proximity. An observed weak FRET responses of the dye-labelled DC-SIGNR to both QD-EG₃-Man and QD-PEG₁₃-Man (Figure 6-4C&D) were barely stronger than those for the monomeric CRD (Figure 6-4E) and for the DHLA-capped control QD (data not shown), demonstrating minimal QD-DC-SIGNR binding. Ratiometric analysis of donor and acceptor signals was used. This detection of FRET changes could provide more accurate results than analysing only the absolute fluorescence intensity by reducing instrument noise and signal perturbations. Also, an accurate measurement of the concentration of the fluorophore is not required when measuring the ratio changes. The apparent FRET ratio (I_{626}/I_{554}) for DC-SIGN was found to follow typical binding curves (Figure 6-4F), whereas the signals measured for DC-SIGNR remained low and comparable to non-specific adsorption throughout the concentrations tested. In spite of the high overall amino acid sequence identity of the two proteins, these FRET data suggested that QD-PEG_n-Man could remarkably discriminate DC-SIGN over DC-SIGNR, notably in the case of QD-EG₃-Man. Therefore, this rapid, sensitive and recently established QD-FRET technique could be used for probing multivalent carbohydrate-protein interactions as well as for opening up a new method for targeting DC-SIGN- from DC-SIGNR-mediated viral infection.

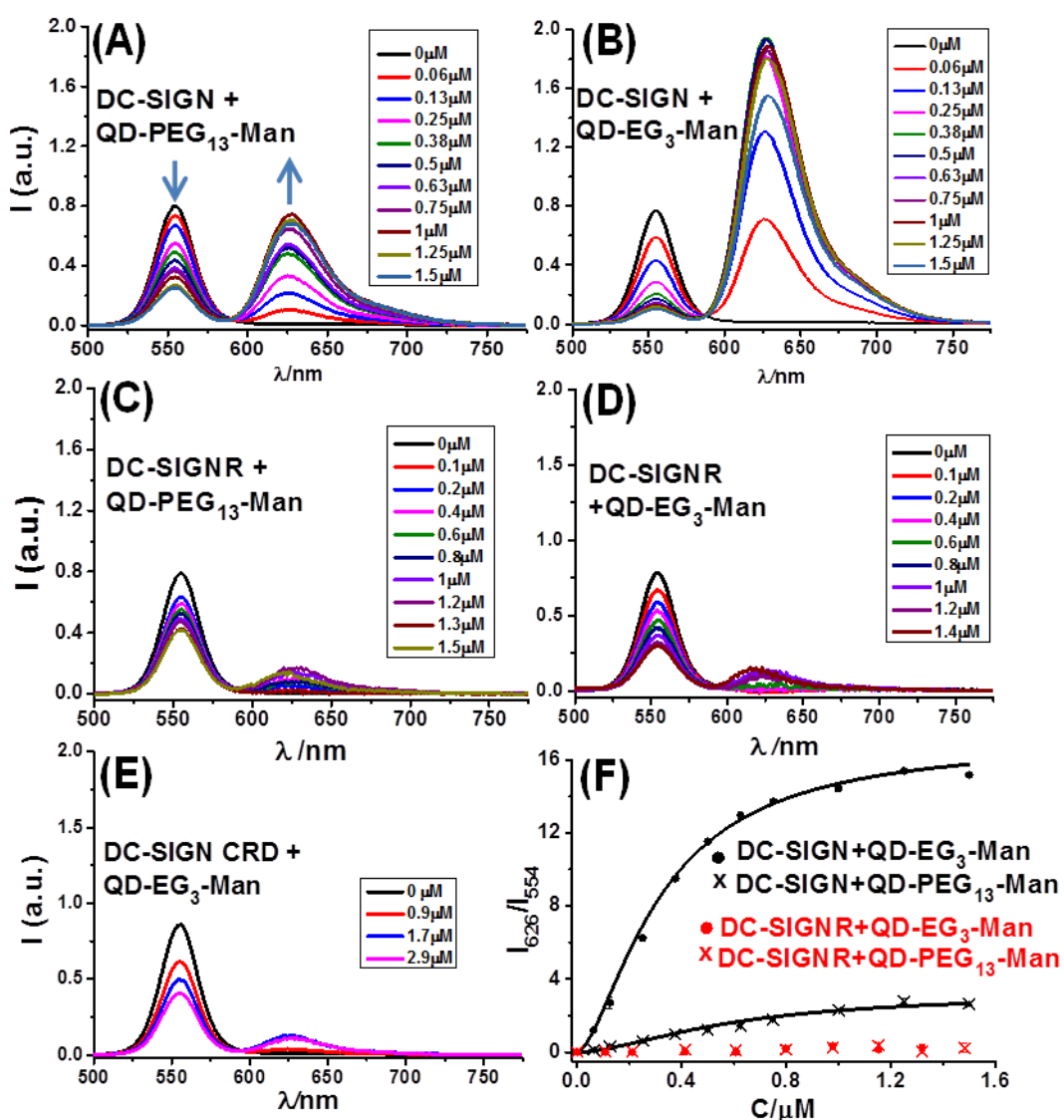


Figure 6-4.¹⁵⁶ Fluorescence spectra of the donor-acceptor pair: (A) DC-SIGN + QD-PEG₁₃-Man; (B) DC-SIGN + QD-EG₃-Man; (C) DC-SIGNR + QD-PEG₁₃-Man; (D) DC-SIGNR + QD-EG₃-Man; (E) DC-SIGN CRD monomer + QD-EG₃-Man. (F) Correlation between the FRET ratio and the protein concentrations, figure reproduced from reference 156.

6.5.2 Viral inhibition assays

This part of the work was performed by Dr. I. Nehlmeier and Dr. S. Pöhlmann (Infection Biology Unit, German Primate Center, Göttingen, Germany). The binding specificity between QD-EG₃-Man and DC-SIGN was further verified by viral inhibition assays, following Pöhlmann and Hofmann-Winkler's published method.¹⁵⁸ Briefly, human embryonic kidney cells (293T) were transfected with plasmids encoding DC-SIGN and DC-SIGNR or a control transfected with empty plasmid (pcDNA). The cells were washed at 6 h post transfection and further cultivated at 37 °C, 5% CO₂ in Dulbecco's

modified eagle medium (DMEM) containing 10% fetal bovine serum (FBS). At 48 h post transfection, after twice treatments with different concentrations of QD-EG₃-Man, murine leukemia virus (MLV) vectors, retroviral vector encoding luciferase gene, bearing either Ebola virus glycoprotein (EBOV-GP) or vesicular stomatitis virus glycoprotein (VSV-G), as a control, was used to transduced with the cells. At 72 h after transduction, luciferase activities were measured in cell lysates. The EBOV-GP-bearing MLV vector (MLV-EBOV-GP) would bind specifically to cell surface DC-SIGN and DC-SIGNR and facilitate vector cell entry and enhance gene transduction, whereas VSV-G bearing MLV vector (MLV-VSV-G) would not bind to DC-SIGN and DC-SIGNR and hence did not affect transduction efficiency via these receptors. An increase in transduction efficiency was observed on expression of DC-SIGN and DC-SIGNR comparing to the pcDNA negative controls (Figure 6-5A). QD-EG₃-Man treatment significantly reduced the transduction efficiency of DC-SIGN positive cells in a dose-dependent manner, presumably by inhibiting cell surface DC-SIGN from binding to the MLV-EBOV-GP vector and did not induce the vector entry. In contrast, transduction of cells expressing DC-SIGNR was unaffected by QD-EG₃-Man. Moreover, QD-EG₃-Man did not affect the transduction driven by the control MLV vector bearing vesicular stomatitis virus glycoprotein (MLV-VSV-G), which did not bind to DC-SIGN and DC-SIGNR (Figure 6-5B). These observations matched to our previous results on the QD's high affinity to DC-SIGN, but minimal to DC-SIGNR, confirming the specific QD-DC-SIGN binding was responsible for the observed inhibition.

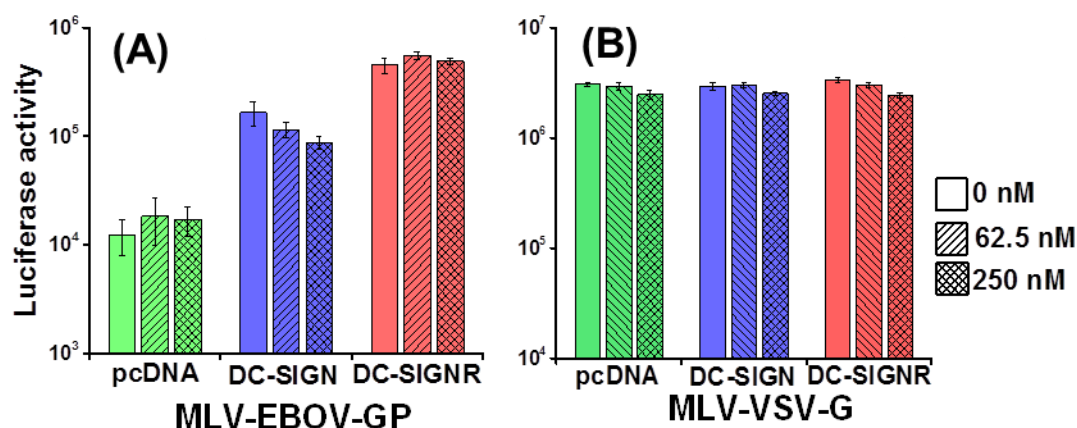


Figure 6-5.¹⁵⁶ Impact of QD-EG₃-Man on viral inhibition. Human 293T cells expressing DC-SIGN, DC-SIGNR or empty plasmid (pcDNA) were treated with QD-EG₃-Man (at 0, 62.5 and 250 nM). Cells were transfected with: (A) murine leukaemia virus (MLV) vectors bearing Ebola virus glycoprotein (MLV-EBOV-GP) or (B) the control vesicular stomatitis virus glyco-protein (MLV-VSV-G) for delivering luciferase gene. Luciferase activities in the lysates were determined. In the case of MLV-EBOV-GP, the difference between untreated and treated with 250 nM QD-EG₃-Man is statistically significant ($p = 0.024$, from two-tailed students t-test), figure reproduced from reference 156.

According to QD-FRET study and cell-based assay, QD-PEG_n-Man has specificity for DC-SIGN over DC-SIGNR. We reasoned that the CRDs tetramer of DC-SIGN are disposed differently comparing to that of DC-SIGNR, that is, the CRDs of DC-SIGN are facing upwardly along the coiled-coil axes, which are readily accessible for multivalent binding with the QD-PEG_n-Man. In contrast, the CRDs of DC-SIGNR tetramer are projecting sideways, which render it unavailable to bind multivalently to the QD (Figure 6-6). These models were consistent with those proposed from small angle X-ray scattering studies.¹⁰³

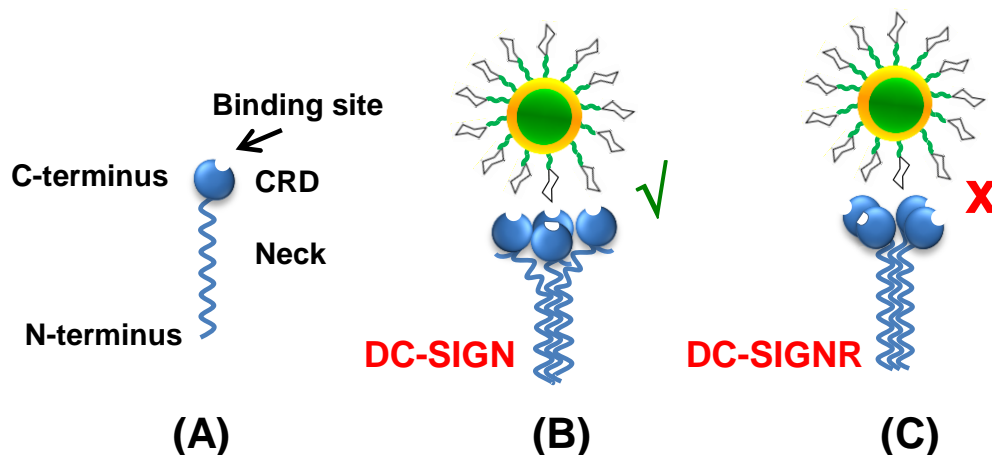


Figure 6-6.¹⁵⁶ (A) Schematic representation of the structure of DC-SIGN and DC-SIGNR monomer; proposed ligand-receptor binding modes between the QDs and: (B) DC-SIGN or (C) DC-SIGNR due to their different orientations of tetrameric CRDs, figure reproduced from reference 156.

From this perspective, the different spatial CRD arrangements between DC-SIGN and DC-SIGNR are potentially associated with their distinct ligand-binding properties and their non-identical physiological roles. By presenting all of the DC-SIGN binding sites in the same direction, DC-SIGN on dendritic cells would allow interactions with a wider range of glycan ligands, compared to DC-SIGNR, as well as rapid antigen internalisation and presentation to T-cells.^{99,117} On the other hand, the binding of the outward-facing CRDs of the endothelial cell surface adhesion receptor DC-SIGNR could only occur with certain spatial orientations of ligands.

6.6 Synthesis of the azido-disaccharide analogue

α 1,2-Mannobiose is thought to be a better ligand for DC-SIGN¹⁵⁹ and its disaccharide mimics have been reported to be good ligands for DC-SIGN.⁴¹ The objective of this section was therefore to synthesise azide-bearing 1,2-mannobiose **31** (Figure 6-7) and evaluate further the binding of DC-SIGN and DC-SIGNR and carbohydrate-capped QDs, comparing with the mono-mannose capped QDs.

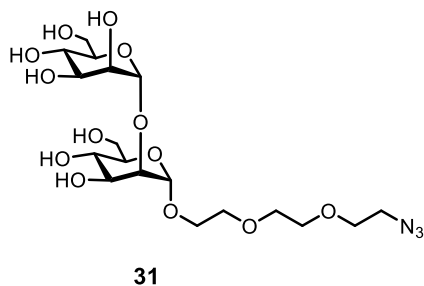
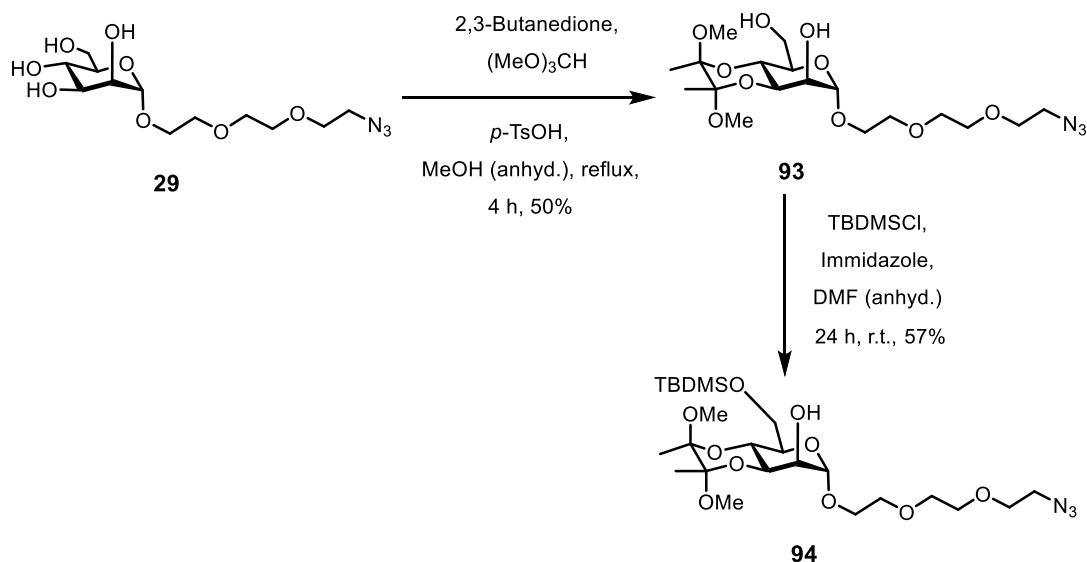


Figure 6-7. Structure of target dimannosyl azide **31**.

6.6.1 Attempted synthesis of the azido-disaccharide analogue starting from the azido-monosaccharide version

An attempt was made to synthesise the target dimannosyl azide using azido-mannopyranoside **29** as a starting material. Diacetal **93** was synthesised by the method of Ley and co-workers:¹⁶⁰ Azido-mannopyranoside **29** was selectively protected at the O-3 and O-4 positions by treatment with 2,3-butanedione and trimethylorthoformate in the presence of *p*-toluene sulfonic acid in refluxing methanol, giving the corresponding butane diacetal **93** in 50% yield (Scheme 6-3). The primary alcohol of the resulting diol **93** was further reacted with *tert*-butyldimethylsilyl chloride (TBDMSCl) and imidazole to selectively protect the O-6 position, providing mannopyranoside **94**.



Scheme 6-3. Synthetic route to azido-mannopyranoside **94**.

A small sample of resulting mannopyranoside **94** was acetylated using pyridine-acetic anhydride, catalysed by DMAP. ^1H NMR analysis of its acetylated derivative demonstrated that the acetate group was attached to the O-2 position on basis of the downfield shift of the proton attached to C-2 bearing an acetate group (Figure 6-8). This indicates that the *tert*-butyldimethylsilyl (TBDMS) ether protecting group was attached at the O-6-position. With a free hydroxyl group at the position C-2, azido-mannopyranoside **94** was used as a glycosyl acceptor for attempts to glycosylate with another mannose residue.

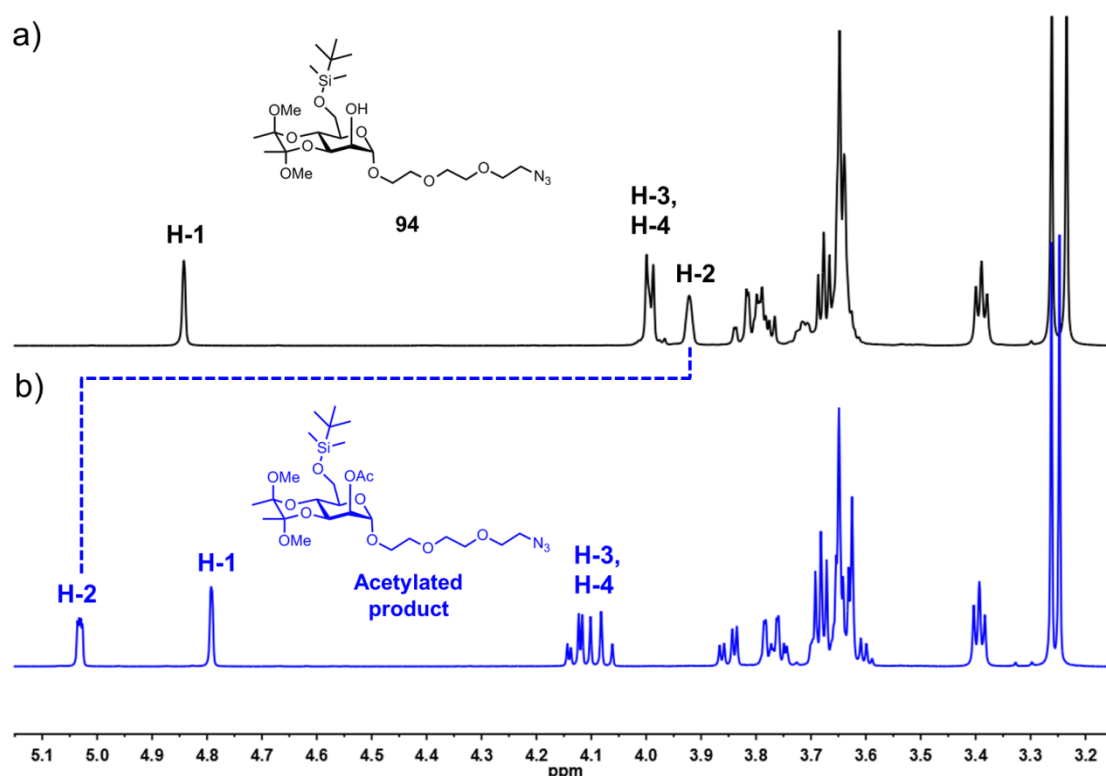
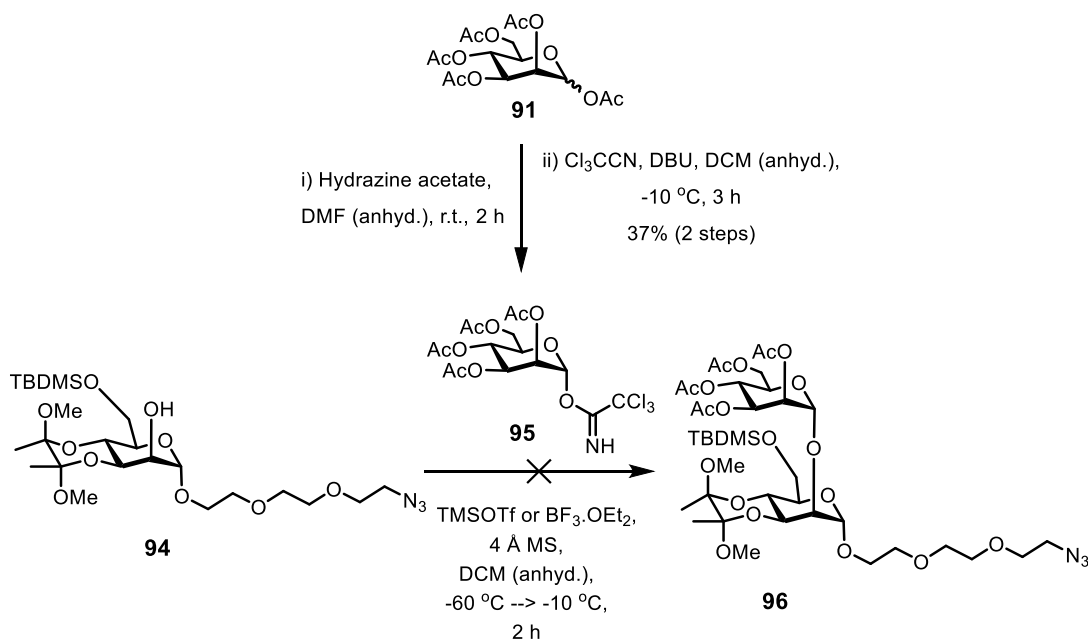


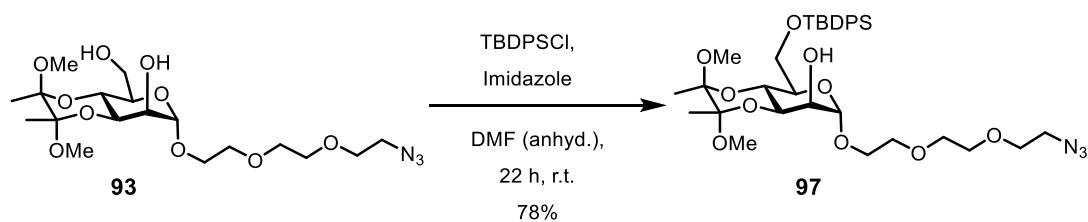
Figure 6-8. ^1H NMR spectra of a) mannopyranoside **94** and b) its acetylated product (500 MHz, CDCl_3), confirming that an acetyl protecting group was attached at the O-2 position and a *tert*-butyldimethylsilyl (TBDMS) ether protecting group was at the O-6-position (cf. proton numbering in Figure 8-1).

Next, trichloroacetimidate donor **95** was prepared in a two-step process from mannose pentaacetate **91** (Scheme 6-4). Glycosylation reactions of mannopyranosyl imidate **95** with the earlier synthesised azido-mannopyranoside **94** were carried out in DCM using either TMSOTf or $\text{BF}_3 \cdot \text{OEt}_2$ as a promoter. In the case of TMSOTf, the formation of the desired product **96** was not observed by LC-MS analysis. Instead, one of the LC-MS peaks at a m/z ratio of 804.3 correlated to a disaccharide analogue without a TBDMS ether protecting group. The resulting loss of the latter protecting group was probably caused by using excessive TMSOTf in the reaction.



Scheme 6-4. Attempted synthesis to azido-disaccharide analogue **96**.

Nevertheless, changing the promoter to BF₃·OEt₂ still did not yield the desired product **96**, suggesting the trichloroacetimidate donor **95** was not reactive enough for the glycosylation of this glycosyl acceptor or *vice versa*. Thus, another type of glycosyl donor, such as thioethyl glycoside was investigated and is discussed further in this section (*cf.* Scheme 6-6). Also, as in the previous glycosylation reaction, the use of excessive TMSOTf probably caused the removal of the TBDMS ether protecting group. Alternatively, *tert*-butyldiphenylsilyl (TBDPS) ether was used as for protection of C-6 hydroxyl group because its more bulky substituents could increase resistance to hydrolysis. Moreover, according to the literature, this TBDPS ether protecting group has been used to protect the O-6 position of a fluoroglycoside bearing butane-2,3-diacetal protecting group.¹⁶¹ To synthesise azido-mannopyranoside **97**, the previously synthesised diol **93** was treated with TBDPSCI in the presence of imidazole (Scheme 6-5).



Scheme 6-5. Synthetic route to azido-mannopyranoside **97**.

A small sample of azido-mannopyranoside **97** was acetylated using pyridine-acetic anhydride, catalysed by DMAP. ^1H NMR analysis of the acetylated compound showed an acetate group was attached to the O-2 position, implying that the TBDPS ether protecting group was successfully attached to the O-6 position (Figure 6-9). Azido-mannopyranoside **97** would be therefore used as a glycosyl acceptor for further glycosylation.

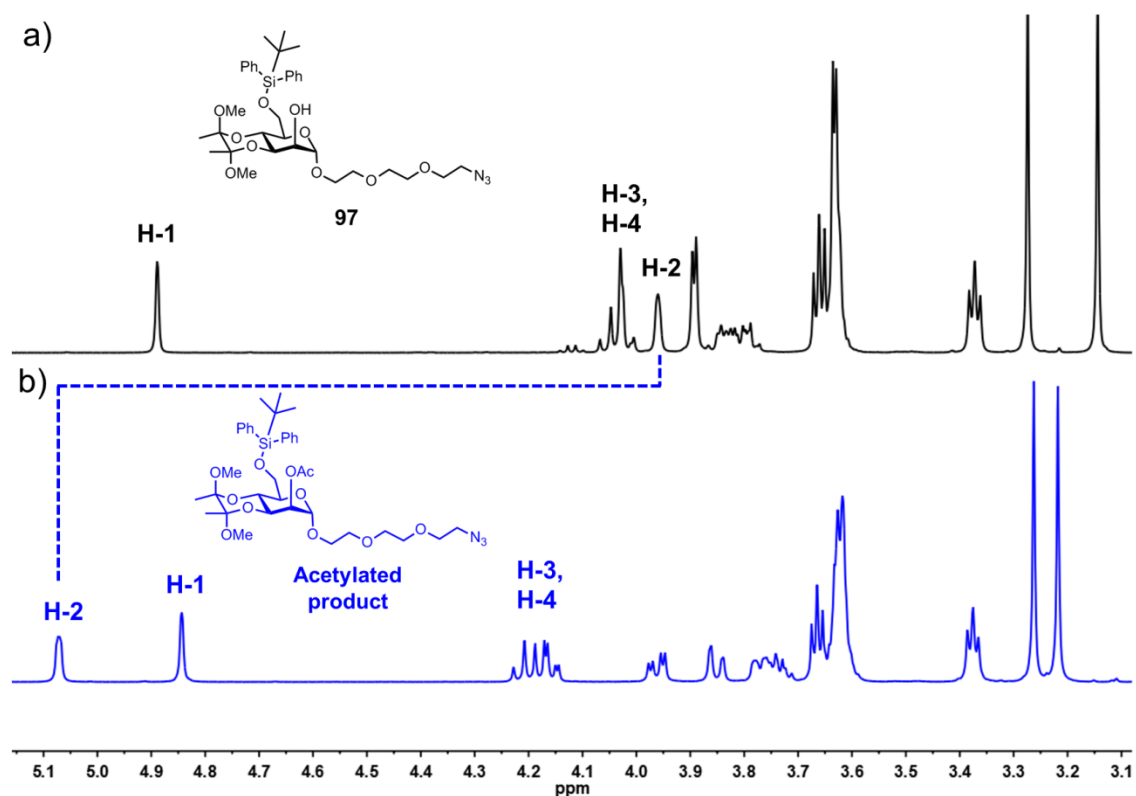
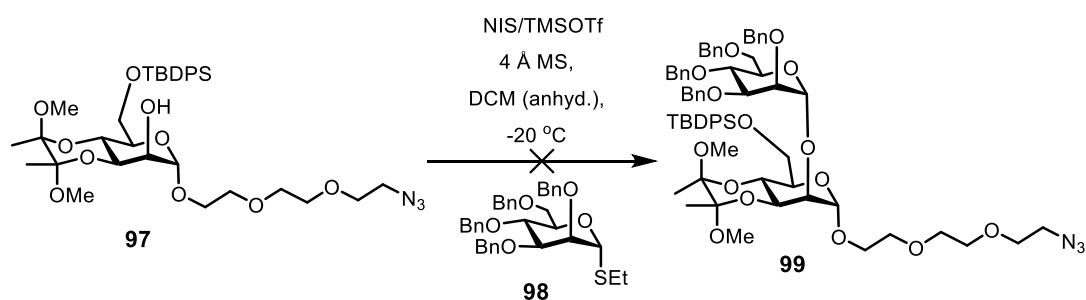


Figure 6-9. ^1H NMR spectra of a) mannopyranoside **97** and b) its acetylated product (500 MHz, CDCl_3), confirming that an acetyl protecting group was attached at the O-2 position and a *tert*-butyldiphenylsilyl (TBDPS) ether protecting group was at the O-6-position (cf. proton numbering in Figure 8-1).

An attempt was made to couple glycosyl acceptor **97** with thioethyl glycosyl donor **98** \ddagger using NIS/TMSOTf as a promoter system (Scheme 6-6). TLC and LC-MS analyses demonstrated that the activated glycosyl donor was formed, but it did not react with the acceptor. The hydrolysed donor was also present in the reaction mixture, implying that the acceptor **97** was not reactive enough to engage in the glycosylation. Low reactivity might be caused by either the presence of the bulky TBDPS group at the O-6 position of the glycosyl acceptor or by the presence of the polyethylene glycol (PEG)-azide at

\ddagger Thioethyl glycoside was supplied by Dr. P. Mandal, a former postdoc in the Turnbull research group.

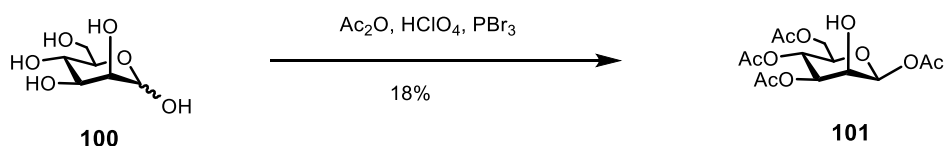
the anomeric position that makes the free hydroxyl group less accessible for glycosylation reaction.



Scheme 6-6. Attempted synthesis of azido-mannopyranoside **99**.

6.6.2 Successful synthesis of the azido-disaccharide analogue starting from D-mannose tetraacetate

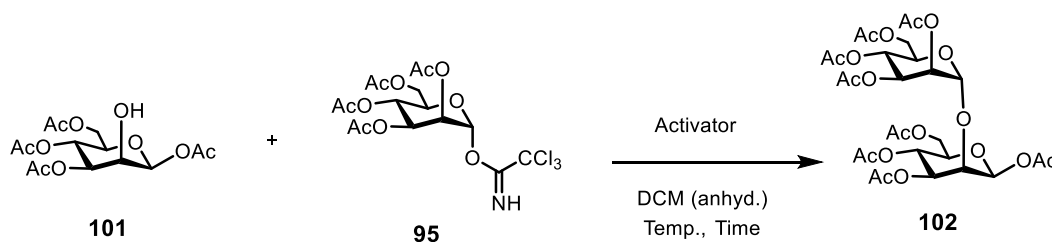
An alternative approach was to synthesise mannopyranosyl acetate **101** (Scheme 6-7), having a free hydroxyl group at C-2 position, following a procedure of Deferrari *et al.*,¹⁶² mannopyranosyl acetate **101** was successfully prepared from D-mannose **100** in a yield of 18%, which was similar to the yield reported in the literature.



Scheme 6-7. Synthetic route to mannopyranosyl acetate **101**.

Next, the couplings of acceptor **101** and mannosyl imidate **95** using either TMSOTf or BF₃·OEt₂ as an activator were successfully performed, giving fully-acetylated manno-**102** (Table 6-1). The use of BF₃·OEt₂ gave a better yield comparing to TMSOTf. However, performing BF₃·OEt₂-mediated reactions for 4.5 h or 20 h did not give any significant difference in term of yields.

Table 6-1. Glycosylation reactions of acceptor **101** with mannosyl imidate **95** under different conditions.



Acceptor 101 (equiv.)	Donor 95 (equiv.)	Activator	Temperature	Time	Yield
1	2	TMSOTf	-30 °C → -8 °C	3 h	21%
1	1	BF ₃ ·OEt ₂	-50 °C → 2 °C	4.5 h	41%
1	1	BF ₃ ·OEt ₂	-50 °C → r.t.	20 h	47%

The ¹³C - ¹H coupling constants of anomeric carbons of acetylated mannoside **102** were determined by a gated decoupled method (Figure 6-10). The observed coupling constants for the anomeric carbon atoms were 174 Hz and 162 Hz, supporting the assignment of α- and β-configurations, respectively.¹⁵⁵ Interestingly, a doublet of doubles with large and small coupling constants (174 Hz and 6 Hz) for the α-anomeric carbon signal resonating at 98.3 ppm was observed. This splitting pattern is probably due to the couplings of the anomeric carbon to the attached proton (H-1) as well as to the proton at C-2 position (H-2) and possibly is arise from the specific conformation of this protected disaccharide. However, there does not appear to be any literature precedent for this type of couplings in mannosyl oligosaccharides.

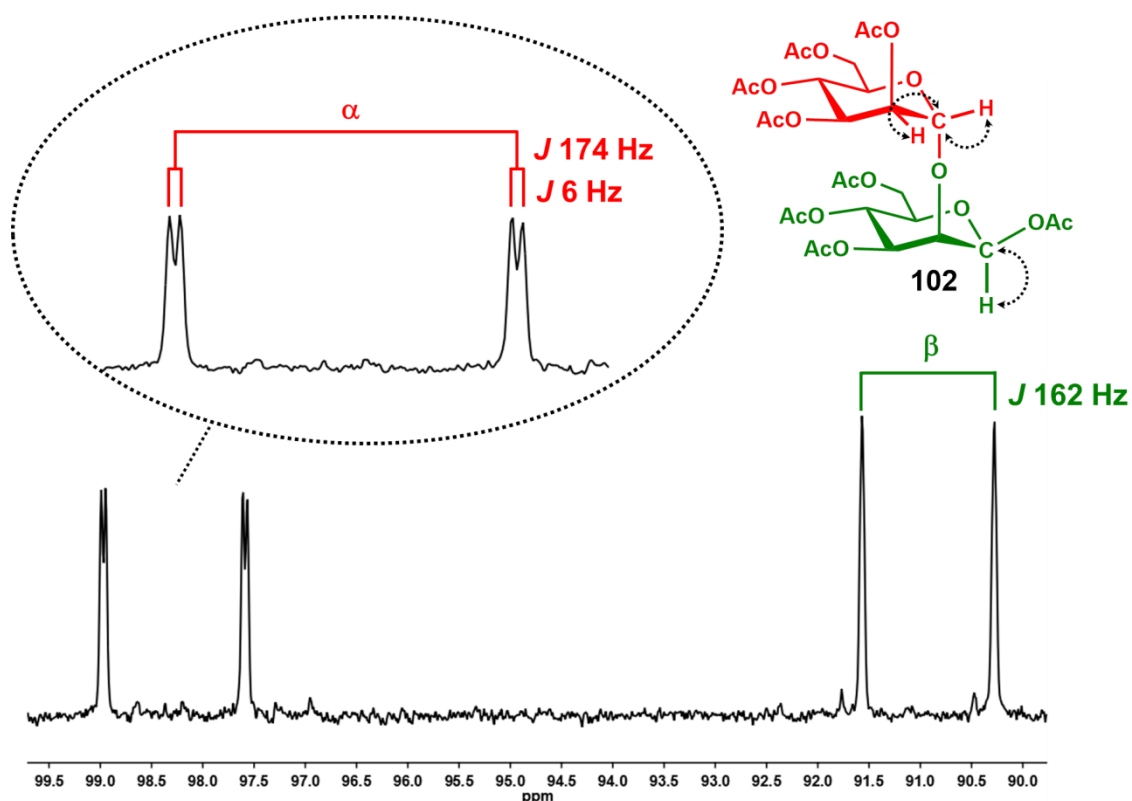


Figure 6-10. Gated decoupled ^{13}C spectrum of dimannose **102** (500 MHz, CDCl_3) showing a doublet of doublets with a large and a small coupling constants (174 Hz and 6 Hz), resonating at 98.3 ppm and a double with a coupling constant of 162 Hz resonating at 91.0 ppm. α -, β -Configurations were determined according to their coupling constants.

As the ^1H -decoupled carbon (^{13}C) spectrum enabled α - and β -configurations of individual mannose residue to be distinguished; it was therefore possible to determine the direct carbon to hydrogen connectivity using HMQC spectroscopy. The corresponding HMQC spectrum showed the correlation between the anomeric carbon and the anomeric proton of each mannose residue, permitting the assignment of dimannosyl azide **102** (Figure 6-11).

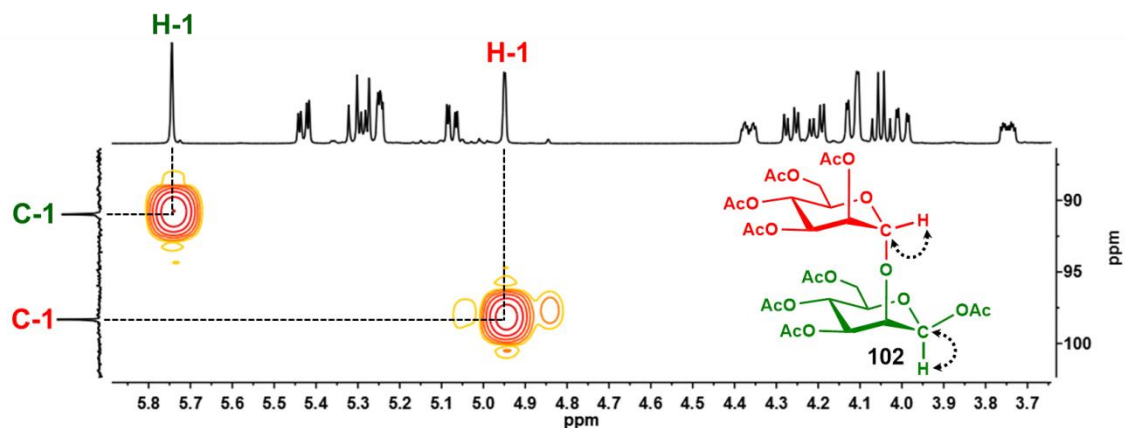
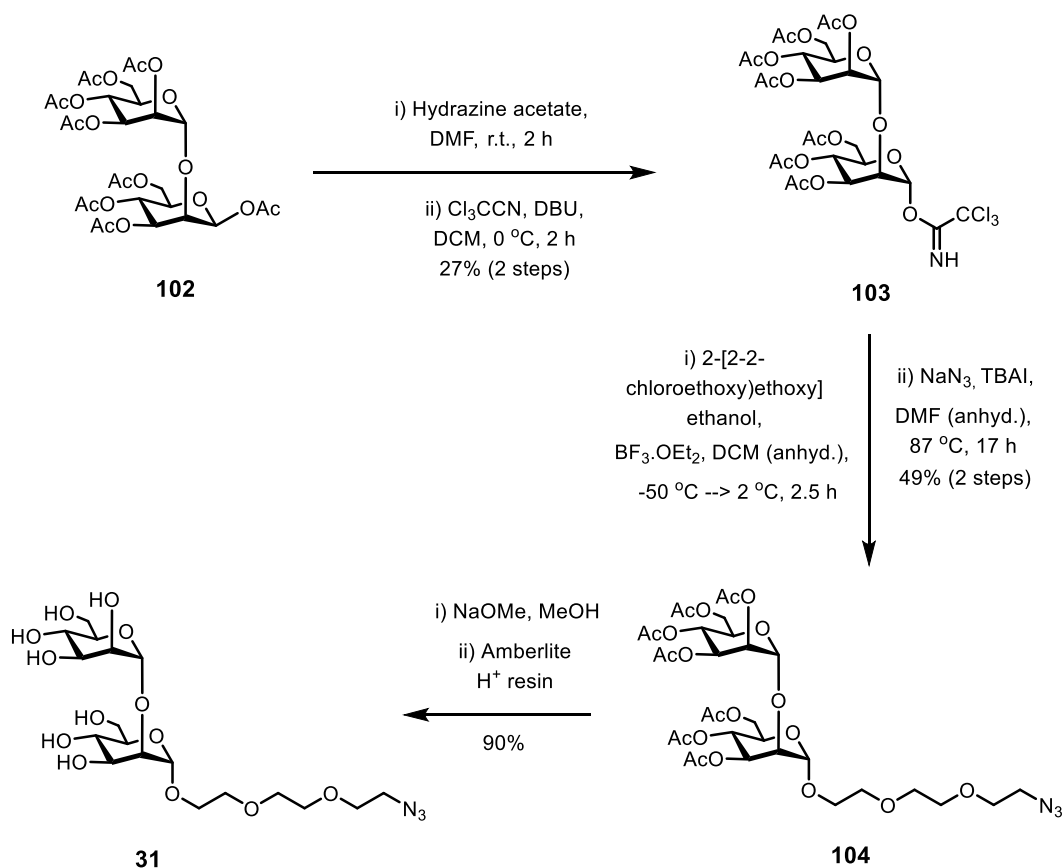


Figure 6-11. The $^1\text{H} - ^{13}\text{C}$ HMQC spectrum of acetylated mannosyl residue **102** (500 MHz, CDCl_3), showing the correlation between anomeric carbon and anomeric proton of each mannose residue.

Anomeric deacetylation of acetylated mannosyl residue **102** with hydrazine acetate and subsequent reaction with trichloroacetonitrile gave of mannosyl imidate **103** (Scheme 6-8). Boron trifluoride diethyl etherate-mediated coupling of 2-[2-(2-chloroethoxy)ethoxy]ethanol with imidate **103** yielded acetylated dimannosyl azide **104**. The obtained compound was deacetylated under Zemplén conditions to give fully deprotected dimannosyl azide **31**.



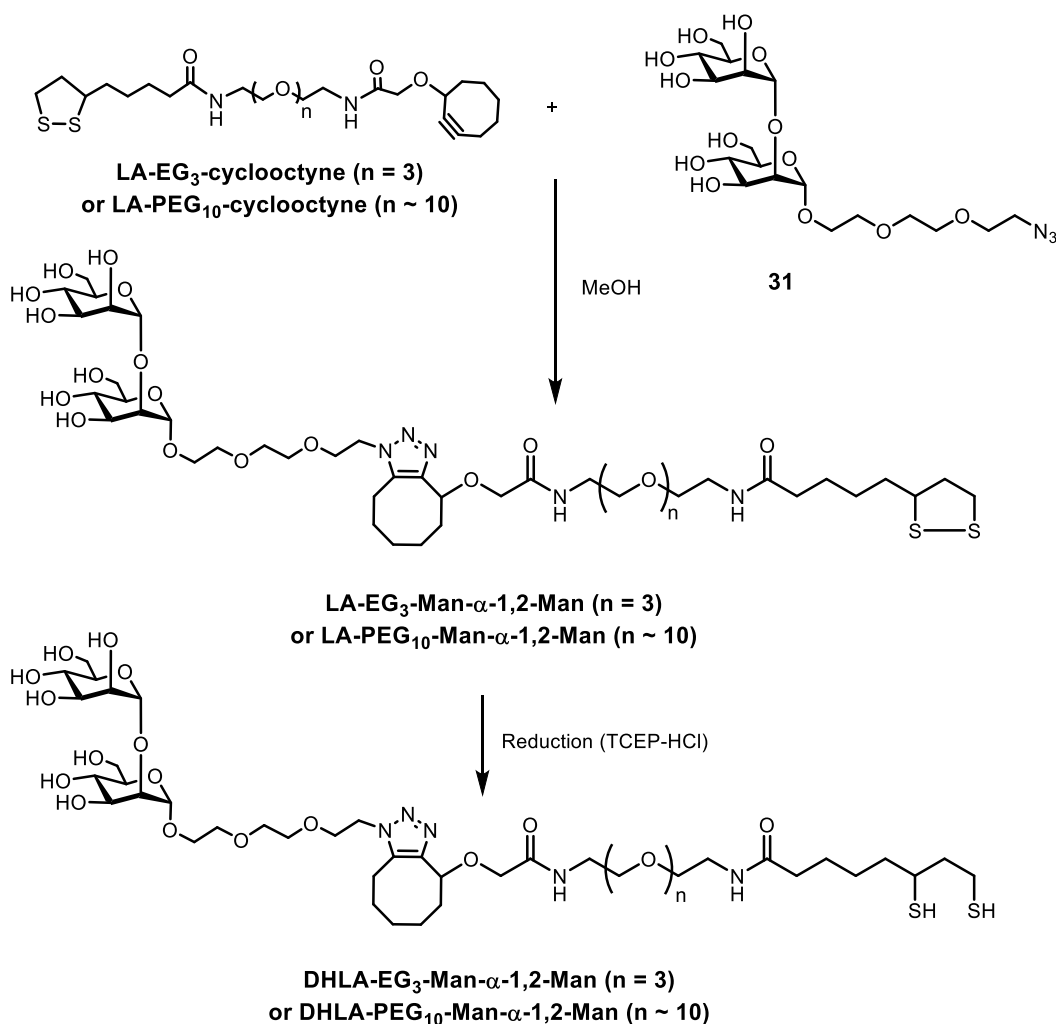
Scheme 6-8. Synthetic route to fully deprotected azido-mannopyranoside **31**.

6.7 Multivalent di-mannose quantum dots for the study of carbohydrate and DC-SIGN and DC-SIGNR interactions

This part of the work was performed by E. Poole and Dr. Y. Guo. In a similar fashion to the preparation of mono-mannose-capped QDs, azido-di-mannose residue **31** was attached to either LA-EG₃-cyclooctyne^{§§} or LA-PEG₁₀-cyclooctyne,^{***} by strain-promoted alkyne-azide cycloaddition, giving LA-EG₃-Man- α -1,2-Man and LA-PEG₁₀-Man- α -1,2-Man (Scheme 6-9). After reduction, the corresponding dihydrolipoic forms (DHLA-EG₃-Man- α -1,2-Man and DHLA-PEG₁₀-Man- α -1,2-Man) were obtained. DHLA-ZW was also used as a control QD, of which the preparation was previously described in Section 6.4 (Scheme 6-2b).

^{§§} Linker was supplied by Dr. D. Zhou, School of Chemistry, University of Leeds.

^{***} Linker was synthesised by E. Poole, a Ph.D. student under supervision of Dr. Y. Guo and Dr. D. Zhou.



Scheme 6-9. Preparation of dihydrolipoic acid-poly(ethylene glycol)-dimannose (DHLA-PEG_n-Man- α -1,2-Man, where n = 3 or ~10). N.B. Both LA-EG₃-cyclooctyne and LA-PEG₁₀-cyclooctyne were used as a mixture of stereoisomers. Both LA-EG₃-Man- α -1,2-Man and LA-PEG₁₀-Man- α -1,2-Man were formed as a mixture of regioisomers, only the predominant stereoisomer is shown.

Di-mannose-capped QDs with varying PEG linker lengths (QD-EG₃-Man- α -1,2-Man and QD-PEG₁₀-Man- α -1,2-Man; collectively called QD-PEG_n-Man- α -1,2-Man, where n = 3 or n ~10) were successfully synthesised using the same procedures as for the preparation of mono-mannose capped QDs. Thus, di-mannose capped QDs and the control DHLA-ZW were available to be used for the QD-FRET experiments.

6.8 Binding studies using QD-FRET technique

This part of the work was performed by E. Poole and Dr. Y. Guo. Similarly to the previous experiments, QD-PEG_n-Man- α -1,2-Man was employed as a FRET donor to assess DC-SIGN and DC-SIGNR-carbohydrate interactions. Two labelled proteins DC-SIGN and DC-SIGNR were prepared and used as FRET acceptors. Preliminary data

suggested an overall view of a preferential interaction of the di-mannose capped QDs with DC-SIGN over DC-SIGNR (Figure 6-12), which was likewise the case of mono-mannose capped QDs that showed a high selectivity with DC-SIGN. This observation was confirmed by analysis of the FRET ratio data plotted against DC-SIGN and DC-SIGNR concentration (Figure 6-13). Di-mannose-functionalised QDs with a long-length PEG linker (QD-PEG₁₀-Man- α -1,2-Man) bound to DC-SIGN with a K_d of 60 nM (Table 6-2), whereas the binding of the QD-PEG₁₀-Man- α -1,2-Man to DC-SIGNR was approximately 10-fold weaker (K_d of 607 nM). While the binding of QD-PEG₁₀-Man- α -1,2-Man to DC-SIGN could be described by a simple one site binding isotherm, the QD-EG₃-Man- α -1,2-Man/DC-SIGN binding could only be fit to Hill equation as the data showed apparent positive cooperativity (Hill coefficient $n = 2.55$; Table 6-2). The fitting of QD-PEG₁₀-Man- α -1,2-Man to DC-SIGN using the Hill equation yielded superimposable binding curve that was well fit by a one-site binding model, a Hill coefficient of 1.02 and an effective concentration for half maximal binding (EC_{50}) that was the same as K_d for the simple one site binding model. EC_{50} value for QD-EG₃-Man- α -1,2-Man was higher than that of the QD-PEG₁₀-Man- α -1,2-Man (104 nM vs. 60 nM). DC-SIGNR bound to QD-EG₃-Man- α -1,2-Man even more weakly than to the other functionalised quantum dots and it was not possible to derive any accurate estimates of K_d or EC_{50} . On the whole, di-mannose capped QDs enhanced the binding affinities of the QD probe to DC-SIGN and DC-SIGNR. EC_{50} for the mono-mannosyl quantum dots estimated from Fig 6-4(F) were around 300-500 nM, whereas EC_{50} values for the dimannosyl quantum dots were 60-100 nM. This di-mannosyl probe could still distinguish DC-SIGN and DC-SIGNR that could further lead to a new insight into their binding modes and biological roles. However, there is still a need for performing additional experiments on the multivalent interactions of QD-PEG_n-Man- α -1,2-Man and DC-SIGN to validate this hypothesis.

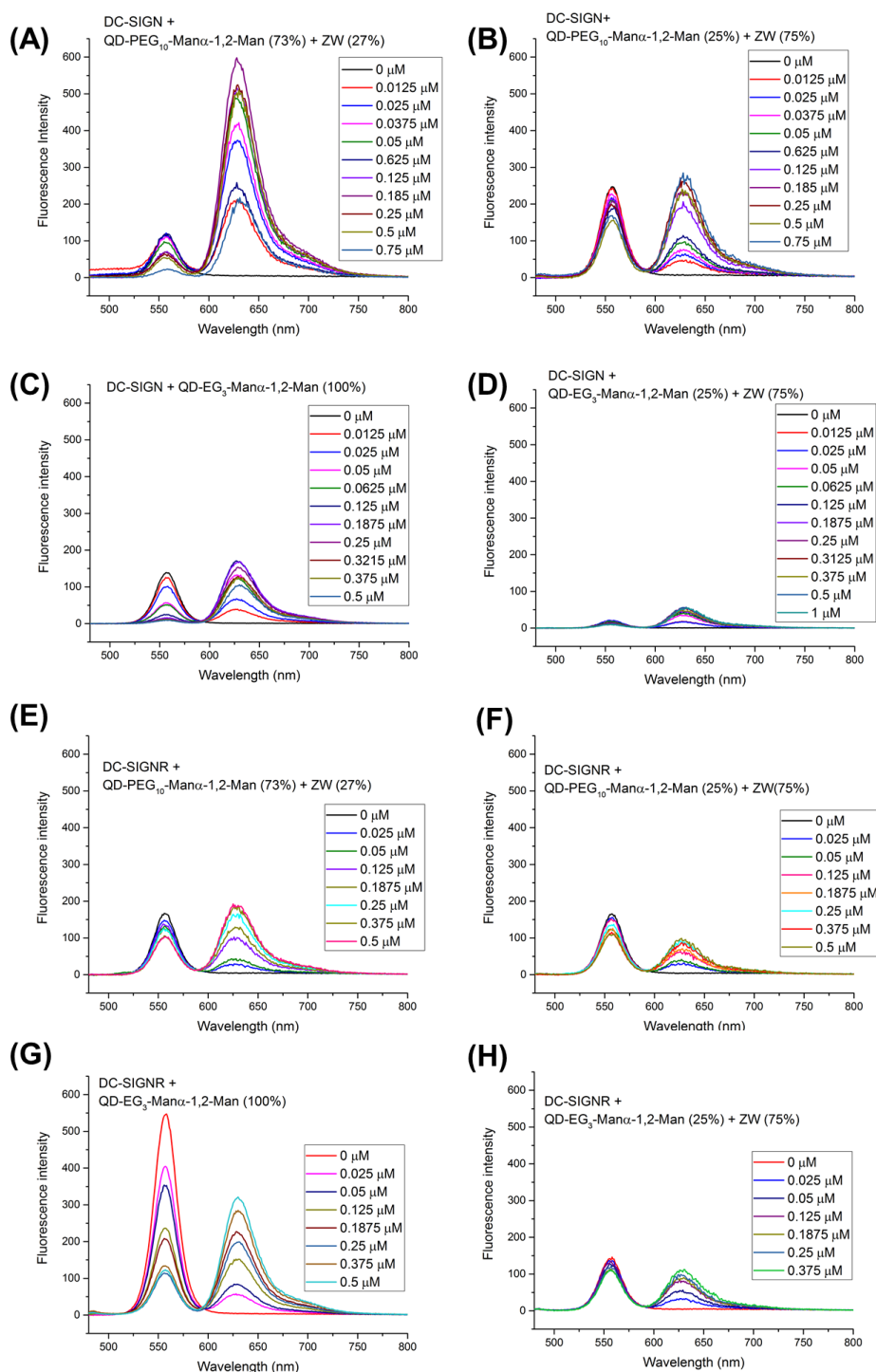


Figure 6-12. (A-H) Preliminary data on fluorescence spectra of QD-PEG_n-Man α -1,2-Man ($\lambda_{EM} = 554$ nm, final QD concentration, CQD = 40 nM) after binding to Atto-594 labelled proteins: (A) DC-SIGN + QD-PEG₁₀-Man α -1,2-Man (73%) + ZW (27%); (B) DC-SIGN + QD-EG₃-Man α -1,2-Man (25%) + ZW (75%); (C) DC-SIGN + QD-PEG₁₀-Man α -1,2-Man (100%); (D) DC-SIGN + QD-EG₃-Man α -1,2-Man (25%) + ZW (75%); (E) DC-SIGNR + QD-PEG₁₀-Man α -1,2-Man (73%) + ZW (27%); (F) DC-SIGNR + QD-PEG₁₀-Man α -1,2-Man (25%) + ZW (75%); (G) DC-SIGNR + QD-EG₃-Man α -1,2-Man (100%); (H) DC-SIGNR + QD-EG₃-Man α -1,2-Man (25%) + ZW (75%).

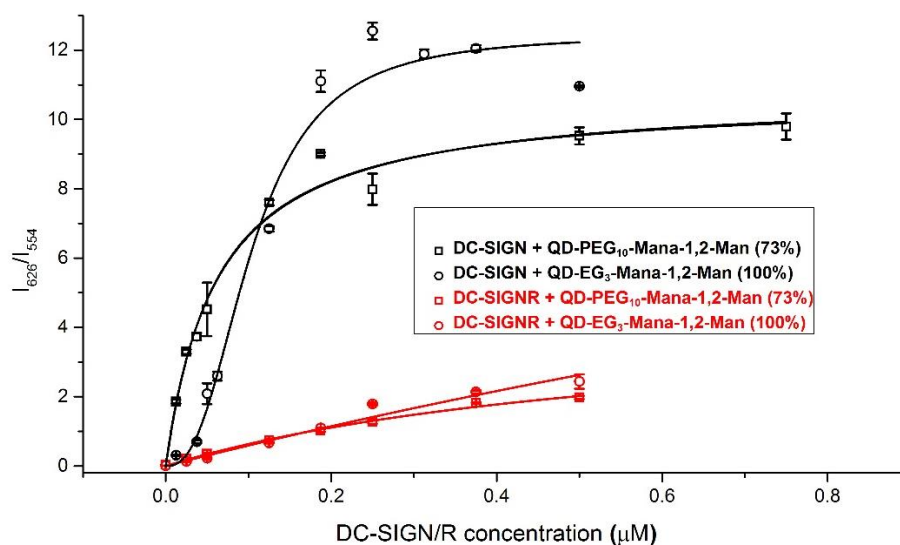


Figure 6-13. FRET ratio (I_{626}/I_{554}) between di-mannose capped QDs donors and dye-labelled DC-SIGN and DC-SIGNR acceptors (collectively called DC-SIGN/R).

Table 6-2. The binding data for dimannose capped QDs binding to DC-SIGN and DC-SIGNR

Protein	Linker between quantum dot and Man- α -1,2-Man	Model				
		One site binding		Hill equation		
		$\frac{I_{626}}{I_{554}} = \frac{\left(\frac{I_{626}}{I_{554}}\right)_{\max} [\text{protein}]}{K_d + [\text{protein}]}$		$\frac{I_{626}}{I_{554}} = \frac{\left(\frac{I_{626}}{I_{554}}\right)_{\max} [\text{protein}]^n}{EC_{50}^n + [\text{protein}]^n}$		
	$(I_{626}/I_{554})_{\max}$	K_d / nM	$(I_{626}/I_{554})_{\max}$	EC_{50} / nM	n	
DC-SIGN	PEG ₁₀	10.7±0.4	62±7	10.6±0.8	60±13	1.02±0.14
DC-SIGN	EG ₃	- ^a	- ^a	12.4±0.8	104±11	2.55±0.33
DC-SIGNR	PEG ₁₀	4.5±0.8	607±165	- ^b	- ^b	- ^b
DC-SIGNR	EG ₃	- ^c	- ^c	- ^c	- ^c	- ^c

^a not determined as equation did not fit the data

^b not determined as fitting was over parameterised

^c not determined as an insufficient portion of the binding isotherm was recorded for analysis

6.9 Conclusions

The synthetic routes to azido-mannopyranosides in form of mono- and disaccharides have been successfully developed. The azido-disaccharide version was unfortunately difficult to synthesise from the previously-prepared azido-monosaccharide as a starting material. The synthesis of disaccharide analogue was achieved by performing O-2-selective de-acetylation of D-mannose pentaacetate to render 2-OH available for glycosylation with another mannosyl donor, and further attachment to azido-PEG-alcohol. Azido-mannopyranosides were functionalised with DHLA-PEG linkers via strain-promoted alkyne-azide cycloaddition before conjugating to commercially available CdSe/ZnS core/shell QDs via an efficient newly established method to make the functionalised QDs dense, compact and biocompatible. Mono and di-mannose capped QDs (Man-QDs) were employed to probe multivalent receptor-glycan interactions for DC-SIGN and DC-SIGNR via FRET. The results showed that multivalent Man-QDs exhibited higher binding affinities to DC-SIGN than its related receptor DC-SIGNR. This distinct function may be due to different arrangements of the CRDs of DC-SIGN and DC-SIGNR. Moreover, mono-mannose capped QDs specifically inhibited DC-SIGN- but not DC-SIGNR-mediated *pseudo*-Ebola viral entry of target cells. This work thus establishes a new strategy for targeting DC-SIGN from DC-SIGNR mediated viral infection.

Chapter 7: Conclusions and future work

This thesis contributes to the development of multivalent galactose-based compounds for targeting LOX-1 and the other mannose-based compounds for probing multivalent DC-SIGN/ligand interaction.

7.1 LOX-1 project

7.1.1 Summary

The previous work of Dr. K. Lacey, Dr. P. Mandal and Dr. S. Ponnambalam (University of Leeds) has led to the identification, both *in vitro* and *in vivo*, of a trisaccharide inhibitor of LOX-1, a receptor involved in atherosclerosis. However, enhancement of inhibition was thought to be possible by the attachment of multiple copies of the lead trisaccharide epitopes on a multivalent scaffold. As a consequence, to build such multivalent structures, two main questions were raised: 1) what type of a scaffold would be used for the multivalent presentation of the sugars? and 2) what functional group on the sugar would be amenable for the multivalent scaffold attachment?

In collaboration with Dr. C. Mahon and Dr. D. Fulton (University of Newcastle), aldehyde-functionalised polymers were used for the attachment of mannosyl- and galactosyl hydrazides, permitting the production of carbohydrate-functionalised polymer scaffold dynamic combinatorial libraries (PS-DCLs). Thereafter, this type of polymer was used as a multivalent scaffold for the attachment of LOX-1 inhibitors. The preparation of a trisaccharide containing a 4-nitrophenyl was first considered. It was anticipated that the final compound with a nitro group could be converted to the corresponding amine, which would then be treated with dimethyl squarate ester and used to conjugate to Dr. C. Mahon's aldehyde-bearing polymer. The synthesis of a 4-nitrophenyl trisaccharide resulted in a very low yield, due to poor regioselectivity of allylation and low α -selectivity of glycosylations. Prior to improving the synthesis, a more simple sugar containing a 4-aminophenyl group was used as a model to react with a squarate ester and subsequently treated with hydrazine; however, this method was ineffective probably because of hydrazine was too reactive or it could cleave the initial group of dimethyl squarate. Hence, the linkage of this squarate ester with the trisaccharide was thus likely to be unattainable.

An alternative strategy was to synthesise a trisaccharide containing an aryl ester as this could be reacted with hydrazine to form the corresponding hydrazide and used for polymer conjugation. Before developing an improved synthetic strategy to a trisaccharide containing an aryl ester based on the initial synthesis, the simplification of the molecular structure of the lead compound was performed by replacing the central

galactose residue with cyclic diols. The other objective of this simplified model system, which was achieved at the same time, was to optimise the glycosylation conditions. Related glycosyl donors were also prepared. According to the results, the use of a glycosyl donor with ester group at O-4 instead of perbenzylated glycoside demonstrated a significant improvement in α -selectivity, possibly owing to the remote protecting group participation. Unfortunately, it was even more difficult to perform glycosylation with the cyclic diols to produce more simple analogues of the lead compound.

To improve the trisaccharide synthesis, controlling the regioselectivity of protecting group chemistry and stereochemical outcome of glycosylation reactions was indeed necessary. The synthesis of a trisaccharide having a 4-methoxycarbonylphenyl aglycone was therefore reinvented. Several attempts to perform tin-mediated regioselective allylation reactions with an unprotected 4-methoxycarbonylphenyl galactopyranoside were unsuccessful. An alternative approach was employed to protect the same galactopyranoside at the O-1 and O-6 positions and make only O-3 and O-4 positions available for the tin-mediated allylation. This method led to a regioselective O-3-allylation. The other challenging problem to deal with was the α -selectivity of glycosylation. Similar to the case of cyclohexanediol, the glycosylation involved a glycosyl donor having an O-4 substituted ester group gave the best α -selectivity. On the whole, the synthetic route towards a trisaccharide containing 4-methoxycarbonylphenyl aglycone was greatly improved in terms of the α -selectivity, regioselectivity and overall yield. Converting the obtained 4-methoxycarbonylphenyl trisaccharide to the corresponding hydrazide was attempted in D₂O; however, this hydrazinolysis resulted in the hydrolysed product having a carboxylic acid instead. The trisaccharide with an aryl ester group was successfully converted to the corresponding hydrazide in refluxing MeOH. Subsequently, 4-benzoylhydrazide trisaccharide was used for the attachment to a multivalent polymeric scaffold by Dr. C. Mahon. A monosaccharide version was also synthesised and attached to the same type of multivalent scaffold. This work establishes new and improved synthetic methods towards a trisaccharide, and its multivalent version, which could be suitable candidates for inhibiting LOX-1 and therefore reducing the incidence of atherosclerosis.

7.1.2 Achievements

The key achievements of this LOX-1 project are as follows:

- The use of a glycosyl donor having an *O*-4 PMBz group for glycosylation on a cyclohexane diol or a galactose residue demonstrated a great improvement of α -selectivity.
- A *pseudo*-trisaccharide having a central cyclohexane ring was successfully synthesised; however in a very low yield.
- Synthetic strategy towards a trisaccharide analogue of the lead inhibitor of LOX-1 was improved, notably on the regioselectivity of allylation and α -selectivity of glycosylation.
- A trisaccharide analogue of the lead inhibitor was successfully synthesised. This trisaccharide contains an ester functional group with could be converted to the corresponding hydrazide that was ready for the attachment to a multivalent scaffold.
- Multivalent glycopolymers bearing mono- and tri-saccharide units were successfully prepared by Dr. C. Mahon. These were anticipated to be better candidates for LOX-1 inhibitors.

7.1.3 Challenges and limitations

The challenges and limitations of this LOX-1 project are as follows.

- The glycosylation reactions with a more simple, non-sugar moiety (*i.e.*, 1,2-cis-cyclohexanediol) were even more difficult to manipulate than glycosylation with sugar residues. Generating more diverse structures of compounds, *i.e.*, trisaccharide in which its central galactose was replaced with different cyclic diols was not yet possible.
- LOX-1 binding domain and its recognition mode are still not yet fully understood; therefore, it is difficult to find a functional and appropriate inhibitor for LOX-1. As LOX-1 was proved to be inhibited by a trisaccharide, modifying the carbohydrate structures still required challenging and consecutive reactions, which were attributed to the need of elaborate protecting group strategies and the difficulties to perform glycosylation of building blocks in a stereoselective fashion.

7.1.4 Future work

It would be of interest to test the synthesised carbohydrate-based compounds both in mono- and multivalent forms in cellular assays for their inhibitory effects for LOX-1. Porcine aortic endothelial cells expressing LOX-1 were established by Ms. I. Abul Zani and Dr. S. Ponnambalam (University of Leeds) and will be used to assess whether these carbohydrates or glycopolymers could inhibit OxLDL binding and uptake by LOX-1-expressing cells using similar protocols which was developed by Dr. K. Lacey. After the treatment of cells expressing LOX-1 with carbohydrates or glycopolymers, the binding of Dil-OxLDL to LOX-1 transfected cells will be detected by confocal microscopy. A decrease in Ox-LDL particles bound to LOX-1 expressing cells is expected.

Moreover, any relevant analogues exhibiting effective inhibition *in vitro* would then be selected to evaluate further for anti-atherogenic effects in animal models of atherosclerosis, e.g., in mouse lacking Apo-E, which could develop atherosclerotic lesions after feeding a high-fat 'Western diet'. These *in vitro* and *in vivo* results would provide the molecular basis of the interaction between LOX-1 and the carbohydrate epitopes and also an insight into the development of a more potent inhibitor of LOX-1. This could ultimately lead to a new therapeutic approach for the atherosclerosis treatment. Expanding the sugar structures to determine which part of the trisaccharide is more essential to be recognised by LOX-1 may also be beneficial for further studies.

Although many carbohydrate-binding proteins have been identified and could be potential drug targets, the development of new carbohydrate-based therapeutics is still a challenge. One of the main obstacles is that carbohydrates exhibit poor pharmacokinetic properties – in particular, low bioavailability and serum half-life. These are possibly due to high polarity of carbohydrates, which limits passive intestinal absorption and therefore oral availability. In addition, after parenteral administration, carbohydrates are potentially excreted rapidly from the kidney.¹⁶³ Possible strategies to improve pharmacokinetic properties are the bioisoteric replacement of crucial groups¹⁶⁴ or a pro-drug approach.¹⁶⁵ A successful example of the pro-drug strategy is oseltamivir, an ethyl ester pro-drug, which is able to be converted to active metabolite oseltamivir carboxylate.¹⁶⁶ Its bioavailable of the ester pro-drug is high (80%). Following dosing, Oseltamivir is detectable in plasma within 30 minutes and reaches maximal concentrations after 3-4 hours.¹⁶⁷ Another approach is to conjugate sugars with carriers, e.g., peptides, polymers, antisense oligonucleotides (ASOs). A recent example is the conjugation of ASOs with triantennary N-acetyl galactosamine (GalNAc₃), a high-affinity

ligand for hepatocyte-specific asialoglycoprotein receptor (ASGPR). The resulting ASOs conjugate could improve drug distribution to target cells, thus, it greatly enhances the targeted distribution of these molecules to hepatocytes and resulted in significant improvement in potency in cells and mice.^{168,169} Moreover, Tanaka *et al.* successfully prepared glycopolymers bearing triazole-linked sialyloligosaccharides which could strongly bind to both human and avian influenza A viruses.¹⁷⁰ On the other hand, Synsorb-Pk, a shigatoxin-binding molecule, was one of the examples of carbohydrate compounds that reached phase II clinical trials in patients but it did not reduce the severity of hemolytic uremic syndrome. Evaluation of the Synsorb-Pk in phase II clinical trials was therefore abandoned.^{171,172} PEGylation (i.e., the covalent conjugation with polyethylene glycol (PEG)), is a widely used technique to achieve long blood circulation times of protein-polymer conjugates for clinical use.^{173,174} The process of PEGylation can be extended to carbohydrates.¹⁷⁵

However, the use of the newly synthesised glycopolymer bearing trisaccharide from this PhD project as a therapeutic agent depends on the results from biological testings. The pharmacokinetic properties and toxicity of the synthesised trisaccharide-conjugated polymer are needed to be evaluated in the future.

There is also a need to perform parallel experiments such as molecular dynamics, crystallographic data, NMR-based structural analysis, to gain a better understanding of structural knowledge of LOX-1 receptor and carbohydrate ligands. This information would also be useful to predict more correct binding orientations of both receptor and relevant ligands.

Another potential application of these carbohydrate-based compounds could be targeted delivery of drugs to LOX-1 expressing cells.

7.2 DC-SIGN project

7.2.1 Summary

Two different mannose-based ligands containing either mono- or dimannose units were developed and used, in collaboration with Dr. Y. Guo, as QD-based FRET probes for the study of DC-SIGN/ligand interaction. An azido-mannopyranoside was prepared from the glycosylation of peracetyl protected mannose with a chloro-PEG-alcohol and converted to the corresponding compound with an azido-PEG linker. Following a Zemplén deacetylation, the desired azido-mannopyranoside was obtained.

The azido-mannopyranoside was further functionalised with DHLA-PEG linkers via strain-promoted alkyne-azide cycloaddition and conjugated to commercially available CdSe/ZnS core/shell QDs. Mono-mannose capped QDs were used as a tool to probe multivalent receptor/glycan interactions for DC-SIGN and DC-SIGNR via FRET technique. Mono-mannose capped QDs were shown to preferentially bind to DC-SIGN over DC-SIGNR. The functional differences between these two receptors may arise from the different spatial aspects of CRDs arrangements of DC-SIGN and DC-SIGNR. Furthermore, the binding specificity of mono-mannose capped QDs with DC-SIGN and DC-SIGNR were confirmed by Ebola virus inhibition assays using *pseudo*-types, which were performed by Dr. I. Nehlmeier and Dr. S. Pöhlmann (German Primate Center, Gottingen, Germany). Their results showed that the mono-mannose capped QDs could specifically inhibit DC-SIGN- but not DC-SIGNR-mediated *pseudo*-Ebola viral entry of target cells.

A more complex carbohydrate epitope, Man α -1,2-Man was thought to be a better ligand for DC-SIGN. Synthesis of an azido-disaccharide version starting from the available off-the-shelf azido-mannopyranoside proved to be problematic. The synthesis of Man α -1,2-Man was eventually accomplished by another approach, which was firstly the preparation of a mannose building block having solely a 2-OH available to perform glycosylation. After the optimised glycosylation step, the acetylated disaccharide was converted to the corresponding imidate and used for the preparation of a manno-*biose* containing an azido-PEG chain via the same experimental procedures as for the mono-Man version.

The azido-Man α -1,2-Man was also conjugated with QDs in a similar manner to that of azido-Man. The preliminary QD-FRET data of di-mannose capped QDs showed higher binding affinities to both lectins in comparison to the mono-mannose capped QDs and exhibited a more intimate binding with DC-SIGN than its related receptor DC-SIGNR.

The interaction between lectin (e.g., DC-SIGN and DC-SIGNR) with synthetic glyco-QDs was investigated for the first time by QD-based FRET technique. This work also provides a new strategy for probing multivalent interactions between the lectin and its ligand.

7.2.2 Achievements

The key achievements of this DC-SIGN project are as follows:

- Azido-mannopyranosides in form of mono- and disaccharide were successfully synthesised.
- Conjugations between both azido-compounds and CdSe/ZnS core/shell QDs were achieved.
- Man-QDs were used to probe multivalent interactions of DC-SIGN and DC-SIGNR by QD-FRET experiments and viral entry inhibition assays. Man-QDs exhibited higher binding affinities to DC-SIGN than DC-SIGNR, confirming their distinct functions potentially due to differences in the CRD orientations.

7.2.3 Challenges and limitations

The challenges and limitations of this DC-SIGN project are as follows.

- The azido-disaccharide could not be synthesised from the mannoside bearing an azido-PEG chain. The disaccharide could only be prepared by first synthesising a disaccharide donor and then performing glycosylation of the chloro-PEG-alcohol.

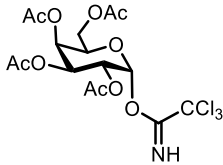
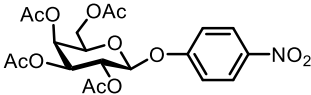
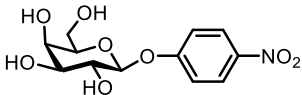
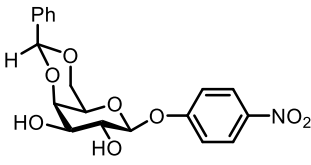
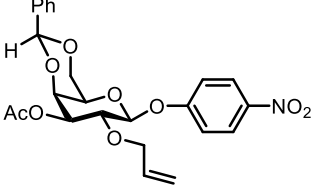
7.2.4 Future work

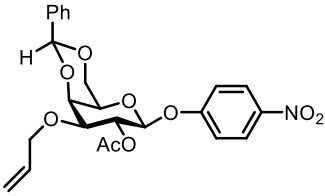
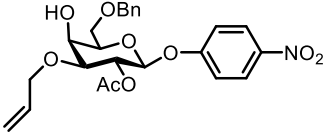
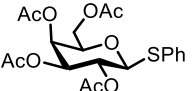
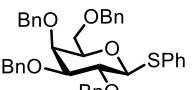
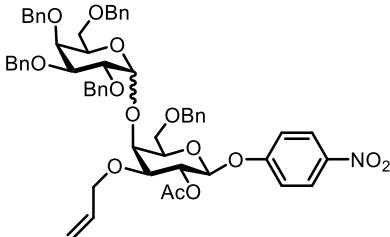
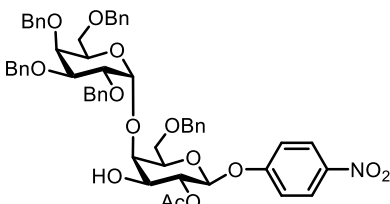
The evaluation of di-Man-QDs for the binding effects with DC-SIGN and DC-SIGNR using FRET will be performed by Dr. Y. Guo, Dr. I. Nehlmeier and Dr. S. Pöhlmann. It would also be of interest to test the di-Man-QDs with the same Ebola virus inhibition assays using virus-like particles to compare its effect with the mono-Man-QDs. It is anticipated that these QD-based FRET probes will have a great impact on DC-SIGN-mediated HIV-1 inhibition. HIV inhibition assays would give an insight into the interaction and the fundamental roles of DC-SIGN in HIV infection. This could be a starting point leading to a rational design of potential DC-SIGN inhibitors as therapeutic drugs for the treatment of viral infections and other related diseases in the future. Similar to the case of glycopolymers, pharmacokinetic and toxicity assessments of the mannose-conjugated QDs are needed to be taken into account. However, the toxicity of quantum-dots is still of a great concern because they contain metal ions, e.g. Cd²⁺,

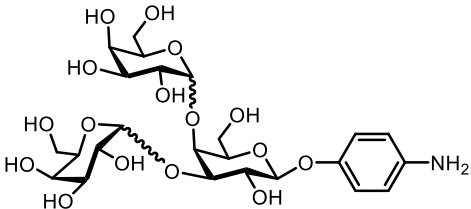
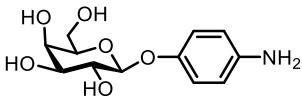
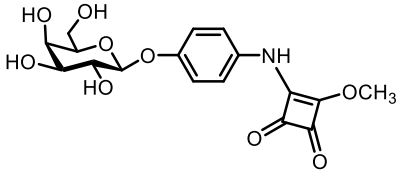
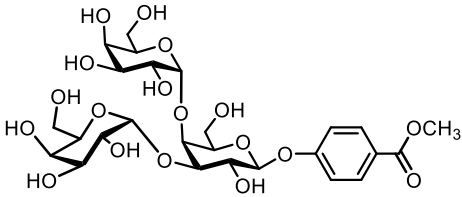
which are known to be toxic to cells. Another option is to prepare carbohydrate-conjugated gold-nanoparticles since gold-nanoparticles has been reported to be nontoxic and used to treat rheumatoid arthritis.¹⁷⁶ Moreover, a recent review showed that the tumour-targeting applications of nanoparticles still resulted in low delivery efficiency as nanoparticles may interact with other components in tumour matrix. A higher dosage may enhance the delivery efficiency but potentially increase toxicity.¹⁷⁷ Furthermore, this newly established conjugation method to produce dense and compact carbohydrate-functionalised QDs could be further applied for the investigation of other lectins by varying the carbohydrate epitopes on the surfaces of the QDs. FRET or other fluorescent imaging methods could be employed to detect glyco-conjugated QDs.

Tables of compounds

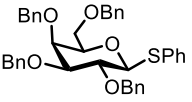
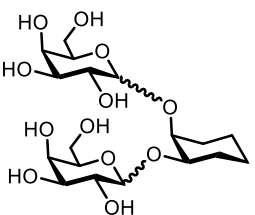
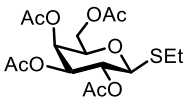
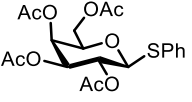
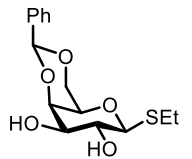
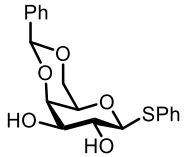
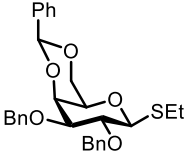
Chapter 2

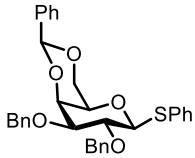
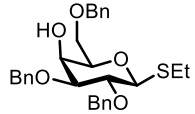
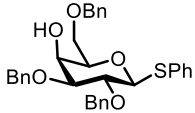
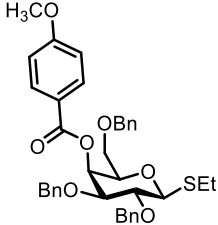
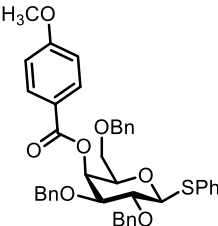
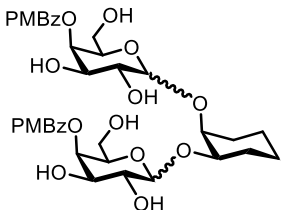
Structure	Compound number	Page number in experimental section
	34	150
	35	151
	36	152
	37	152
	38a	153

Structure	Compound number	Page number in experimental section
	38b	153
	39	155
	40	156
	41	157
	42	158
	43	159

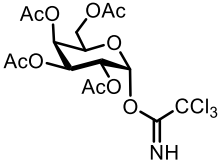
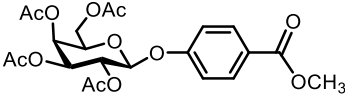
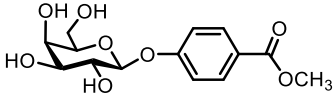
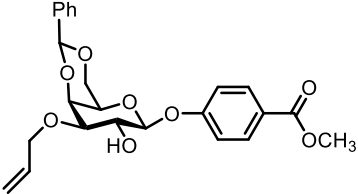
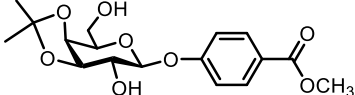
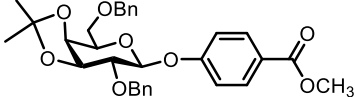
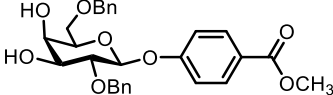
Structure	Compound number	Page number in experimental section
	44	160
	45	161
	47	161
	27	148

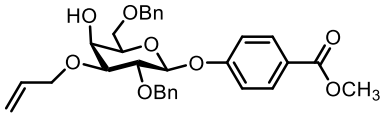
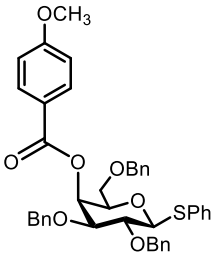
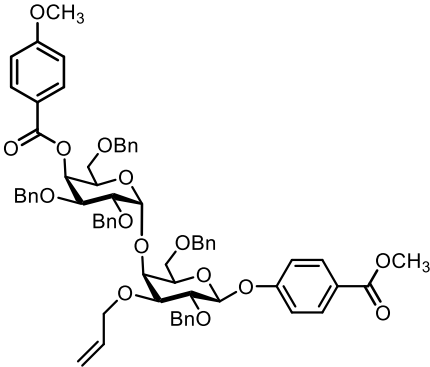
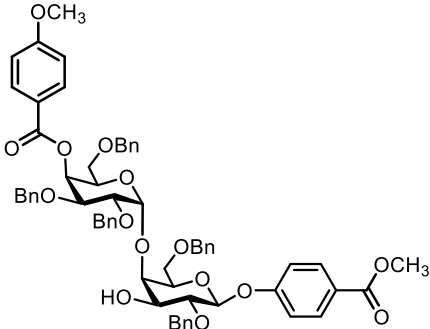
Chapter 3

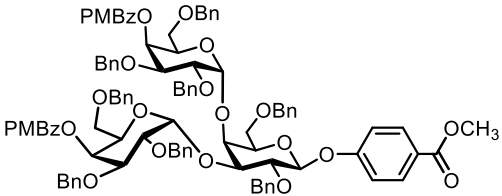
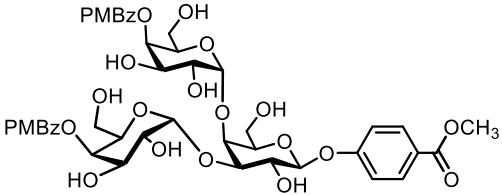
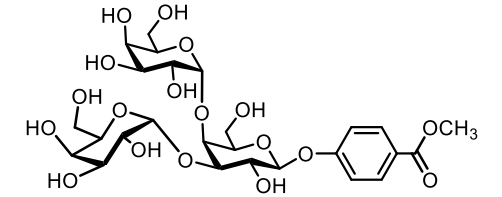
Structure	Compound number	Page number in experimental section
	41	157
	51	162
	61	165
	40	156
	62	166
	63	167
	64	168

Structure	Compound number	Page number in experimental section
	65	169
	66	170
	67	171
	68	172
	55	164
	70	173

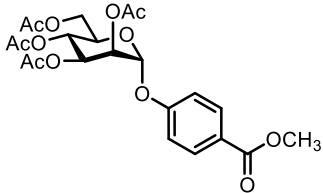
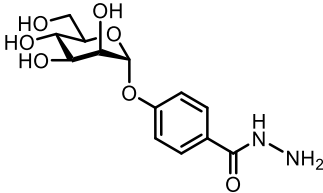
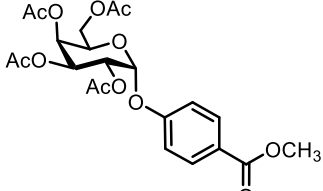
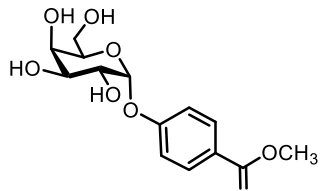
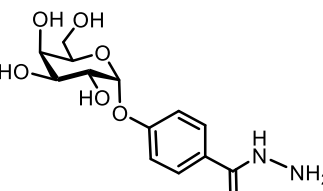
Chapter 4

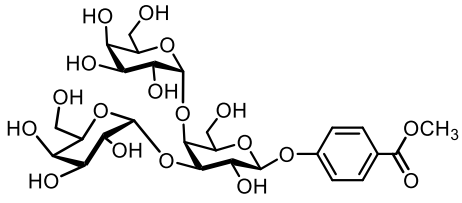
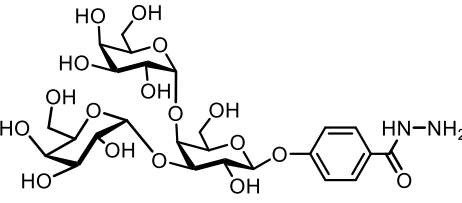
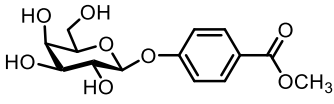
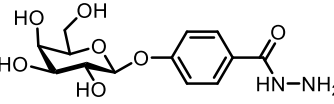
Structure	Compound number	Page number in experimental section
	34	150
	72	175
	73	176
	75	177
	76	178
	77	179
	78	180

Structure	Compound number	Page number in experimental section
	79	180
	55	164
	80	181
	81	183

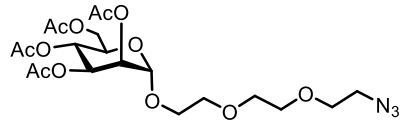
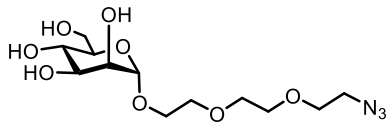
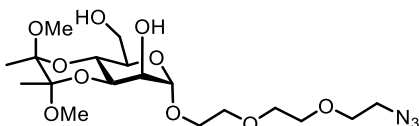
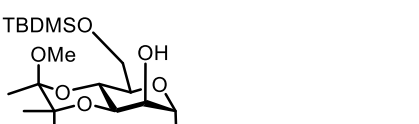
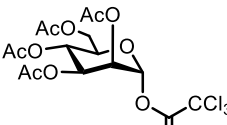
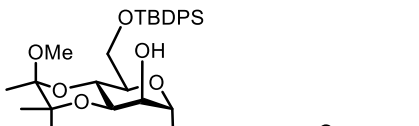
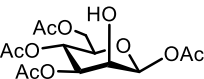
Structure	Compound number	Page number in experimental section
	82	184
	83	186
	27	148

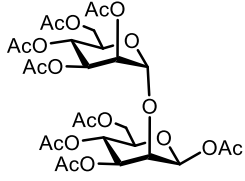
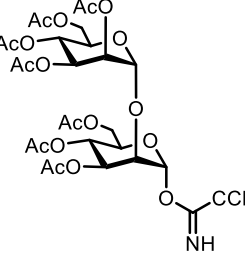
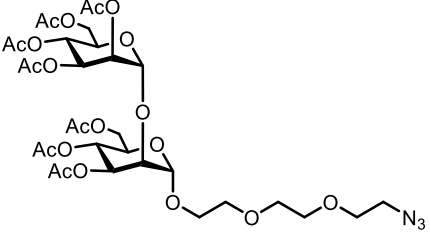
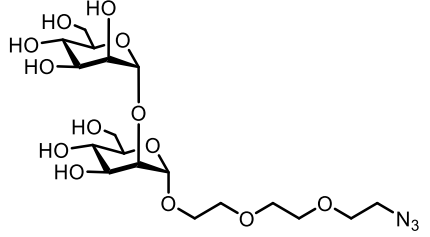
Chapter 5

Structure	Compound number	Page number in experimental section
	85	187
	86	188
	87	188
	88	189
	89	190

Structure	Compound number	Page number in experimental section
	27	148
	90	191
	73	176
	91	191

Chapter 6

Structure	Compound number	Page number in experimental section
	92	192
	29	149
	93	193
	94	194
	95	195
	97	196
	101	197

Structure	Compound number	Page number in experimental section
	102	198
	103	199
	104	200
	31	149

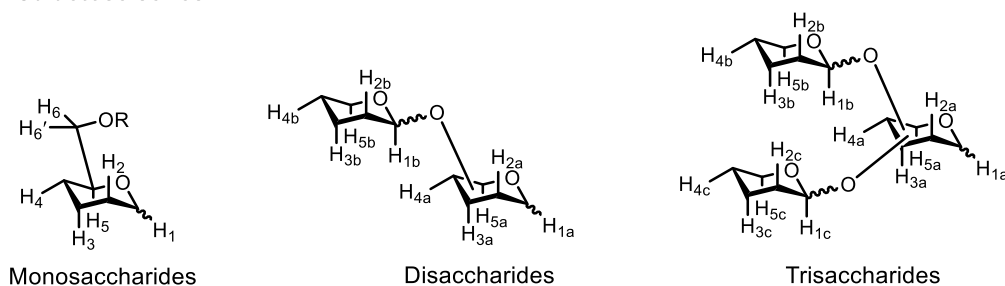
Chapter 8: Experimental

8.1 General methods

Dry DCM, THF, MeOH, MeCN, EtOAc were obtained through an Innovative Technology solvent drying system. Anhydrous DMF and DCE were purchased from Sigma-Aldrich, and all other commercially available reagents were used as received. Boron trifluoride diethyl etherate ($\text{BF}_3 \cdot \text{OEt}_2$) and triflic anhydride (Tf_2O) were distilled prior to use. All solvents used for flash chromatography were GPR grade, except hexane and ethyl acetate, for which HPLC grade was used. All concentrations were performed *in vacuo*, unless otherwise stated. CdSe/ZnS core/shell QDs with λ_{EM} of 560 nm were purchased commercially from PlasmaChem GmbH (Berlin, Germany). The QDs were supplied as dry powder, capped with mixed hydrophobic ligands including trioctyl-phosphine oxide (TOPO), hexadecylamine and oleic acid.

NMR spectra were acquired at room temperature (r.t.), unless noted otherwise. ^1H NMR spectra were recorded at 500 MHz on a Bruker Avance 500 instrument or at 600 MHz on a JEOL Resonance ECA600II spectrometer. ^{13}C NMR spectra were recorded at 75 MHz on a Bruker Avance 300 instrument or at 500 MHz on a Bruker Avance 500 machine. Chemical shifts (δ) are reported in parts per million (ppm) using ^{13}C and residual ^1H signals from deuterated solvents as references. Assignments of NMR spectra were achieved using 2D methods (COSY, TOCSY, NOESY, HMBC, HMQC) when necessary. Splitting patterns are described by using the following abbreviations: br, broad; s, singlet; d, doublet; t, triplet; q, quartet; m, multiplet; or combinations thereof. ^1H NMR data of mono-, di- and trisaccharides were assigned in agreement with Figure 8-1.

a) Galactose series



b) Mannose series

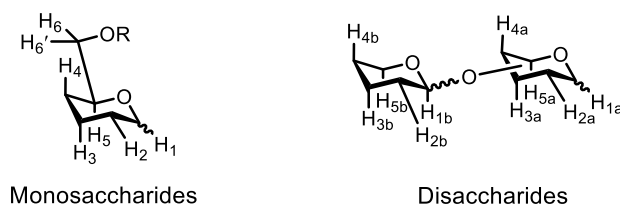


Figure 8-1. Proton numbering in ^1H NMR for a) galacto-configured mono- and di- and trisaccharides b) manno-configured mono- and disaccharides.

Low resolution electrospray (ES^+) ionisation mass spectra were obtained on a Bruker HCTUltra mass spectrometer, and high resolution ES^+ were performed on a Bruker Daltonics MicroTOF or a Bruker maXis ImpactTM mass spectrometer. Infra-red (IR) spectra were recorded on a PerkinElmer Spectrum One FT-IR spectrometer. Melting points were obtained on a Griffin melting point apparatus. Optical rotations were measured at the sodium D-line with a Schmidt+Haensch Polartronic H532 polarimeter. Specific rotation $[\alpha]_D$ values are given in units of $10^{-1} \text{ deg cm}^2 \text{ g}^{-1}$. All solution reactions were monitored by thin layer chromatography (TLC) on silica gel plates 60-F²⁵⁴ (Merck) with visualisation under UV (254 nm) and/or by staining with iodine vapour or detection charring following immersion in a 5% $\text{H}_2\text{SO}_4/\text{MeOH}$ solution, unless otherwise indicated. Column chromatography was carried out using silica gel (60 mesh) with elution solvents as described. Gel filtrations were performed on Sephadex LH-20 eluting with water/MeOH or on Bio-Beads SX-1 eluting with toluene. Water soluble compounds were freeze dried using Virtis Benchtop K freeze dryer.

UV-vis absorption spectra were recorded on a Varian Cary 50 bio UV-Visible spectrophotometer over 200-800 nm using a 1 mL-quartz cuvette with an optical path of 1 cm or on a Nanodrop 2000 spectrophotometer (Thermo scientific) over the range of 200-800 nm using 1 drop of the solution with an optical path length of 1 mm. All centrifugations were carried out on a Thermo Scientific Heraeus Fresco 21 microcentrifuge using 1.5 mL-microcentrifuge tubes at room temperature, unless

otherwise stated. The QD purification was performed by Amicon ultra-centrifugal filter tubes with a molecular weight cut-off (MWCO) of 30,000. DLS was performed using a Zetasizer NanoZS (Malvern) using a laser wavelength of 633 nm in disposable polystyrene cuvettes. Readings of 10 scans were taken in triplicate and the average values were calculated.

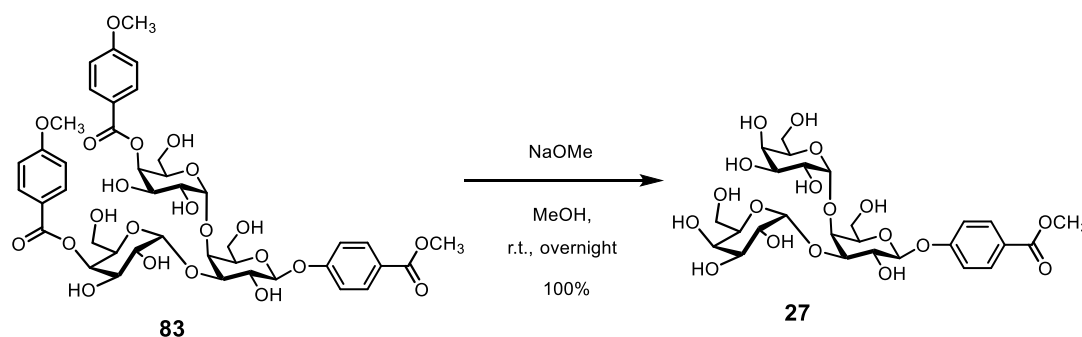
8.2 Chemical synthesis

8.2.1 Synthesis of carbohydrates

4-Methoxycarbonylphenyl

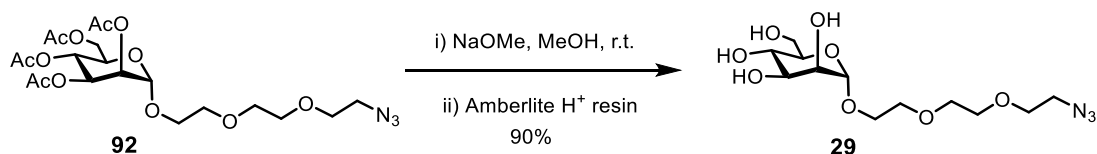
3,4-bis-O-(α -D-galactopyranosyl)- β -D-

galactopyranoside (**27**)



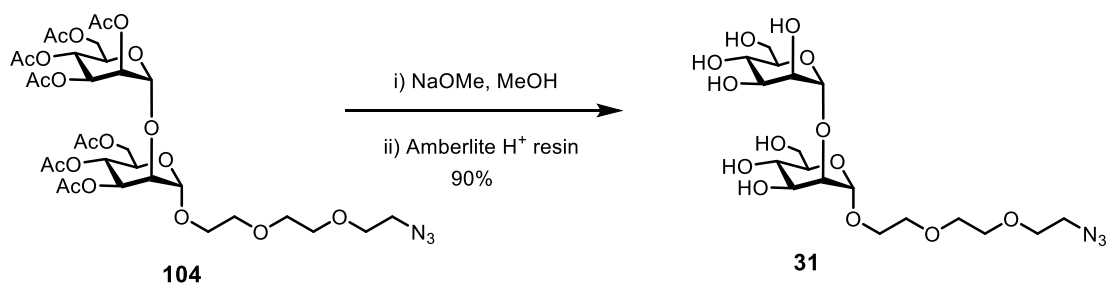
Sodium methoxide (3.2 mg, 0.1 mmol) was added to a solution of 4-methoxycarbonylphenyl-3,4-bis-O-(4-O-4-methoxybenzoyl- α -D-galactopyranosyl) β -D-galactopyranoside **83** (24 mg, 0.03 mmol) in MeOH (1 mL). The reaction mixture was stirred for 48 h at r.t., neutralised with Amberlite[®] IRC 86 H⁺ resin, filtered and concentrated to give 4-methoxycarbonyl 3,4-bis-O-(α -D-galactopyranosyl)- β -D-galactopyranoside **27** as a colourless oil (17 mg, 100%); R_f 0.38 (6:4:1 Chloroform–MeOH–H₂O); $[\alpha]_D^{25}$ 10.64 (c, 0.1, H₂O); δ_H (500 MHz, D₂O); 8.04 (d, 2H, J 8.8 Hz, ArH), 7.24 (d, 2H, J 8.8 Hz, ArH), 5.34 (d, 1H, $J_{1a,2a}$ 7.5 Hz, H-1a), 5.29 (d, 1H, $J_{1c,2c}$ 4.0 Hz, H-1c), 5.14 (d, 1H, $J_{1b,2b}$ 3.6 Hz, H-1b), 4.42 (d, 1H, J 2.2 Hz, H-4a), 4.29 (t, 1H, J 6.4 Hz, H-5), 4.20 (t, 1H, J 6.5 Hz, H-5), 4.08–3.63 (m, 18H, H-2a, H-2b, H-2c, H-3a, H-3b, H-3c, H-4b, H-4c, H-5a, H-6a, H-6'a, H-6b, H-6'b, H-6c, H-6'c, OCH₃); δ_C (75 MHz, D₂O); 168.9 (C=O), 160.4 (C-O), 131.7 (ArC), 124.0 (C-O), 116.3 (ArC), 101.0 (C-1a), 99.9 (C-1c), 95.5 (C-1b), 76.5, 75.5, 75.1, 71.7, 70.8, 69.6, 69.1, 68.9, 68.8, 68.6, 60.9, 60.9, 60.6 (3 \times C-2, 3 \times C-3, 3 \times C-4, 3 \times C-5, 3 \times C-6), 52.5 (OCH₃); **IR** (ν_{\max} /cm⁻¹): 3375 (OH), 1704 (C=O); **HRMS**: Found $[M+Na]^+$ 661.1960, C₂₆H₃₈NaO₁₈ requires 661.1950.

1-Azido-3,6-dioxaoct-8-yl α -D-mannopyranoside (**29**)¹⁷⁸



Sodium methoxide (103 mg, 2 mmol) was added to a solution of 1-azido-3,6-dioxaoct-8-yl 2,3,4,6-tetra-O-acetyl- α -D-mannopyranoside **92** (1.20 g, 2.4 mmol) in anhydrous MeOH (50 mL). After stirring for 3 h at r.t., the reaction mixture was diluted with MeOH and neutralised with Amberlite[®] IRC 86 H⁺ resin, filtered, re-dissolved in hot MeOH, cooled down, filtered through Celite[®] pad and concentrated to afford compound **29** (0.72 g, 90%) as a colourless oil; R_f 0.10 (9:1 DCM–MeOH); $[\alpha]_D^{22}$ 54.24 (c, 0.25, MeOH) (lit.¹⁷⁹ $[\alpha]_D^{25}$ 38.7 (c, 1.0, MeOH)); δ_H (500 MHz, D₂O); 4.91 (d, 1H, J 1.6 Hz, H-1), 3.99 (dd, 1H, $J_{2,3}$ 3.5 Hz, $J_{1,2}$ 1.6 Hz, H-2), 3.92–3.88 (m, 2H, ManOCH₂), 3.86–3.83 (m, 1H, H-3), 3.80–3.66 (m, 12H, H-4, H-5, H-6, H-6', 4 × OCH₂), 3.52 (t, 2H, J 5.1 Hz, CH₂-N); δ_C (75 MHz, D₂O); 100.0 ($J_{C,H}$ 169 Hz, α , C-1), 72.7 (C-4), 70.5 (C-3), 70.0 (C-2), 69.6, 69.5, 69.5, 69.3 (4 × CH₂O), 66.7 (C-5), 66.4 (ManOCH₂), 60.9 (C-6), 50.2 (CH₂-N); IR (ν_{max}/cm^{-1}): 3373 (OH), 2106 (N₃); HRMS: Found $[M+Na]^+$ 360.1377, C₁₂H₂₃N₃NaO₈ requires 360.1381.

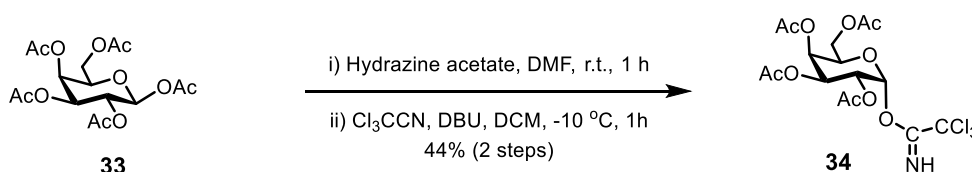
1-Azido-3,6-dioxaoct-8-yl 2-O- α -D-mannopyranosyl- α -D-mannopyranoside (**31**)



Sodium methoxide (5.3 mg, 0.10 mmol) was added to a solution of 1-azido-3,6-dioxaoct-8-yl 3,4,6-tri-O-acetyl-2-O-(2,3,4,6-tetra-O-acetyl- α -D-mannopyranosyl)- α -D-mannopyranoside **104** (38 mg, 0.05 mmol) in anhydrous MeOH (1 mL). After stirring for 17 h at r.t., the reaction mixture was neutralised with Amberlite[®] IRC 86 H⁺ resin, filtered and concentrated to afford compound **31** (22 mg, 90%) as a colourless oil; R_f 0.38 (6:4:1 Chloroform–MeOH–H₂O); $[\alpha]_D^{21}$ 0.94 (C, 0.1, H₂O); δ_H (500 MHz, D₂O); 5.14 (d, 1H, $J_{1a,2a}$ 1.7 Hz, H-1a), 5.05 (d, 1H, $J_{1b,2b}$ 1.7 Hz, H-1b), 4.09 (dd, 1H, $J_{2b,3b}$ 3.4

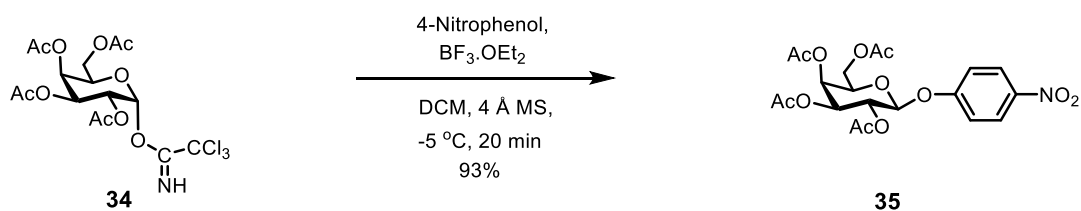
Hz, $J_{1b,2b}$ 1.7 Hz, H-2b), 4.01 (dd, 1H, $J_{2a,3a}$ 3.4 Hz, $J_{1a,2a}$ 1.7 Hz, H-2a), 3.95 (dd, 1H, $J_{3a,4a}$ 9.2 Hz, $J_{2a,3a}$ 3.4 Hz, H-3a), 3.93-3.84 (m, 4H, H-3b, H-6, H-6', CH_2O), 3.82-3.61 (m, 15H, C-4a, C-4b, C-5a, C-5b, C-6, C-6', CH_2O), 3.55-3.51 (t, 2H, J 4.87 Hz, $\text{CH}_2\text{-N}$); δ_{c} (75 MHz, D_2O); 102.3 ($J_{\text{C,H}}$ 171 Hz, 4.1 Hz, α , C-1b), 98.4 ($J_{\text{C,H}}$ 172 Hz, α , C-1a), 78.6 (C-2a), 73.3, 72.8, 66.6, 61.1 (2 \times C-4, 2 \times C-5), 70.3, 70.2 (C-3b), 69.9 (C-2b), 69.6 (C-3a), 69.5, 69.5, 69.3, 66.9 (4 \times CH_2O), 60.9, 50.2 (2 \times C-6); **IR** ($\nu_{\text{max}}/\text{cm}^{-1}$): 3331 (OH), 2103 (N_3); **HRMS**: Found $[\text{M}+\text{NH}_4]^+$ 517.2372, $\text{C}_{18}\text{H}_{37}\text{N}_4\text{O}_{13}$ requires 517.2352.

2,3,4,6-Tetra-O-acetyl- α -D-galactopyranosyl trichloroacetimidate (**34**)¹⁸⁰



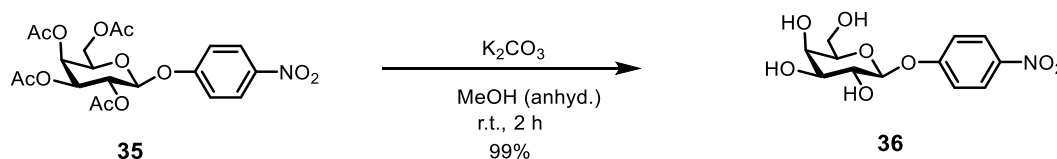
Hydrazine acetate (8.86 g, 96.1 mmol) was added to a solution of β -D-galactose pentaacetate **33** (25.0 g, 64 mmol) in DMF (80 mL), and the reaction mixture was stirred at r.t. for 1 h, concentrated to leave a pale yellow oil, which was purified by flash column chromatography (silica; 2:1 hexane–EtOAc) to afford a hemiacetal intermediate as a colourless oil (17.6 g). The oil was dissolved in anhydrous DCM (40 mL). Trichloroacetonitrile (24.5 mL, 244 mmol) and DBU (2.5 mL) were added to the solution, which was stirred at -10 $^\circ\text{C}$ for 1 h, concentrated and purified by flash column chromatography (silica; 4:1 hexane–EtOAc), yielded trichloroacetimidate **34** (13.9 g, 44% over two steps) as a pale yellow solid; R_f 0.14 (double-run, 2:1 hexane–EtOAc); m.p. 124-125 $^\circ\text{C}$ (from diethyl ether–hexane) (lit.¹⁸⁰ m.p. 126-127 $^\circ\text{C}$); $[\alpha]_{\text{D}}^{24}$ 128 (c, 1, CHCl_3) (lit.¹⁸⁰ $[\alpha]_{\text{D}}^{25}$ 124 (c, 1, CHCl_3)); δ_{H} (500 MHz, CDCl_3); 8.66 (s, 1H, NH), 6.59 (d, 1H, $J_{1,2}$ 3.5 Hz, H-1), 5.55 (dd, 1H, $J_{4,5}$ 1.23 Hz, $J_{3,4}$ 3.2 Hz, H-4), 5.42 (dd, 1H, $J_{2,3}$ 10.9 Hz, $J_{3,4}$ 3.2 Hz, H-3), 5.35 (dd, 1H, $J_{1,2}$ 3.5 Hz, $J_{2,3}$ 10.9 Hz, H-2), 4.45-4.41 (m, 1H, H-5), 4.15 (dd, 1H, $J_{6,5}$ 6.7 Hz, $J_{6,6'}$ 11.3 Hz, H-6), 4.07 (dd, 1H, $J_{6,5}$ 6.7 Hz, $J_{6,6'}$ 11.3 Hz, H-6'), 2.16 (s, 3H, $\text{C}(\text{O})\text{CH}_3$), 2.10-2.00 (m, 9H, 3 \times $\text{C}(\text{O})\text{CH}_3$); δ_{c} (75 MHz, CDCl_3); 170.4, 170.2, 170.2, 170.1 (C=O), 161.1 (C-N), 93.7 (C-1), 90.9 (CCl_3), 69.1 (C-5), 67.6 (C-3), 67.5 (C-2), 67.0 (C-4), 61.4 (C-6), 20.8, 20.8, 20.7, 20.6 (4 \times $\text{C}(\text{O})\text{CH}_3$); **IR** ($\nu_{\text{max}}/\text{cm}^{-1}$): 3349 (NH), 1747 (C=O), 1645 (C=N); **HRMS**: Found $[\text{M}+\text{Na}]^+$ 514.0055, $\text{C}_{16}\text{H}_{20}\text{Cl}_3\text{NNaO}_{10}$ requires 514.0045.

4-Nitrophenyl 2,3,4,6-tetra-O-acetyl- β -D-galactopyranoside (35)^{181,182}



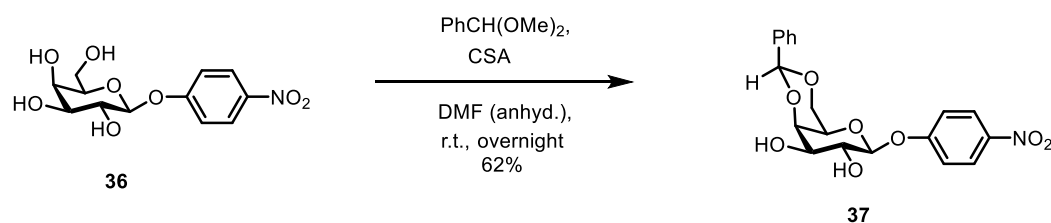
A solution of 2,3,4,6-tetra-O-acetyl α -D-galactopyranosyl trichloroacetimidate **34** (14.0 g, 28 mmol), 4-nitrophenol (5.9 g, 42 mmol) and 4 Å MS (7.0 g) in anhydrous DCM (80 mL) was stirred at -5°C for 5 min before freshly distilled boron trifluoride diethyl etherate (0.7 mL, 5 mmol) was added dropwise. After 15 min the reaction mixture was washed with saturated aq. NaHCO_3 (3×20 mL) and extracted with DCM (3×20 mL). The organic layer was dried (MgSO_4) and concentrated to afford a colourless oil. The crude oil was purified by flash column chromatography (silica; 3:1 hexane–EtOAc \rightarrow 2:1 hexane–EtOAc) to afford compound **35** (12.3 g, 93%) as a colourless solid; R_f 0.21 (3:1 hexane–EtOAc); m.p. $145\text{--}146^\circ\text{C}$ (from EtOH) (lit.¹⁸¹ m.p. $146\text{--}147^\circ\text{C}$); $[\alpha]_{\text{D}}^{21}$ -9.8 (c, 2, CHCl_3) (lit.¹⁸² $[\alpha]_{\text{D}}^{25}$ -10 (c, 2, CHCl_3)); δ_{H} (500 MHz, CDCl_3); 8.22–8.18 (m, 2H, ArH), 7.10–7.05 (m, 2H, ArH), 5.51 (dd, 1H, $J_{2,3}$ 10.4 Hz, $J_{1,2}$ 7.9 Hz, H-2), 5.47 (d, 1H, $J_{3,4}$ 3.4 Hz, H-4), 5.17 (d, 1H, $J_{1,2}$ 7.9 Hz, H-1), 5.13 (dd, 1H, $J_{2,3}$ 10.4 Hz, $J_{3,4}$ 3.4 Hz, H-3), 4.23–4.09 (m, 3H, H-5, H-6, H-6'), 2.18 (s, 3H, $\text{C}(\text{O})\text{CH}_3$), 2.06 (s, 6H, $2 \times \text{C}(\text{O})\text{CH}_3$), 2.01 (s, 3H, $\text{C}(\text{O})\text{CH}_3$); δ_{C} (75 MHz, CDCl_3); 170.5, 170.3, 170.2, 169.5 (C=O), 161.4, 143.5, 126.0, 116.8 (ArC), 98.8 (C-1), 71.7 (C-5), 70.8 (C-3), 68.5 (C-2), 66.9 (C-4), 61.6 (C-6), 20.9, 20.9, 20.8, 20.7 ($4 \times \text{C}(\text{O})\text{CH}_3$); IR ($\nu_{\text{max}}/\text{cm}^{-1}$): 1752 (C=O), 1520, 1342 (NO_2); HRMS: Found $[\text{M}+\text{Na}]^+$ 492.1096, $\text{C}_{20}\text{H}_{23}\text{NNaO}_{12}$ requires 492.1112.

4-Nitrophenyl β -D-galactopyranoside (**36**)¹⁸³



Anhydrous potassium carbonate (0.8 g, 5.1 mmol) was added to a solution of 4-nitrophenyl 2,3,4,6-tetra-*O*-acetyl- β -D-galactopyranoside **35** (11.8 g, 25 mmol) in anhydrous MeOH (150 mL), and stirred at r.t. for 2 h. The reaction mixture was then neutralised by adding acetic acid dropwise. The solvent was evaporated to afford compound **36** (8.08 g, 99%) as a yellow oil. This material was used for the next reaction without purification. The spectroscopic and analytical data are obtained from a partially purified material by recrystallisation from EtOH to give colourless needles; R_f 0.29 (9:1 DCM–MeOH); m.p. 177–179 °C (from EtOH) (lit.¹⁸³ m.p. 180–182 °C); $[\alpha]_D^{25}$ -74.0 (c, 0.5, H₂O) (lit.¹⁸³ $[\alpha]_D$ -80.6 (c, 0.5, H₂O)); δ_H (500 MHz, CD₃OD); 8.23–8.19 (m, 2H, ArH), 7.27–7.23 (m, 2H, ArH), 5.02 (d, 1H, $J_{1,2}$ 7.7 Hz, H-1), 3.92 (d, 1H, $J_{3,4}$ 3.3 Hz, H-4), 3.84 (dd, 1H, $J_{1,2}$ 7.7 Hz, $J_{2,3}$ 9.7 Hz, H-2), 3.80–3.73 (m, 3H, H-5, H-6, H-6'), 3.61 (dd, 1H, $J_{2,3}$ 9.7 Hz, $J_{3,4}$ 3.3 Hz, H-3); δ_C (75 MHz, CD₃OD); 164.0, 143.9, 126.6, 117.8 (ArC), 102.3 (C-1), 77.3 (C-5), 74.8 (C-3), 72.0 (C-2), 70.2 (C-4), 62.4 (C-6); IR ($\nu_{\max}/\text{cm}^{-1}$): 3368 (OH), 1509, 1347 (NO₂); HRMS: Found $[\text{M}+\text{Na}]^+$ 324.0694, C₁₂H₁₅NNaO₈ requires 324.0690.

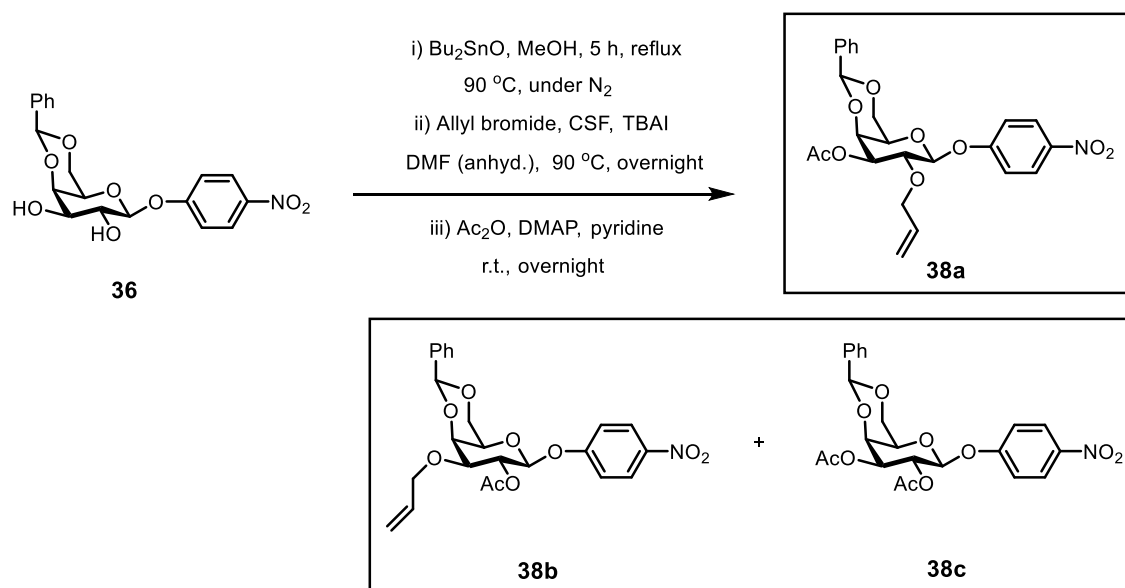
4-Nitrophenyl 4,6-*O*-benzylidene- β -D-galactopyranoside (**37**)^{184,185}



Benzaldehyde dimethylacetal (5.31 g, 34.9 mmol) was added to a solution of 4-nitrophenyl β -D-galactopyranoside **36** (8.08 g, 26.8 mmol) in DMF (30 mL). (+/-)-10-Camphorsulfonic acid was added to the solution dropwise until the reaction mixture was acidic. The reaction mixture was then stirred at r.t. overnight. Triethylamine (33 mL, 22 mmol) was added to the solution mixture and concentrated to give a crude product, which was purified by flash column chromatography (silica; 4:1 EtOAc–hexane) to

afford compound **37** (6.55 g, 62%) as a colourless solid; R_f 0.46 (EtOAc); m.p. 231-233 °C (from EtOH) (lit.¹⁸⁴ m.p. 236-238 °C); $[\alpha]_D^{21}$ -112.5 (c, 1, DMF) (lit.¹⁸⁵ $[\alpha]_D$ -120 (c, 0.6, DMF)); δ_H (500 MHz, DMSO-*d*₆); 8.22 (d, 2H, *J* 8.3 Hz, ArH), 7.48-7.34 (m, 5H, ArH), 7.27 (d, 2H, *J* 8.3 Hz, ArH), 5.60 (s, 1H, PhCHO₂), 5.44 (d, 1H, *J* 5.0 Hz, OH), 5.20 (d, 1H, *J*_{1,2} 7.4 Hz, H-1), 5.16 (d, 1H, *J* 5.9 Hz, OH), 4.19 (s, 1H, H-4), 4.07 (q, 2H, *J*_{6,6'} 12.5 Hz, H-6, H-6'), 3.86 (s, 1H, H-5), 3.73-3.61 (m, 2H, H-2, H-3); δ_C (75 MHz, DMSO-*d*₆); 162.3, 141.6, 138.5, 128.7, 127.9, 126.2, 125.7, 116.5 (ArC), 100.0 (C-1), 99.8 (PhCHO₂), 75.7 (C-4), 71.6 (C-2), 69.5 (C-3), 68.3 (C-6), 66.4 (C-5); **IR** ($\nu_{\max}/\text{cm}^{-1}$): 3468 (OH), 1666, 1390 (NO₂); **HRMS**: Found $[\text{M}+\text{Na}]^+$ 412.1002, C₁₉H₁₉NNaO₈ requires 412.1003.

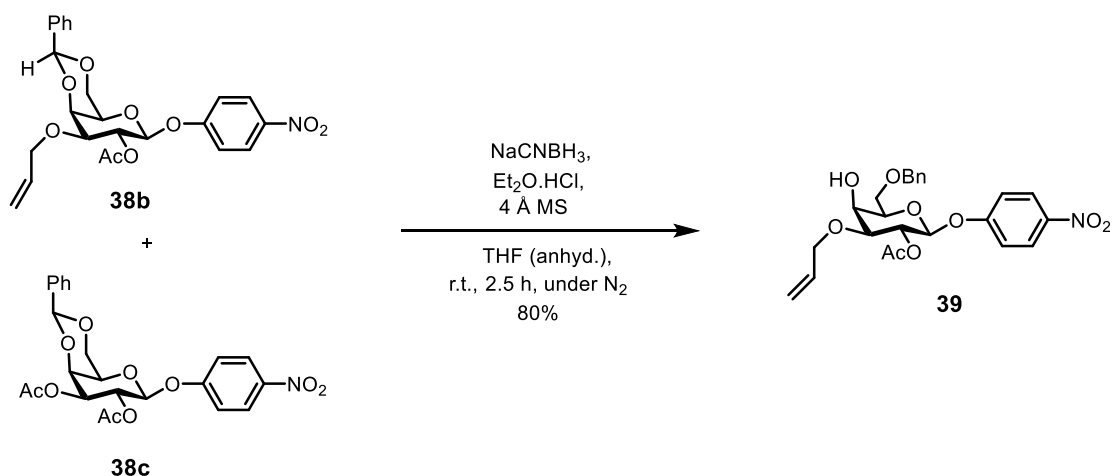
4-Nitrophenyl 3-O-acetyl-2-O-allyl-4,6-O-benzylidene-β-D-galactopyranoside (38a) and 4-nitrophenyl 2-O-acetyl-3-O-allyl-4,6-O-benzylidene-β-D-galactopyranoside (38b)



Dibutyltin oxide (5.44 g, 21.9 mmol) was added to a solution of 4-nitrophenyl 4,6-O-benzylidene-β-D-galactopyranoside **36** (6.55 g, 16.8 mmol) in MeOH (200 mL), and the reaction mixture was heated under reflux at 90 °C for 5 h under N₂(g) atmosphere. After removal of the solvent under vacuum, cesium fluoride (3.07 g 20.2 mmol) was added to the residue which was coevaporated and dried with toluene two times. Dimethylformamide (100 mL) was added to the resulting residue, followed by the addition of tetrabutylammonium iodide (0.4 g, 1 mmol). The reaction mixture was

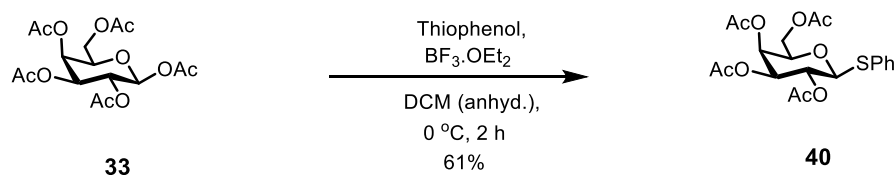
stirred at 90 °C overnight and was concentrated to leave a solid which was dissolved in pyridine (50 mL). 4-Dimethylaminopyridine (0.5 g, 4 mmol) and acetic anhydride (4 mL) were added to the reaction mixture, which was stirred at r.t. overnight. The reaction mixture was concentrated to leave a crude solid, which was purified by flash column (silica; 4:1 hexane–EtOAc → 3:1 hexane–EtOAc → 2:1 hexane–EtOAc → 1:1 hexane–EtOAc) to afford first compound **38a** (2.20 g, 28%) as a pale yellow solid; R_f 0.35 (2:1 hexane–EtOAc); m.p. 170–171 °C (from EtOH); $[\alpha]_D^{21}$ 24.9 (c, 1, CHCl₃); δ_H (500 MHz, CDCl₃); 8.22–8.18 (m, 2H, ArH), 7.55–7.49 (m, 2H, ArH), 7.43–7.34 (m, 3H, ArH), 7.12 (m, 2H, ArH), 5.92–5.82 (m, 1H, CH₂=CHCH₂), 5.54 (s, 1H, PhCHO₂), 5.25 (m, 1H, CH₂=CHCH₂), 5.17–5.13 (m, 2H, CH₂=CHCH₂, H-1), 4.99 (dd, 1H, $J_{3,4}$ 3.6 Hz, $J_{2,3}$ 10.5 Hz, H-3), 4.45 (d, 1H, $J_{3,4}$ 3.6 Hz, H-4), 4.38–4.32 (m, 2H, H-6, CH₂=CHCH₂), 4.26–4.21 (m, 1H, CH₂=CHCH₂), 4.11 (dd, 1H, $J_{5,6}$ 1.7 Hz, $J_{6,6'}$ 12.53 Hz, H-6'), 4.06 (dd, 1H, $J_{1,2}$ 7.7 Hz, $J_{2,3}$ 10.5 Hz, H-2), 3.69 (d, 1H, $J_{5,6}$ 1.7 Hz, H-5), 2.17 (s, 1H, C(O)CH₃); δ_C (75 MHz, CDCl₃); 170.8 (C=O), 162.0, 143.0, 137.6, 129.3, 128.4, 126.4, 125.9, 116.8 (ArC), 134.6 (CH₂=CHCH₂), 117.1 (CH₂=CHCH₂), 101.2 (PhCHO₂), 101.1 (C-1), 75.4 (C-2), 74.2 (CH₂=CHCH₂), 73.5 (C-4), 73.3 (C-3), 68.9 (C-6), 66.8 (C-5), 21.2 (C(O)CH₃); IR (ν_{max}/cm^{-1}): 1746 (C=O), 1592, 1345 (NO₂); HRMS: Found [M+Na]⁺ 494.1440, C₂₄H₂₅NNaO₉ requires 494.1422. Further elution gave an inseparable mixture of **38b** and **38c** (4.84 g containing **38b** and **38c** in a ratio of 3:2), which was used for the next step; R_f 0.19 (2:1 hexane–EtOAc); δ_H (500 MHz, CDCl₃) only signals for compound **38b** are listed; 8.22–8.14 (m, 2H, ArH), 7.57–7.48 (m, 2H, ArH), 7.42–7.30 (m, 3H, ArH), 7.14–7.07 (m, 2H, ArH), 5.95–5.81 (m, 1H, CH₂=CHCH₂), 5.63 (dd, 1H, $J_{1,2}$ 7.9 Hz, $J_{2,3}$ 10.1 Hz, H-2), 5.59 (s, 1H, PhCHO₂), 5.17 (d, 1H, $J_{1,2}$ 7.9 Hz, H-1), 4.37 (d, 1H, $J_{3,4}$ 3.4 Hz, H-4), 3.71 (dd, 1H, $J_{2,3}$ 10.1, $J_{3,4}$ 3.4 Hz, H-3), 3.64 (d, 1H, J 1.0 Hz, H-5), 4.16–4.09 (m, 4H, H-6), 2.09 (s, 3H, C(O)CH₃); δ_C (75 MHz, CDCl₃); 170.8, 169.3, 169.3, 161.9, 161.6, 143.1, 143.0, 137.4, 134.6, 128.4, 128.3, 126.5, 125.8, 117.6, 116.9, 116.7, 101.4, 101.2, 99.0, 98.9, 73.1, 71.7, 70.7, 69.6, 69.0, 67.3, 67.0, 21.0, 21.0, 20.9; IR (ν_{max}/cm^{-1}): 1750 (C=O), 1593, 1518 (NO₂); HRMS: Found [M+Na]⁺ 494.1436, C₂₄H₂₅NNaO₉ requires 494.1422.

4-Nitrophenyl 2-O-acetyl-3-O-allyl-6-O-benzyl-β-D-galactopyranoside (39)¹⁸⁶



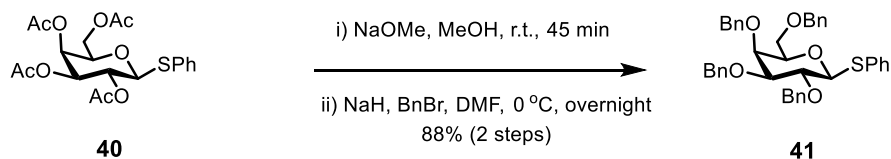
4 Å MS (2.5 g) were added to a solution of the crude product mixture (4.84 g, 10.2 mmol) of the previous step containing **38b** (6.15 mmol) in anhydrous THF (100 mL) and the reaction was stirred at 0 °C for 10 min under N₂(g) atmosphere. Sodium cyanoborohydride (3.23 g, 51.38 mmol) was added to the reaction mixture, which was stirred for further 10 h. Etheral hydrochloric acid (12 mL) was added dropwise to the reaction mixture until the solution was acidic. The reaction mixture was stirred at r.t. for 2 h and was washed with saturated aq. NaHCO₃ (25 mL). The aqueous phase was washed with DCM (2 × 25 mL). The organic phase was collected, dried (MgSO₄) and concentrated to leave a crude oil, which was purified by flash column chromatography (silica; 2:1 hexane–EtOAc) to afford galactopyranoside **39** (2.33 g, 80%) as a colourless oil; *R*_f 0.14 (2:1 hexane–EtOAc); m.p. 90-91 °C (from hexane–EtOAc) (lit.¹⁸⁶ m.p. 89.5-90 °C); $[\alpha]_D^{22}$ -1.1 (c, 1, MeOH); δ_H (500 MHz, CDCl₃); 8.18-8.08 (m, 2H, ArH), 7.35-7.25 (m, 5H, ArH), 7.15- 7.05 (m, 2H, ArH), 5.92-5.80 (m, 1H, CH₂=CHCH₂), 5.48 (dd, 1H, *J*_{1,2} 8.1 Hz, *J*_{2,3} 9.5 Hz, H-2), 5.33-5.16 (m, 2H, CH₂=CHCH₂), 5.09 (d, 1H, *J*_{1,2} 8.1 Hz, H-1), 4.60-4.49 (m, 1H, PhCHO₂), 4.25-4.14 (m, 1H, H-6), 4.12 (d, 1H, *J*_{3,4} 3.2 Hz, H-4), 4.07-3.95 (m, 1H, H-6'), 3.91-3.76 (m, 3H, H-5, CH₂=CHCH₂), 3.61 (dd, 1H, *J*_{2,3} 9.5 Hz, *J*_{3,4} 3.2 Hz, H-3), 2.97 (s, 1H, OH), 2.10 (s, 3H, C(O)CH₃), δ_C (75 MHz, CDCl₃); 107.0 (C=O), 161.7, 142.7, 134.5, 137.7 (ArC), 128.4 (CH₂=CHCH₂), 127.8, 127.6, 125.6 (ArC), 117.7 (CH₂=CHCH₂), 116.6 (ArC), 98.5 (C-1), 78.5 (C-3), 74.5 (C-5), 73.7 (PhCHO₂), 70.2 (C-6), 70.0 (C-2), 69.3 (CH₂=CHCH₂), 66.2 (C-4), 20.8 (C(O)CH₃); **IR** (ν_{max}/cm^{-1}): 1746 (C=O), 1592, 1514 (NO₂); **HRMS**: Found [M+Na]⁺ 496.1581 C₂₄H₂₇NNaO₉ requires 496.1578.

Phenyl 2,3,4,6-tetra-O-acetyl-1-thio-β-D-galactopyranoside (40)¹⁸⁷



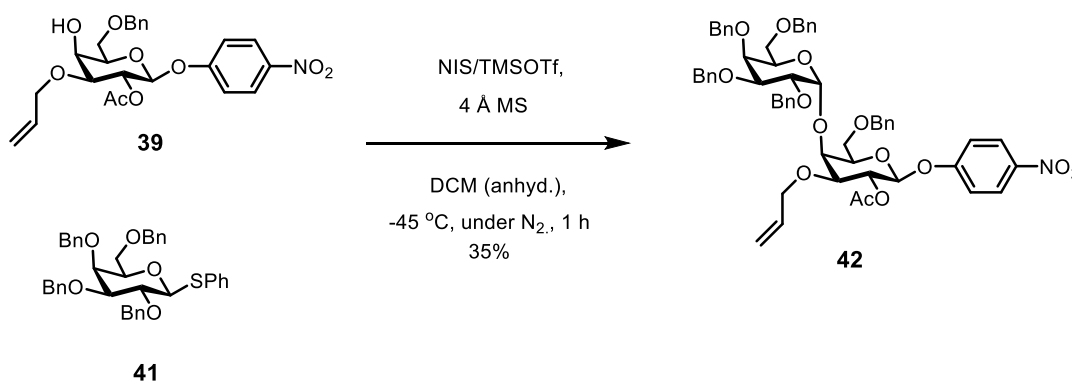
Thiophenol (6.8 mL, 66 mmol) was added to a solution of β-D-galactose pentaacetate **33** (20.0 g, 51 mmol) in anhydrous DCM (200 mL) and the reaction was stirred at 0 °C for 10 min. Freshly distilled boron trifluoride diethyl etherate (9.5 mL, 77 mmol) was added to the reaction mixture, which was stirred at 0 °C for further 2 h. The reaction mixture was washed with water (2 × 50 mL). The aqueous phase was washed with DCM (2 × 50 mL). The organic phase was collected and washed with saturated aq. NaHCO₃ (2 × 50 mL), dried (MgSO₄) and concentrated to leave a crude oil, which was purified by flash column chromatography (silica; 6:1 hexane–EtOAc → 5:1 hexane–EtOAc → 4:1 hexane–EtOAc → 3:1 hexane–EtOAc → 2.5:1 hexane–EtOAc) to afford galactopyranoside **40** (13.7 g, 61%) as a colourless solid; *R*_f 0.21 (2:1 hexane–EtOAc); m.p. 82–83 °C (from diethyl ether–hexane) (lit.¹⁸⁸ m.p. 80–81 °C); $[\alpha]_{\text{D}}^{22}$ 4.5 (c, 1, CHCl₃) (lit.¹⁸⁹ $[\alpha]_{\text{D}}^{25}$ 4.9 (c, 1, CHCl₃)); δ_{H} (500 MHz, CDCl₃); 7.53–7.48 (m, 2H, ArH), 7.33–7.29 (m, 3H, ArH), 5.41 (d, 1H, *J*_{3,4} 3.2 Hz, H-4), 5.24 (t, 1H, *J*_{1,2} 10.0 Hz, H-2), 5.05 (dd, 1H, *J*_{3,4} 3.2 Hz, *J*_{2,3} 10.0 Hz, H-3), 4.71 (d, 1H, *J*_{1,2} 10.0 Hz, H-1), 4.21–4.08, (m, 2H, H-6, H-6'), 3.94 (t, 1H, *J*_{5,6=5,6'} 6.6 Hz, H-5), 2.12 (s, 3H, C(O)CH₃), 2.09 (s, 3H, C(O)CH₃), 2.04 (s, 3H, C(O)CH₃), 1.97 (s, 3H, C(O)CH₃); δ_{C} (75 MHz, CDCl₃); 170.5, 170.3, 170.2, 169.6, 132.7, 132.6, 129.0, 128.3 (4 × C=O, ArC), 86.7 (C-1), 74.6 (C-5), 72.2 (C-3), 67.4, 67.4 (C-2, C-4), 61.8 (C-6), 21.0, 20.8, 20.7, 20.7 (4 × C(O)CH₃); IR (*v*_{max}/cm⁻¹): 1751 (C=O); HRMS: Found [M+Na]⁺ 463.1044, C₂₄H₂₅NNaO₉ requires 463.1033.

Phenyl 2,3,4,6-tetra-O-benzyl-1-thio-β-D-galactopyranoside (41)¹⁸⁷



Sodium methoxide (5 mL, 88 mmol) was added dropwise to a solution of phenyl 2,3,4,6-tetra-O-acetyl-1-thio-β-D-galactopyranoside **40** (13.7 g, 31 mmol) in MeOH (100 mL) and the reaction was stirred at r.t. for 45 min. The reaction mixture was neutralised by slow addition of acetic acid and concentrated to give a crude oil, which was dissolved in DMF (120 mL). Sodium hydride (7.2 g, 300 mmol) was added portionwise to the reaction mixture, which was stirred at 0 °C for 5 min. Benzylbromide (18.5 g, 155 mmol) was slowly added to the mixture, which was stirred at r.t. overnight. Methanol (20 mL) was added to the solution to remove trace sodium hydride. The solvent was evaporated and the residue was recrystallised from EtOH to give compound **41** (17.4 g, 88%, 2 steps) as a colourless solid; R_f 0.23 (6:1 hexane–EtOAc); m.p. 86–88 °C (from diethyl ether–hexane) (lit.¹⁸⁷ m.p. 86–88 °C); $[\alpha]_D^{22}$ 0.8 (c, 1, CHCl₃) (lit.¹⁸⁷ $[\alpha]_D$ 5 (c, 1, CHCl₃)); δ_H (500 MHz, CDCl₃); 7.55–7.48 (m, 2H, ArH), 7.38–7.08 (m, 23H, ArH), 4.91 (d, 1H, J 11.5 Hz, OCH₂Ph), 4.76–4.63 (m, 4H, OCH₂Ph), 4.59 (d, 1H, J 9.8 Hz, H-1), 4.55 (d, 1H, J 11.5 Hz, OCH₂Ph), 4.45–4.34 (m, 2H, OCH₂Ph), 3.93 (d, 1H, J 2.4, H-4), 3.89 (t, 1H, $J_{1,2=2,3}$ 9.4 Hz, H-2), 3.64–3.52 (m, 4H, H-3, H-5, H-6, H-6'); δ_C (75 MHz, CDCl₃); 138.9, 138.5, 138.4, 138.0, 134.3, 131.6, 128.9, 128.5, 128.4, 128.3, 128.0, 127.9, 127.9, 127.8, 127.8, 127.7, 127.6, 127.1 (ArC), 87.8 (C-1), 84.3 (C-3), 77.4 (C-2, C-5), 75.7 (OCH₂Ph), 74.6 (OCH₂Ph), 73.7 (C-4, OCH₂Ph), 72.8 (OCH₂Ph), 68.9 (C-6); **IR** (ν_{max}/cm^{-1}): 2915, 2864 (C-H), 1098 (C-OR); **HRMS**: Found $[M+Na]^+$ 655.2493, C₄₀H₄₀NaO₅S requires 655.2489.

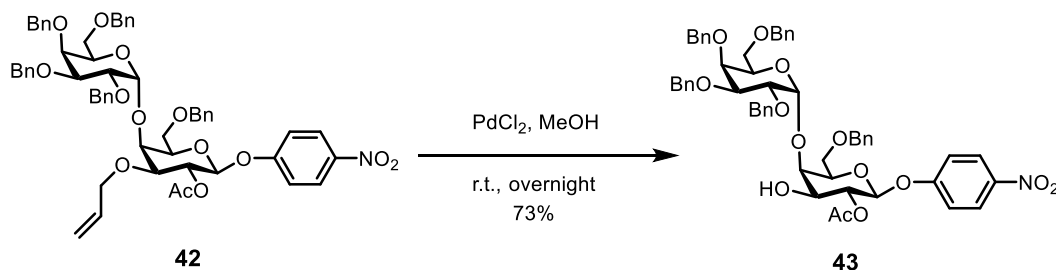
4-Nitrophenyl 2-O-acetyl-3-O-allyl-6-O-benzyl-4-O-(2,3,4,6-tetra-O-benzyl- α -D-galactopyranosyl)- β -D-galactopyranoside (42)



Donor **41** (1.0 g, 2 mmol) was added to a solution of acceptor **39** (1.74 g, 2.8 mmol) and 4 Å MS (1.4 g) in anhydrous DCM (40 mL), and the reaction was stirred at r.t. for 30 min under N₂(g) atmosphere. The reaction mixture was cooled to -45 °C and NIS (0.68 g, 3.0 mmol) and TMSOTf (0.083 mL, 0.42 mmol) were added to the reaction mixture, which was stirred at the same temperature for 20 min. The reaction mixture was washed with saturated aq. NaHCO₃ (20 mL) and sodium thiosulfate (20 mL) to remove traces of acid and iodine. The aqueous phase was washed with DCM (2 × 30 mL). The organic phase was collected, dried (MgSO₄), filtered and concentrated to leave a crude oil, which was purified by flash column chromatography (silica; 8:1 → 4.5:1 hexane–EtOAc) to afford disaccharide **42** (0.73 g, 35%) as a yellow oil; *R*_f 0.12 (3:1 hexane–EtOAc); $[\alpha]_{\text{D}}^{27}$ 57.1 (c, 0.5, CHCl₃); δ_{H} (500 MHz, CDCl₃); 8.07 (d, 2H, *J* 9.2 Hz, ArH), 7.36–6.99 (m, 27H, ArH), 5.76–5.68 (m, 1H, CH₂=CHCH₂), 5.47 (dd, 1H, *J*_{2a,3a} 10.2 Hz, *J*_{1a,2a} 7.7 Hz, H-2a), 5.16 (dd, 1H, *J* 17.3, *J* 1.5 Hz, CH₂=CHCH₂), 5.06 (d, 1H, *J* 10.6 Hz, CH₂=CHCH₂), 4.99 (d, 1H, *J*_{1a,2a} 7.7 Hz, H-1a), 4.91 (d, 1H, *J*_{1b,2b} 2.5 Hz, H-1b), 4.89–4.83 (m, 2H, OCH₂Ph), 4.73 (s, 1H, OCH₂Ph), 4.60 (d, 1H, *J* 11.8 Hz, OCH₂Ph), 4.52 (d, 1H, *J* 11.2 Hz, OCH₂Ph), 4.45–4.34 (m, 3H, OCH₂Ph, H-5b), 4.19–4.02 (m, 7H, CH₂=CHCH₂, H-4a, H-2b, H-3b, H-4b, OCH₂Ph), 3.89–3.79 (m, 2H, H-6a, CH₂=CHCH₂), 3.69 (t, 1H, *J*_{5a,6a}=*J*_{5a,6'a} 6.5 Hz, H-5a), 3.63–3.53 (m, 1H, H-6'a, H-6'b), 3.45–3.38 (m, 2H, H-6b, H-3a), 1.93 (s, 3H, C(O)CH₃); δ_{C} (75 MHz, CDCl₃); δ 169.4 (C=O), 161.8, 142.8, 139.1, 138.9, 138.8, 138.4, 137.9, 134.5, 128.6, 128.4, 128.4, 128.3, 128.3, 128.2, 128.1, 128.0, 127.8, 127.7, 127.6, 127.5, 127.5, 127.5, 125.7, 117.0 (ArC, CH₂=CHCH₂), 117.3 (CH₂=CHCH₂), 100.4 (C-1b), 99.2 (C-1a), 79.3, 76.4, 73.4 (CH₂=CHCH₂, C-4a, C-2b, C-3b, C-4b, OCH₂Ph), 78.3 (C-3a), 75.1 (OCH₂Ph), 74.8 (C-5a), 74.1 (OCH₂Ph), 73.2, 69.4 (C-5b, OCH₂Ph), 72.5 (OCH₂Ph), 71.2 (CH₂=CHCH₂), 70.1 (C-2a), 68.2, 68.1 (C-6a, C-6b), 21.0 (C(O)CH₃); IR (ν_{max} /cm⁻¹):

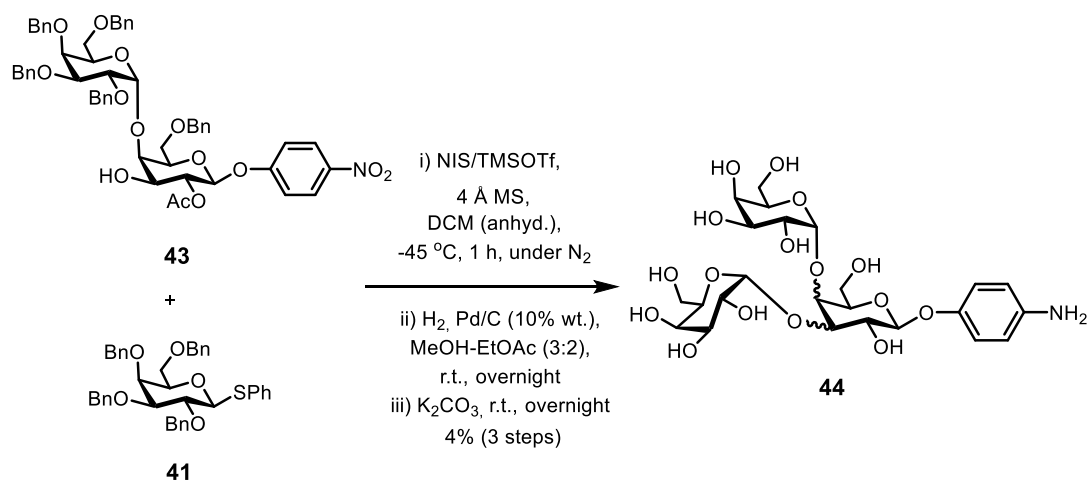
3435 (CH=CH₂), 2917, 2870 (C-H), 1754 (C=O), 1517 (NO₂), 1079, 1099, 1054 (C-OR);
HRMS: Found [M+Na]⁺ 1018.3974, C₅₈H₆₁NNaO₁₄ requires 1018.3984.

4-Nitrophenyl 2-O-acetyl-6-O-benzyl-4-O-(2,3,4,6-tetra-O-benzyl- α -D-galactopyranosyl)- β -D-galactopyranoside (43)



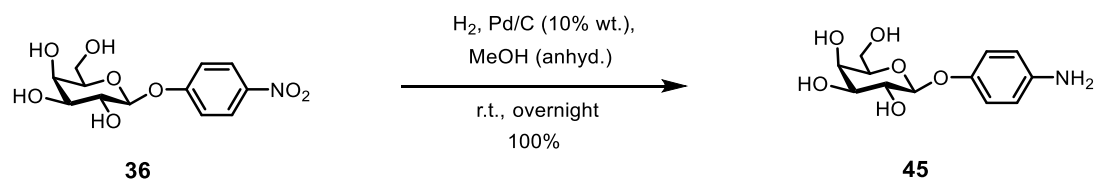
A catalytic amount of palladium (II) chloride (0.1 g, 0.6 mmol) was added to a solution of 4-nitrophenyl 2-O-acetyl-3-O-allyl-6-O-benzyl-4-O-(2,3,4,6-tetra-O-benzyl- α -D-galactopyranosyl)- β -D-galactopyranoside **42** (0.73 g, 0.7 mmol) in MeOH (40 mL), and the reaction was stirred at r.t. overnight. The reaction mixture was concentrated to leave a crude product, which was purified by flash column chromatography (silica; 4:1 hexane–EtOAc \rightarrow 3:1 hexane–EtOAc \rightarrow 2:1 hexane–EtOAc) to afford disaccharide **43** (0.51 g, 73%) as a colourless solid; R_f 0.21 (3:1 hexane–EtOAc); m.p. 138–139 °C (from EtOH); $[\alpha]_D^{23}$ 23.6 (c, 0.5, CHCl₃); δ_H (500 MHz, CDCl₃); 8.19–8.12 (m, 2H, ArH), 7.43–7.20 (m, 25H, ArH), 7.16–7.11 (m, 2H, ArH), 5.31 (dd, 1H, $J_{2a,3a}$ 10.4 Hz, $J_{1a,2a}$ 7.8 Hz, H-2a), 5.08 (d, 1H, $J_{1a,2a}$ 7.8 Hz, H-1a), 5.00 (d, 1H, $J_{1b,2b}$ 3.8 Hz, H-1b), 4.94 (d, 1H, J 11.3 Hz, OCH₂Ph), 4.88 (d, 1H, J 11.6 Hz, OCH₂Ph), 4.82–4.75 (m, 2H, OCH₂Ph), 4.66 (d, 1H, J 11.6 Hz, OCH₂Ph), 4.60 (dd, 2H, J 11.6, 6.6 Hz, OCH₂Ph), 4.52 (d, 1H, J 11.6 Hz, OCH₂Ph), 4.36 (t, 1H, J 6.7 Hz, H-5b), 4.28–4.22 (m, 2H, OCH₂Ph), 4.16 (dd, 1H, $J_{2b,3b}$ 10.2 Hz, $J_{1b,2b}$ 3.8 Hz, H-2b), 4.11–4.01 (m, 3H, H-4a, H-3b, OH), 3.97 (d, 1H, J 2.4 Hz, H-4b), 3.92 (dd, 1H, J 10.9, 5.4 Hz, H-6a), 3.84–3.76 (m, 2H, H-5a, H-6'a), 3.73–3.61 (m, 2H, H-3a, H-6b), 3.56–3.48 (m, 1H, H-6'b), 2.09 (s, 3H, C(O)CH₃); δ_C (75 MHz, CDCl₃); 170.0 (C=O), 161.8, 142.9, 138.6, 138.5, 138.5, 138.2, 138.1, 128.5, 128.4, 128.3, 128.3, 128.0, 127.8, 127.8, 127.7, 127.6, 127.5, 127.5, 125.8, 116.7 (ArC), 101.5 (C-1b), 98.9 (C-1a), 8.16 (C-4b), 78.9, 76.3, 74.3 (C-2b, C-3b, C-4a), 75.3 (C-6b), 74.9, 74.2, 73.6, 73.2 (OCH₂Ph), 72.8 (C-3a), 72.3 (C-2a), 71.8 (OCH₂Ph), 71.1 (C-5b), 69.6 (C-5a), 68.4 (C-6b), 21.0 (C(O)CH₃); **IR** (ν_{\max} /cm⁻¹): 3445, (OH), 1749 (C=O), 1592, 1517 (NO₂); **HRMS:** Found [M+Na]⁺ 978.3684, C₅₅H₅₇NNaO₁₄ requires 978.3671.

4-Nitrophenyl bis-O-(α -D-galactopyranosyl)- β -D-galactopyranoside (**44**)



Donor **41** (167 mg, 0.26 mmol) was added to a solution of acceptor **43** (180 mg, 0.19 mmol) and 4 Å MS (200 mg) in anhydrous DCM (25 mL), and the reaction was stirred at r.t. for 30 min under N₂(g) atmosphere. The reaction mixture was cooled to -45 °C and NIS (65 mg, 0.6 mmol) and TMSOTf (7 μL, 0.08 mmol) were added to the reaction mixture, which was stirred at the same temperature for further 30 min. The reaction mixture was washed with saturated aq. NaHCO₃ (30 mL) and sodium thiosulfate (30 mL) to remove traces of acid and iodine. The aqueous phase was washed with DCM (2 × 30 mL). The organic phase was collected, dried (MgSO₄), filtered and concentrated to leave a crude oil, which was partially purified by flash column chromatography (silica; 7:1 → 5.5:1 hexane–EtOAc). The mixture was then dissolved in a mixture of EtOAc and MeOH (2:3, v/v, 25 mL). Palladium on carbon (10% wt., 200 mg) was added to the solution, which was stirred at r.t. under hydrogen atmosphere overnight. The reaction mixture was filtered through Celite[®] pad under vacuum eluting with MeOH, and evaporated to dryness. The residue was dissolved in MeOH (30 mL). Potassium carbonate anhydrous (15 mg, 0.1 mmol) was added to the reaction mixture, which was stirred at r.t. overnight. The resulting solution was neutralised with acetic acid, evaporated, purified by size-exclusion chromatography (Sephadex LH-20, MeOH) to give a mixture of compounds **44** with different configurations of glycosidic linkages as colourless oil (8 mg, 4%, 3 steps); only signals for the major compound are listed; δ_{H} (500 MHz, D₂O); 7.09-7.05 (m, 2H, ArH), 6.87-6.84 (m, 2H, ArH), 5.29 (d, $J_{1,2}$ 4.1 Hz, H-1), 5.13 (d, 1H, $J_{1,2}$ 3.7 Hz, H-1), 5.10 (d, 1H, $J_{1,2}$ 7.3 Hz, H-1), 4.39 (bs, 1H, H-4), 4.29 (t, 1H, J 6.4 Hz, H-5), 4.14 (t, 1H, J 6.01 Hz, H-5), 4.08-3.37 (m, 15H, 3 × H-2, 3 × H-3, 2 × H-4, H-5, 3 × H-6, 3 × H-6'); **HRMS**: Found $[M+\text{Na}]^+$ 618.2026, C₂₄H₃₇NNaO₁₆ requires 618.2005.

4-Aminophenyl β -D-galactopyranoside (**45**)¹⁹⁰



Palladium on carbon (10% wt., 50 mg) was added to a solution of 4-nitrophenyl β -D-galactopyranoside **36** (0.34 g, 1.12 mmol) in anhydrous MeOH (14 mL), and the reaction was stirred at r.t. under hydrogen atmosphere overnight. The reaction mixture was filtered through Celite[®] pad under vacuum eluting with MeOH, and evaporated to leave compound **45** (0.32 g, 100%) as a colourless solid; R_f 0.22 (8:2 EtOAc–MeOH); m.p. 156-157 °C (from MeOH) (lit.¹⁹⁰ m.p. 158-159°C); $[\alpha]_D^{23}$ -35.5 (c, 1, MeOH) (lit.¹⁹⁰ $[\alpha]_D$ -40.5 (c, 1, MeOH)); δ_H (500 MHz, DMSO- d_6 with D₂O exchange); 6.75 (d, 2H, J 8.6 Hz, ArH), 6.50 (d, 2H, 8.6 Hz, ArH), 4.53 (d, 1H, $J_{1,2}$ 7.7 Hz, H-1), 3.66 (d, 1H, J 3.0 Hz, H-4), 3.48-3.55 (m, 4H, H-2, H-5, H-6, H-6'), 3.36 (d, 1H, J 12.7 Hz, H-3); δ_C (75 MHz, DMSO- d_6); 148.9, 143.5, 117.7, 114.5 (ArC), 102.7 (C-1), 75.3 (C-3), 73.3 (C-5), 70.4 (C-2), 68.1 (C-4), 60.4 (C-6); **IR** (ν_{max} /cm⁻¹): 3435 (OH, NH), 1642 (NH); **HRMS**: Found $[\text{M}+\text{Na}]^+$ 294.0937, C₁₂H₁₇NNaO₆ requires 294.0946.

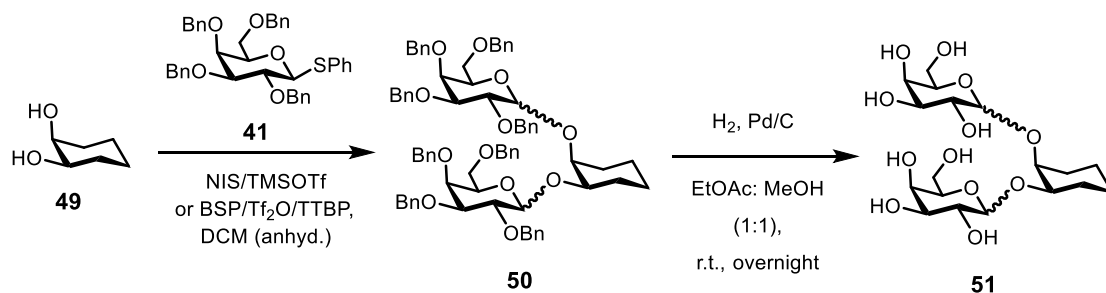
p-[*N*-(2-Methoxy-3,4-dioxocyclobut-1-enyl)amino]phenyl β -D-galactopyranoside (**47**)



3,4-dimethoxy-3-cyclobutene-1,2-dione (0.06 g, 0.4 mmol) was added to a solution of 4-aminophenyl β -D-galactopyranoside **45** (0.095 g, 0.35 mmol) in DMF (2 mL). The reaction mixture was stirred at r.t., filtered under vacuum through Celite[®] pad eluting with MeOH, and evaporated to leave compound **47** (0.32 g, 80%) as a yellow oil; R_f 0.6 (1:1 EtOAc–MeOH); $[\alpha]_D^{24}$ 78.0 (c, 0.5, DMSO); δ_H (500 MHz, DMSO- d_6 with D₂O exchange); 7.18 (bs, 2H, ArH), 6.98 (d, 2H, 8.9 Hz, ArH), 4.73 (d, 1H, $J_{1,2}$ 7.7 Hz, H-1), 4.30 (s, 3H, CH₃), 3.66 (d, 1H, $J_{3,4}$ 3.3 Hz, H-4), 3.51-3.85 (m, 4H, H-2, H-5, H-6, H-6'), 3.37 (dd, 1H, $J_{3,4}$ 3.3 Hz, $J_{2,3}$ 9.7 Hz, H-3); δ_C (75 MHz, DMSO- d_6); 121.0, 116.8 (ArC),

101.5 (C-1), 75.5, 73.5, 73.3, 68.2 (C-2, C-3, C-5), 70.1 (C-4), 60.4 (C-6, OCH₃); **IR** ($\nu_{\max}/\text{cm}^{-1}$): 3466 (OH), 1658 (C=O); **HRMS**: Found [M+Na]⁺ 404.0964, C₁₇H₁₉NNaO₉ requires 404.0952.

meso-1,2-bis-(D-Galactopyranosyloxy)-cyclohexane (51)



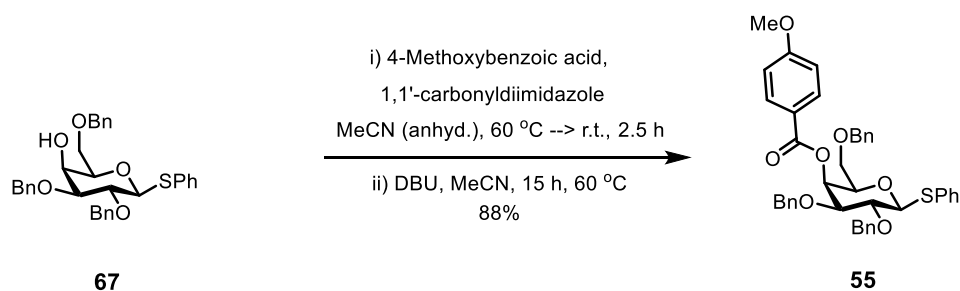
- Glycosylation reaction using NIS/TMSOTf

Thioglycosyl donor **41** (213 mg, 3 mmol) and 1,2-*cis*-cyclohexanediol **49** (150 mg, 1 mmol) were co-evaporated with toluene several times before adding 4 Å MS (120 mg) and anhydrous DCM (25 mL). The reaction was stirred at r.t. for 30 min under N₂(g) atmosphere, cooled to -45 °C and NIS (750 mg, 4 mmol) and TMSOTf (100 μL, 0.5 mmol) were added to the reaction mixture, which was stirred at -45 °C temperature for 3 h. The reaction mixture was washed with saturated aq. NaHCO₃ (20 mL) and 10% aq. Na₂S₂O₃ (20 mL) to remove traces of acid and iodine. The aqueous phase was washed with DCM (2 × 30 mL). The organic phase was collected, dried (MgSO₄), filtered and concentrated to leave a crude yellow oil, which was purified by flash column chromatography (silica; 13:1 → 4:1 hexane–EtOAc). The residue was re-dissolved in a mixture of EtOAc (12 mL) and MeOH (12 mL). Palladium on carbon (Pd/C, 10% wt., 104 mg, 2 mmol) was added to the reaction mixture, which was allowed to stir at r.t. under a positive pressure of hydrogen overnight. The reaction mixture was filtered through a Celite[®] pad and evaporated to dryness to give compound **51** as colourless oil (230 mg, 29% over 2 steps). A mixture of anomers was obtained. The α:β ratio (1:3) was determined by integration of anomeric signals in the ¹H NMR spectrum. Signal integrations are normalised to give a total of 2 anomeric protons across all isomers; δ_H (500 MHz, D₂O); 5.19 (d, 0.25H, *J* 3.9 Hz), 5.11 (d, 0.23H, *J* 4.0 Hz), 4.59 (d, 0.65H, *J* 7.9 Hz), 4.54 (d, 0.23H, *J* 7.9 Hz), 4.45 (d, 0.64H, *J* 7.9 Hz), 4.12-3.47 (m, 14H), 1.94-1.25 (m, 8H); **LC-MS**: Found [M+Na]⁺ 463.1, C₁₈H₃₂NaO₁₂ requires 463.2.

- Glycosylation reaction using BSP/Tf₂O/TTBP

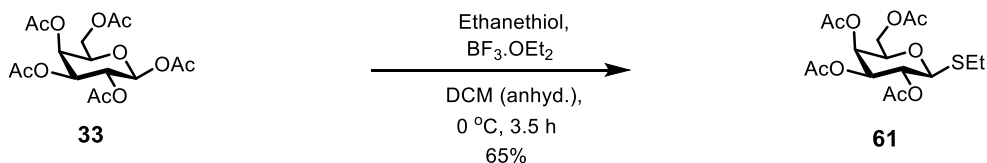
Thioglycosyl donor **41** (188 mg, 0.3 mmol), BSP (68 mg, 0.3 mmol), and TTBP (148 mg, 0.6 mmol) were co-evaporated with toluene several times before adding 4 Å MS (100 mg) and anhydrous DCM (5 mL). The reaction mixture was stirred at r.t. under N₂(g) atmosphere for 1 h. Glycosyl acceptor **49** (15 mg, 0.13 mmol) was also co-evaporated with toluene several times and dissolved in anhydrous DCM (2 mL) in a separate flask. After stirring for 1 h, the mixture of thioglycosyl donor, BSP, TTBP and molecular sieves 4 Å was cooled to -60 °C before freshly distilled triflic anhydride (Tf₂O) (30 µL, 0.17 mmol) was added. The reaction mixture was stirred at -60 °C for further 10 min before a solution of glycosyl acceptor **49** was added. The resulting mixture was stirred at low temperature (-60 °C to -10 °C) for 2 h, quenched with triethyl phosphite (51 µL), triethylamine (2 mL), and washed with sat. aq. NaHCO₃ (2 × 10 mL), followed by brine (2 × 10 mL). The combined organic phase was dried (MgSO₄), and concentrated to leave crude brown oil, which was purified by gel permeation chromatography (*Bio-beads SX-1, toluene*). The residue was re-dissolved in a mixture of EtOAc (3 mL) and MeOH (3 mL). Palladium on carbon (Pd/C, 10% wt., 120 mg, 1 mmol) was added to the reaction mixture, which was allowed to stir at r.t. under a positive pressure of hydrogen overnight. The reaction mixture was filtered through a Celite[®] pad and evaporated to dryness to give compound **51** as colourless oil (72 mg, 87% over 2 steps). A mixture of anomers was obtained. The α:β ratio (2:1) was determined by integration of anomeric signals in the ¹H NMR spectrum. Signal integrations are normalised to give a total of 2 anomeric protons across all isomers; δ_H (500 MHz, D₂O); 5.28 (d, 0.17H, *J* 3.9 Hz), 5.25 (d, 1.08H, *J* 4.0 Hz), 4.65 (d, 0.19H, *J* 7.8 Hz), 4.60 (d, 0.30H, *J* 7.3 Hz), 4.51 (d, 0.26H, *J* 8.0 Hz), 4.12-3.47 (m, 14H), 1.94-1.25 (m, 8H); **HRMS**: Found [M+Na]⁺ 463.1805, C₁₈H₃₂NaO₁₂ requires 463.1786.

Phenyl 2,3,6-tri-O-benzyl-4-O-4-methoxybenzoyl-1-thio-β-D-galactopyranoside (55)¹²⁹

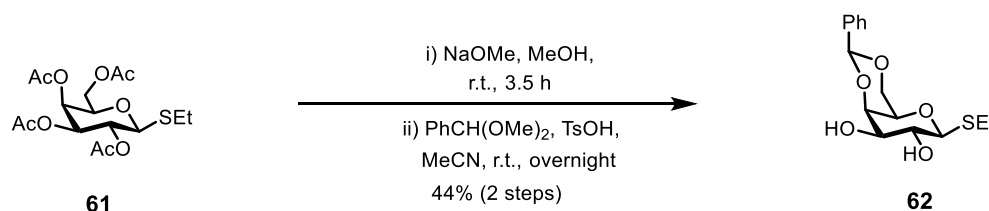


4-Methoxybenzoic acid (589.0 mg, 4 mmol) and 1,1'-carbonyldiimidazole (657 mg, 4 mmol) were dissolved in anhydrous MeCN (25 mL) and stirred at 60 °C under N₂(g) atmosphere for 2.5 h. The reaction mixture was cooled to r.t. before phenyl 2,3,6-tri-O-benzyl-1-thio-β-D-galactopyranoside **67** (1.0 g, 2 mmol) in MeCN (20 mL) was added, followed by DBU (578 μL, 4 mmol). The reaction mixture was stirred at 60 °C under N₂(g) atmosphere for 15 h, cooled to r.t., poured into saturated aq. NaHCO₃, and extracted with DCM (3 × 40 mL). The combined organic layers were washed with brine, dried (MgSO₄), and concentrated. The residue was flash column chromatography (silica; 4:1 hexane–EtOAc), to give compound **55** (1.1 g, 88%) as a colourless oil; *R_f* 0.21 (4:1 hexane–EtOAc); [α]_D²¹ 30.7 (c, 2.4, CHCl₃) (lit.¹²⁹ [α]_D 22.5 (c, 2.2, CHCl₃)); δ_H (500 MHz, CDCl₃); 8.03 (d, 2H, *J* 8.5 Hz, ArH), 7.74–7.70 (m, 2H, ArH), 7.49–7.25 (m, 18H, ArH), 7.01–6.97 (m, 2H, ArH), 5.94 (d, 1H, *J*_{3,4} 2.9 Hz, H-4), 4.92 (d, 1H, *J* 11.2 Hz, OCH₂Ph), 4.82 (s, 2H, OCH₂Ph), 4.78 (d, 1H, *J* 9.1 Hz, H-1), 4.61–4.56 (m, 2H, OCH₂Ph), 4.52 (d, 1H, *J* 11.7 Hz, OCH₂Ph), 3.97–3.92 (m, 4H, OCH₃, H-5), 3.84–3.74 (m, 3H, H-2, H-3, H-6), 3.69–3.63 (m, 1H, H-6'); δ_C (75 MHz, CDCl₃); 165.5 (C=O), 163.7, 138.4, 137.8, 137.7, 133.1, 132.1, 132.9, 132.1, 128.9, 128.5, 128.4, 128.4, 128.3, 128.3, 128.0, 127.8, 127.8, 127.7, 122.3, 113.7 (ArC), 87.2 (C-1), 81.6 (C-2), 76.7 (C-3), 76.5 (C-5), 75.7 (OCH₂Ph), 73.8 (OCH₂Ph), 71.8 (OCH₂Ph), 68.6 (C-6), 67.1 (C-4), 55.6 (OCH₃); IR (ν_{max}/cm⁻¹): 2868 (C-H), 1716 (C=O), 1257 (C-OR); HRMS: Found [M+Na]⁺ 699.2391, C₄₁H₄₀NaO₇S requires 699.2387.

Ethyl 2,3,4,6-tetra-O-acetyl-1-thio- β -D-galactopyranoside (61)¹⁹¹

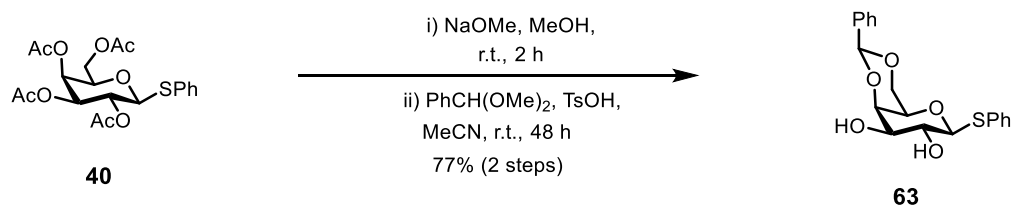


Ethanethiol (4.9 mL, 60 mmol) was added to a solution of β -D-galactose pentaacetate **33** (20.0 g, 51 mmol) in anhydrous DCM (200 mL) and the reaction was stirred at 0 °C for 10 min. Freshly distilled boron trifluoride diethyl etherate (9.5 mL, 77 mmol) was added to the reaction mixture, which was stirred at 0 °C for further 3.5 h. The reaction mixture was washed with water (2 \times 50 mL). The aqueous phase was washed with DCM (2 \times 50 mL). The organic phase was collected and washed with saturated aq. NaHCO_3 (2 \times 50 mL), dried (MgSO_4) and concentrated to leave a crude oil, which was purified by flash column chromatography (silica; 2:1 hexane–EtOAc) to afford compound **61** (13.12 g, 65%) as a colourless solid; R_f 0.44 (2:1 toluene–EtOAc); m.p. 75–77 °C (from diethyl ether–petroleum ether) (lit.¹⁹¹ m.p. 77–78 °C); $[\alpha]_D^{23}$ 13.9 (c, 1, CHCl_3) (lit.¹⁹¹ $[\alpha]_D$ 20.8 (c, 1.3, CHCl_3)); δ_H (500 MHz, CDCl_3); 5.43 (dd, 1H, $J_{3,4}$ 3.4 Hz, $J_{4,5}$ 0.7 Hz, H-4), 5.22 (t, 1H, $J_{1,2=2,3}$ 10.0 Hz, H-2), 5.08 (dd, 1H, $J_{2,3}$ 10.0 Hz, $J_{3,4}$ 3.4 Hz, H-3), 4.56 (d, 1H, $J_{1,2}$ 10.0 Hz, H-1), 4.18–4.09 (m, 2H, H-6, H-6'), 4.01 (td, 1H, $J_{5,6=5,6'}$ 7.0 Hz, $J_{4,5}$ 0.7 Hz, H-5), 2.83–2.65 (m, 2H, SCH_2CH_3), 2.16, 2.07, 2.04, 1.98 (4 s, 12H, 4 \times C(O)CH_3), 1.29 (t, 3H, J 7.5 Hz, SCH_2CH_3); δ_C (75 MHz, CDCl_3); 83.5 (C-1), 74.0 (C-5), 71.5 (C-3), 67.1 (C-4), 66.9 (C-2), 61.2 (C-6), 23.9 (SCH_2CH_3), 20.4, 20.3, 20.2 (4 \times C(O)CH_3), 14.6 (SCH_2CH_3); IR ($\nu_{\text{max}}/\text{cm}^{-1}$): 1750 (C=O); HRMS: Found $[\text{M}+\text{Na}]^+$ 415.1050, $\text{C}_{16}\text{H}_{24}\text{NaO}_9\text{S}$ requires 415.1033

Ethyl 4,6-O-benzylidene-1-thio- β -D-galactopyranoside (**62**)^{193,194}

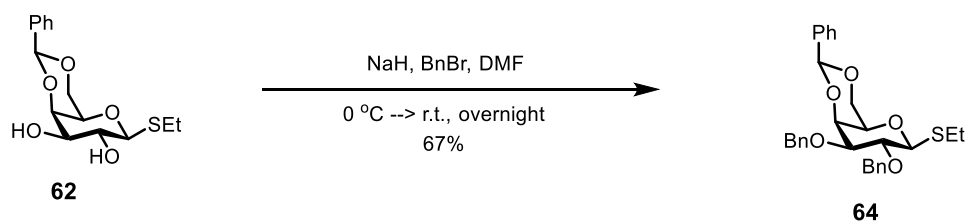
Sodium methoxide (1.83 g, 33.8 mmol) was added to a solution of ethyl 2,3,4,6-tetra-O-acetyl-1-thio- β -D-galactopyranoside **61** (4.74 g, 12.0 mmol) in MeOH (30 mL). After being stirred at r.t. for 3.5 h, the reaction mixture was neutralised by slow addition of acetic acid and concentrated to leave a crude colourless solid, which was dissolved in MeCN (50 mL). Benzaldehyde dimethyl acetal (9 mL, 49 mmol) and *p*-toluenesulfonic acid monohydrate (2 g) were added to the solution, which was stirred at r.t. overnight. The reaction mixture was quenched by triethylamine, and concentrated. The residue was purified by flash column chromatography (silica; 4:1 hexane–EtOAc \rightarrow 3:1 hexane–EtOAc \rightarrow 1:1 hexane–EtOAc with 0.1% triethylamine), yielded compound **62** (1.55 g, 44%, 2 steps) as a colourless solid; R_f 0.46 (10:1 EtOAc–MeOH); m.p. 156–157 °C (from EtOH) (lit.¹⁹³ 154–156 °C); $[\alpha]_D^{21}$ -63.1 (c, 1, CHCl₃) (lit.¹⁹⁴ $[\alpha]_D$ -63.3 (c, 1, CHCl₃)); δ_H (500 MHz, CDCl₃); 7.50–7.47 (m, 2H, ArH), 7.39–7.35 (m, 3H, ArH), 5.54 (s, 1H, PhCH(O)₂), 4.37–4.33 (m, 2H, H-1, H-6), 4.27 (dd, 1H, $J_{4,5}$ 1.2 Hz, $J_{3,4}$ 3.8 Hz, H-4), 4.04 (dd, 1H, $J_{6',5}$ 1.9 Hz, $J_{6,6'}$ 12.4 Hz, H-6'), 3.81 (t, 1H, $J_{1,2=2,3}$ 9.3 Hz, H-2), 3.69 (m, 1H, H-3), 3.53 (m, 1H, H-5), 2.80 (m, 2H, SCH₂CH₃), 2.59 (m, 1H, 2 \times OH), 1.35 (t, 3H, J 7.3 Hz, SCH₂CH₃); δ_C (75 MHz, CDCl₃); 129.5, 128.5, 126.6 (ArC), 101.7 (PhCH), 85.5 (C-1), 75.7 (C-4), 74.1 (C-3), 70.3 (C-5), 69.9 (C-2), 69.5 (C-6), 23.6 (SCH₂CH₃), 15.4 (SCH₂CH₃); IR (ν_{max}/cm^{-1}): 3325 (OH); HRMS: Found $[M+Na]^+$ 335.0935, C₁₅H₂₀NaO₅S requires 335.0935.

Phenyl 4,6-O-benzylidene-1-thio-β-D-galactopyranoside (63)¹⁹⁵



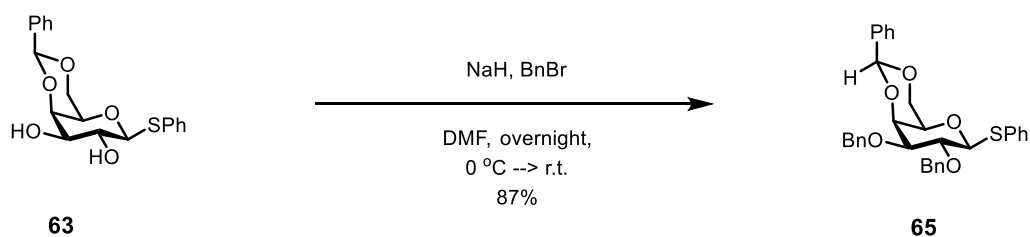
Sodium methoxide (6.5 g, 12 mmol) was added to a solution of phenyl 2,3,4,6-tetra-O-acetyl-1-thio-β-D-galactopyranoside **40** (19 g, 43 mmol) in MeOH (136 mL) and the reaction was stirred at r.t. for 2 h. The reaction mixture was neutralised by slow addition of acetic acid and concentrated to give a crude colourless solid, which was dissolved in MeCN (150 mL). Benzaldehyde dimethyl acetal (28.6 mL, 188 mmol) and *p*-toluenesulfonic acid monohydrate (4.5 g, 24 mmol) added to the reaction mixture, which was stirred at r.t. for 48 h, quenched by triethylamine, concentrated, and purified by flash column chromatography (silica; 4:1 hexane–EtOAc) to afford phenyl 4,6-O-benzylidene-1-thio-β-D-galactopyranoside **63** as colourless solid (12 g, 77% over 2 steps); R_f 0.53 (9:1 EtOAc–MeOH); m.p. 160-161 °C (from EtOH) (lit.¹⁹⁵ m.p. 164-165.5 °C); $[\alpha]_D^{22}$ -28.5 (c, 1.0, CHCl₃) (lit.¹⁹⁵ $[\alpha]_D$ -29.7 (c, 1.3, CHCl₃)); δ_H (500 MHz, CDCl₃); 7.70-7.67 (m, 2H, ArH), 7.42-7.25 (m, 8H, ArH), 5.51 (s, 1H, PhCHO₂), 4.54-4.48 (m, 1H, H-1), 4.39 (dd, 1H, $J_{6,6'}$ 12.5 Hz, $J_{5,6}$ 1.6 Hz, H-6), 4.22 (bd, 1H, $J_{3,4}$ 1.2 Hz, H-4), 4.04 (dd, 1H, $J_{6,6'}$ 12.5 Hz, $J_{5,6}$ 1.6 Hz, H-6'), 3.70 (m, 3H, H-2, H-3), 3.56 (bd, $J_{5,6}$ 1.6 Hz, H-5), 2.58 (s, 1H, OH), 1.61 (s, 1H, OH); δ_C (75 MHz, CDCl₃); 137.7, 133.9, 130.9, 129.5, 129.1, 128.4, 128.4, 126.7, 110.1 (ArC), 101.6 (PhCHO₂), 87.2 (C-1), 75.5 (C-4), 74.0 (C-3), 70.2 (C-5), 69.4 (C-6), 69.0 (C-2); IR (ν_{max}/cm^{-1}): 3294 (OH); HRMS: Found $[M+Na]^+$ 383.0922, C₁₉H₂₀NaO₅S requires 383.0924.

Ethyl 2,3-di-O-benzyl-4,6-O-benzylidene-1-thio-β-D-galactopyranoside (64)¹⁹⁶



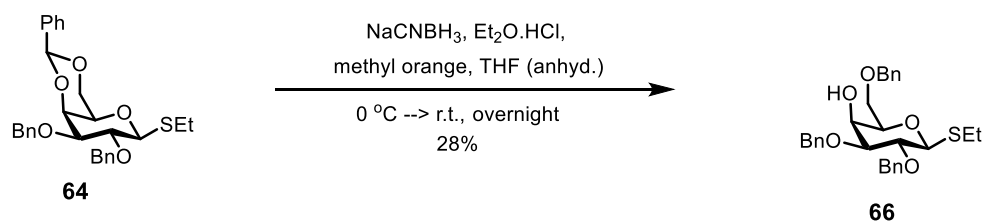
Benzyl bromide (2 mL, 16.2 mmol) was added to a solution of ethyl 4,6-O-benzylidene-1-thio-β-D-galactopyranoside **62** (1.41 g, 4.5 mmol) in DMF (20 mL). After cooling the reaction mixture to 0 °C, sodium hydride (60% in oil dispersion, 2.4 g, 60 mmol) was added. The reaction mixture was stirred at r.t. overnight. The mixture was quenched with water (5 mL), extracted with DCM twice. The organic layers were combined, washed with brine and dried over MgSO₄. The solvent was removed and the crude product was purified by flash column chromatography (silica; 4:1 hexane–EtOAc) to afford compound **64** (1.50 g, 67%) as colourless needles; *R*_f 0.70 (10:1 EtOAc–MeOH); m.p. 153-154 °C (from DCM-petroleum ether) (lit.¹⁹⁶ m.p. 154-156 °C); $[\alpha]_{\text{D}}^{24}$ 3.6 (c, 1.3, CHCl₃) (lit.¹⁹⁶ $[\alpha]_{\text{D}}$ 3.5 (c, 1.3, CHCl₃)); δ_{H} (500 MHz, CDCl₃); 7.58-7.52 (m, 2H, ArH), 7.45-7.23 (m, 13H, ArH), 5.48 (s, 1H, PhCHO₂), 4.90 (d, 1H, *J* 10.2 Hz, OCH₂Ph), 4.84 (d, 1H, *J* 10.2 Hz, OCH₂Ph), 4.79-4.72 (m, 2H, OCH₂Ph), 4.44 (d, 1H, *J*_{1,2} 9.6 Hz, H-1), 4.31 (dd, 1H, *J*_{6,6'} 12.3 Hz, *J*_{5,6} 1.2 Hz, H-6), 4.16 (d, 1H, *J*_{3,4} 3.2 Hz, H-4), 3.97 (dd, 1H, *J*_{6,6'} 12.4 Hz, *J*_{5,6'} 1.2 Hz, H-6'), 3.90 (t, 1H, *J*_{1,2=2,3} 9.6 Hz, H-2), 3.60 (dd, 1H, *J*_{2,3} 9.6 Hz, *J*_{3,4} 3.2 Hz, H-3), 3.36 (d, 1H, *J*_{5,6=5,6'} 1.2 Hz H-5), 2.90-2.70 (m, 2H, SCH₂CH₃), 1.34 (t, 3H, *J* 7.5 Hz, SCH₂CH₃); δ_{C} (75 MHz, CDCl₃); 138.6, 138.4, 138.1, 129.2, 128.5, 128.5, 128.3, 127.9, 127.9, 127.9, 126.7 (ArC), 101.6 (PhCH), 84.6 (C-1), 81.3 (C-3), 77.0 (C-2), 75.9 (OCH₂Ph), 74.1 (C-4), 71.9 (OCH₂Ph), 69.9 (C-5), 69.6 (C-6), 24.0 (SCH₂CH₃), 15.2 (SCH₂CH₃); **IR** (ν_{max} /cm⁻¹): 3019 (C-H), 1215 (C-OR); **HRMS**: Found [M+Na]⁺ 515.1860, C₂₉H₃₂NaO₅S requires 515.1863.

Phenyl 2,3-di-O-benzyl-4,6-O-benzylidene-1-thio-β-D-galactopyranoside (**65**)¹⁹⁷



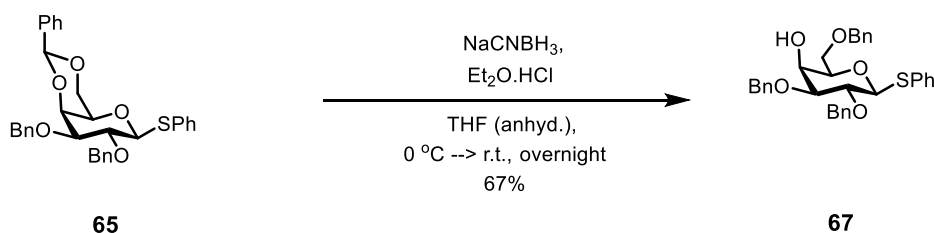
Benzylbromide (3.5 mL, 30 mmol) was added to the solution of 4,6-O-benzylidene-1-thio-β-D-galactopyranoside **63** (11.5 g, 32 mmol) in DMF (100 mL). After cooling the reaction mixture to 0 °C in an ice bath, sodium hydride (60% in oil dispersion, 3.3 g, 138 mmol) was added. The reaction mixture was stirred at r.t. overnight and quenched with water (5 mL), extracted with DCM twice. The organic layers were combined, washed with brine and dried over MgSO₄. The solvent was removed and the crude product was purified by flash column chromatography (silica; 17:3 hexane–EtOAc → 2:1 hexane–EtOAc) to afford compound **65** as a colourless solid (15.0 g, 87%); *R*_f 0.26 (2:1 hexane–EtOAc); m.p. 177-178 °C (from EtOAc–hexane) (lit.¹⁹⁷ m.p. 178-179 °C); $[\alpha]_{\text{D}}^{21}$ -17.3 (c, 1.2, CHCl₃) (lit.¹⁹⁷ $[\alpha]_{\text{D}}$ -19.4 (c, 1.23, CHCl₃)); δ_{H} (500 MHz, CDCl₃); 7.73-7.68 (m, 2H, ArH), 7.57-7.49 (m, 2H, ArH), 7.44-7.16 (m, 16H, ArH), 5.49 (s, 1H, PhCHO₂), 4.75-4.66 (m, 4H, 2 × OCH₂Ph), 4.61 (d, 1H, *J*_{1,2} 9.4 Hz, H-1), 4.36 (dd, 1H, *J*_{6,6'} 12.3 Hz, *J*_{5,6} 1.6 Hz, H-6), 4.15 (d, 1H, *J*_{3,4} 3.2 Hz, H-4), 3.98 (dd, 1H, *J*_{6,6'} 12.3 Hz, *J*_{5,6'} 1.6 Hz, H-6'), 3.90 (t, 1H, *J*_{1,2=2,3} 9.4 Hz, H-2), 3.62 (dd, 1H, *J*_{2,3} 9.4 Hz, *J*_{3,4} 3.2 Hz, H-3), 3.40 (d, 1H, *J*_{5,6} 1.6 Hz, H-5); δ_{C} (75 MHz, CDCl₃); 138.5, 138.1, 137.9, 132.8, 129.1, 128.9, 129.4, 129.3, 129.2, 129.2, 127.7, 127.5, 126.6 (ArC), 101.3 (PhCHO₂), 86.6 (C-1), 81.4 (C-2), 75.5 (OCH₂Ph), 75.4 (C-2), 73.7 (C-4), 71.9 (OCH₂Ph), 69.9 (C-5), 69.4 (C-6); **IR** (ν_{max} /cm⁻¹): 2865 (C-H), 1091 (C-OR); **HRMS**: Found [M+Na]⁺ 563.1861, C₃₃H₃₂NaO₅S requires 563.1863.

Ethyl 2,3,6-tri-O-benzyl-1-thio-β-D-galactopyranoside (66)¹⁹⁸



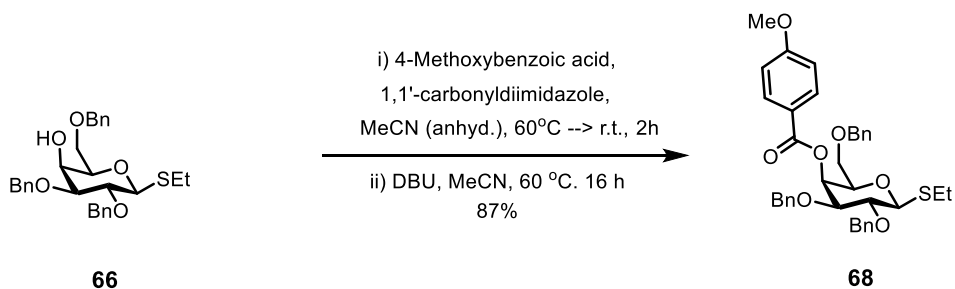
Sodium cyanoborohydride (0.52 g, 8.3 mmol) and methyl orange (28 mg) were added to a stirred solution of ethyl 2,3-di-O-benzyl-4,6-O-benzylidene-1-thio-β-D-galactopyranoside **64** (0.68 g, 1.4 mmol) in anhydrous THF. After cooling the mixture to 0 °C, ethereal HCl was added dropwise until the solution turned pink. The reaction mixture was stirred at r.t. under N₂(g) atmosphere overnight. The reaction mixture was quenched with water, extracted with DCM. The combined organic phases were washed with saturated aq. NaHCO₃ twice, dried (MgSO₄), and concentrated. The residue was purified by flash column chromatography (silica; 2:1 hexane–EtOAc), yielded compound **66** (200 mg, 28%) as a colourless oil; *R*_f 0.32 (2:1 hexane–EtOAc); $[\alpha]_D^{24}$ 3.5 (c, 1, EtOAc) (lit.¹⁹⁸ $[\alpha]_D$ 2 (c, 1, EtOAc)); δ_H (500 MHz, CDCl₃); 7.41–7.36 (m, 2H, ArH), 7.36–7.23 (m, 13H, ArH), 4.86 (d, 1H, *J* 10.3 Hz, OCH₂Ph), 4.76 (d, 1H, *J* 10.3 Hz, OCH₂Ph), 4.69 (d, 1H, *J* 11.7 Hz, OCH₂Ph), 4.66 (d, 1H, *J* 11.7 Hz, OCH₂Ph), 4.55 (s, 2H, OCH₂Ph), 4.42 (d, 1H, *J*_{1,2} 9.7 Hz, H-1), 4.06 (t, 1H, *J* 2.4 Hz, H-4), 3.79–3.64 (m, 3H, H-2, H-6, H-6'), 3.57–3.49 (m, 2H, H-3, H-5), 2.81–2.65 (m, 2H, SCH₂CH₃), 2.62 (d, 1H, *J* 1.9 Hz, -OH), 1.30 (t, 3H, *J* 7.4 Hz, SCH₂CH₃); δ_C (75 MHz, CDCl₃); 138.2, 138.0, 137.8 (C-O), 128.5, 128.4, 128.3, 127.9, 127.8, 127.7 (ArC), 85.0 (C-1), 82.4 (C-3), 77.9 (C-2), 76.9 (C-5), 75.8, 73.7, 72.0 (3 × OCH₂Ph), 69.4 (C-6), 66.9 (C-4), 24.7 (SCH₂CH₃), 15.1 (SCH₂CH₃); IR (ν_{max}/cm^{-1}): 3463 (OH), 2895 (C-H); HRMS: Found [M+Na]⁺ 517.2016, C₂₉H₃₄NaO₅S requires 517.2019.

Phenyl 2,3,6-tri-O-benzyl-1-thio-β-D-galactopyranoside (67)¹⁹⁹



Sodium cyanoborohydride (1.5 g, 24 mmol) and methyl orange (80 mg, 0.2 mmol) were added to a stirred solution of phenyl 2,3-di-O-benzyl-4,6-O-benzylidene-1-thio-β-D-galactopyranoside **65** (2.14 g, 4.0 mmol) in anhydrous THF. After cooling the mixture to 0 °C, ethereal HCl was added dropwise until the solution turned pink. The reaction mixture was stirred at r.t. under N₂(g) atmosphere overnight. The reaction mixture was quenched with water (70 mL), extracted with diethyl ether (3 × 100 mL). The combined organic phases were combined, washed with saturated aq. NaHCO₃ (2 × 100 mL) and water (2 × 100 mL), dried (MgSO₄), and concentrated. The crude product was purified by flash column chromatography (silica; 2:1 hexane–EtOAc), yielded compound **67** (1.4 g, 67%) as a colourless oil; *R_f* 0.34 (2:1 hexane–EtOAc); $[\alpha]_{\text{D}}^{21}$ -6.3 (c, 1.03, CHCl₃) (lit.¹⁹⁹ $[\alpha]_{\text{D}}$ -10.5 (c, 1.06, CHCl₃)); δ_{H} (500 MHz, CDCl₃); 7.64-7.60 (m, 2H, ArH), 7.46-7.43 (m, 2H, ArH), 7.39-7.22 (m, 16H, ArH), 4.87 (d, 1H, *J* 10.4 Hz, OCH₂Ph), 4.78 (d, 1H, *J* 10.4 Hz, OCH₂Ph), 4.74-4.65 (m, 3H, H-1, OCH₂Ph), 4.57 (s, 2H, OCH₂Ph), 4.10 (t, 1H, *J*_{3,4=4,5} 2.8 Hz, H-4), 3.85-3.77 (m, 3H, H-2, H-6, H-6'), 3.63-3.56 (m, 2H, H-3, H-5), 2.74 (d, 1H, *J* 2.5 Hz, OH); δ_{C} (75 MHz, CDCl₃); 138.2, 137.9, 137.7, 134.0, 131.6, 128.8, 128.4, 128.3, 128.3, 128.2, 127.9, 127.8, 127.7, 127.7, 127.7, 127.7, 127.2 (ArC), 87.6 (C-1), 82.5 (C-3), 77.0 (C-5), 77.0 (C-2), 75.6 (OCH₂Ph), 73.6 (OCH₂Ph), 72.0 (OCH₂Ph), 69.5 (C-6), 66.8 (C-4); **IR** (ν_{max} /cm⁻¹): 3552 (OH), 2907, 2870 (CH), 1052 (C-OR) **HRMS**: Found $[\text{M}+\text{Na}]^+$ 565.2031, C₃₃H₃₄NaO₅S requires 565.2019.

Ethyl 2,3,6-tri-O-benzyl-4-O-(4-methoxybenzoyl)-1-thio-β-D-galactopyranoside (68)¹²⁷

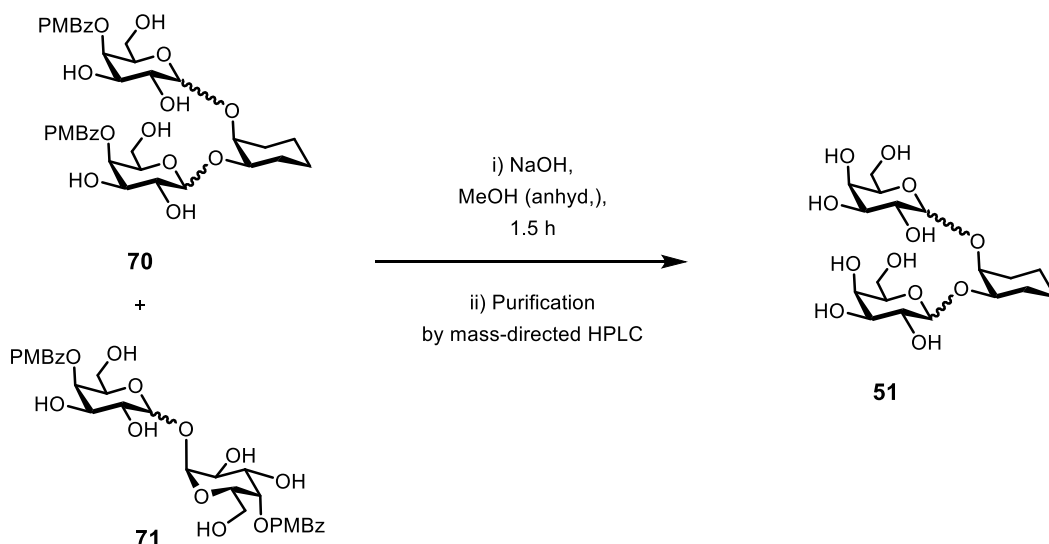


4-Methoxybenzoic acid (127 mg, 0.8 mmol) and 1,1'-carbonyldiimidazole (143 mg, 0.9 mmol) were dissolved in anhydrous MeCN (5 mL) and stirred at 60 °C under N₂(g) atmosphere for 2 h. The reaction mixture was cooled to r.t. before ethyl 2,3,6-tri-O-benzyl-1-thio-β-D-galactopyranoside **66** (196 mg, 0.4 mmol) in MeCN (4 mL) was added, followed by DBU (128 μL, 0.8 mmol). The reaction mixture was stirred at 60 °C under N₂(g) atmosphere for 16 h, cooled to r.t., poured into saturated aq. NaHCO₃, and extracted with DCM. The combined organic layers were washed with brine, dried (MgSO₄), and concentrated. The residue was purified by flash column chromatography (silica; 4:1 hexane–EtOAc), to give compound **68** (220 mg, 87%) as a colourless oil; *R_f* 0.43 (2:1 hexane–EtOAc); $[\alpha]_D^{22}$ 28.4 (c, 1.0, CHCl₃); δ_H (500 MHz, CDCl₃); 8.06 (d, 2H, *J* 8.8 Hz, ArH), 7.39–7.17 (m, 15H, ArH), 6.93 (d, 2H, *J* 8.8 Hz, ArH), 5.87 (d, 1H, *J* 2.7 Hz, H-4), 4.87 (d, 1H, *J* 11.4 Hz, OCH₂Ph), 4.80 (d, 1H, *J* 10.3 Hz, OCH₂Ph), 4.75 (d, 1H, *J* 10.2 Hz, OCH₂Ph), 4.58–4.45 (m, 3H, H-1, OCH₂Ph), 4.42 (d, 1H, *J* 11.7 Hz, OCH₂Ph), 3.88–3.78 (m, 4H, OCH₃, H-5), 3.74–3.60 (m, 3H, H-2, H-3, H-6), 3.58–3.51 (m, 1H, H-6'), 2.86–2.71 (m, 2H, SCH₂CH₃), 1.34 (t, 3H, *J* 7.4 Hz, SCH₂CH₃); δ_C (75 MHz, CDCl₃); 165.5 (C=O), 163.6, 138.2, 137.9, 137.7, 128.5, 128.4, 128.3, 128.2, 128.0, 127.8, 127.7, 113.7 (ArC), 85.5 (C-1), 81.2 (C-2), 77.9 (C-3), 76.3 (C-5), 75.9, 73.8, 71.7 (3 × OCH₂Ph), 68.6 (C-6), 67.2 (C-4), 55.5 (OCH₃); IR (ν_{max}/cm⁻¹): 3054 (C–H), 1714 (C=O), 1265 (C–OR); HRMS: Found [M+Na]⁺ 651.2406, C₃₇H₄₀NaO₇S requires 651.2387.

$[M+Na]^+$ 731.4, $C_{34}H_{44}NaO_{16}$ requires 731.7; for compound **71**: Found $[M+Na]^+$ 633.2, $C_{28}H_{34}NaO_{15}$ requires 633.6.

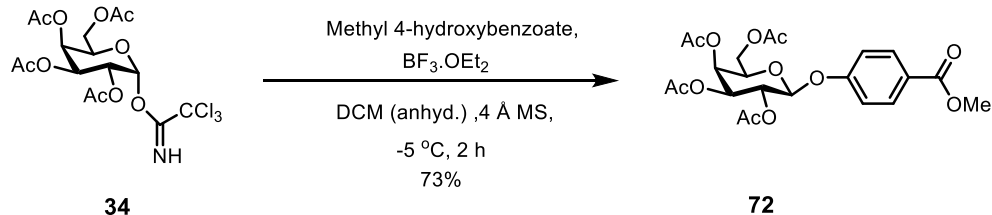
- Glycosylation reaction in DCM gave a mixture of compounds **70** and **71** in a ratio of 5:3 (29 mg of the mixture, 21% of **70** over two steps; calculated from a relative mass of 671.90). A mixture of anomers was obtained. The α : β ratio (5:1) was determined by integration of anomeric signals in the 1H NMR spectrum. Signal integrations are normalised to give a total of 2 anomeric protons across all isomers; δ_H (500 MHz, CD_3OD); 8.03-8.00 (m, 4H), 7.04-6.96 (m, 4H), 5.57-5.51 (m, 2H), 5.34 (d, 0.40H, J 3.7 Hz), 5.31 (d, 0.69H, J 3.8 Hz), 5.25 (d, 0.10H, J 3.6 Hz), 5.13 (d, 0.68H, J 3.8 Hz), 5.11 (d, 0.13H, 3.8 Hz), 4.66 (d, 0.50H, J 7.9 Hz), 4.62 (d, 0.25, J 7.9 Hz), 4.51 (d, 1.25H, J 7.7 Hz), 4.38-3.49 (m, 14H), 2.18-1.24 (m, 8H).
- Glycosylation reaction in DCM:diethyl ether (1:1, v/v) gave a mixture of compounds **70** and **71** in a ratio of 10:7 (45 mg of the mixture, 30% of **70** over two steps; calculated from a relative mass of 668.30); The α : β ratio (5:1) was determined by integration of aromatic signals in the 1H NMR spectrum. Signal integrations are normalised to give a total of 2 anomeric protons across all isomers; δ_H (500 MHz, CD_3OD); 8.06-7.99 (m, 4H), 7.06-6.95 (m, 4), 5.57-5.51 (m, 2H), 5.35 (d, 0.48H, J 3.8 Hz), 5.31 (d, 0.68H, J 3.9 Hz), 5.25 (d, 0.07H, J 3.9 Hz), 5.13 (d, 0.65H, J 3.7 Hz), 5.11 (d, 0.12H, J 3.9 Hz), 4.65 (d, 0.15H, J 7.1 Hz), 4.62 (d, 0.10H, J 7.4 Hz), 4.55-4.49 (m, 1.20H), 4.38-3.51 (m, 14H), 2.11-1.24 (m, 8H).

A mixture of compounds **70** and **71** of the above reactions were combined (62 mg) was dissolved in anhydrous MeOH (5 mL). Sodium hydroxide (14 mg, 0.53 mmol) was added to the reaction mixture, which was stirred for 1.5 h, concentrated and purified by mass-directed HPLC to provide compound **51** as a mixture of anomers (7 mg, α / β ratio of 8:1).



The α : β ratio was determined by integration of aromatic signals in the ^1H NMR spectrum. Signal integrations are normalised to give a total of 2 anomeric protons across all isomers; δ_{H} (500 MHz, D_2O); 5.27 (d, 0.90H, J 4.0 Hz), 5.25 (d, 0.09H, J 3.9 Hz), 5.18 (d, 1.01H, J 4.0 Hz), 4.68 (d, 0.96 H, J 7.3 Hz), 4.56 (d, 1.04H, J 7.8 Hz), 4.30-3.59 (m, 14H), 2.09-1.20 (m, 8H).

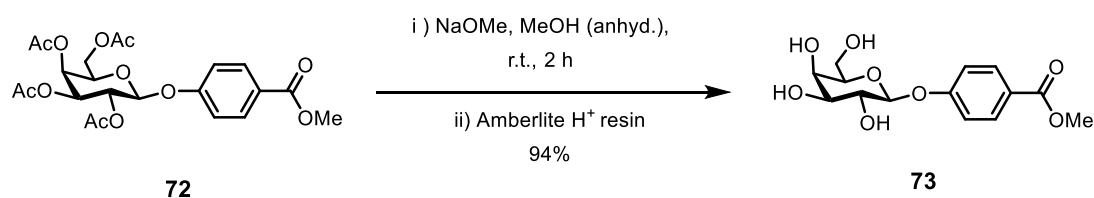
4-Methoxycarbonylphenyl 2,3,4,6-tetra-*O*-acetyl- β -D-galactopyranoside (**72**)²⁰⁰



A solution of 2,3,4,6-tetra-*O*-acetyl- α -D-galactopyranosyl trichloroacetimidate **34** (720.0 mg, 1.46 mmol), methyl 4-hydroxybenzoate (333.0 mg, 2.2 mmol) and 4 Å MS (500 mg) in anhydrous DCM (6 mL) was stirred at -5°C for 1 h before freshly distilled boron trifluoride diethyl etherate (40 μL , 0.3 mmol) was added dropwise. After stirring at -5°C for 1 h, the reaction mixture was washed with saturated aq. NaHCO_3 three times and extracted with DCM three times. The combined organic layers were dried (MgSO_4) and concentrated to afford a colourless oil, which was purified by flash column chromatography (silica; 2:1 hexane–EtOAc) to afford compound **72** (515 mg, 73%) as a colourless solid; R_f 0.13 (2:1 hexane–EtOAc); m.p. 146-147 $^\circ\text{C}$ (from EtOH); $[\alpha]_{\text{D}}^{22}$ 1.0 (c, 1, CHCl_3) (lit.²⁰⁰ $[\alpha]_{\text{D}}^{25}$ 1.7 (c 0.8, CHCl_3)); δ_{H} (500 MHz, CDCl_3); 8.01-7.98 (m, 2H,

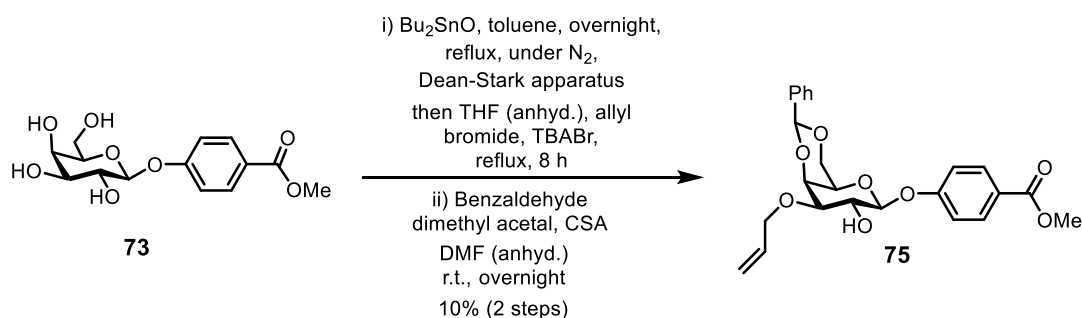
ArH), 7.03-7.00 (m, 2H, ArH), 5.51 (dd, 1H, $J_{2,3}$ 10.4, $J_{1,2}$ 7.9 Hz, H-2), 5.47 (d, 1H, $J_{3,4}$ 3.1 Hz, H-4), 5.15-5.10 (m, 2H, H-1, H-3), 4.24-4.20 (m, 1H, H-6), 4.19-4.14 (m, 1H, H-6'), 4.13-4.08 (m, 1H, H-5), 3.90 (s, 3H, OCH₃), 2.18 (s, 3H, C(O)CH₃), 2.06 (s, 3H, C(O)CH₃), 2.02 (s, 3H, C(O)CH₃); δ_c (75 MHz, CDCl₃); 170.5, 170.3, 170.2, 169.5 (4 × C(O)CH₃), 166.6 (C=O), 160.4, 131.7, 125.2, 116.3 (ArC), 99.0 (C-1), 71.4 (C-5), 70.9 (C-3), 68.6 (C-2), 67.0 (C-4), 61.5 (C-6), 52.2 (OCH₃), 20.8, 20.8, 20.8, 20.7 (4 × C(O)CH₃), **IR** ($\nu_{\max}/\text{cm}^{-1}$): 1755 (C=O); **HRMS**: Found $[\text{M}+\text{Na}]^+$ 505.1334, C₂₂H₂₆O₁₂Na requires 505.1316.

4-Methoxycarbonylphenyl β -D-galactopyranoside (**73**)



Sodium methoxide (34.5 mg, 0.6 mmol) was added to a suspension of 4-methoxycarbonylphenyl 2,3,4,6-tetra-O-acetyl- β -D-galactopyranoside **72** (370 mg, 0.8 mmol) in anhydrous MeOH (7 mL). After stirring for 2 h at r.t., the reaction mixture was diluted with MeOH and neutralised with Amberlite IRC 86 H⁺ resin, filtered and concentrated to afford compound **73** (236 mg, 94%) as a colourless solid; R_f 0.10 (9:1 DCM–MeOH); m.p. 190-191 °C; $[\alpha]_D^{23}$ 0.8 (c, 1.0, DMSO); δ_H (500 MHz, DMSO-*d*₆) 7.91 (d, 2H, J 8.8 Hz, ArH), 7.11 (d, 2H, J 8.8 Hz, ArH), 5.30 (s, 1H, OH), 5.04 (s, 1H, OH), 4.95 (d, 1H, $J_{1,2}$ 7.7 Hz, H-1), 4.74 (s, 1H, OH), 4.66 (s, 1H, OH), 3.82 (s, 3H, OCH₃), 3.72 (s, 1H, H-5), 3.64-3.40 (m, 5H, H-2, H-3, H-4, H-6, H-6'); δ_c (75 MHz, DMSO-*d*₆); 161.2 (C=O), 131.0 (ArC), 122.8 (ArC), 116.0 (ArC), 100.4 (ArC), 75.6 (C-1), 73.2 (C-5), 70.2, 68.0, 60.2 (C-2, C-3, C-4), 51.9 (OCH₃); **IR** ($\nu_{\max}/\text{cm}^{-1}$): 3589 (OH), 1694 (C=O); **HRMS**: Found $[\text{M}+\text{Na}]^+$ 337.0908, C₁₄H₁₈O₈Na requires 337.0894.

4-Methoxycarbonylphenyl 3-O-allyl-4,6-O-benzylidene- β -D-galactopyranoside (**75**)

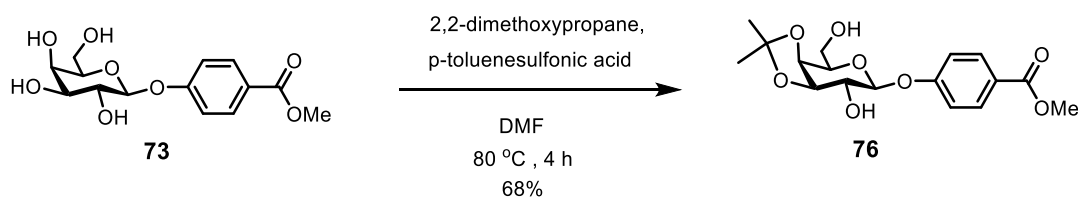


A suspension of 4-methoxycarbonylphenyl 2,3,4,6-tetra-*O*-acetyl- β -D-galactopyranoside **73** (5 g, 16 mmol) and dibutyl tin oxide (4 g, 16 mmol) in toluene (110 mL) was refluxed overnight under azeotropic conditions. Toluene was removed *in vacuo* and the residue was dissolved in anhydrous THF (70 mL). Allyl bromide (6.9 mL, 80 mmol) and tetrabutyl aluminium bromide (5.12 g, 16 mmol) were added to the reaction mixture, which was refluxed for 8 h, filtered, evaporated, and partially purified by flash column chromatography (silica; 1:4 hexane–EtOAc). One fourth of the semi crude product (500 mg, 1.45 mmol) was dissolved in anhydrous DMF (3 mL). Benzaldehyde dimethylacetal (2.6 mL, 1.73 mmol) and (+/-)-10-camphorsulfonic acid were added to the solution until the reaction mixture was acidic. The reaction mixture was then stirred at r.t. overnight. Triethylamine was added to neutralise the solution mixture, which was then concentrated, and recrystallised from EtOH to afford compound **75** (190 mg, 10%, 2 steps); R_f 0.50 (1:4 hexane–EtOAc); m.p. 230–231 °C (from EtOH); $[\alpha]_D^{22}$ –61.4 (c, 1.0, CHCl_3); δ_H (500 MHz, CDCl_3); 8.01–7.94 (m, 2H, ArH), 7.55–7.50 (m, 2H, ArH), 7.39–7.30 (m, 3H, ArH), 7.12–7.05 (m, 2H, ArH), 5.93–6.04 (m, 1H, $\text{CH}_2=\text{CHCH}_2$), 5.57 (s, 1H, PhCHO_2), 5.39–5.33 (m, 1H, $\text{CH}_2=\text{CHCH}_2$), 5.27–5.22 (m, 1H, $\text{CH}_2=\text{CHCH}_2$), 5.06 (d, 1H, $J_{1,2}$ 7.7 Hz, H-1), 4.39–4.19 (m, 5H, H-2, H-4, H-6, $\text{CH}_2=\text{CHCH}_2$), 4.15–4.10 (m, 1H, H-6'), 3.89 (s, 3H, OCH_3), 3.64–3.55 (m, 2H, H-3, H-5); δ_C (75 MHz, CDCl_3); 166.8 (C=O), 160.9, 137.7, 134.8 ($\text{CH}_2=\text{CHCH}_2$), 131.6, 129.2, 128.3, 126.5, 124.6 (ArC), 118.1 ($\text{CH}_2=\text{CHCH}_2$), 116.5 (ArC), 101.3 (PhCHO_2), 100.6 (C-1), 79.0 (C-3), 72.9 (C-4), 70.9 ($\text{CH}_2=\text{CHCH}_2$), 69.6 (C-2), 69.3 (C-6), 67.1 (C-5), 52.1 (OCH_3); IR ($\nu_{\text{max}}/\text{cm}^{-1}$): 3419 (OH), 1718 (C=O); HRMS: Found $[\text{M}+\text{Na}]^+$ 465.1524, $\text{C}_{24}\text{H}_{26}\text{O}_8\text{Na}$ requires 465.1520.

A small sample (30 mg) of this purified product was acetylated using pyridine-acetic anhydride catalysed by DMAP and purified by flash column chromatography (silica; 1:1 hexane–EtOAc) to give 4-methoxycarbonylphenyl 2-*O*-acetyl-3-*O*-allyl-4,6-*O*-benzylidene- β -D-galactopyranoside as colourless solid; R_f 0.25 (1:1 hexane–EtOAc);

$[\alpha]_{\text{D}}^{25}$ -22.93 (c, 1.0, CHCl_3); m.p. 166-168 °C (from hexane-EtOAc); δ_{H} (500 MHz, CDCl_3); 7.96 (d, 2H, J 8.7 Hz, ArH), 7.56-7.51 (m, 2H, ArH), 7.35 (q, 3H, J 7.6 Hz, ArH), 7.02 (d, 2H, J 8.7 Hz, ArH), 5.88 (m, 1H, $\text{CH}_2=\text{CHCH}_2$), 5.62-5.53 (m, 2H, PhCHO_2 , H-2), 5.33-5.26 (m, 1H, $\text{CH}_2=\text{CHCH}_2$), 5.22-5.18 (m, 1H, $\text{CH}_2=\text{CHCH}_2$), 5.10 (d, 1H, $J_{1,2}$ 7.9 Hz, H-1), 4.38-4.31 (m, 2H, H-4, H-6), 4.22-4.16 (m, 1H, $\text{CH}_2=\text{CHCH}_2$), 4.15-4.07 (m, 2H, $\text{CH}_2=\text{CHCH}_2$, H-6'), 3.88 (s, 3H, OCH_3), 3.68 (dd, 1H, $J_{2,3}$ 10.1 Hz, $J_{3,4}$ 3.5 Hz, H-3), 3.58 (bs, 1H, H-5), 2.07 (s, 3H, $\text{C}(\text{O})\text{CH}_3$); δ_{C} (75 MHz, CDCl_3); 169.4, 166.8 (C=O), 160.9, 137.6, 134.7 ($\text{CH}_2=\text{CHCH}_2$), 131.5, 129.1, 128.3, 126.5, 124.6 (ArC), 117.5 ($\text{CH}_2=\text{CHCH}_2$), 116.4 (ArC), 101.3 (PhCHO_2), 99.1 (C-1), 77.1 (C-3), 73.3 (C-4), 70.6 ($\text{CH}_2=\text{CHCH}_2$), 69.9 (C-2), 69.0 (C-6), 67.1 (C-5), 52.1 (OCH_3), 21.0 ($\text{C}(\text{O})\text{CH}_3$); IR ($\nu_{\text{max}}/\text{cm}^{-1}$): 1716 (C=O); HRMS: Found $[\text{M}+\text{Na}]^+$ 507.1633, $\text{C}_{26}\text{H}_{28}\text{NaO}_9$ requires 507.1626.

4-Methoxycarbonylphenyl 3,4-O-isopropylidene- β -D-galactopyranoside (**76**)

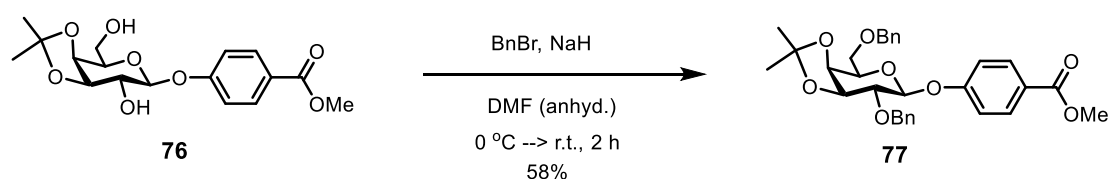


4-Methoxycarbonylphenyl β -D-galactopyranoside **73** (3.16 g, 10 mmol) in DMF (30 mL) was stirred at 80 °C, and *p*-toluenesulfonic acid (0.7 g, 3.6 mmol) was added portionwise, followed by adding 2,2-dimethoxypropane (3.7 mL, 30 mmol) dropwise. The resulting mixture was stirred for 4 h at 80 °C. The reaction was quenched with triethylamine (3 mL) and concentrated to leave pale yellow syrup, which was suspended in EtOAc (30 mL) and MeOH (10 mL). Aqueous TFA (0.2 mL, 50% v/v) was added to the mixture. After stirring for further 1 h, the reaction mixture was again quenched with triethylamine (2 mL) and evaporated onto silica. Flash column chromatography (silica, 19:1 EtOAc–hexane) gave compound **76** as colourless foam (2.41 g, 68%); R_f 0.58 (19:1 EtOAc–MeOH); $[\alpha]_{\text{D}}^{22}$ -35.4 (c, 1.0, CHCl_3); δ_{H} (500 MHz, CD_3OD); 8.00-7.92 (m, 2H, ArH), 7.16-7.10 (m, 2H, ArH), 4.97 (d, 1H, $J_{1,2}$ 8.0 Hz, H-1), 4.29 (dd, 1H, $J_{3,4}$ 5.5 Hz, $J_{4,5}$ 2.1 Hz, H-4), 4.16 (1H, dd, $J_{2,3}$ 7.1 Hz, $J_{3,4}$ 5.5 Hz, H-3), 4.11-4.06 (m, 1H, H-5), 3.87 (s, 1H, OCH_3), 3.81-3.77 (m, 2H, H-6, H-6'), 3.71 (dd, 1H, $J_{1,2}$ 8.0 Hz, $J_{2,3}$ 7.1 Hz, H-2), 1.52 (s, 3H, $\text{C}(\text{CH}_3)_2$), 1.36 (s, 3H, $\text{C}(\text{CH}_3)_2$); δ_{C} (75 MHz, CD_3OD); 168.2 (C=O), 162.7, 132.4, 125.1, 117.3 (ArC), 111.2 ($\text{C}(\text{CH}_3)_2$), 101.1 (C-1),

80.7 (C-3), 75.3 (C-5), 74.9 (C-4), 73.9 (C-2), 62.4 (C-6), 52.5 (OCH₃), 28.4, 26.5 (2 × CH₃); IR (ν_{max}/cm⁻¹): 3365 (OH), 1722 (C=O); HRMS: Found [M+Na]⁺ 377.1212, C₁₇H₂₂O₈Na requires 377.1207.

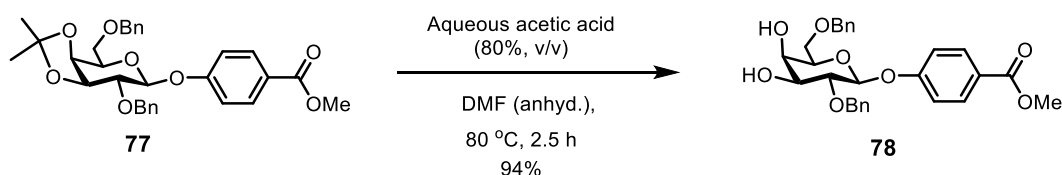
**4-Methoxycarbonylphenyl
galactopyranoside (76)**

3,4-O-isopropylidene-2,6-di-O-benzyl-β-D-



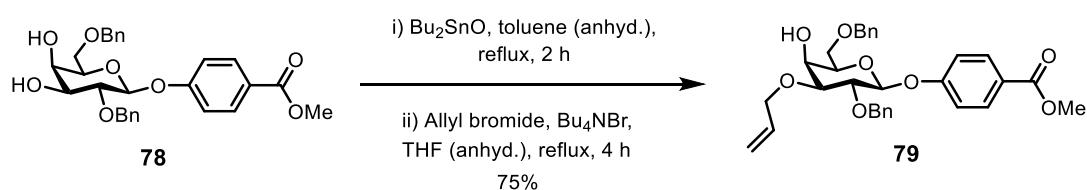
4-Methoxycarbonylphenyl 3,4-O-isopropylidene β-D-galactopyranoside **76** (2.23 g, 6.2 mmol) was dissolved in anhydrous DMF (50 mL), the reaction mixture was cooled to 0 °C, to which NaH (60%, 1.13 g, 47.2 mmol) was added portionwise. After stirring at 0 °C for 15 min, benzyl bromide (2.7 mL, 22.7 mmol) was added. The resulting mixture was stirred at r.t. for 2 h before MeOH (18 mL) was added to quench the reaction. Solvent removal gave a crude oil, which was purified by flash column chromatography (silica; 3:1 Petroleum ether–EtOAc), yielded compound **77** as colourless oil (1.96, 58%); *R_f* 0.67 (19:1 Petroleum ether–EtOAc); [α]_D²² 4.13 (c, 1.0, CHCl₃); δ_H (500 MHz, CDCl₃); 7.99-7.95 (m, 2H, ArH), 7.41-7.24 (m, 10H, ArH), 7.09-7.05 (m, 2H, ArH), 5.01 (d, 1H, *J*_{1,2} 7.8 Hz, H-1), 4.87 (s, 2H, OCH₂Ph), 4.61 (d, 1H, *J* 11.8 Hz, OCH₂Ph), 4.53 (d, 1H, *J* 11.8 Hz, OCH₂Ph), 4.29 (t, 1H, *J*_{2,3-3,4} 6.1 Hz, H-3), 4.23 (dd, 1H, *J*_{3,4} 6.1 Hz, *J*_{4,5} 1.9 Hz, H-4), 4.09 (m, 1H, H-5), 3.90 (s, 3H, OCH₃), 3.86-3.75 (m, 2H, H-6, H-6'), 3.71 (dd, 1H, *J*_{1,2} 7.8 Hz, *J*_{2,3} 6.1 Hz, H-2), 1.42 (s, 3H, C(CH₃)), 1.36 (s, 3H, C(CH₃)); δ_C (75 MHz, CDCl₃); 166.8 (C=O), 160.9, 138.2, 138.0, 131.7, 128.5, 128.4, 128.3, 127.9, 127.9, 127.7, 124.5, 116.3 (Arc), 110.5 (C(CH₃)₂), 100.2 (C-1), 79.1 (C-2), 79.1 (C-3), 73.8 (OCH₂Ph), 73.8 (OCH₂Ph), 73.7 (C-4), 73.0 (C-5), 69.6 (C-6), 52.1 (OCH₃), 27.8, 26.4 (2 × CH₃); IR (ν_{max}/cm⁻¹): 1750 (C=O); HRMS: Found [M+Na]⁺ 557.2155, C₃₁H₃₄O₈Na requires 557.2146.

4-Methoxycarbonylphenyl 2,6-di-O-benzyl-β-D-galactopyranoside (78)



An aqueous acetic acid (80% v/v, 17 mL) was added to 200 mg of 4-methoxycarbonylphenyl 3-O-allyl-2,6-di-O-benzyl-β-D-galactopyranoside **77**. The reaction mixture was stirred at 80 °C for 2.5 h, brought to r.t., concentrated to give compound **78** as a colourless oil (172 mg, 94%); R_f 0.06 (1:1 Hexane–EtOAc); $[\alpha]_D^{27}$ -12.0 (c, 0.7, CHCl₃); δ_H (500 MHz, CDCl₃); 7.99 (d, 2H, J 8.8 Hz, ArH), 7.37-7.27 (m, 10H, ArH), 7.09 (d, 2H, J 8.8 Hz, ArH), 5.05 (s, 1H, $J_{1,2}$ 7.7 Hz, H-1), 5.01 (d, 1H, J 11.3 Hz, OCH₂Ph), 4.78 (d, 1H, J 11.4 Hz, OCH₂Ph), 4.57 (s, 2H, OCH₂Ph), 4.07 (d, 1H, $J_{3,4}$ 3.3 Hz, H-4), 3.90 (s, 3H, OCH₃), 3.86-3.77 (m, 4H, H-2, H-5, H-6, H-6'), 3.71 (dd, 1H, $J_{2,3}$ 9.4 Hz, $J_{3,4}$ 3.3 Hz, H-3), 2.68, (s, 1H, OH), 2.56 (s, 1H, OH); δ_C (75 MHz, CDCl₃); 166.8 (C=O), 160.8, 138.1, 137.8, 131.7, 128.8, 128.6, 128.4, 128.3, 128.0, 128.0, 127.9, 124.6, 116.3 (ArC), 101.1 (C-1), 78.8 (C-2), 75.1 (OCH₂Ph), 74.1 (C-5), 74.0 (OCH₂Ph), 73.3 (C-3), 69.5 (C-6), 69.0 (C-4), 52.1 (OCH₃); IR (ν_{\max} /cm⁻¹): 3438 (OH), 1717 (C=O); HRMS: Found $[M+Na]^+$ 517.1838, C₂₈H₃₀O₈Na requires 517.1833.

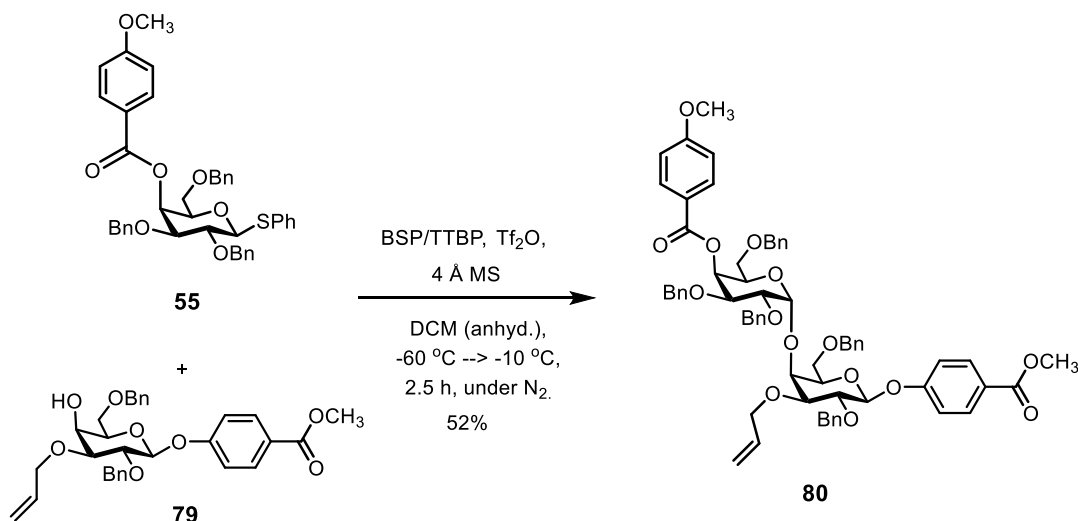
4-Methoxycarbonylphenyl 3-O-allyl-2,6-di-O-benzyl-β-D-galactopyranoside (79)



A suspension of 4-methoxycarbonylphenyl 2,6-di-O-benzyl β-D-galactopyranoside **78** (103 mg, 0.2 mmol) and dibutyl tin oxide (49 mg, 0.2 mmol) in anhydrous toluene (3 mL) was refluxed under azeotropic conditions. Toluene was removed *in vacuo* and the residue was co-evaporated with several times toluene, and then was dissolved in anhydrous THF (2 mL). Allyl bromide (90 μL, 1.0 mmol) and tetrabutyl aluminium bromide (64 mg, 0.2 mmol) were added to the reaction mixture, which was refluxed for 4 h, filtered, evaporated, and the residue was purified by flash column chromatography (silica; 2:1 hexane–EtOAc) to give compound **79** (80 mg, 75%) as a colourless solid; R_f

0.52 (1:1 hexane–EtOAc); m.p. 136-138 °C (from EtOH); $[\alpha]_D^{27}$ -33.0 (c, 1.0, CHCl₃); δ_H (500 MHz, CDCl₃); 7.98 (d, 2H, *J* 8.8 Hz, ArH), 7.40-7.26 (m, 10H, ArH), 7.08 (d, 2H, *J* 8.8 Hz, ArH), 6.00-5.90 (m, 1H, CH₂=CHCH₂), 5.32 (dd, 1H, *J* 17.2, 1.7 Hz, CH₂=CHCH₂), 5.22 (dd, 1H, *J* 1.07, 10.37 Hz, CH₂=CHCH₂), 5.04 (d, 1H, *J*_{1,2} 7.8 Hz, H-1), 4.93 (d, 1H, *J* 11.0 Hz, OCH₂Ph), 4.82 (d, 1H, *J* 11.0 Hz, OCH₂Ph), 4.58 (s, 2H, OCH₂Ph), 4.24-4.22 (m, 2H, CH₂=CHCH₂), 4.09 (d, 1H, *J*_{3,4} 3.5 Hz, H-4), 3.90 (s, 3H, OCH₃), 3.86-3.74 (m, 4H, H-2, H-5, H-6, H-6'), 3.53 (dd, *J*_{2,3} 9.3 Hz, *J*_{3,4} 3.5 Hz, H-3), 2.58 (s, 1H, OH); δ_C (75 MHz, CDCl₃); 166.8 (C=O), 161.0, 138.3, 138.0 (ArC), 134.5 (CH₂=CHCH₂), 131.7, 128.6, 128.5, 128.3, 128.0, 127.9, 124.4 (ArC), 117.8 (CH₂=CHCH₂), 116.3, 110.1 (ArC), 101.0 (C-1), 80.5 (C-3), 78.5 (C-2), 75.6 (OCH₂Ph), 74.0 (C-5), 74.0 (OCH₂Ph), 71.8 (CH₂=CHCH₂), 69.4 (C-6), 67.0 (C-4), 52.1 (OCH₃); IR (ν_{max}/cm^{-1}): 3029 (OH), 1716 (C=O); HRMS: Found [M+Na]⁺ 557.2163, C₃₁H₃₄O₈Na requires 557.2146.

4-Methoxycarbonylphenyl 3-O-allyl-2,6-di-O-benzyl-4-O-(2,3,6-tri-O-benzyl-4-O-(4-methoxybenzoyl)- α -D-galactopyranosyl)- β -D-galactopyranoside (80)

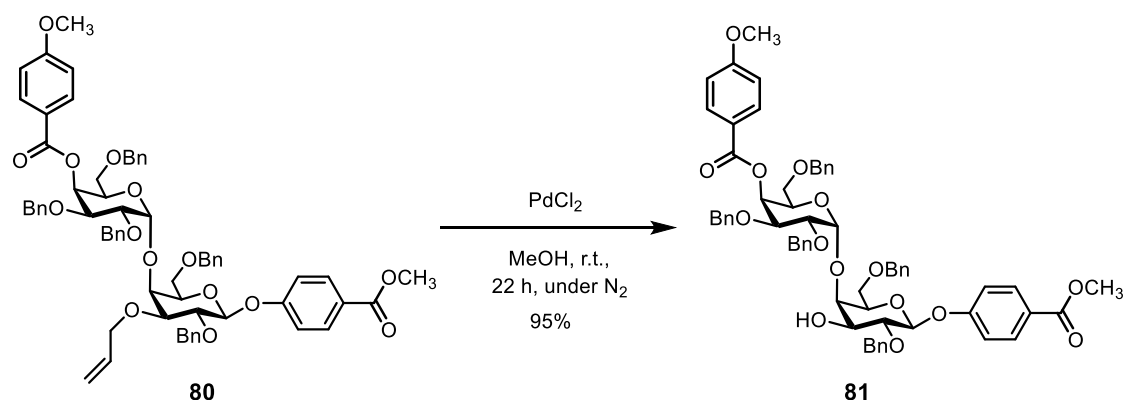


Thioglycosyl donor **55** (1.67 g, 2.4 mmol), 1-benzenesulfinyl piperidine (0.57 g, 2.7 mmol), and 2,4,6-tri-*tert*-butylpyrimidine (1.26 g, 4.9 mmol) were co-evaporated with toluene several times before adding molecular sieves 4 Å and anhydrous DCM (72 mL). The reaction mixture was stirred at r.t. under N₂(g) atmosphere for 1.5 h. Glycosyl acceptor **79** (1.08 g, 2.0 mmol) was also co-evaporated with toluene several times and dissolved in anhydrous DCM (36 mL) in a separate flask. After stirring for 1.5 h, the mixture of thioglycosyl donor, BSP, TTBP and molecular sieves 4 Å was cooled to -

60 °C before freshly distilled triflic anhydride (Tf₂O) (0.5 mL, 3 mmol) was added. The reaction mixture was stirred for 10 min at -60 °C before a solution of acceptor was added. The resulting mixture was stirred at low temperature (-60 °C to -10 °C) for 2 h, quenched with triethyl phosphate (0.4 mL), triethylamine (9.6 mL), and washed with sat. aq. NaHCO₃ (2 × 150 mL), followed by brine (2 × 150 mL). The combined organic phase was dried over MgSO₄, and concentrated to leave a crude yellow oil, which was purified by Biotage® flash column chromatography (Redisef®Rf 40 g silica column, 1.5 g of sample loaded each time, hexane:EtOAc (0% EtOAc (1 col. vol.) → 0-30% EtOAc (over 19 col. vol.) → 30-100% EtOAc (over 3 col. vol.)). The partially purified products were further purified by size exclusion chromatography (BioBeads SX-1, 500 mg of sample loaded each time, toluene). Further purification was performed by Biotage® flash column chromatography (Redisef®Rf 40 g silica column, Hexane:EtOAc (0% EtOAc (1 col. vol.) → 0-30% EtOAc (over 8 col. vol.) → 30% EtOAc (over 9 col. vol.)) to give compound **80** as colourless oil (1.15 g, 52%); *R*_f 0.25 (2:1 hexane–EtOAc); $[\alpha]_{\text{D}}^{22}$ 47.5 (c, 1.0, CHCl₃); δ_{H} (500 MHz, CDCl₃); 8.03-7.96 (m, 4H, ArH), 7.35-7.15 (m, 25H, ArH), 7.15 (d, 2H, *J* 8.9 Hz, ArH), 6.93 (d, 2H, *J* 8.9 Hz, ArH), 5.97 (dd, 1H, *J*_{3b,4b} 3.1 Hz, *J*_{4b,5b} 1.4 Hz, H-4b), 5.88 (m, 1H, CH₂=CHCH₂), 5.27 (dd, 1H, *J* 17.3 Hz, 1.7 Hz, CH₂=CHCH₂), 5.13 (dd, 1H, *J* 10.5, 1.4 Hz, CH₂=CHCH₂), 5.04 (d, 1H, *J*_{1b,2b} 3.6 Hz, H-1b), 5.02 (d, 1H, *J*_{1a,2a} 7.6 Hz, H-1a), 4.93 (d, 1H, *J* 10.8 Hz, OCH₂Ph), 4.88-4.80 (m, 3H, OCH₂Ph), 4.72-4.68 (m, 1H, H-5b), 4.59 (d, 1H, *J* 11.3 Hz, OCH₂Ph), 4.55 (d, 1H, *J* 10.9 Hz, OCH₂Ph), 4.46-4.38 (m, 2H, OCH₂Ph), 4.32-4.21 (m, 3H, OCH₂Ph, CH₂=CHCH₂), 4.18 (dd, 1H, *J*_{2b,3b} 10.1 Hz, *J*_{3b,4b} 3.2 Hz, H-3b), 4.14-4.08 (m, 2H, H-4a, CH₂=CHCH₂), 3.99-3.91 (m, 3H, H-2a, H-2b, H-6a), 3.88 (s, 6H, 2 × OCH₃), 3.70 (t, 1H, *J*_{5a,6a=5a,6'a} 6.3 Hz, H-5a), 3.63 (m, 1H, H-6'a), 3.54 (m, 1H, H-6b), 3.50-3.43 (m, 2H, H-6'b, H-3a); δ_{C} (75 MHz, CDCl₃); 166.8, 165.5 (C=O), 163.5, 161.1 (C-O), 138.7, 138.4, 138.1, 137.9 (ArC), 135.1 (CH₂=CHCH₂), 132.0, 131.6, 128.5, 128.4, 128.4, 128.3, 128.3, 128.3, 128.2, 128.1, 127.9, 127.8, 127.7, 127.6, 127.5, 124.3, 122.8 (ArC), 117.2 (CH₂=CHCH₂), 116.4, 113.7 (ArC), 101.3 (C-1a), 100.3 (C-1b), 80.3 (C-3a), 78.1 (C-2a), 76.7 (C-3b), 75.4 (C-2b, OCH₂Ph), 74.4 (C-4a, C-5a), 73.9 (2 × OCH₂Ph), 77.8 (OCH₂Ph), 73.4 (OCH₂Ph), 72.2 (CH₂=CHCH₂), 71.5 (C-5b), 68.3 (C-6b), 68.2 (C-4b), 68.2 (C-6a), 55.6 (OCH₃), 52.1 (OCH₃); **IR** (ν_{max} /cm⁻¹): 3013 (CH=CH₂), 2924, 2870 (C-H), 1714 (C=O), 1097, 1048 (C-OR); **HRMS**: Found [M+NH₄]⁺ 1118.4909, C₆₆H₇₂NO₁₅ requires 1118.4896.

4-Methoxycarbonylphenyl

2,6-di-O-benzyl-4-O-(2,3,6-tri-O-benzyl-4-O-(4-

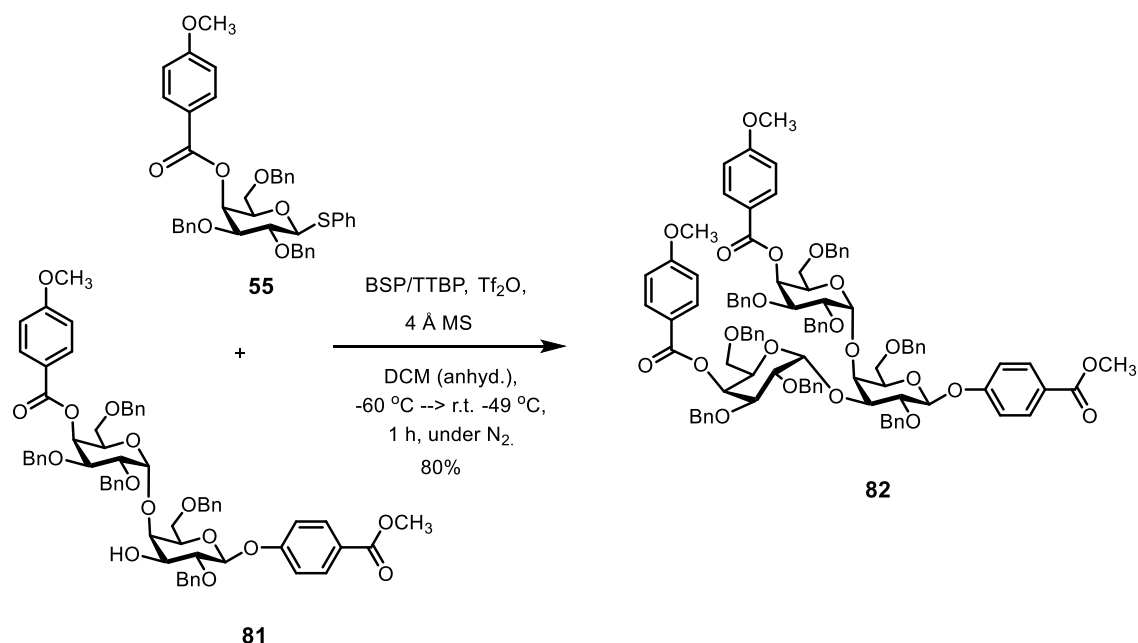
methoxybenzoyl)- α -D-galactopyranosyl)- β -D-galactopyranoside (**81**)

4-Methoxycarbonylphenyl

3-O-allyl-2,6-di-O-benzyl-4-O-(2,3,6-tri-O-benzyl-4-O-4-

methoxybenzoyl- α -D-galactopyranosyl)- β -D-galactopyranoside **80** (100 mg, 0.09 mmol) was stirred in MeOH (6 mL) for 1 h before adding palladium (II) chloride (12.8 mg, 0.072 mmol) to the reaction mixture, which was stirred at r.t. under N₂(g) atmosphere for 22 h. The resulting mixture was filtered through Celite[®] pad. The filtrate was concentrated, purified by Biotage[®] flash column chromatography (Redisef[®]Rf 12 g silica column, Hexane:EtOAc (0% EtOAc (1 col. vol.) → 0-30% EtOAc (over 11 col. vol.) → 30% EtOAc (over 6 col. vol.) → 30-40% (over 2 col. vol.) → 40% EtOAc (over 16 col. vol.)) to afford compound **81** as a colourless oil (90 mg, 95%); *R*_f 0.45 (1:1 hexane–EtOAc); $[\alpha]_{\text{D}}^{22}$ 39.1 (c, 1.0, CHCl₃); δ_{H} (500 MHz, CDCl₃); 7.99-7.94 (m, 4H, ArH), 7.34-7.17 (m, 25H, ArH), 7.10-7.05 (m, 2H, ArH), 6.93-6.90 (m, 2H, ArH), 5.80 (dd, 1H, $J_{3b,4b}$ 3.1 Hz, $J_{4b,5b}$ 1.2 Hz, H-4b), 5.08 (d, 1H, $J_{1b,2b}$ 3.7 Hz, H-1b), 5.03 (d, 1H, $J_{1a,2a}$ 7.0 Hz, H-1a), 4.90-4.78 (m, 4H, 2 × OCH₂Ph), 4.62-4.31 (m, 5H, 2 × OCH₂Ph, H-5b), 4.31-4.24 (m, 2H, OCH₂Ph), 4.16-4.09 (m, 1H, H-3b), 4.02 (d, 1H, $J_{3a,4a}$ 2.0 Hz, H-4a), 3.95 (dd, 1H, $J_{2b,3b}$ 10.1 Hz, $J_{1b,2b}$ 3.7 Hz, H-2b), 3.90-3.82 (m, 8H, 2 × OCH₃, H-5a, H-6a), 3.79-3.70 (m, 3H, H-2a, H-3a, H-6'a), 3.68-3.64 (m, 1H, H-3a), 3.57 (m, 1H, H-6b), 3.51 (m, 1H, H-6'b); δ_{C} (75 MHz, CDCl₃); 166.8, 165.6 (C=O), 163.7, 161.0 (C-O), 138.5, 138.3, 138.2, 137.4, 132.1, 131.6, 128.4, 128.4, 127.9, 124.4, 122.2, 116.3, 113.8 (ArC), 101.2 (C-1a, C-1b), 80.9 (C-4a), 80.1, 74.1 (C2a, C-3a), 76.6 (C-3b), 75.5 (C-2b), 75.4 (OCH₂Ph), 74.8 (C-5a), 74.2 (OCH₂Ph), 73.7 (OCH₂Ph), 73.3 (OCH₂Ph), 71.7 (OCH₂Ph), 70.0 (C-5b), 69.5 (C-6a), 69.3 (C-6b), 68.3 (C-4b), 55.6 (OCH₃), 52.0 (OCH₃); IR (ν_{max} /cm⁻¹): 3471 (OH), 2917, 1714 (C=O), 1097, 1048, (C-OR); HRMS: Found [M+Na]⁺ 1083.4147, C₆₃H₆₄NaO₁₅ requires 1083.4137.

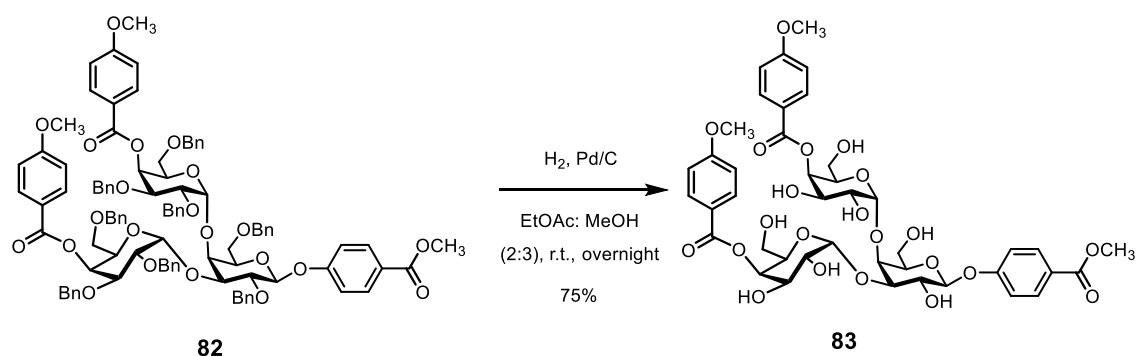
4-Methoxycarbonylphenyl 2,6-di-O-benzyl-3,4-bis-O-(2,3,6-tri-O-benzyl-4-O-(4-methoxybenzoyl)- α -D-galactopyranosyl)- β -D-galactopyranoside (82)



Thioglycosyl donor **55** (84 mg, 0.12 mmol), 1-benzenesulfinyl piperidine (30 mg, 0.14 mmol), and 2,4,6-tri-*tert*-butylpyrimidine (64 mg, 0.25 mmol) were co-evaporated with toluene several times before adding molecular sieves 4 Å and anhydrous DCM (6 mL). The reaction mixture was stirred at r.t. under $\text{N}_2(\text{g})$ atmosphere for 1.5 h. Glycosyl acceptor **81** (88 mg, 0.08 mmol) was also co-evaporated with toluene several times and dissolved in anhydrous DCM (2.8 mL) in a separate flask. After stirring for 1.5 h, the mixture of thioglycosyl donor, BSP, TTBP and molecular sieves 4 Å was cooled to $-60\text{ }^\circ\text{C}$ before freshly distilled triflic anhydride (Tf_2O) (23 μL , 0.14 mmol) was added. The reaction mixture was stirred for 10 min at $-60\text{ }^\circ\text{C}$ before a solution of acceptor was added. The resulting mixture was stirred at low temperature ($-60\text{ }^\circ\text{C}$ to $-49\text{ }^\circ\text{C}$) for 1 h, quenched with triethyl phosphite (20 μL), triethylamine (450 μL), and washed with sat. aq. NaHCO_3 (2 \times 10 mL), followed by brine (2 \times 10 mL). The combined organic phase was dried over MgSO_4 , and concentrated to leave crude yellow oil. The residue was purified by Biotage® flash column chromatography (Redisef®Rf 12 g silica column, Hexane:EtOAc (0% EtOAc (1 col. vol.) \rightarrow 0-25% EtOAc (over 12 col. vol.) \rightarrow 25% EtOAc (over 3 col. vol.) \rightarrow 25-35% EtOAc (over 10 col. vol.)) to give compound **82** as a pale yellow oil (100 mg, 80%); R_f 0.2 (2:1 hexane–EtOAc); $[\alpha]_D^{24}$ 56.34 (c, 1.0, CHCl_3); δ_{H} (500 MHz, CDCl_3 , 327 K); 8.03-8.00 (m, 2H, ArH), 8.00-7.96 (m, 4H, ArH), 7.35-7.11 (m, 40H, ArH), 7.08-7.04 (m, 2H, ArH), 6.96-6.92 (m, 2H, ArH), 6.87-6.83 (m, 2H, ArH),

5.83 (d, 1H, $J_{3b,4b}$ 2.39 Hz H-4b), 5.75 (d, 1H, $J_{3c,4c}$ 2.26 Hz, H-4c), 5.57 (d, 1H, $J_{1b,2b}$ 2.27 Hz, H-1b), 5.27 (d, 1H, $J_{1c,2c}$ 3.30 Hz, H-1c), 5.00 (d, 1H, $J_{1a,2a}$ 6.67 Hz, H-1a), 4.91-4.77 (m, 5H, OCH_2Ph), 4.66 (d, 2 H, J 11.6 Hz, OCH_2Ph), 4.62 (td, 1H, $J_{5c,6c=5c,6'c}$ 6.2 Hz, $J_{4c,5c}$ 1.4 Hz, H-5c), 4.60-4.51 (m, 3H, H-5b, OCH_2Ph), 4.51-4.40 (m, 3H, OCH_2Ph), 4.33-4.22 (m, 6H, H-3c, H-4a, OCH_2Ph), 4.11-4.06 (m, 2H, H-3c, H-2a), 4.00 (dd, 1H, $J_{2c,3c}$ 10.0 Hz, $J_{1c,2c}$ 3.3 Hz, H-2c), 3.92 (s, 3H, OCH_3), 3.89 (s, 3H, OCH_3), 3.86-3.80 (m, 5H, H-3a, H-2b, OCH_3), 3.78-3.65 (m, 4H, H-5a, H-6a, H-6'a, H-6b), 3.59-3.64 (m, 1H, H-6'b), 3.48-3.43 (m, 1H, H-6c), 3.42-3.37 (m, 1H, H-6'c); δ_c (75 MHz, CDCl_3 , 331 K); 166.8, 165.7, 165.7 (C=O), 163.7, 163.7, 161.3 (C-O), 139.0, 138.8, 138.7, 138.6, 138.3, 138.2, 132.0, 132.0, 131.7, 128.6, 128.5, 128.5, 128.4, 128.4, 128.4, 128.4, 128.3, 128.3, 128.1, 128.1, 128.0, 128.0, 127.9, 127.8, 127.8, 127.7, 127.7, 127.6, 127.6, 127.6, 127.5, 127.5, 124.9, 123.1, 123.1, 116.5, 113.9 (ArC), 101.7 (C-1a), 99.2 (C-1c), 98.9 (C-1b), 78.7 (C-2a), 77.4 (C-2b), 77.2 (C-3a), 77.1 (C-4a), 77.0 (C-3c), 76.8 (C-2c), 76.7 (C-3b), 75.7 (C-5a), 75.2, 74.3, 73.9, 73.8, 73.5, 73.5, 72.0, 71.7 (OCH_2Ph), 71.0 (C-6a), 69.7 (C-5b), 69.5 (C-6b), 69.2 (C-6c), 69.2 (C-5c), 69.0 (C-4c), 68.8 (C-4b), 55.6, 51.9 (3 \times OCH_3); **IR** ($\nu_{\text{max}}/\text{cm}^{-1}$): 2926 (C-H), 1716 (C=O), 1263 (C-O), 1098 (C-OR); **HRMS**: Found $[\text{M}+\text{Na}]^+$ 1649.6443, $\text{C}_{98}\text{H}_{98}\text{NaO}_{22}$ requires 1649.6442.

4-Methoxycarbonylphenyl

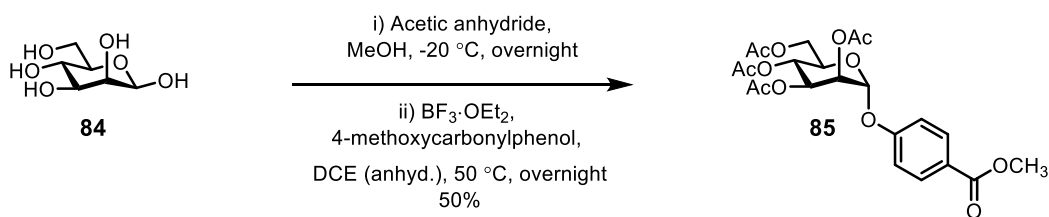
3,4-bis-O-(4-O-(4-methoxybenzoyl)- α -D-galactopyranosyl)- β -D-galactopyranoside (**83**)

4-Methoxycarbonylphenyl

2,6-di-O-benzyl-3,4-bis-O-(2,3,6-tri-O-benzyl-4-O-4-

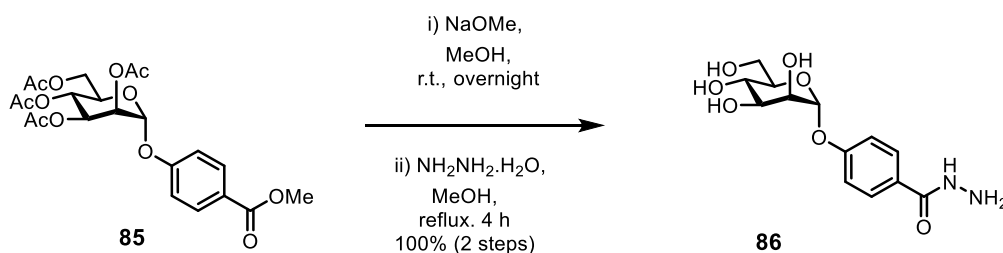
methoxybenzoyl- α -D-galactopyranosyl)- β -D-galactopyranoside **82** (87 mg, 0.05 mmol) was dissolved in a mixture of MeOH (9 mL) and EtOH (6 mL) and stirred at r.t. under $N_2(g)$ atmosphere for 15 min. Palladium on carbon (Pd/C, 10% wt., 104 mg, 0.98 mmol) was added to the solution. The reaction mixture was allowed to stir at r.t. under a positive pressure of hydrogen overnight. The reaction mixture was filtered through a Celite[®] pad and evaporated to dryness to give trisaccharide **83** as a white powder (36 mg, 75%); R_f 0.57 (9:1 EtOAc–MeOH); $[\alpha]_D^{25}$ 97.88 (c, 1.0, MeOH); δ_H (500 MHz, MeOD); 8.03–7.97 (m, 6H, ArH), 7.19–7.15 (m, 2H, ArH), 7.01–6.97 (m, 4H, ArH), 5.59 (dd, 1H, $J_{3b,4b}$ 3.4 Hz, $J_{4b,5b}$ 1.3 Hz, H-4b), 5.54 (d, 1H, $J_{3c,4c}$ 3.37 Hz, H-4c), 5.35 (d, 1H, $J_{1c,2c}$ 3.8 Hz, H-1c), 5.28 (d, 1H, $J_{1b,2b}$ 3.6 Hz, H-1b), 5.17 (d, 1H, $J_{1a,2a}$ 7.4 Hz, H-1a), 4.66–4.62 (m, 1H, H-5c), 4.44–4.41 (m, 2H, H-4a, H-5b), 4.22–4.16 (m, 2H, H-3b, H-3c), 4.07–3.83 (m, 16H, H-2a, H-2b, H-2c, H-3a, H-5a, H-6a, H-6'a, 3 \times OCH₃), 3.65 (d, 2H, $J_{5b,6b=6b,6'b}$ 6.3 Hz, H-6b, H-6'b), 3.55 (d, 2H, $J_{5c,6c=6c,6'c}$ 6.4 Hz, H-6c, H-6'c); δ_C (75 MHz, MeOD); 168.2, 167.7, 167.7 (C=O), 165.3, 162.7 (C-O), 132.9, 132.5, 125.2, 123.4, 117.2, 114.8 (ArC), 103.1 (C-1b), 102.0 (C-1a), 97.8 (C-1c), 78.7 (C-2c), 77.1 (C-4a), 76.0 (C-5a), 73.1 (C-4c), 73.0 (C-4b), 72.9 (C-5b), 71.6 (C-3a), 71.4 (C-5c), 71.2 (C-2b), 70.8 (C-2a), 70.1 (C-3b), 69.6 (C-3c), 62.2 (C-6b, C-6c), 61.4 (C-6a), 56.0 (2 \times OCH₃), 52.5 (OCH₃); IR (ν_{max}/cm^{-1}): 3359 (OH), 2921 (C-H), 1698 (C=O), 1021 (C-OR); HRMS: Found $[M+NH_4]^+$ 924.3143, C₄₂H₅₄NaO₂₂ requires 924.3132.

4-Methoxycarbonylphenyl 2,3,4,6-tetra-O-acetyl- α -D-mannopyranoside (**85**)¹²⁵



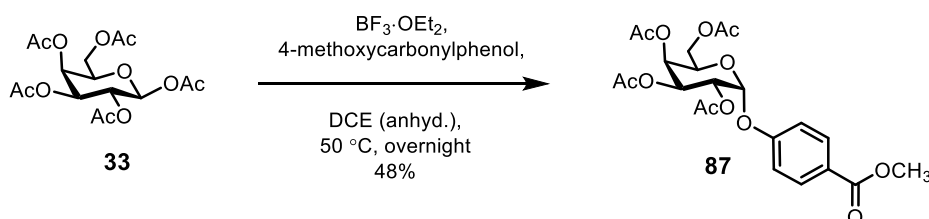
Acetic anhydride (21 mL, 222 mmol) was added to a solution of β -D-mannopyranose **84** (4 g, 22.2 mmol) in pyridine at 0 °C. The reaction mixture was sealed and stored at -20 °C overnight. The reaction mixture was slowly poured into ice water (100 mL) and extracted with ethyl acetate (3 \times 150 mL). The organic layer was washed with sat. aq. NaHCO₃ (3 \times 150 mL), distilled water (2 \times 100 mL), and brine (1 \times 150 mL). The organic phase was dried (MgSO₄) and concentrated to leave a crude oil, which was dissolved in anhydrous dichloroethane (50 mL). 4-methoxycarbonylphenol (6.7 g, 44 mmol) and freshly distilled boron trifluoride diethyl etherate (8.2 mL, 66 mmol) were added to the reaction mixture, which was heated to 50 °C and stirred overnight. The reaction was quenched by addition of sat. aq. NaHCO₃ (50 mL). The organic layer was then washed with sat. aq. NaCl (50 mL), dried (MgSO₄), concentrated, and purified by flash column chromatography (silica; 2:1hexane–EtOAc). Semi crude product was recrystallised from MeOH to give compound **85** (5.9 g, 50%) as colourless solid; *R*_f 0.34 (1:1 Hexane–EtOAc); m.p. 147-149 °C (from MeOH); $[\alpha]_{\text{D}}^{22}$ 89.6 (c, 1.5, CHCl₃) (lit.¹²⁵ $[\alpha]_{\text{D}}^{25}$ 88.8 (c, 0.65, CHCl₃)); δ_{H} (500 MHz, CDCl₃); 8.01 (d, 2H, *J* 8.7 Hz, ArH), 7.14 (d, 2H, *J* 8.7 Hz, ArH), 5.62 (d, 1H, *J*_{1,2} 1.8 Hz, H-1), 5.55 (dd, 1H, *J*_{3,4} 10.1 Hz, *J*_{3,2} 3.5 Hz, H-3), 5.46 (dd, 1H, *J*_{2,3} 3.5 Hz, *J*_{2,1} 1.8 Hz, H-2), 5.37 (t, 1H, *J*_{4,3=4,5} 10.1 Hz, H-4), 4.28 (dd, 1H, *J*_{6,6'} 12.3 Hz, *J*_{5,6} 5.7 Hz, H-6), 4.10-4.03 (m, 2H, H-5, H-6'), 3.89 (s, 3H, OCH₃), 2.21 (s, 3H, C(O)CH₃), 2.06 (s, 3H, C(O)CH₃), 2.05 (s, 3H, C(O)CH₃), 2.02 (s, 3H, C(O)CH₃); δ_{C} (75 MHz, CDCl₃); 170.3, 169.8, 169.6, 166.3 (C=O), 158.0, 131.5, 124.9, 116.0 (ArC), 95.4 (C-1), 69.4 (C-5), 69.1 (C-2), 68.7 (C-3), 65.7 (C-4), 62.0 (C-6), 52.0 (OCH₃), 20.8, 20.6, 20.6, 20.6 (4 \times COCH₃); **IR** (ν_{max} /cm⁻¹): 1753 (C=O); **HRMS**: Found $[\text{M}+\text{Na}]^+$ 505.1316, C₂₂H₂₆NaO₁₂ requires 505.1316.

4- α -D-Mannopyranosyloxy benzoylhydrazide (**86**)¹²⁵



Sodium methoxide (470 mg, 8 mmol) was added to a solution of 4-methoxycarbonylphenyl 2,3,4,6-tetra-O-acetyl- α -D-mannopyranoside **85** (5.2 g, 10 mmol) in anhydrous MeOH (100 mL). The reaction mixture was stirred overnight at r.t., neutralised with Amberlite IRC 86 H⁺ resin, filtered and concentrated to give a colourless solid, which was dissolved in MeOH (12 mL). Hydrazine monohydrate (3.2 mL, 63 mmol) was added to the mixture, which was heated at reflux for 4 h. The solution was then concentrated and lyophilized from water to afford compound **86** (1.03 g, 100%, 2 steps) as colourless lyophilisate; *R_f* 0.23 (6:4:1 Chloroform–MeOH–H₂O); m.p. 174–176 °C; $[\alpha]_{\text{D}}^{23}$ 109.2 (c, 1.0, H₂O) (lit.¹²⁵ $[\alpha]_{\text{D}}^{25}$ 94.2 (c, 0.52, H₂O); δ_{H} (500 MHz, D₂O); 7.72 (d, 2H, *J* 8.8 Hz, ArH), 7.21 (d, 2H, *J* 8.8 Hz, ArH), 5.69 (d, 1H, *J*_{1,2} 1.8 Hz, H-1), 4.18 (dd, 1H, *J*_{2,3} 3.5 Hz, *J*_{1,2} 1.8 Hz, H-2), 4.06 (dd, 1H, *J*_{3,4} 9.6 Hz, *J*_{2,3} 3.5 Hz, H-3), 3.81–3.71 (m, 3H, H-4, H-6, H-6'), 3.69–3.64 (m, 1H, H-5); δ_{C} (75 MHz, D₂O); 169.4 (C=O), 158.4, 128.9, 126.2, 116.7 (ArC), 97.7 (C-1), 73.5 (C-5), 70.3 (C-3), 69.8 (C-2), 66.5 (C-4), 60.6 (C-6); IR (ν_{max} /cm⁻¹): 3373 (OH, NH), 1605 (C=O); HRMS: Found [M+H]⁺ 315.1183, C₁₃H₁₉N₂O₇ requires 315.1187.

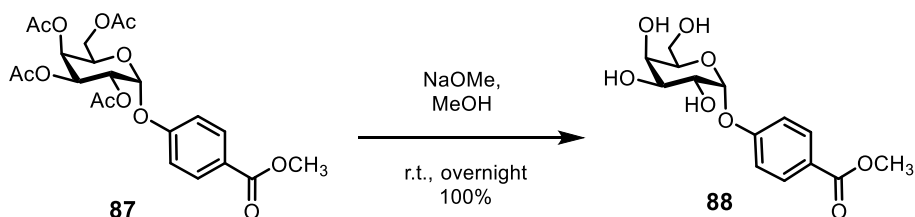
4-Methoxycarbonylphenyl 2,3,4,6-tetra-O-acetyl- α -D-galactopyranoside (**87**)¹²⁵



Freshly distilled boron trifluoride diethyl etherate (4.84 mL, 38.4 mmol) was added dropwise to a solution of β -D-galactose pentaacetate **33** (5 g, 12.8 mmol) and 4-(methoxycarbonyl)phenol (3.89 g, 25.6 mmol) in anhydrous dichloroethane (30 mL). The resulting solution was warmed to 50 °C, and stirred for a further 22 h at 50 °C

before quenching by addition of aq. NaHCO_3 (3 × 30 mL). The organic layer was then separated and washed with aq. NaCl (2 × 50 mL), dried (MgSO_4), concentrated Biotage[®] flash column chromatography (Redisef[®]Rf 80 g silica column, Hexane:EtOAc (0% EtOAc (1 col. vol.) → 0-50% EtOAc (over 10 col. vol.) → 50% EtOAc (over 10 col. vol.) to give a mixture of two anomers. The mixture was then recrystallised from MeOH to afford compound **87** as colourless plates as only the α -anomer (2.97 g, 48%); R_f 0.38 (1:1 Hexane–EtOAc); m.p. 114-119°C (from MeOH) (Lit.¹²⁵ 112-117 °C from MeOH); $[\alpha]_D^{23}$ 208.27 (c, 0.22, CH_2Cl_2) (Lit.¹²⁵ $[\alpha]_D^{25}$ 212.7 (c, 0.22, CH_2Cl_2); δ_H (500 MHz, CDCl_3); 8.01-7.95 (m, 2H, ArH), 7.08 (m, 1H, ArH), 5.83 (d, 1H, $J_{1,2}$ 3.4 Hz, H-1), 5.54 (dd, 1H, $J_{2,3}$ 10.8 Hz, $J_{3,4}$ 3.1 Hz, H-3), 5.50 (dd, 1H, $J_{3,4}$ 3.1 Hz, $J_{4,5}$ 1.4 Hz, H-4), 5.28 (dd, 1H, $J_{2,3}$ 10.8 Hz, $J_{1,2}$ 3.4 Hz, H-2), 4.27 (t, 1H, $J_{5,6=5,6'}$ 6.2 Hz, H-5), 4.15-4.09 (m, 1H, H-6), 4.09-4.03 (m, 1H, H-6'), 3.86 (s, 1H, OCH_3), 2.14 (s, 1H, C(O)CH_3), 2.04 (s, 1H, C(O)CH_3), 2.00 (s, 1H, C(O)CH_3), 1.89 (s, 1H, C(O)CH_3); δ_C (75 MHz, CDCl_3); 170.4, 170.3, 170.2, 170.0, 166.5 (C=O), 159.8, 131.7, 124.9, 116.3 (ArC), 94.6 (C-1), 67.8 (C-4), 67.7 (C-2), 67.6 (C-5), 67.5 (C-3), 61.5 (C-6), 52.1 (OCH_3), 20.8 (C(O)CH_3), 20.7 (C(O)CH_3), 20.7 (C(O)CH_3), 20.6 (C(O)CH_3); IR ($\nu_{\text{max}}/\text{cm}^{-1}$): 1746 (C=O); HRMS: Found $[\text{M}+\text{Na}]^+$ 505.1327, $\text{C}_{22}\text{H}_{26}\text{O}_{12}\text{Na}$ requires 505.1316.

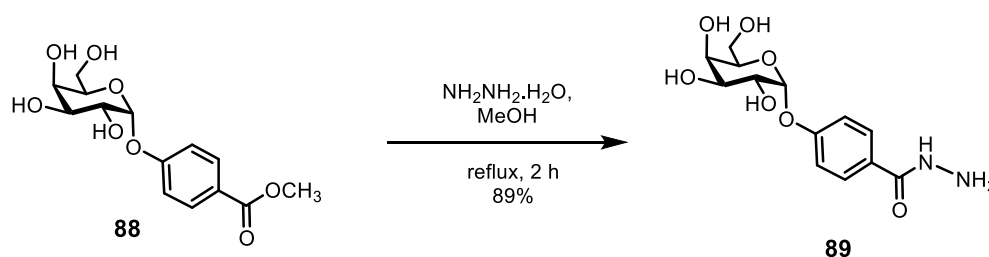
4-Methoxycarbonylphenyl α -D-galactopyranoside (**88**)¹²⁵



Sodium methoxide (152 mg, 2.8 mmol) was added to a solution of 4-methoxycarbonylphenyl 2,3,4,6-tetra-*O*-acetyl- α -D-galactopyranoside **87** (1.7 g, 3.5 mmol) in anhydrous MeOH (30 mL). The reaction mixture was stirred for 18 h at r.t., neutralised with Amberlite[®] IRC 86 H^+ resin, filtered and concentrated to afford compound **88** (1.17 g, 100%) as a colourless glassy solid; R_f 0.14 (6:4:1 Chloroform–MeOH– H_2O); $[\alpha]_D^{23}$ 222.47 (c, 0.17, H_2O) (Lit.¹²⁵ $[\alpha]_D^{25}$ 231.8 (c, 0.17, H_2O); δ_H (500 MHz, $\text{DMSO}-d_6$ with D_2O exchange); 7.92-7.88 (m, 2H, ArH), 7.20-7.14 (m, 2H, ArH), 5.54 (d, 1H, $J_{1,2}$ 3.4 Hz, H-1), 3.81 (s, 3H, OCH_3), 3.80-3.77 (m, 2H, H-2, H-4), 3.75 (dd, 1H, $J_{2,3}$ 10.2 Hz, $J_{3,4}$ 3.0 Hz, H-3), 3.65-3.62 (m, 1H, H-5), 3.51 (dd, 1H, $J_{6,6'}$ 10.9 Hz, $J_{5,6=5,6'}$ 6.3 Hz, H-6), 3.35 (dd, 1H, $J_{6,6'}$ 10.9 Hz, $J_{5,6=5,6'}$ 6.3 Hz, H-6'); δ_C (75

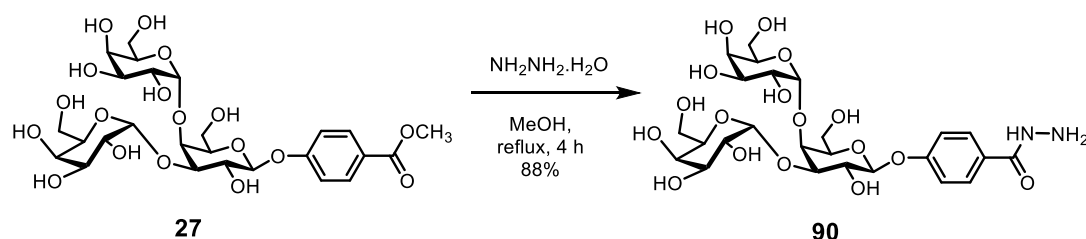
MHz, DMSO-*d*₆ with D₂O exchange); 166.0 (C=O), 161.2, 131.1, 122.8, 116.6 (ArC), 97.9 (C-1), 72.6 (C-5), 69.3, 68.4, 67.8 (C-2, C-3, C-4), 60.2 (C-6), 52.0 (OCH₃); **IR** ($\nu_{\max}/\text{cm}^{-1}$): 3293 (OH), 1613 (C=O); **HRMS**: Found [M+Na]⁺ 337.0895, C₁₄H₁₈O₈Na requires 337.0894.

4- α -D-galactopyranosyloxy benzoylhydrazide (**89**)¹²⁵



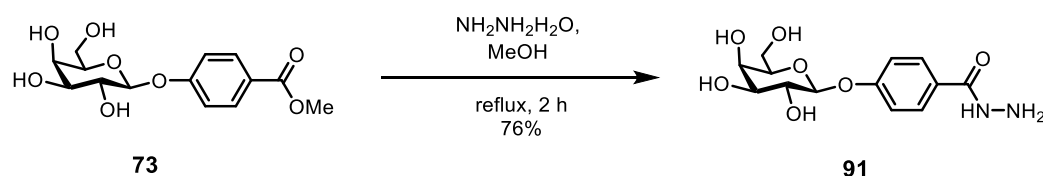
Hydrazine monohydrate (719 μL , 14.8 mmol) was added to a solution of 4-methoxycarbonylphenyl α -D-galactopyranoside **88** (230 mg, 0.79 mmol) in MeOH (3 mL) and heated at reflux for 2 h. The solvent was evaporated and the residue was lyophilized from water to afford compound **89** (220 mg, 89%) as colourless lyophilisate; R_f 0.24 (6:4:1 Chloroform–MeOH–H₂O); $[\alpha]_D^{23}$ 171.9 (c, 0.2, H₂O) (Lit.¹²⁵ $[\alpha]_D^{25}$ 141.0 (c, 0.2, H₂O)); δ_H (500 MHz, DMSO-*d*₆ with D₂O exchange); 8.43 (s, 1H, NH), 7.78-7.73 (m, 2H, ArH), 7.13-7.07 (m, 2H, ArH), 5.48 (d, 1H, $J_{1,2}$ 3.2 Hz, H-1), 3.81-3.73 (m, 3H, C-2, C-3, C-4), 3.65 (t, 1H, $J_{5,6=5,6'}$ 6.4 Hz, H-5), 3.50 (dd, 1H, $J_{6,6'}$ 11.0 Hz, $J_{5,6=5,6'}$ 6.3 Hz, H-6), 3.35 (dd, 1H, $J_{6,6'}$ 11.0 Hz, $J_{5,6=5,6'}$ 6.3 Hz, H-6); δ_C (75 MHz, DMSO-*d*₆ with D₂O exchange); 166.7 (NH), 166.0 (C=O), 128.8, 126.6, 116.5, 109.8 (ArC), 98.1 (C-1), 72.6 (C-5), 69.45, 68.6, 68.0 (C-2, C-3, C-4), 60.4 (C-6); **IR** ($\nu_{\max}/\text{cm}^{-1}$): 3278 (OH, NH), 1618 (C=O); **HRMS**: Found [M+H]⁺ 315.1189, C₁₃H₁₉N₂O₇ requires 315.1187.

4-(3,4-bis-O-(α -D-galactopyranosyl)- β -D-galactopyranosyloxy benzoylhydrazide (90)



Hydrazine monohydrate (15.7 μ L, 0.3 mmol) was added to a suspension of 4-methoxycarbonylphenyl bis-O-(α -D-galactopyranosyl)- β -D-galactopyranoside **27** in MeOH (2 mL). The resulting mixture was heated at reflux for 4 h. The solution was then concentrated and lyophilized from water to afford compound **90** (9 mg, 88%) as colourless lyophilisate; R_f 0.80 (6:4:1 Chloroform–MeOH–H₂O); $[\alpha]_D^{24}$ 24.72 (c, 0.2, H₂O); δ_H (500 MHz, D₂O); 7.75 (d, 2H, J 8.7 Hz, ArH), 7.24 (d, 2H, J 8.7 Hz, ArH), 5.32 (d, 1H, $J_{1a,2a}$ 7.5 Hz, H-1a), 5.29 (d, 1H, $J_{1c,2c}$ 4.0 Hz, H-1c), 5.13 (d, 1H, $J_{1b,2b}$ 3.7 Hz, H-1b), 4.42 (d, 1H, J 2.3 Hz, H-4a), 4.29 (t, 1H, J 6.4 Hz, H-5), 4.19 (t, 1H, J 6.4 Hz, H-5), 4.07–3.68 (m, 15H, H-2a, H-2b, H-2c, H-3a, H-3b, H-3c, H-4b, H-4c, H-5a, H-6a, H-6'a, H-6b, H-6'b, H-6c, H-6'c); δ_C (75 MHz, D₂O); 169.4 (C=O), 159.2 (C-O), 129.0 (ArC), 126.7 (C-O), 116.5 (ArC), 100.9 (C-1a), 100.0 (C-1c), 95.5 (C-1b), 76.5, 75.5, 75.1, 71.7, 70.8, 69.6, 69.1, 68.9, 68.8, 68.6, 61.0, 60.9, 60.7 (3 \times C-2, 3 \times C-3, 3 \times C-4, 3 \times C-5, 3 \times C-6); IR (ν_{max}/cm^{-1}): 3375 (OH, NH), 1606 (C=O); HRMS: Found $[M+H]^+$ 639.2246, C₂₅H₃₉N₂O₁₇ requires 639.2243.

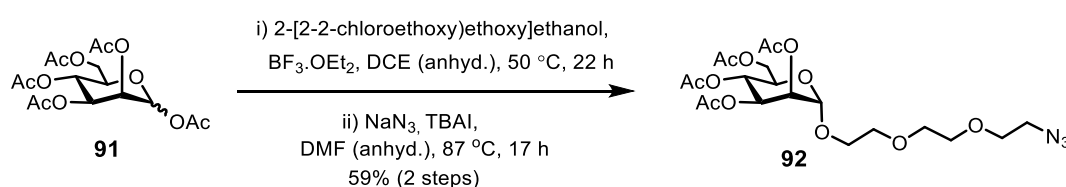
4- β -D-Galactopyranosyloxy benzoylhydrazide (91)



Hydrazine monohydrate (937 μ L, 19.1 mmol) was added to a suspension of 4-methoxycarbonylphenyl β -D-galactopyranoside **73** (300 mg, 0.95 mmol) in MeOH (4 mL) and heated at reflux for 2 h, over the course of which a colourless solid precipitated. The solid was filtered and lyophilized from water to afford compound **91** (226 mg, 76%) as colourless lyophilisate; R_f 0.19 (6:4:1 Chloroform–MeOH–H₂O);

$[\alpha]_D^{24}$ 23.3 (c, 1.0, DMSO); δ_H (500 MHz, DMSO-*d*6); 9.62 (s, 1H, NH), 7.78 (d, 2H, *J* 8.4 Hz, ArH), 7.05 (d, 2H, *J* 8.4 Hz, ArH), 4.90 (d, 1H, *J*_{1,2} 7.7 Hz, H-1), 3.70 (d, 1H, *J*_{3,4} 3.8 Hz, H-4), 3.63-3.38 (m, 5H, H-2, H-3, H-5, H-6, H-6'); δ_C (75 MHz, DMSO-*d*6); 165.5 (C=O), 159.6, 128.5, 126.6, 115.6 (ArC), 100.6 (C-1), 75.6, 73.3, 70.2 (C-2, C-3, C-5), 68.1 (C-4), 60.6 (C-6); IR ($\nu_{\max}/\text{cm}^{-1}$): 3435 (OH, NH), 1662 (C=O); HRMS: Found $[\text{M}+\text{Na}]^+$ 337.1014, C₁₃H₁₈N₂NaO₇ requires 337.1006.

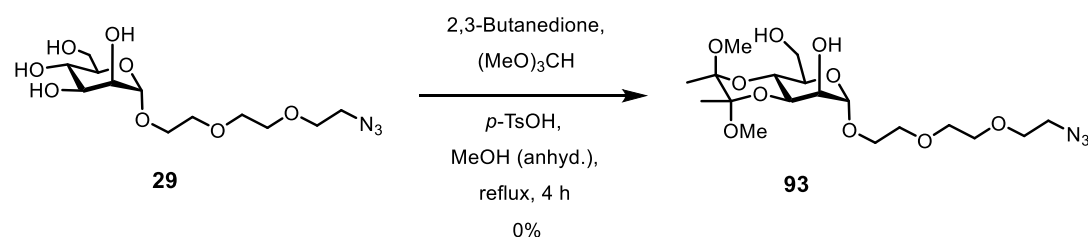
1-Azido-3,6-dioxaoct-8-yl 2,3,4,6-tetra-O-acetyl- α -D-mannopyranoside (**92**)²⁰¹



Freshly distilled boron trifluoride diethyl etherate (23.70 mL, 192.2 mmol) were added dropwise to a solution of mannose pentaacetate **91** (25.0 g, 64 mmol), and 2-[2-(2-chloroethoxy)ethoxy]ethanol (18.62 mL, 128.1 mmol) in anhydrous dichloroethane (250 mL) at 0 °C. The reaction mixture was heated to 50 °C and stirred for 22 h. The reaction was washed with sat. aq. NaHCO₃ (2 × 250 mL), with brine (2 × 250 mL), dried (MgSO₄), concentrated to leave a brown crude oil, which was partially purified by flash column chromatography (silica; 1:1 hexane–EtOAc). Partially separated product (2 g, 4 mmol) was then dissolved in anhydrous DMF (100 mL). Sodium azide (1.3 mg, 20 mmol) and TBAI (1.48 g, 4 mmol) were added to the reaction mixture, which was stirred at 87 °C for 17 h. The solvent was removed and the residue was purified by flash column chromatography (silica; 1:1 Petroleum ether–EtOAc) to give compound **92** (1.02 mg, 59%, 2 steps) as a colourless oil; *R*_f 0.16 (1:1 petroleum ether–EtOAc); $[\alpha]_D^{22}$ 41.01 (c, 2.2, CHCl₃) (lit.²⁰¹ $[\alpha]_D^{20}$ 61.5 (c, 0.22, CHCl₃)); δ_H (500 MHz, CDCl₃); 5.28 (dd, 1H, *J*_{2,3} 10.0 Hz, *J*_{3,4} 3.5 Hz, H-3), 5.23-5.19 (m, 2H, H-2, H-4), 4.80 (d, 1H, *J*_{1,2} 1.7 Hz, H-1), 4.22 (dd, 1H, *J*_{6,6'} 12.1 Hz, *J*_{5,6} 4.9 Hz, H-6), 4.06-3.97 (m, 2H, H-5, H-6'), 3.79-3.71 (m, 1H, ManOCH₂), 3.66-3.56 (m, 9H, ManOCH₂, 4 × CH₂O), 3.33 (t, 2H, *J* 5.1 Hz, CH₂-N), 2.08 (s, 3H, C(O)CH₃), 2.03 (s, 3H, C(O)CH₃), 1.97 (s, 3H, C(O)CH₃), 1.92 (s, 3H, C(O)CH₃); δ_C (75 MHz, CDCl₃); 170.6, 170.0, 169.8, 169.7 (4 × C=O), 97.7 (C-1), 70.8, 70.6, 70.1, 70.0 (4 × CH₂O), 69.5 (C-2), 69.1 (C-3), 68.4 (C-5), 67.4 (ManOCH₂), 66.1 (C-4), 62.4 (C-6), 50.7 (CH₂-N), 20.9, 20.7, 20.7, 20.6 (4 × C(O)CH₃); IR ($\nu_{\max}/\text{cm}^{-1}$): 1741 (C=O), 2106 (N₃); HRMS: Found $[\text{M}+\text{Na}]^+$ 528.1805, C₂₀H₃₁N₃NaO₁₂ requires 528.1800.

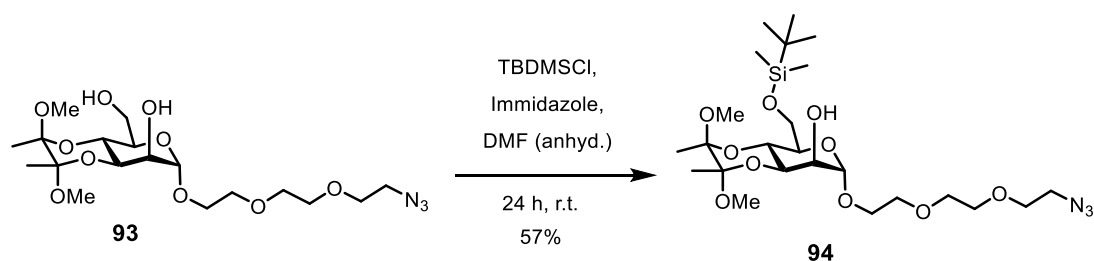
**1-Azido-3,6-dioxaoct-8-yl
mannopyranoside (29)**

3,4-di-O-(2,3-dimethoxybutane-2,3-diyl)- α -D-



Trimethyl orthoformate (525 μL , 4.8 mmol), 2,3-butanedione (120 μL , 1.32 mmol), and *p*-toluenesulfonic acid (136 mg, 0.72 mmol) were added to a solution of 1-azido-3,6-dioxaoct-8-yl α -D-mannopyranoside **29** (400 mg, 1.2 mmol) in anhydrous MeOH (4 mL). The reaction mixture was stirred at reflux for 4 h and then quenched with triethylamine (500 μL). The mixture was concentrated and purified by flash column chromatography (silica; EtOAc) to give compound **93** (272 mg, 50%) as a pale yellow oil; R_f 0.16 (EtOAc); $[\alpha]_D^{25}$ 175.0 (c, 0.5, CHCl_3); δ_{H} (500 MHz, CDCl_3); 4.90 (d, 1H, $J_{1,2}$ 1.4 Hz, H-1), 4.08 (t, 1H, $J_{3,4}$ 10.0 Hz, H-4), 4.02 (dd, 1H, $J_{2,3}$ 3.1 Hz, $J_{3,4}$ 10.0 Hz, H-3), 3.96 (bs, 1H, H-2), 3.85-3.72 (m, 4H, H-5, H-6, OCH_2), 3.71-3.63 (m, 9H, 4 \times OCH_2 , H-6'), 3.40 (t, 2H, J 5.1 Hz, $\text{CH}_2\text{-N}$), 3.28 (s, 3H, OCH_3), 3.25 (s, 3H, OCH_3), 2.83 (s, 1H, OH), 2.34 (s, 1H, OH), 1.32 (s, 3H, CH_3), 1.28 (s, 3H, CH_3); δ_{C} (75 MHz, CDCl_3); 100.4, 99.9 (2 \times $(\text{CH}_3)\underline{\text{C}}(\text{OCH}_3)$), 100.3 ($J_{\text{C,H}}$ 171 Hz, α , C-1), 70.8 (2 \times OCH_2), 70.8 (C-5), 70.4 (OCH_2), 70.2 (OCH_2), 69.7 (C-2), 68.2 (C-4), 66.8 (C-6), 63.2 (C-3), 61.5 (OCH_2), 50.8 ($\text{CH}_2\text{-N}$), 48.2 (OCH_3), 48.0 (OCH_3), 17.9 (CH_3), 17.8 (CH_3); **IR** ($\nu_{\text{max}}/\text{cm}^{-1}$): 3445 (OH), 2926 (OCH_3), 2109 (N_3); **HRMS**: Found $[\text{M}+\text{Na}]^+$ 474.2074, $\text{C}_{18}\text{H}_{33}\text{N}_3\text{O}_{10}\text{Na}$ requires 474.2058.

1-Azido-3,6-dioxaoct-8-yl

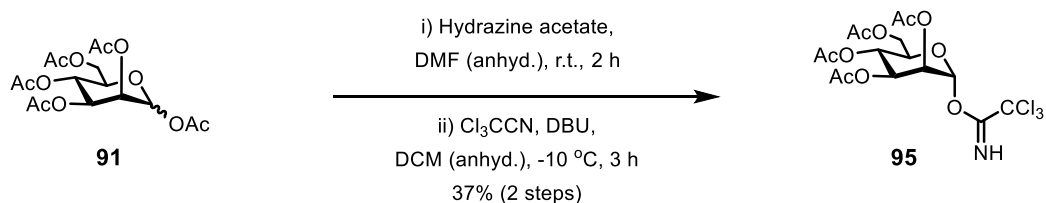
6-*O*-*tert*-butyldimethylsilyl-3,4-di-*O*-(2,3-dimethoxybutane-2,3-diyl)- α -D-mannopyranoside (**94**)

tert-Butyldimethylsilyl chloride (98 mg, 0.78 mmol) and imidazole (106 mg, 1.56 mmol) were added to a solution of 1-azido-3,6-dioxaoct-8-yl 3,4-di-*O*-(2,3-dimethoxybutane-2,3-diyl)- α -D-mannopyranoside **93** (253 mg, 0.52 mmol) in anhydrous DMF (2 mL) in an ice bath. The reaction mixture was stirred at r.t. for 24 h, diluted with EtOAc (12 mL) and quenched with distilled water (2 mL). The organic layer was washed with distilled water (2 \times 10 mL) and brine (10 mL), dried (MgSO₄), concentrated and purified by flash column chromatography (silica; 2:1 hexane–EtOAc) to give compound **94** (168 mg, 57%) as colourless oil; *R*_f 0.12 (2:1 hexane–EtOAc); $[\alpha]_{\text{D}}^{25}$ 111.1 (c, 1.0, CHCl₃); δ_{H} (500 MHz, CDCl₃); 4.84 (d, 1H, *J*_{1,2} 1.4 Hz, H-1), 4.01-3.98 (m, 2H, H-3, H-4), 3.92 (bs, 1H, H-2), 3.80 (m, 3H, H-6, OCH₂), 3.73-3.61 (m, 10H, H-5, H-6', 4 \times OCH₂), 3.39 (t, 2H, *J* 5.1 Hz, CH₂-N), 3.26 (s, 3H, OCH₃), 3.23 (s, 3H, OCH₃), 2.31 (s, 1H, OH), 1.31 (s, 3H, CH₃), 1.27 (s, 3H, CH₃), 0.37 (s, 9H, C(CH₃)₃), 0.06 (s, 3H, SiCH₃), 0.04 (s, 3H, SiCH₃); δ_{C} (75 MHz, CDCl₃); 100.4, 100.0, 99.9 (C-1, 2 \times (CH₃)C(OCH₃)), 71.7 (C-5), 70.8, 70.4, 70.2 (4 \times OCH₂), 69.4 (C-2), 68.5 (C-4), 66.4 (C-6), 63.0 (C-3), 61.8 (OCH₂), 50.8 (CH₂-N), 48.2 (OCH₃), 48.0 (OCH₃), 26.0 (C(CH₃)₃), 18.5 (C(CH₃)₃), 17.9 (CH₃), 17.9 (CH₃), -5.0 (SiCH₃), -5.2 (SiCH₃); IR (ν_{max} /cm⁻¹): 3460 (OH), 2928 (OCH₃), 2104 (N₃); HRMS: Found [M+Na]⁺ 588.2915, C₂₄H₄₇N₃O₁₀SiNa requires 588.2923.

A small sample (30 mg) of this purified product was acetylated using pyridine-acetic anhydride catalysed by DMAP and purified by flash column chromatography (silica; 2:1 hexane–EtOAc) to give 6-*O*-acetyl-1-azido-3,6-dioxaoct-8-yl 3,4-di-*O*-(2,3-dimethoxybutane-2,3-diyl)-6-*O*-*tert*-butyldimethylsilyl- α -D-mannopyranoside as a colourless oil; *R*_f 0.25 (2:1 hexane–EtOAc); $[\alpha]_{\text{D}}^{25}$ 284.3 (c, 1.0, CHCl₃); δ_{H} (500 MHz, CDCl₃); 5.03 (dd, 1H, *J*_{1,2} 1.5 Hz, *J*_{2,3} 3.2 Hz, H-2), 4.79 (d, 1H, *J*_{1,2} 1.5 Hz, H-1), 4.16-4.04 (m, 2H, H-3, H-4), 3.85 (m, 1H, OCH₂), 3.77 (m, 2H, H-6, OCH₂), 3.71-3.57 (m, 10H, H-5, H-6', 4 \times OCH₂), 3.39 (t, 2H, *J* 5.0 Hz, CH₂-N), 3.26 (s, 3H, OCH₃), 3.25 (s, 3H, OCH₃), 2.10 (s, 3H, C(O)CH₃), 1.27 (s, 3H, CH₃), 1.26 (s, 3H, CH₃), 0.88 (s, 9H, C(CH₃)₃), 0.06 (s, 3H, SiCH₃), 0.04 (s, 3H, SiCH₃); δ_{C} (75 MHz, CDCl₃); 170.6 (C=O),

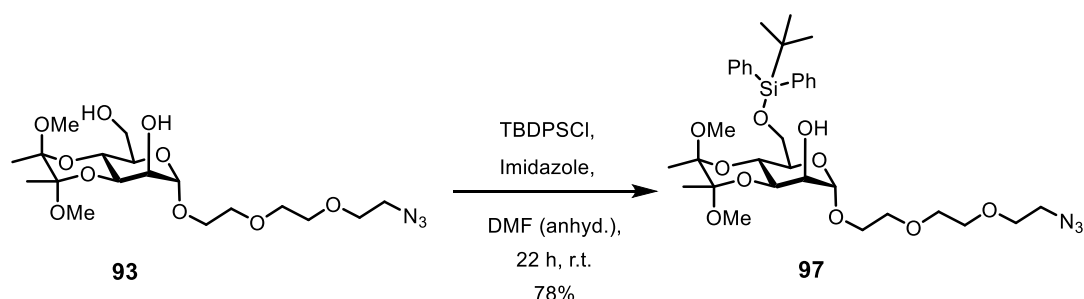
100.3, 99.8, 98.1 (C-1, 2 × (CH₃)C(OCH₃)), 71.7 (C-2), 71.0 (2 × OCH₂), 70.8 (C-5), 70.3 (2 × OCH₂), 66.8 (C-6), 66.2 (C-4), 62.9 (C-3), 61.4 (OCH₂), 50.8 (CH₂-N), 48.2 (OCH₃), 48.0 (OCH₃), 25.0 (C(CH₃)₃), 21.3 (C(O)CH₃), 18.4 (C(CH₃)₃), 18.0 (CH₃), 17.8 (CH₃), -5.0 (SiCH₃), -5.23 (SiCH₃); **IR** ($\nu_{\max}/\text{cm}^{-1}$): 2930 (OCH₃), 2109 (N₃), 1742 (C=O); **HRMS**: Found [M+Na]⁺ 630.3027, C₂₆H₄₉N₃O₁₁SiNa requires 630.3029.

2,3,4,6-Tetra-O-acetyl α -D-mannopyranosyl trichloroacetimidate (**95**)²⁰²



Hydrazine acetate (1.06 g, 11.5 mmol) was added to a solution of α -D-mannose pentaacetate **91** (3.00 g, 7.7 mmol) in DMF (10 mL). The reaction mixture was stirred at r.t. for 2 h, concentrated to leave dark brown oil, which was dissolved in anhydrous DCM (7 mL). Trichloroacetonitrile (3.97 mL, 38.5 mmol) and DBU (1.16 mL, 11.5 mmol) were added dropwise to the reaction mixture at -10 °C, which was stirred for 3 h, concentrated and purified by flash column chromatography (silica; 9:1 DCM–EtOAc) to leave a yellow oil. The partially purified products was then purified by another flash column chromatography (silica; 3:1 hexane–EtOAc), yielded trichloroacetimidate **95** (1.35 g, 37%, 2 steps) as a colourless oil; R_f 0.20 (2:1 hexane–EtOAc); $[\alpha]_D^{25}$ 44.1 (c, 1.0, CHCl₃) (lit.²⁰² $[\alpha]_D^{25}$ 42.7 (c, 1.0, CHCl₃)); δ_H (500 MHz, CDCl₃); 8.78 (s, 1H, NH), 6.26 (d, 1H, $J_{1,2}$ 1.9 Hz, H-1), 5.46-5.44 (m, 1H, H-2), 5.41-5.34 (m, 2H, H-3, H-4), 4.26 (dd, 1H, $J_{5,6}$ 4.8 Hz, $J_{6,6'}$ 12.1 Hz, H-6), 4.20-4.07 (m, 2H, H-5, H-6'), 2.18 (s, 3H, C(O)CH₃), 2.06 (s, 3H, C(O)CH₃), 2.05 (s, 3H, C(O)CH₃), 1.99 (s, 3H, C(O)CH₃); δ_C (75 MHz, CDCl₃); 170.6, 169.9, 169.8, 169.7, 159.8 (4 × C=O, CN), 94.6 ($J_{C,H}$ 180 Hz, α , C-1), 90.6 (CCl₃), 71.3 (C-5), 68.0 (C-2), 68.9, 65.5 (C-3, C-4), 62.1 (C-6), 20.9, 20.8, 20.7 (4 × C(O)CH₃); **IR** ($\nu_{\max}/\text{cm}^{-1}$): 3020 (NH), 1752 (C=O), 1677 (C=N); **HRMS**: Found [2M+Na]⁺ 1005.0175, C₃₂H₄₀Cl₃N₂O₂₀Na requires 1005.0198.

1-Azido-3,6-dioxaoct-8-yl

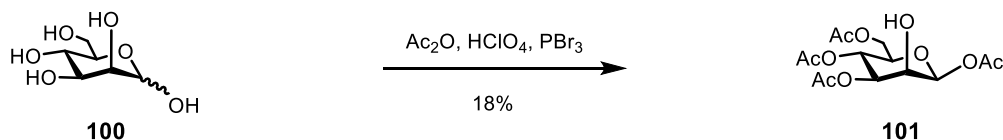
6-O-*tert*-butyldiphenylsilyl-3,4-di-O-(2,3-dimethoxybutane-2,3-diyl)- α -D-mannopyranoside (**97**)

tert-Butyldiphenylsilyl chloride (141 μ L, 0.5 mmol) and imidazole (76 mg, 1.2 mmol) were added to a solution of 1-azido-3,6-dioxaoct-8-yl 3,4-di-O-(2,3-dimethoxybutane-2,3-diyl)- α -D-mannopyranoside **93** (200 mg, 0.4 mmol) in anhydrous DMF (1 mL). The reaction mixture was stirred at r.t. for 22 h and quenched with distilled water (1 mL). The product was extracted with EtOAc (3 \times 10 mL). The organic extracts were combined, dried (MgSO₄), concentrated and purified by flash column chromatography (silica; 2:1 hexane–EtOAc) to give compound **97** (236 mg, 78%) as a colourless oil; R_f 0.35 (1:1 hexane–EtOAc); $[\alpha]_D^{24}$ 116.4 (c, 1.0, CHCl₃); δ_H (500 MHz, CDCl₃); 7.73-7.69 (m, 4H, ArH), 7.45-7.33 (m, 6H, ArH), 4.89 (d, 1H, $J_{1,2}$ 1.3 Hz, H-1), 4.07-4.00 (m, 2H, H-3, H-4), 3.96 (bs, 1H, H-2), 3.89 (d, 2H, J 3.6 Hz, OCH₂), 3.87-3.77 (m, 2H, H-5, H-6), 3.68-3.61 (m, 9H, H-6', 4 \times OCH₂), 3.37 (t, 2H, J 5.1 Hz, CH₂-N), 3.28 (s, 3H, OCH₃), 3.15 (s, 3H, OCH₃), 2.38 (s, 1H, OH), 1.31 (s, 3H, CH₃), 1.26 (s, 3H, CH₃), 1.04 (s, 9H, C(CH₃)₃); δ_C (75 MHz, CDCl₃); 136.0, 135.7, 134.1, 133.6, 129.6, 127.7, 127.6, 100.4, 99.9, 99.9 (C-1, 2 \times (CH₃)C(OCH₃)), 71.8 (C-5), 70.8, 70.3, 70.2 (OCH₂), 69.8 (C-2), 68.6, 63.1 (C-3, C-4), 66.4 (C-6), 62.6 (OCH₂), 50.8 (CH₂-N), 48.3 (OCH₃), 48.1 (OCH₃), 26.9 (C(CH₃)₃), 19.5 (C(CH₃)₃), 17.9 (CH₃), 17.9 (CH₃); IR (ν_{\max} /cm⁻¹): 3053 (OH), 2930 (OCH₃), 2107 (N₃); HRMS: Found [M+Na]⁺ 712.3247, C₃₄H₅₁N₃O₁₀SiNa requires 712.3236.

A small sample (30 mg) of this purified product was acetylated using pyridine-acetic anhydride catalysed by DMAP and purified by flash column chromatography (silica; 2:1 hexane–EtOAc) to give 6-O-acetyl-1-azido-3,6-dioxaoct-8-yl 3,4-di-O-(2,3-dimethoxybutane-2,3-diyl)-6-O-*tert*-butyldiphenylsilyl- α -D-mannopyranoside as colourless oil; R_f 0.21 (2:1 hexane–EtOAc); $[\alpha]_D^{24}$ 86.4 (c, 1.0, CHCl₃); δ_H (500 MHz, CDCl₃); 7.68-7.74 (m, 4H, ArH), 7.45-7.30 (m, 6H, ArH), 5.07 (dd, 1H, $J_{1,2}$ 1.6 Hz, $J_{2,3}$ 3.1 Hz, H-2), 4.84 (bs, 1H, H-1), 4.24-4.13 (m, 2H, H-3, H-4), 3.96 (dd, 1H, J 11.3, 4.0 Hz, OCH₂), 3.85 (dd, 1H, J 11.3, 2.0 Hz, OCH₂), 3.79-3.71 (m, 2H, H-5, H-6), 3.69-3.59

(m, 9H, H-6', 4 × OCH₂), 3.38 (t, 2H, *J* 5.1 Hz, CH₂-N), 3.26 (s, 3H, OCH₃), 3.22 (s, 3H, OCH₃), 2.13 (s, 3H, C(O)CH₃), 1.27 (s, 3H, CH₃), 1.28 (s, 3H, CH₃), 1.06 (s, 9H, C(CH₃)₃); δ_c (75 MHz, CDCl₃); 170.8 (C=O), 100.3, 99.8 (2 × (CH₃)C(OCH₃)), 98.0 (C-1), 71.7 (C-5), 70.9 (OCH₂), 70.9 (C-2), 70.8 (OCH₂), 70.2 (C-6), 66.8 (C-4), 66.3 (C-3), 63.0 (OCH₂), 50.8 (CH₂-N), 48.2 (OCH₃), 48.1 (OCH₃), 26.9 (C(CH₃)₃), 21.3 (C(O)CH₃), 19.6 (C(CH₃)₃), 18.0 (CH₃), 17.8 (CH₃); IR (ν_{max}/cm⁻¹): 2930 (OCH₃), 2109 (N₃), 1742 (C=O); HRMS: Found [M+Na]⁺ 754.3348, C₃₆H₅₃N₃O₁₁SiNa requires 754.3342.

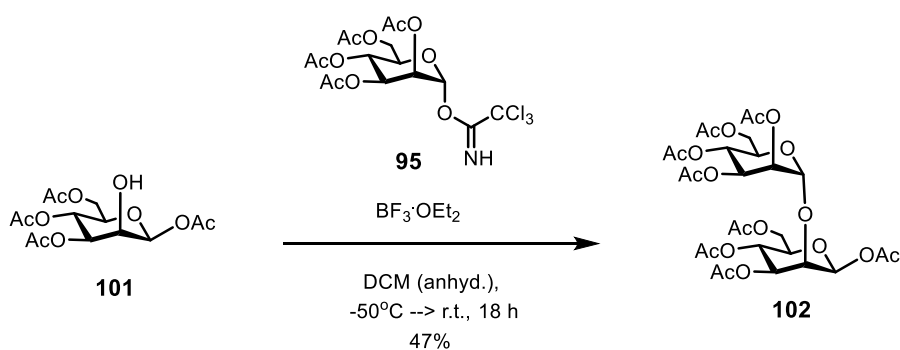
1,3,4,6-Tetra-O-acetyl-β-D-mannopyranoside (**101**)^{162,203}



Acetic anhydride (50 mL, 49 mmol) was placed in a 3-neck round bottom flask, equipped with a thermometer. D-Mannose (50 mg, 0.28 mmol) **100** was added, followed by perchloric acid (70%, 4 drops from a Pasteur pipette). D-Mannose **100** (13.2 g, 73 mmol) was added in small portions of a period of 1 h, keeping the reaction temperature in the range of 40-45 °C. Once the addition was complete, the orange-brown solution was stirred for 1 h at r.t. The reaction mixture was cooled to 10 °C (in an ice bath) and phosphorus tribromide (10.45 mL, 110 mmol) was added dropwise. This led to the formation of HBr and was quite exothermic; the reaction was cooled in an ice bath to maintain an internal temperature of 20-25 °C. Once the addition was complete, the mixture was stirred at r.t. for 1.5 h. The reaction mixture was cooled to 5 °C in an ice bath and a solution of sodium acetate trihydrate (39.9 g, 293 mmol) in water (50 mL) also at 5 °C was added dropwise. With cooling, the temperature was kept at 20-25 °C and the addition completed in 30 min. The reaction mixture was stirred at r.t. for 20 min. The mixture was then poured onto ice and extracted with chloroform (3 × 60 mL). The extracts were combined and washed with ice-water (150 mL), sat. aq. NaHCO₃ containing ice (150 mL) and ice-water (150 mL) again. The organic layer was dried (MgSO₄), filtered and concentrated. Diethyl ether (100 mL) was added and the product crystallised out of solution. The flask was left in the freezer overnight and the product collected by filtration and washed with a little with cold ether, to give mannopyranoside **101** as a colourless solid (4.6 g, 18%); *R*_f 0.39 (1:4 Hexane–EtOAc);

m.p. 132-133 °C (from EtOH) (lit.²⁰⁴ 131 °C from EtOH); $[\alpha]_{\text{D}}^{23}$ -26.3 (c, 1.0, CHCl₃) (lit.¹⁶² $[\alpha]_{\text{D}}^{30}$ -23.6 (c, 1.4, CHCl₃)); δ_{H} (500 MHz, CDCl₃); 5.77 (d, 1H, $J_{1,2}$ 1.0 Hz, H-1), 5.37 (t, 1H, $J_{3,4=4,5}$ 9.8 Hz, H-4), 5.02 (dd, 1H, $J_{3,4}$ 9.8 Hz, $J_{2,3}$ 3.0 Hz, H-3), 4.28 (dd, 1H, $J_{5,6}$ 5.0 Hz, $J_{6,6'}$ 12.4 Hz, H-6), 4.18 (td, 1H, $J_{2,3}$ 3.0 Hz, $J_{1,2}$ 1.0 Hz, H-2), 4.11 (dd, 1H, $J_{5,6'}$ 2.4 Hz, $J_{6,6'}$ 12.4 Hz, H-6'), 3.76 (m, 1H, H-5), 2.49 (d, 1H, J 4.0 Hz, OH), 2.16 (s, 3H, C(O)CH₃), 2.09 (s, 3H, C(O)CH₃), 2.06 (s, 3H, C(O)CH₃), 2.03 (s, 3H, C(O)CH₃); δ_{C} (75 MHz, CDCl₃); 170.9, 170.2, 169.7, 168.6 (C=O), 91.8 ($J_{\text{C,H}}$ 163 Hz, β , C-1), 73.2 (C-5), 73.0 (C-3), 68.5 (C-2), 65.4 (C-4), 62.1 (C-6), 21.0, 20.9, 20.9, 20.8 (4 × C(O)CH₃); IR (ν_{max} /cm⁻¹): 3453 (OH), 1712 (C=O); HRMS: Found $[\text{M}+\text{NH}_4]^+$ 366.1400, C₁₄H₂₄NO₁₀ requires 366.1395.

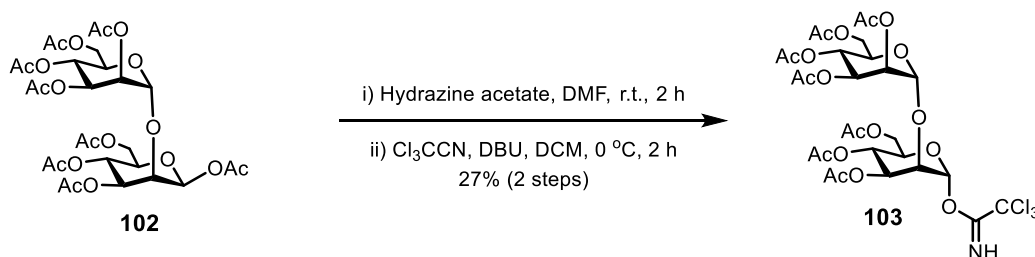
1,3,4,6-Tetra-O-acetyl-2-O-(2,3,4,6-tetra-O-acetyl- α -D-mannopyranosyl)- β -D-mannopyranose (**102**)²⁰⁵



1,3,4,6-Tetra-O-acetyl- β -D-mannopyranoside **101** (1.70 g, 4.9 mmol) and 2,3,4,6-tetra-O-acetyl- α -D-mannopyranosyl trichloroacetimidate **95** (2.40, 4.9 mmol) were co-evaporated with toluene several times before adding molecular sieves 4 Å (2.0 g) and anhydrous DCM (17 mL). The resulting mixture was stirred at r.t. under N₂(g) for 2 h, and cooled to -50 °C. Freshly distilled BF₃·OEt₂ was added to the reaction mixture, which was stirred at low temperature and slowly warmed up to r.t. over 18 h. The reaction mixture was quenched with sodium hydrogen carbonate (1.28 g), filtered through a Celite[®] pad, concentrated to leave a yellow oil. The crude residue was purified by Biotage[®] flash column chromatography (Redisef[®]Rf 40 g silica column, Hexane:EtOAc (0% EtOAc (1 col. vol.) → 0-33% EtOAc (over 3 col. vol.) → 33% EtOAc (over 2 col. vol.) → 33-50% EtOAc (over 16 col. vol.) → 50% EtOAc (over 13 col. vol.)) to give compound **102** as a white fluffy solid (1.54, 47%); R_f 0.36 (3:7 Hexane–EtOAc); m.p. 70 °C (from hexane–EtOAc) (lit.²⁰⁵ m.p. 72 °C); $[\alpha]_{\text{D}}^{22}$ 0.73 (c,

0.25, CHCl₃) (lit.²⁰⁶ $[\alpha]_D^{18}$ 0.7 (c, 0.6, CHCl₃)); δ_H (500 MHz, CDCl₃); 5.81 (d, 1H, $J_{1a,2a}$ 1.1 Hz, H-1a), 5.50 (dd, 1H, $J_{2b,3b}$ 10.0 Hz, $J_{3b,4b}$ 3.3 Hz, H-3b), 5.40-5.34 (m, 2H, H-4a, H-4b), 5.33-5.30 (m, 1H, H-2b), 5.14 (dd, 1H, $J_{2a,3a}$ 9.7 Hz, $J_{3a,4a}$ 2.9 Hz, H-3a), 5.02 (d, 1H, $J_{1b,2b}$ 1.9 Hz, H-1b), 4.44 (ddd, 1H, $J_{4b,5b}$ 10.1 Hz, $J_{5b,6b}$ 4.4 Hz, $J_{5b,6'b}$ 2.5 Hz, H-5b), 4.33 (dd, 1H, $J_{6b,6'b}$ 12.2 Hz, $J_{5b,6b}$ 4.4 Hz, H-6b), 4.27 (dd, 1H, $J_{6a,6'a}$ 12.4 Hz, $J_{5a,6a}$ 4.7 Hz, H-6a), 4.21-4.16 (m, 2H, H-2a, H-6'a), 4.07 (dd, 1H, $J_{6b,6'b}$ 12.2 Hz, $J_{5b,6'b}$ 2.5 Hz, H-6'b), 3.82 (ddd, 1H, $J_{4a,5a}$ 9.6 Hz, $J_{5a,6a}$ 4.7 Hz, $J_{5a,6'a}$ 2.5 Hz, H-5a), 2.16 (s, 6H, 2 × C(O)CH₃), 2.13 (s, 3H, C(O)CH₃), 2.10 (s, 3H, C(O)CH₃), 2.09 (s, 3H, C(O)CH₃), 2.05 (s, 3H, C(O)CH₃), 2.04 (s, 3H, C(O)CH₃), 2.03 (s, 3H, C(O)CH₃); δ_C (75 MHz, CDCl₃); 170.9, 170.6, 170.2, 169.8, 169.6, 169.5, 169.3, 169.4 (8 × C=O), 98.3 ($J_{C,H}$ 174 Hz, 5.5 Hz, α , C-1b), 91.0 ($J_{C,H}$ 162 Hz, β , C-1a), 74.7 (C-2a), 73.1 (C-5a), 72.2 (C-3a), 69.9 (C-2b), 68.9 (C-5b), 68.4 (C-3b), 66.2 (C-4a), 65.8 (C-4b), 62.2 (C-6b), 61.8 (C-6a), 20.9, 20.7, 20.6, 20.5 (8 × C(O)CH₃); IR (ν_{max}/cm^{-1}): 1739 (C=O); HRMS: Found $[M+Na]^+$ 701.1904, C₂₈H₃₈NaO₁₉ requires 701.1900.

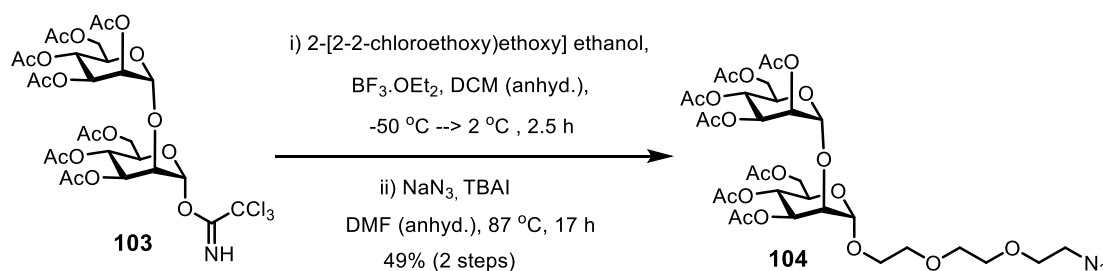
3,4,6-Tri-O-acetyl-2-O-(2,3,4,6-tetra-O-acetyl- α -D-mannopyranosyl)- α -D-mannopyranosyl trichloroacetimidate (103**)²⁰⁵**



Hydrazine acetate (56 mg, 0.6 mmol) was added to a solution of 1,3,4,6-tetra-O-acetyl-2-O-(2,3,4,6-tetra-O-acetyl- α -D-mannopyranosyl)- β -D-mannopyranose **102** (275 mg, 0.4 mmol) in DMF (1 mL). The reaction mixture was stirred at r.t. for 2 h, concentrated to leave dark brown oil, which was dissolved in anhydrous DCM (1 mL). Trichloroacetonitrile (212 μ L, 2.1 mmol) and DBU (62 μ L, 0.6 mmol) were added dropwise to the reaction mixture at 0 °C, which was stirred for 2 h at r.t., concentrated and purified by Biotage® flash column chromatography (Redisef® Rf 24 g silica column, Hexane:EtOAc (0% EtOAc (1 col. vol.) → 0-33% EtOAc (over 16 col. vol.) → 33% EtOAc (over 25 col. vol.) → 33-50% EtOAc (over 5 col. vol.) 50% EtOAc (over 10 col. vol.)) to give compound **103** as a yellow oil (86 mg, 27%); R_f 0.23 (1:1 Hexane–EtOAc); $[\alpha]_D^{22}$ 32.2 (c, 1.0, CHCl₃) (lit.²⁰⁵ $[\alpha]_D^{25}$ 31.2 (c, 1.4, CHCl₃)); δ_H (500 MHz, CDCl₃); 8.71

(s, 1H, NH), 6.40 (d, 1H, $J_{1a,2a}$ 2.2 Hz, H-1a), 5.45 (t, 1H, $J_{3a,4a=4a,5a}$ 10.0 Hz, H-4a), 5.39 (dd, 1H, $J_{3b,4b}$ 10.0 Hz, $J_{2b,3b}$ 3.4 Hz, H-3b), 5.32 (dd, 1H, $J_{3a,4a}$ 9.9 Hz, $J_{2a,3a}$ 3.1 Hz, H-3a), 5.30-5.24 (m, 2H, H-2b, H-4b), 4.97 (d, 1H, $J_{1b,2b}$ 1.8 Hz, H-1b), 4.27 (t, 1H, J 2.7 Hz, H-2a), 4.24-4.06 (m, 6H, H-5a, H-5b, H-6a, H-6'a, H-6b, H-6'b), 2.13 (s, 3H, C(O)CH₃), 2.11 (s, 3H, C(O)CH₃), 2.07 (s, 3H, C(O)CH₃), 2.03 (s, 3H, C(O)CH₃), 2.02 (s, 3H, C(O)CH₃), 2.01 (s, 3H, C(O)CH₃), 1.99 (s, 3H, C(O)CH₃); δ_c (75 MHz, CDCl₃); 170.9, 170.7, 170.4, 170.0, 169.8, 169.6, 169.4, 160.2 (7 × C=O, NH), 99.3 ($J_{C,H}$ 173 Hz, 4.6 Hz, α , C-1b), 95.6 ($J_{C,H}$ 180 Hz, α , C-1a), 75.1 (C-2a), 71.4, 69.9, 69.7, 69.6, 68.5, 66.2, 65.4, 62.4, 61.8, 60.5, 21.1, 20.9, 20.8, 20.7 (7 × C(O)CH₃); IR (ν_{max}/cm^{-1}): 3056 (NH), 1745 (C=O), 1676 (C=N); HRMS: Found [M+Na]⁺ 802.0906, C₂₈H₃₆Cl₃NaNO₁₈ requires 802.0906.

1-Azido-3,6-dioxaoct-8-yl 3,4,6-tri-O-acetyl-2-O-(2,3,4,6-tetra-O-acetyl- α -D-mannopyranosyl)- α -D-mannopyranoside (104)

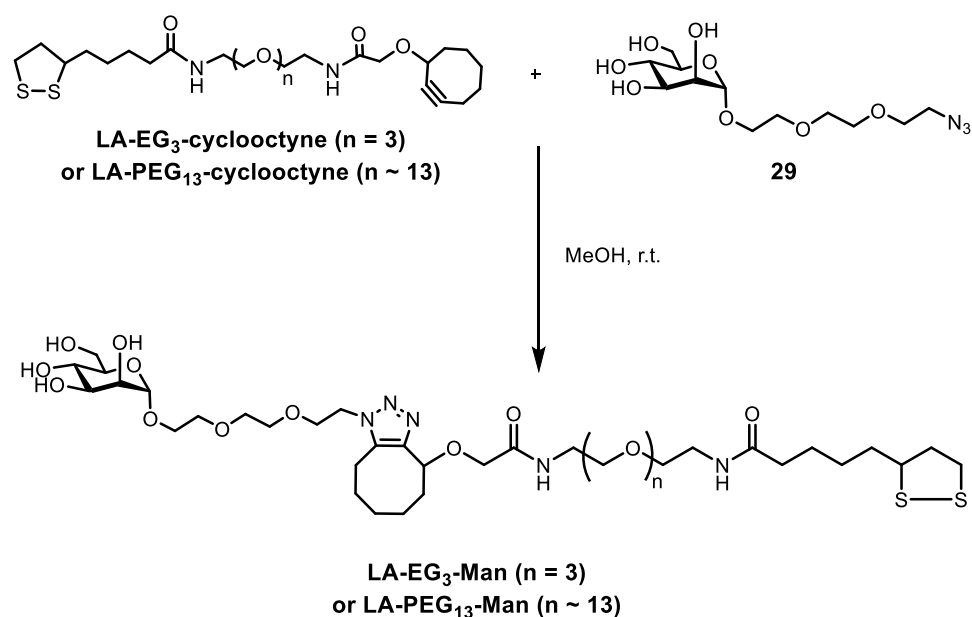


3,4,6-Tri-O-acetyl-2-O-(2,3,4,6-tetra-O-acetyl- α -D-mannopyranosyl)- α -D-mannopyranosyl trichloroacetimidate **103** (82 mg, 0.11 mmol) was co-evaporated with toluene several times before adding molecular sieves 4 Å (50 mg), anhydrous DCM (1 mL) and 2-[2-(2-chloroethoxy)ethoxy]ethanol (279 μ L, 1.5 mmol). The resulting mixture was stirred at r.t. under N₂(g) atmosphere for 1.5 h, and cooled to -50 °C. Freshly distilled BF₃·OEt₂ (14 μ L, 0.11 mmol) was added to the reaction mixture, which was stirred at low temperature and slowly warmed up to 2 °C, over 2.5 h. The reaction mixture was washed with sat. aq. NaHCO₃ (2 × 2 mL), followed by brine (2 mL). The combined organic phase was dried over MgSO₄, and concentrated to leave crude yellow oil, which was purified by Biotage[®] flash column chromatography (Redisef[®]Rf 24 g silica column, Hexane:EtOAc (0% EtOAc (1 col. vol.) → 0-70% EtOAc (over 12 col. vol.) → 70% EtOAc (over 12 col. vol.)). The partially purified mixture was dissolved in anhydrous DMF (3.5 mL). Sodium azide (32 mg, 0.1 mmol) and TBAI (37 mg, 0.1 mmol) were added to the reaction mixture, which was stirred at 87 °C for 17 h. The reaction

mixture was cooled to r.t., concentrated, and purified by Biotage[®] flash column chromatography (Redise[®]Rf 24 g silica column, Hexane:EtOAc (0% EtOAc (1 col. vol.) → 0-70% EtOAc (over 12 col. vol.) → 70% EtOAc (over 12 col. vol.) to give compound **104** as a colourless oil (43 mg, 49%, 2 steps); R_f 0.30 (3:7 Hexane–EtOAc); $[\alpha]_D^{25}$ 27.2 (c, 1.0, CHCl₃); δ_H (500 MHz, CDCl₃); 5.40 (dd, 1H, $J_{3b,4b}$ 9.9 Hz, $J_{2b,3b}$ 3.6 Hz, H-3b), 5.36-5.23 (m, 4H, H-2b, H-3a, H-4a, H-4b), 4.97 (d, 1H, $J_{1a,2a}$ 2.0 Hz, H-1a), 4.91 (d, 1H, $J_{1b,2b}$ 1.9 Hz, H-1b), 4.21 (dd, 2H, $J_{6,6'}$ 12.1 Hz, $J_{5,6=5,6'}$ 4.9 Hz, H-6, H-6'), 4.12 (m, 3H, H-5b, H-6, H-6'), 4.04 (bs, 1H, H-2a), 4.01-3.95 (m, 1H, H-5a), 3.81 (m, 1H, CH₂O), 3.70-3.60 (m, 9H, CH₂O), 3.37 (t, 2H, J 5.1 Hz, CH₂-N), 2.14 (s, 3H, C(O)CH₃), 2.13 (s, 3H, C(O)CH₃), 2.07 (s, 3H, C(O)CH₃), 2.06 (s, 3H, C(O)CH₃), 2.02 (s, 3H, C(O)CH₃), 2.01 (s, 3H, C(O)CH₃), 1.99 (s, 3H, C(O)CH₃); δ_C (75 MHz, CDCl₃); 171.0, 170.6, 170.5, 170.0, 169.8, 169.6, 169.5 (7 × C=O), 99.3 ($J_{C,H}$ 173.3 Hz, 5.1 Hz, α , C-1b), 98.5 ($J_{C,H}$ 172 Hz, α , C-1a), 77.2 (C-2a), 70.9, 70.8 (2 × CH₂O), 70.4 (C-3a), 70.2 (2 × CH₂O), 69.9 (C-2b), 69.3 (C-5b), 68.6 (C-3b), 69.5 (C-5a), 67.6 (ManOCH₂), 66.5, 66.3 (C-4a, C-4b), 62.6, 62.2 (C-6a, C-6b), 50.8 (CH₂-N), 21.0, 20.8, 20.8 (7 × OCH₃); IR (ν_{max}/cm^{-1}): 2107 (N₃), 1744 (C=O); HRMS: Found [M+Na]⁺ 816.2660, C₃₂H₄₇N₃NaO₂₀ requires 816.2645.

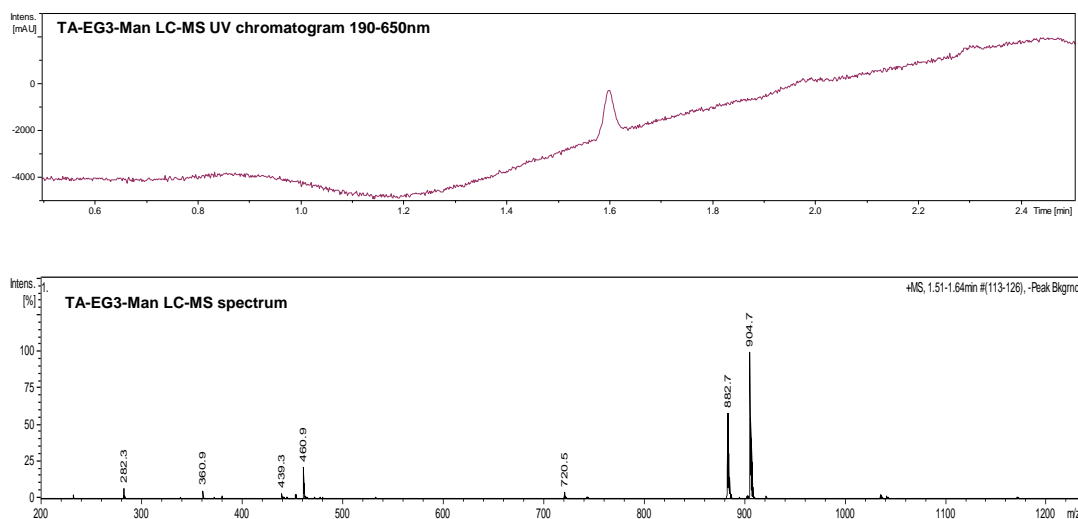
8.2.2 Synthesis of carbohydrate-functionalised quantum dots

8.2.2.1 LA-PEG_n-Man (n = ~ 13 or 3)^{†††}

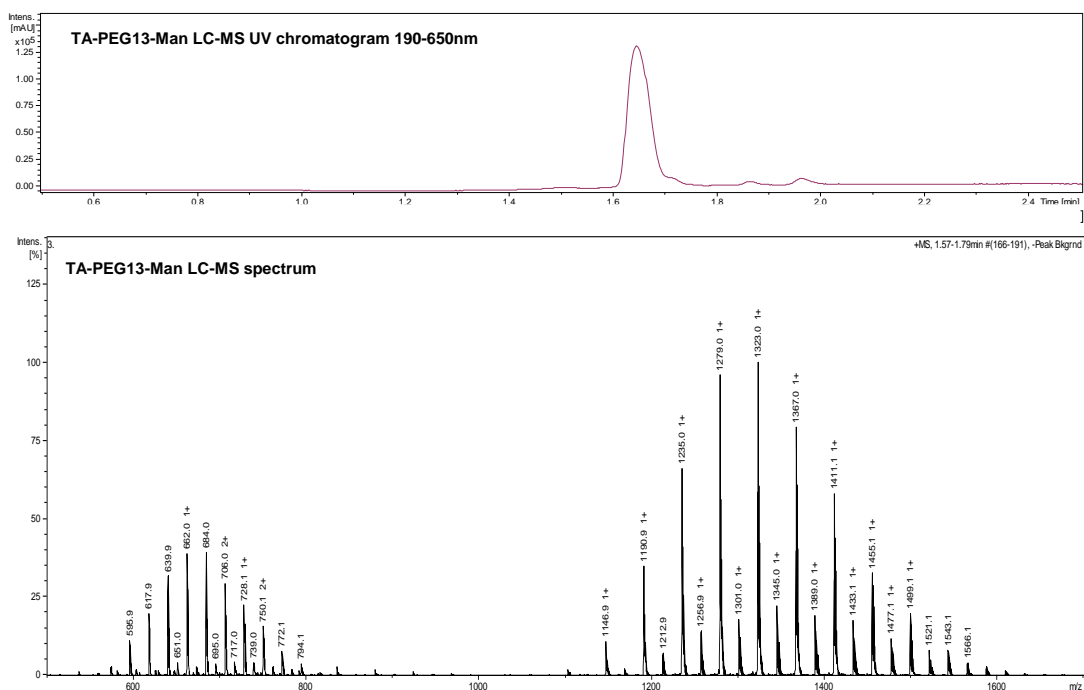


LA-PEG₁₃-cyclooctyne (0.175 M, 114 μL, 20 μmol in EtOH) or LA-EG₃-cyclooctyne (0.144 M, 138 μL, 19.8 μmol, in EtOH) was mixed with 1-azido-3,6-dioxaoct-8-yl α-D-mannopyranoside **29** (0.200 M in MeOH, 120 μL, 24 μmol) and allowed to react at r.t. for 48 h for efficient conjugation. The reaction mixture was concentrated and purified by Sephadex LH-20 column chromatography using MeOH as eluting solvent. The desired product fractions were collected, combined and analysed by HRMS. For LA-EG₃-Man, LC-MS analysis revealed a single UV absorption band with a retention time of ~1.6 min. The MS spectrum displayed two peaks with m/z values of 882.7 and 904.7, corresponding to the [M+H]⁺ and [M+Na]⁺ peaks, respectively. HRMS analysis found [M+Na]⁺ 904.4046, C₃₈H₆₇N₅NaO₁₄S₂ requires 904.4018.

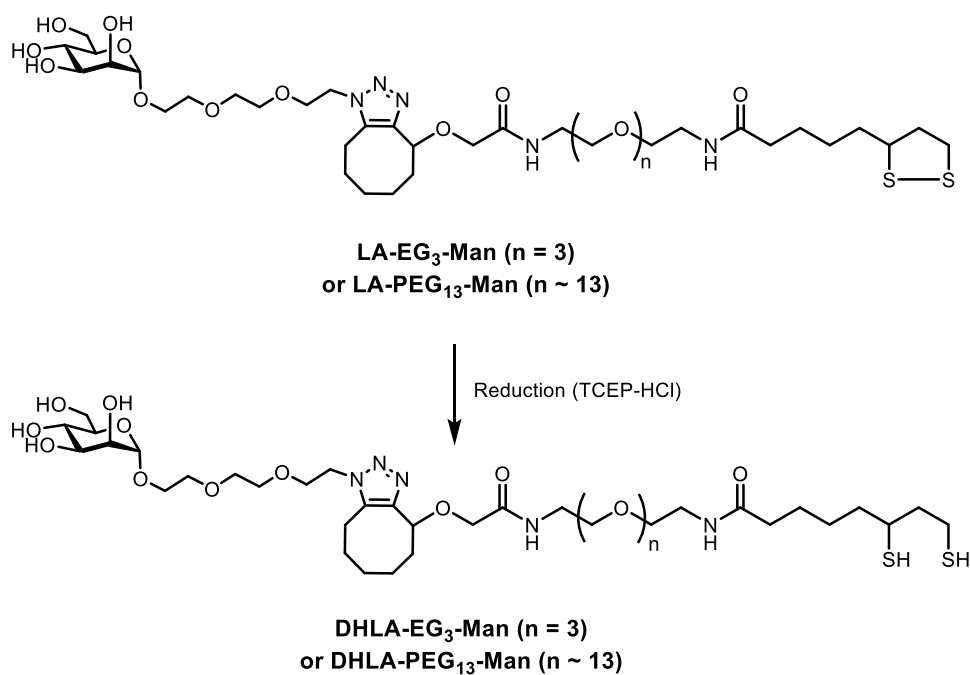
^{†††} Both LA-EG₃-cyclooctyne and LA-PEG₁₃-cyclooctyne were used as a mixture of stereoisomers. Both LA-EG₃-Man and LA-PEG₁₃-Man were formed as a mixture of regioisomers, only the predominant stereoisomer is shown.



For LA-PEG₁₃-Man, LC-MS analysis provided a single absorption band with a retention time of ~1.65 min. The corresponding MS spectrum displayed a series of peaks that were separated by 44 m/z units, corresponding to different PEG chain lengths in the mixed length PEG₁₃ linker: found: m/z peaks at 1190.9, 1235.0, 1235.0, 1323.0, 1367.0, 1411.1, 1455.1. The calculated corresponding [M+H]⁺ peaks for LA-PEG_n-Man where n = 10, 11, 12, 13, 14, 15 and 16 were 1191, 1235, 1279, 1323, 1367, 1411 and 1455, respectively. HRMS analysis showed a series of species with m/z ratios separated by multiple numbers of 44 (the molecular weight of the EG unit): 537.7932, 595.8059, 617.8188, 639.8318, 661.8450, 683.8584, 705.8713, and 727.8832. The corresponding expected [M+2H]²⁺ peaks with PEG repeat number of 9, 10, 11, 12, 13, 14, 15 and 16 were 573.7922, 595.8059, 617.8184, 639.8315, 661.8446, 683.8576, 705.8709 and 727.8840, respectively.



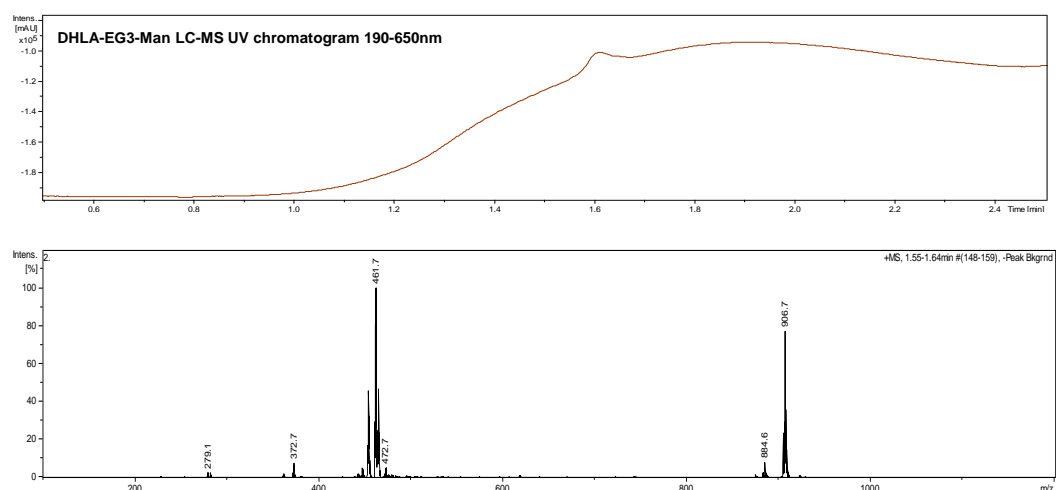
8.2.2.2 DHLA-PEG_n-Man (n = ~13 or 3)##



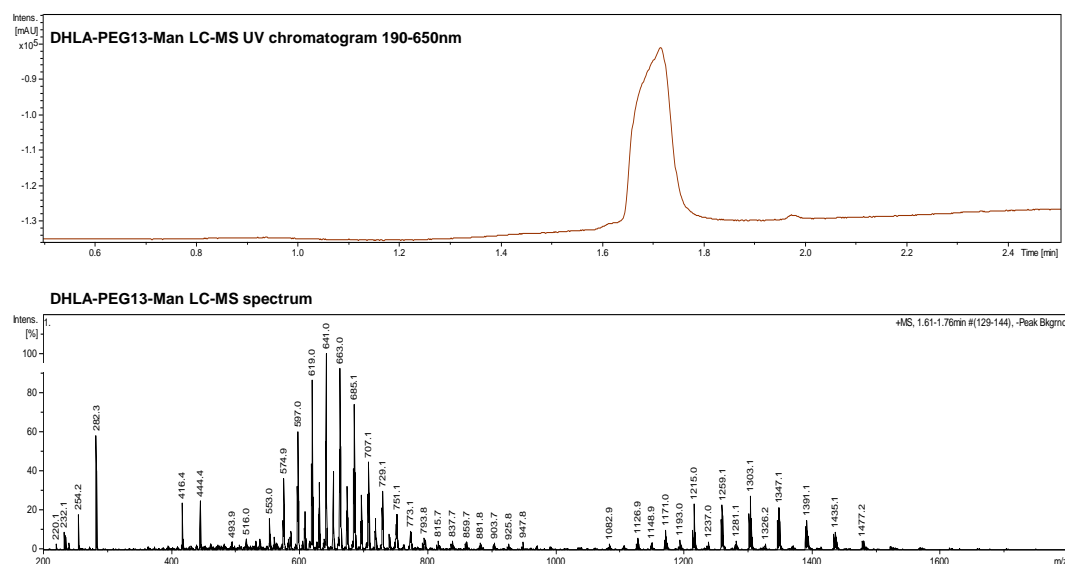
Tris(2-carboxyethyl)phosphine hydrochloride (TCEP·HCl, 1.2 eq) was dissolved in H₂O and added to a solution of LA-PEG₁₃-Man or LA-EG₃-Man in EtOH. The resulting mixture was allowed to stand at r.t. for 30 min to reduce disulphide bonds. After evaporation of solvent, DHLA-PEG₁₃-Man or DHLA-EG₃-Man was purified by flash

Both DHLA-EG₃-Man and DHLA-PEG₁₃-Man were formed as a mixture of regioisomers, only the predominant stereoisomer is shown.

column chromatography (silica; 5:1 Chloroform–MeOH). The fractions containing reduced ligands were combined and evaporated. The purified DHLA-PEG₁₃-Man or DHLA-EG₃-Man was further analysed by LC-MS. For DHLA-EG₃-Man, a single UV band with a retention time of ~1.6 min from the HPLC elution profile gave two MS peaks with m/z ratios of 884.6 and 906.7, corresponding to the required [M+H]⁺ and [M+Na]⁺ peaks.



For DHLA-PEG₁₃-Man, a single UV absorption band from the HPLC eluting profile was found. The corresponding MS spectrum revealed a series of m/z ratios separated by 44 mass units, corresponding to the different PEG lengths of the average of 13.



The reduced DHLA-EG₃-Man and DHLA-PEG₁₃-Man ligands were concentrated and dissolved in chloroform. The concentrations of mannose were determined by phenol-sulfuric acid method as described in the following section.

8.2.2.3 Determination of mannose loading on the QDs¹⁵⁷

Mannose amount was determined by phenol-sulfuric acid method. D-Mannose stock (100 mg/mL in H₂O) was diluted 100 times to give 1 mg/mL stock in H₂O. Different amounts of stock solution were then mixed with 5% phenol in H₂O and H₂SO₄ to generate a calibration curve as follows: to a solution of D-mannose in H₂O (125 μL) in a 5 mL-glass vial was added 125 μL of 5% phenol in H₂O followed by 625 μL of concentrated H₂SO₄. The mixture was vortexed and allowed to stand at r.t. for 30 min. The absorbance of the solution at 490 nm was measured against a blank pure water control solution to generate a calibration curve.¹⁵⁷ Unconjugated DHLA-PEG_n-Man ligands collected from hexane precipitation supernatant (after removal of organic solvent and dissolving in H₂O) and spin column filtrate were combined to make a total volume of 1300 μL for DHLA-PEG₁₃-Man and 1430 μL for DHLA-EG₃-Man. One hundred twenty five μL of each solution was then mixed with 125 μL of phenol and 625 μL of H₂SO₄ as above to determine the amounts of unconjugated mannose ligand. The dilution factors were then corrected to calculate the total amount of unconjugated mannose ligand. Assuming the difference between the amounts of ligand added and unconjugated were those that have bound to the QD,^{207,208} the average number of mannose molecules conjugated to each QD was then calculated as 170±40 and 330±70 for QD-PEG₁₃-Man and QD-EG₃-Man, respectively. A lower mannose valency in the former is likely due to a relatively long PEG chain that may sterically limit very high ligand packing on the QD surface, leading to a lower ligand density.

8.2.2.4 Preparation of DHLA-ZW capped QDs

TOPO capped hydrophobic QDs (1 nmole, 20 μL in hexane) were first precipitated by adding 500 μL of EtOH followed by centrifugation to remove any free TOPO ligands. The QD precipitate was then dissolved in 50 μL of chloroform followed by addition of 20 μL of EtOH, resulting in QD solution. In a separate Eppendorf tube, LA-ZW (0.10 M, 2.0 μL in H₂O) was reacted with TCEP·HCl (0.10 M, 2.0 μL in H₂O) for 10 min to reduce the LA-ZW into DHLA-ZW. NaOH (0.10 M in EtOH, 12 μL) was added to fully deprotonate the DHLA thiol-groups and to neutralise acid groups in TCEP. The resulting mixture was mixed with the previously-prepared QD solution, forming a homogenous solution. After a brief shaking by hand, the QDs were found to rise to the top aqueous layer within 1 min. The phase separation became clearer after addition of 50 μL of H₂O, followed by a brief centrifugation. The QD was found to be completely transferred to the top aqueous phase, leaving the bottom organic layer colourless, indicating a full QD water-solubilisation. The top aqueous layer was then carefully

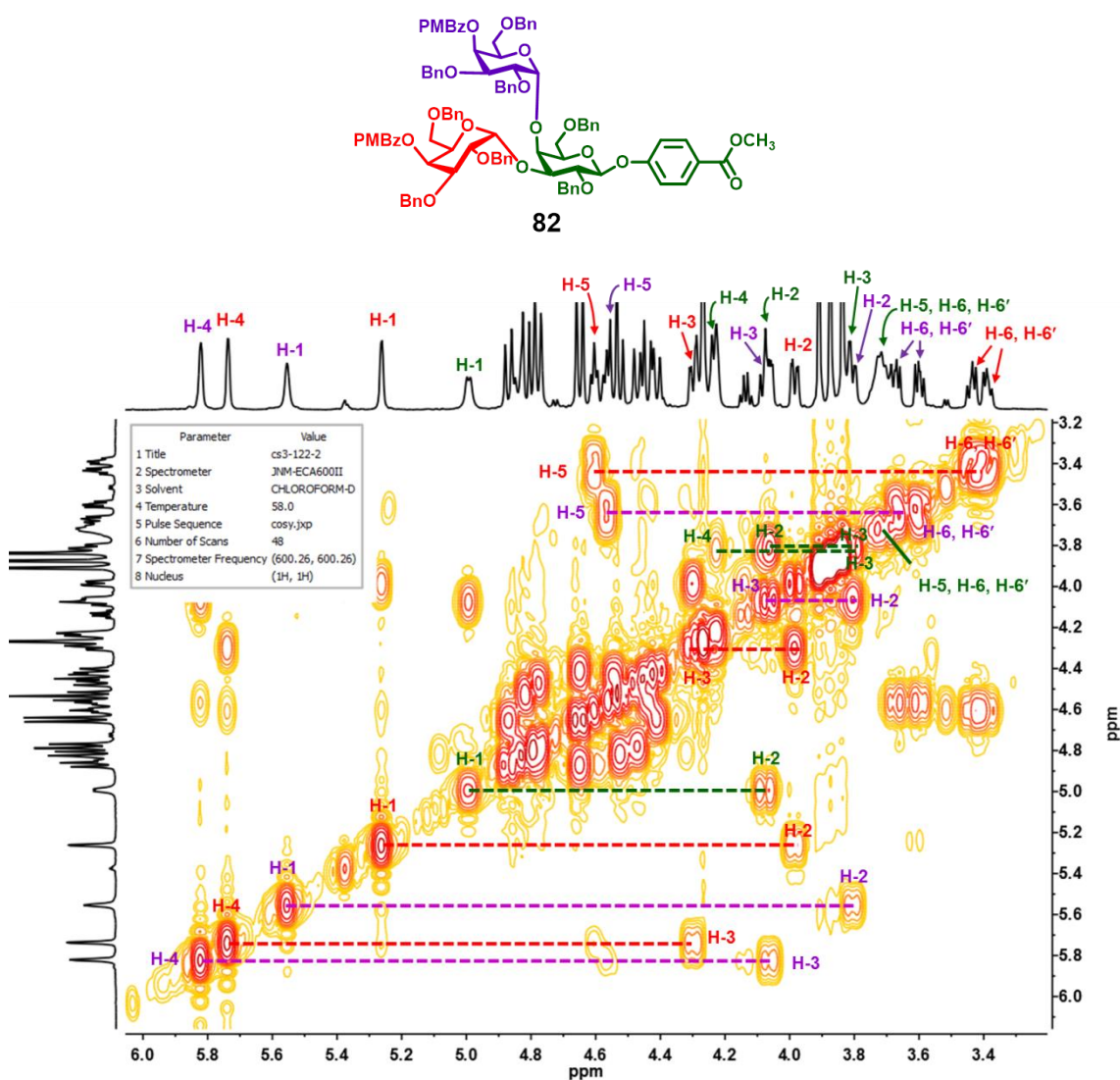
separated from the bottom chloroform layer and transferred to an Amicon ultra-centrifugal tube equipped with a 30,000 MW cut-off (MWCO) filter membrane and centrifuged for 1 min at 3000 rpm. The residue was further washed with H₂O (200 μ L) and followed by centrifugation. The process was repeated three times to remove any unbound ligands. This yielded a stable, water soluble QD stock solution. The stock QD concentration was determined from its UV-vis absorption at the first excitation peak and using the respective extinction coefficient as previously established.^{207,209}

8.2.2.5 Preparation of QD-PEG₁₃-Man and QD-EG₃-Man

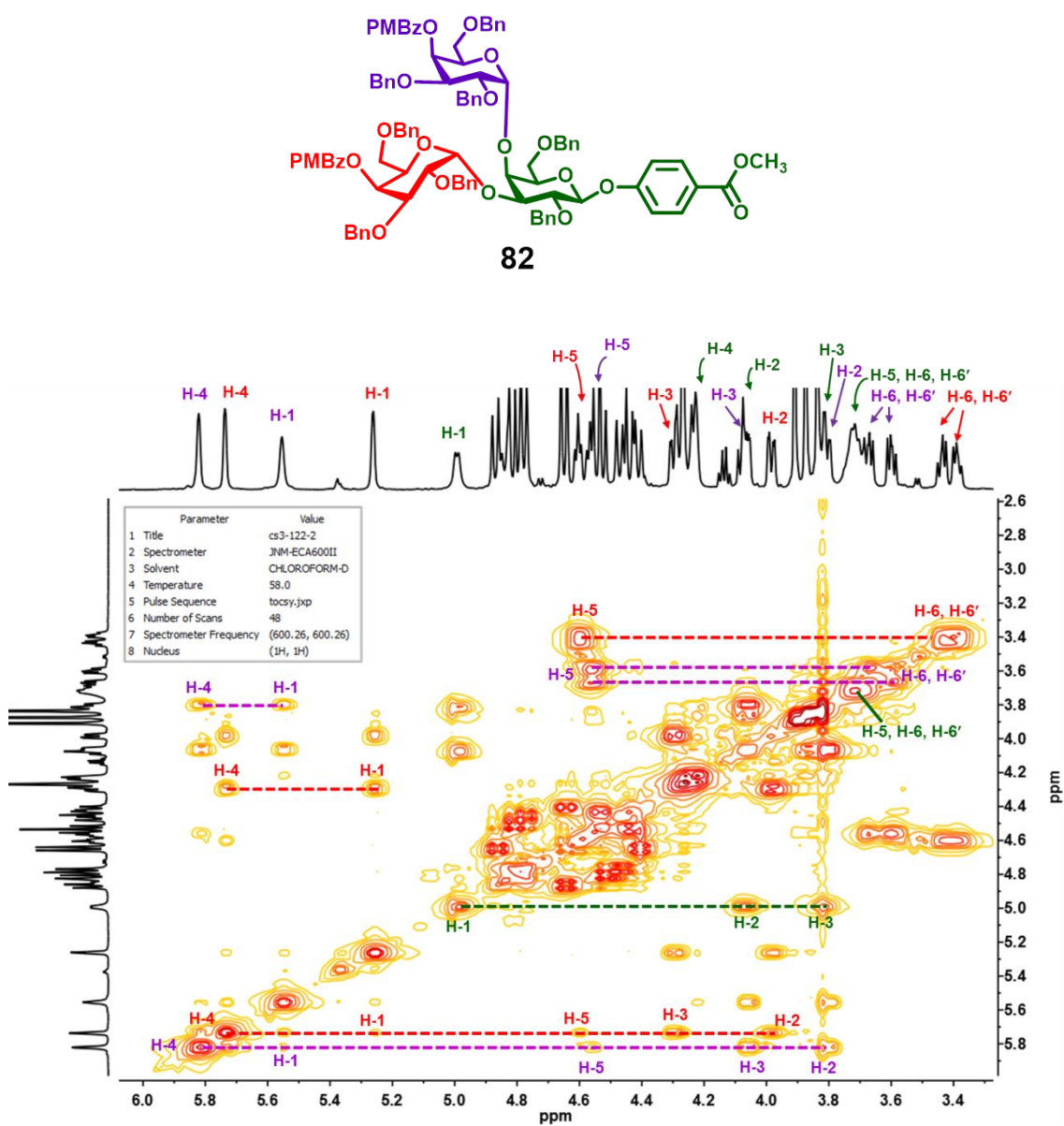
CdSe/ZnS core/shell QDs ($\lambda_{EM} = 560$ nm, 1 nmol) in 0.2 mL of toluene were precipitated with EtOH (1 mL) and separated by centrifugation at 10 \times kg for 3 min.^{193,194} The resultant QDs were re-dissolved in chloroform (50 μ L). After being deprotonated by adding NaOH in EtOH (0.10 M, 600 nmol in total), previously prepared DHLA-PEG₃-Man or DHLA-EG₃-Man (500 nmol, in chloroform) was added to the QD solution together with some extra MeOH to make a homogenous solution (Chloroform–MeOH 1:1, v/v). The reaction mixture was stirred at r.t. in the dark for 30 min. Hexane was then added to the reaction mixture until the solution became cloudy. The resulting mixture was then centrifuged at 10 \times kg for 5 min to obtain QD-PEG₁₃-Man/QD-EG₃-Man pellet. After removal of clear supernatant (checked by UV to ensure no QD fluorescence), the pellet was dissolved in 100 μ L of H₂O. The QD-conjugate-solution was then transferred to a 30 KD MWCO spin column and washed with H₂O (3 \times 100 μ L) to remove any unbound ligands. The QD stock concentration was determined by measuring the absorbance at 546 nm using extinction coefficient of 1.3×10^5 M⁻¹·cm⁻¹.^{207,208}

Chapter 9: Appendix

Appendix A: $^1\text{H} - ^1\text{H}$ COSY spectrum of trisaccharide **82** (600 MHz, CDCl_3 , 331 K) with the complete assignments of sugar proton resonances. N.B. Couplings from H-5 to H-4 from TOCSY (*cf.* Appendix B).



Appendix B: ^1H - ^1H TOCSY spectrum of trisaccharide **82** (600 MHz, CDCl_3 , 331 K) with the complete assignments of sugar proton resonances.



Chapter 10: References

- (1) Nieuwdorp, M.; Meuwese, M. C.; Vink, H.; Hoekstra, J. B.; Kastelein, J. J.; Stroes, E. S. *Curr. Opin. Lipidol.* **2005**, *16*, 507.
- (2) Schroter, S.; Osterhoff, C.; McArdle, W.; Ivell, R. *Hum. Reprod. Update* **1999**, *5*, 302.
- (3) Diekman, A. B. *Cell. Mol. Life Sci.* **2003**, *60*, 298.
- (4) Lowe, J. B. *Curr. Opin. Cell. Biol.* **2003**, *15*, 531.
- (5) Sacchettini, J. C.; Baum, L. G.; Brewer, C. F. *Biochemistry* **2001**, *40*, 3009.
- (6) Campbell, B. J.; Yu, L. G.; Rhodes, J. M. *Glycoconj. J.* **2001**, *18*, 851.
- (7) Takenaka, Y.; Fukumori, T.; Raz, A. *Glycoconj. J.* **2004**, *19*, 543.
- (8) Liu, F. T.; Rabinovich, G. A. *Nat. Rev. Cancer.* **2005**, *5*, 29.
- (9) Imberty, A.; Varrot, A. *Curr. Opin. Struct. Biol.* **2008**, *18*, 567.
- (10) Mandal, P. K.; Branson, T. R.; Hayes, E. D.; Ross, J. F.; Gavin, J. A.; Daranas, A. H.; Turnbull, W. B. *Angew. Chem. Int. Ed. Engl.* **2012**, *51*, 5143.
- (11) Heggelund, J. E.; Burschowsky, D.; Bjornestad, V. A.; Hodnik, V.; Anderluh, G.; Krengel, U. *PLoS Pathog.* **2016**, *12*, e1005567.
- (12) Bundle, D. R.; Young, N. M. *Curr. Opin. Struct. Biol.* **1992**, *2*, 666.
- (13) Naismith, J. H.; Field, R. A. *J. Biol. Chem.* **1996**, *271*, 972.
- (14) Quioco, F. A.; Spurlino, J. C.; Rodseth, L. E. *Structure* **1997**, *5*, 997.
- (15) Hudson, K. L.; Bartlett, G. J.; Diehl, R. C.; Agirre, J.; Gallagher, T.; Kiessling, L. L.; Woolfson, D. N. *J. Am. Chem. Soc.* **2015**, *137*, 15152.
- (16) Asensio, J. L.; Cañada, F. J.; Bruix, M.; González, C.; Khiar, N.; Rodríguez-Romero, A.; Jiménez-Barbero, J. *Glycobiology* **1998**, *8*, 569.
- (17) Nagahori, N.; Lee, R. T.; Nishimura, S.; Page, D.; Roy, R.; Lee, Y. C. *ChemBioChem* **2002**, *3*, 836.
- (18) del Carmen Fernandez-Alonso, M.; Diaz, D.; Berbis, M. A.; Marcelo, F.; Canada, J.; Jimenez-Barbero, J. *Curr. Protein Pept. Sci.* **2012**, *13*, 816.
- (19) Somers, W. S.; Tang, J.; Shaw, G. D.; Camphausen, R. T. *Cell* **2000**, *103*, 467.
- (20) Lindhorst, T. K. In *Carbohydrate-modifying biocatalysts*; Ed. Grunwald P; CRC Press: 2012, p 144.

- (21) Navarre, N.; Amiot, N.; van Oijem, A.; Imberty, A.; Poveda, A.; Jiménez-Barbero, J.; Cooper, A.; Nutley, M. A.; Boons, G. J. *Chem. Eur. J.* **1999**, *5*, 2281.
- (22) Weis, W. I.; Drickamer, K. *Annu. Rev. Biochem.* **1996**, *65*, 441.
- (23) Lee, Y. C.; Lee, R. T. *Acc. Chem. Res.* **1995**, *28*, 321.
- (24) Bertozzi, C. R.; Kiessling, L., L. *Science* **2001**, *291*, 2357.
- (25) Sandvig, K. *Toxicon* **2001**, *39*, 1629.
- (26) Ling, H.; Boodhoo, A.; Hazes, B.; Cummings, M. D.; Armstrong, G. D.; Brunton, J. L.; Read, R. J. *Biochemistry* **1998**, *37*, 1777.
- (27) Cambi, A.; de Lange, F.; van Maarseveen, N. M.; Nijhuis, M.; Joosten, B.; van Dijk, E. M. H. P.; de Bakker, B. I.; Fransen, J. A. M.; Bovee-Geurts, P. H. M.; van Leeuwen, F. N.; Van Hulst, N. F.; Figdor, C. G. *J. Cell Biol.* **2004**, *164*, 145.
- (28) Feinberg, H.; Tso, C. K. W.; Taylor, M. E.; Drickamer, K.; Weis, W. I. *J. Mol. Biol.* **2009**, *394*, 613.
- (29) Bernardi, A.; Jimenez-Barbero, J.; Casnati, A.; De Castro, C.; Darbre, T.; Fieschi, F.; Finne, J.; Funken, H.; Jaeger, K. E.; Lahmann, M.; Lindhorst, T. K.; Marradi, M.; Messner, P.; Molinaro, A.; Murphy, P. V.; Nativi, C.; Oscarson, S.; Penades, S.; Peri, F.; Pieters, R. J.; Renaudet, O.; Reymond, J. L.; Richichi, B.; Rojo, J.; Sansone, F.; Schaffer, C.; Turnbull, W. B.; Velasco-Torrijos, T.; Vidal, S.; Vincent, S.; Wennekes, T.; Zuilhof, H.; Imberty, A. *Chem. Soc. Rev.* **2013**, *42*, 4709.
- (30) Turhan A.; Weiss L.A.; Mohandas N.; Coller B.S.; Frenette P.S. *Proc. Natl. Acad. Sci. USA* **2002**, *99*, 3047.
- (31) Chang, J.; Patton, J. T.; Sarkar, A.; Ernst, B.; Magnani, J. L.; Frenette, P. S. *Blood* **2010**, *116*, 1779.
- (32) Scheffler, K.; Brisson, J. R.; Weisemann, R.; Magnani, J. L.; Wong, W. T.; Ernst, B.; Peters, T. *J. Biomol. NMR* **1997**, *9*, 423.
- (33) Rinnbauer, M.; Ernst, B.; Wagner, B.; Magnani, J.; Benie, A. J.; Peters, T. *Glycobiology* **2003**, *13*, 435.
- (34) Geijtenbeek, T. B.; Kwon, D. S.; Torensma, R.; van Vliet, S. J.; van Duijnhoven, G. C.; Middel, J.; Cornelissen, I. L.; Nottet, H. S.; KewalRamani, V. N.; Littman, D. R.; Figdor, C. G.; van Kooyk, Y. *Cell* **2000**, *100*, 587.
- (35) Bernardi, A.; Cheshev, P. *Chem. Euro. J.* **2008**, *14*, 7434.
- (36) Sattin, S.; Daggetti, A.; Thépaut, M.; Berzi, A.; Sánchez-Navarro, M.; Tabarani, G.; Rojo, J.; Fieschi, F.; Clerici, M.; Bernardi, A. *ACS Chem. Biol.* **2010**, *5*, 301.
- (37) Berzi, A.; Reina, J. J.; Otria, R.; Sutkeviciute, I.; Antonazzo, P.; Sanchez-Navarro, M.; Chabrol, E.; Biasin, M.; Trabattoni, D.; Cetin, I.; Rojo, J.; Fieschi, F.; Bernardi, A.; Clerici, M. *AIDS* **2012**, *26*, 127.

- (38) Luczkowiak, J.; Sattin, S.; Sutkevičiūtė, I.; Reina, J. J.; Sánchez-Navarro, M.; Thépaut, M.; Martínez-Prats, L.; Daggetti, A.; Fieschi, F.; Delgado, R.; Bernardi, A.; Rojo, J. *Bioconjugate Chem.* **2011**, *22*, 1354.
- (39) Berzi, A.; Varga, N.; Sattin, S.; Antonazzo, P.; Biasin, M.; Cetin, I.; Trabattoni, D.; Bernardi, A.; Clerici, M. *Viruses* **2014**, *6*, 391.
- (40) Reina, J. J.; Sattin, S.; Invernizzi, D.; Mari, S.; Martinez-Prats, L.; Tabarani, G.; Fieschi, F.; Delgado, R.; Nieto, P. M.; Rojo, J.; Bernardi, A. *ChemMedChem* **2007**, *2*, 1030.
- (41) Varga, N.; Sutkeviciute, I.; Guzzi, C.; McGeagh, J.; Petit-Haertlein, I.; Gugliotta, S.; Weiser, J.; Angulo, J.; Fieschi, F.; Bernardi, A. *Chemistry* **2013**, *19*, 4786.
- (42) Varga, N.; Sutkeviciute, I.; Ribeiro-Viana, R.; Berzi, A.; Ramdasi, R.; Daggetti, A.; Vettoretti, G.; Amara, A.; Clerici, M.; Rojo, J.; Fieschi, F.; Bernardi, A. *Biomaterials* **2014**, *35*, 4175.
- (43) Ordanini, S.; Varga, N.; Porkolab, V.; Thepaut, M.; Belvisi, L.; Bertaglia, A.; Palmioli, A.; Berzi, A.; Trabattoni, D.; Clerici, M.; Fieschi, F.; Bernardi, A. *Chem. Commun.* **2015**, *51*, 3816.
- (44) Taylor, M. E.; Drickamer, K. In *Introduction to glycobiology*; Oxford University Press: 2011, p 139.
- (45) Feinberg, H.; Mitchell, D. A.; Drickamer, K.; Weis, W. I. *Science* **2001**, *294*, 2163.
- (46) Drickamer, K. *Curr. Opin. Struct. Biol.* **1999**, *9*, 585.
- (47) Ross, R. *N. Engl. J. Med.* **1999**, *340*, 1929.
- (48) Landmesser, U.; Hornig, B.; Drexler, H. *Circulation* **2004**, *109*, 1127.
- (49) Saito, Y.; Morimoto, T.; Ogawa, H.; Nakayama, M.; Uemura, S.; Doi, N.; Jinnouchi, H.; Waki, M.; Soejima, H.; Sugiyama, S.; Okada, S.; Akai, Y. *Diabetes Care* **2011**, *34*, 280.
- (50) Jain, M. K.; Ridker, P. M. *Nat. Rev. Drug Discov.* **2005**, *4*, 977.
- (51) Libby, P.; Ridker, P. M.; Hansson, G. K. *Nature* **2011**, *473*, 317.
- (52) Sawamura, T.; Kume, N.; Aoyama, T.; Moriwaki, H.; Hoshikawa, H.; Aiba, Y.; Tanaka, T.; Miwa, S.; Katsura, Y.; Kita, T.; Masaki, T. *Nature* **1997**, *386*, 73.
- (53) Mehta, J. L.; Chen, J.; Hermonat, P. L.; Romeo, F.; Novelli, G. *Cardiovasc. Res.* **2006**, *69*, 36.
- (54) Chen, M. Y.; Kakutani, M.; Minami, M.; Kataoka, H.; Kume, N.; Narumiya, S.; Kita, T.; Masaki, T.; Sawamura, T. *Arterioscler. Thromb. Vasc. Biol.* **2000**, *20*, 1107.
- (55) Kataoka, H.; Kume, N.; Miyamoto, S.; Minami, M.; Moriwaki, H.; Murase, T.; Sawamura, T.; Masaki, T.; Hashimoto, N.; Kita, T. *Circulation* **1999**, *99*, 3110.

- (56) Hayashida, K.; Kume, N.; Murase, T.; Minami, M.; Nakagawa, D.; Inada, T.; Tanaka, M.; Ueda, A.; Kominami, G.; Kambara, H.; Kimura, T.; Kita, T. *Circulation* **2005**, *112*, 812.
- (57) Mehta, J. L.; Sanada, N.; Hu, C. P.; Chen, J.; Dandapat, A.; Sugawara, F.; Satoh, H.; Inoue, K.; Kawase, Y.; Jishage, K.; Suzuki, H.; Takeya, M.; Schnackenberg, L.; Beger, R.; Hermonat, P. L.; Thomas, M.; Sawamura, T. *Circ. Res.* **2007**, *100*, 1634.
- (58) Kita, T.; Kume, N.; Yokode, M.; Ishii, K.; Arai, H.; Horiuchi, H.; Moriwaki, H.; Minami, M.; Kataoka, H.; Wakatsuki, Y. *Ann. N. Y. Acad. Sci.* **2000**, *902*, 95.
- (59) Dunn, S.; Vohra, R. S.; Murphy, J. E.; Homer-Vanniasinkam, S.; Walker, J. H.; Ponnambalam, S. *Biochem. J.* **2008**, *409*, 349.
- (60) Insull, W., Jr. *Am. J. Med.* **2009**, *122*, S3.
- (61) Chen, M.; Masaki, T.; Sawamura, T. *Pharmacol. Ther.* **2002**, *95*, 89.
- (62) Kume, N.; Mitsuoka, H.; Hayashida, K.; Tanaka, M.; Kominami, G.; Kita, T. *J. Cardiol.* **2010**, *56*, 159.
- (63) Yoshida, H.; Kondratenko, N.; Green, S.; Steinberg, D.; Quehenberger, O. *Biochem. J.* **1998**, *334*, 9.
- (64) Kakutani, M.; Masaki, T.; Sawamura, T. *Proc. Natl. Acad. Sci. USA* **2000**, *97*, 360.
- (65) Draude, G.; Hrboticky, N.; Lorenz, R. L. *Biochem. Pharmacol.* **1999**, *57*, 383.
- (66) Chen, M. Y.; Inoue, K.; Narumiya, S.; Masaki, T.; Sawamura, T. *FEBS Lett.* **2001**, *499*, 215.
- (67) Chen, M. Y.; Narumiya, S.; Masaki, T.; Sawamura, T. *Biochem. J.* **2001**, *355*, 289.
- (68) Park, H.; Adsit, F. G.; Boyington, J. C. *J. Biol. Chem.* **2005**, *280*, 13593.
- (69) Ohki, I.; Ishigaki, T.; Oyama, T.; Matsunaga, S.; Xie, Q.; Ohnishi-Kameyama, M.; Murata, T.; Tsuchiya, D.; Machida, S.; Morikawa, K.; Tate, S. *Structure* **2005**, *13*, 905.
- (70) Francone, O. L.; Tu, M.; Royer, L. J.; Zhu, J.; Stevens, K.; Oleynek, J. J.; Lin, Z.; Shelley, L.; Sand, T.; Luo, Y.; Kane, C. D. *J. Lipid Res.* **2009**, *50*, 546.
- (71) Marshe, G.; Levak-Frank, S.; Quehenberger, O.; Heller, R.; Sattler, W.; Malle, E. *FASEB J.* **2001**, *15*, 1095.
- (72) Jono, T.; Miyazaki, A.; Nagai, R.; Sawamura, T.; Kitamura, T.; Horiuchi, S. *FEBS Lett.* **2002**, *511*, 170.
- (73) Oka, K.; Sawamura, T.; Kikuta, K.; Itokawa, S.; Kume, N.; Kita, T.; Masaki, T. *Proc. Natl. Acad. Sci. USA* **1998**, *95*, 9535.

- (74) Murphy, J. E.; Tacon, D.; Tedbury, P. R.; Hadden, J. M.; Knowling, S.; Sawamura, T.; Peckham, M.; Phillips, S. E. V.; Walker, J. H.; Ponnambalam, S. *Biochem. J.* **2006**, *393*, 107.
- (75) Shimaoka, T.; Kume, N.; Minami, M.; Hayashida, K.; Sawamura, T.; Kita, T.; Yonehara, S. *J. Immunol.* **2001**, *166*, 5108.
- (76) Fujita, Y.; Kakino, A.; Nishimichi, N.; Yamaguchi, S.; Sato, Y.; Machida, S.; Cominacini, L.; Delneste, Y.; Matsuda, H.; Sawamura, T. *Clin. Chem.* **2009**, *55*, 285.
- (77) Shih, H. H.; Zhang, S.; Cao, W.; Hahn, A.; Wang, J.; Paulsen, J. E.; Harnish, D. C. *Am. J. Physiol. Heart Circ. Physiol.* **2009**, *296*, H1643.
- (78) Xie, J.; Zhu, H.; Guo, L.; Ruan, Y.; Wang, L.; Sun, L.; Zhou, L.; Wu, W.; Yun, X.; Shen, A.; Gu, J. *J. Immunol.* **2010**, *185*, 2306.
- (79) Delneste, Y.; Magistrelli, G.; Gauchat, J. F.; Haeuw, J. F.; Aubry, J. P.; Nakamura, K.; Kawakami-Honda, N.; Goetsch, L.; Sawamura, T.; Bonnefoy, J.-Y.; Jeannin, P. *Immunity* **2002**, *17*, 353.
- (80) Moriwaki, H.; Kume, N.; Sawamura, T.; Aoyama, T.; Hoshikawa, H.; Ochi, H.; Nishi, E.; Masaki, T.; Kita, T. *Arterioscler. Thromb. Vasc. Biol.* **1998**, *18*, 1541.
- (81) Lacey, K., University of Leeds, 2012.
- (82) Nishizuka, T.; Fujita, Y.; Sato, Y.; Nakano, A.; Kakino, A.; Ohshima, S.; Kanda, T.; Yoshimoto, R.; Sawamura, T. *Proc. Jpn. Acad. Ser. B Phys. Biol. Sci.* **2011**, *87*, 431.
- (83) Lee, W. J.; Ou, H. C.; Hsu, W. C.; Chou, M. M.; Tseng, J. J.; Hsu, S. L.; Tsai, K. L.; Sheu, W. H. *J. Vasc. Surg.* **2010**, *52*, 1290.
- (84) Ou, H. C.; Song, T. Y.; Yeh, Y. C.; Huang, C. Y.; Yang, S. F.; Chiu, T. H.; Tsai, K. L.; Chen, K. L.; Wu, Y. J.; Tsai, C. S.; Chang, L. Y.; Kuo, W. W.; Lee, S. D. *J. Appl. Physiol.* **2010**, *108*, 1745.
- (85) Shibata, Y.; Kume, N.; Arai, H.; Hayashida, K.; Inui-Hayashida, A.; Minami, M.; Mukai, E.; Toyohara, M.; Harauma, A.; Murayama, T.; Kita, T.; Hara, S.; Kamei, K.; Yokode, M. *Atherosclerosis* **2007**, *193*, 20.
- (86) Mehta, J. L.; Li, D. Y. *Biochem. Biophys. Res. Commun.* **1998**, *248*, 511.
- (87) Li, D.; Mehta, J. L. *Arterioscler. Thromb. Vasc. Biol.* **2000**, *20*, 1116.
- (88) Mehta, J. L.; Li, D. Y.; Chen, H. J.; Joseph, J.; Romeo, F. *Biochem. Biophys. Res. Commun.* **2001**, *289*, 857.
- (89) Mehta, J. L.; Chen, J.; Yu, F.; Li, D. Y. *Cardiovasc. Res.* **2004**, *64*, 243.
- (90) Li, L.; Renier, G. *Atherosclerosis* **2009**, *204*, 40.
- (91) Matarazzo, S.; Quitadamo, M. C.; Mango, R.; Ciccone, S.; Novelli, G.; Biocca, S. *Mol. Pharmacol.* **2012**, *82*, 246.

- (92) Biocca, S.; Iacovelli, F.; Matarazzo, S.; Vindigni, G.; Oteri, F.; Desideri, A.; Falconi, M. *Cell cycle* **2015**, *14*, 1583.
- (93) Falconi, M.; Ciccone, S.; D'Arrigo, P.; Viani, F.; Sorge, R.; Novelli, G.; Patrizi, P.; Desideri, A.; Biocca, S. *Biochem. Biophys. Res. Commun.* **2013**, *438*, 340.
- (94) Thakkar, S.; Wang, X.; Khaidakov, M.; Dai, Y.; Gokulan, K.; Mehta, J. L.; Varughese, K. I. *Sci. Rep.* **2015**, *5*, 16740.
- (95) Curtis, B. M.; Scharnowske, S.; Watson, A. J. *Proc. Natl. Acad. Sci. USA* **1992**, *89*, 8356.
- (96) Probert, F.; Whittaker, S. B.; Crispin, M.; Mitchell, D. A.; Dixon, A. M. *J. Biol. Chem.* **2013**, *288*, 22745.
- (97) Geijtenbeek, T. B.; Torensma, R.; van Vliet, S. J.; van Duijnhoven, G. C.; Adema, G. J.; van Kooyk, Y.; Figdor, C. G. *Cell* **2000**, *100*, 575.
- (98) Soilleux, E. J.; Barten, R.; Trowsdale, J. *J. Immunol.* **2000**, *165*, 2937.
- (99) Guo, Y.; Feinberg, H.; Conroy, E.; Mitchell, D. A.; Alvarez, R.; Blixt, O.; Taylor, M. E.; Weis, W. I.; Drickamer, K. *Nat. Struct. Mol. Bio.* **2004**, *11*, 591.
- (100) Yu, Q. D.; Oldring, A. P.; Powlesland, A. S.; Tso, C. K.; Yang, C.; Drickamer, K.; Taylor, M. E. *J. Mol. Biol.* **2009**, *387*, 1075.
- (101) Bashirova, A. A.; Geijtenbeek, T. B.; van Duijnhoven, G. C.; van Vliet, S. J.; Eilering, J. B.; Martin, M. P.; Wu, L.; Martin, T. D.; Viebig, N.; Knolle, P. A.; KewalRamani, V. N.; van Kooyk, Y.; Carrington, M. *J. Exp. Med.* **2001**, *193*, 671.
- (102) Feinberg, H.; Guo, Y.; Mitchell, D. A.; Drickamer, K.; Weis, W. I. *J. Biol. Chem.* **2005**, *280*, 1327.
- (103) Tabarani, G.; Thépaut, M.; Stroebel, D.; Ebel, C.; Vivès, C.; Vachette, P.; Durand, D.; Fieschi, F. *J. Biol. Chem.* **2009**, *284*, 21229.
- (104) Mitchell, D. A.; Fadden, A. J.; Drickamer, K. *J. Biol. Chem.* **2001**, *276*, 28939.
- (105) Menon, S.; Rosenberg, K.; Graham, S. A.; Ward, E. M.; Taylor, M. E.; Drickamer, K.; Leckband, D. E. *Proc. Natl. Acad. Sci. USA* **2009**, *106*, 11524.
- (106) Pederson, K.; Mitchell, D. A.; Prestegard, J. H. *Biochemistry* **2014**, *53*, 5700.
- (107) Azad, A. K.; Torrelles, J. B.; Schlesinger, L. S. *J. Leukoc. Biol.* **2008**, *84*, 1594.
- (108) Engering, A.; Geijtenbeek, T. B.; van Vliet, S. J.; Wijers, M.; van Liempt, E.; Demaurex, N.; Lanzavecchia, A.; Fransen, J.; Figdor, C. G.; Piguet, V.; van Kooyk, Y. *J. Immunol.* **2002**, *168*, 2118.
- (109) Soilleux, E. J.; Barten, R.; Trowsdale, J. *J. Immunol.* **2000**, *165*, 2937.
- (110) Geijtenbeek, T. B. H.; Engering, A.; van Kooyk, Y. *J. Leukoc. Biol.* **2002**, *71*, 921.

- (111) Pöhlmann, S.; Soilleux, E. J.; Baribaud, F.; Leslie, G. J.; Morris, L. S.; Trowsdale, J.; Lee, B.; Coleman, N.; Doms, R. W. *Proc. Natl. Acad. Sci. USA* **2001**, *98*, 2670.
- (112) van Liempt, E.; Bank, C. M. C.; Mehta, P.; García-Vallejo, J. J.; Kwar, Z. S.; Geyer, R.; Alvarez, R. A.; Cummings, R. D.; Kooyk, Y. v.; van Die, I. *FEBS Lett.* **2006**, *580*, 6123.
- (113) Lai, W. K.; Sun, P. J.; Zhang, J.; Jennings, A.; Lalor, P. F.; Hubscher, S.; McKeating, J. A.; Adams, D. H. *Am. J. Pathol.* **2006**, *169*, 200.
- (114) Simmons, G.; Reeves, J. D.; Grogan, C. C.; Vandenberghe, L. H.; Baribaud, F.; Whitbeck, J. C.; Burke, E.; Buchmeier, M. J.; Soilleux, E. J.; Riley, J. L.; Doms, R. W.; Bates, P.; Pöhlmann, S. *Virology* **2003**, *305*, 115.
- (115) Su, S. V.; Hong, P.; Baik, S.; Negrete, O. A.; Gurney, K. B.; Lee, B. *J. Biol. Chem.* **2004**, *279*, 19122.
- (116) Davis, C. W.; Nguyen, H. Y.; Hanna, S. L.; Sánchez, M. D.; Doms, R. W.; Pierson, T. C. *J. Virol.* **2006**, *80*, 1290.
- (117) Cambi, A.; Beeren, I.; Joosten, B.; Fransen, J. A.; Figdor, C. G. *Eur. J. Immunol.* **2009**, *39*, 1923.
- (118) Bleul, C. C.; Wu, L.; Hoxie, J. A.; Springer, T. A.; Mackay, C. R. *Proc. Natl. Acad. Sci. USA* **1997**, *94*, 1925.
- (119) Wilen, C. B.; Tilton, J. C.; Doms, R. W. *Cold Spring Harb. Perspect. Med.* **2012**, *2*.
- (120) Lambert, A. A.; Gilbert, C.; Richard, M.; Beaulieu, A. D.; Tremblay, M. J. *Blood* **2008**, *112*, 1299.
- (121) Wu, L.; KewalRamani, V. N. *Nat. Rev. Immunol.* **2006**, *6*, 859.
- (122) Boily-Larouche, G.; Iscache, A. L.; Zijenah, L. S.; Humphrey, J. H.; Moulard, A. J.; Ward, B. J.; Roger, M. *PLoS ONE* **2009**, *4*, e7211.
- (123) Alvarez, C. P.; Lasala, F.; Carrillo, J.; Muñoz, O.; Corbí, A. L.; Delgado, R. *J. Virol.* **2002**, *76*, 6841.
- (124) Mahon, C. S.; Jackson, A. W.; Murray, B. S.; Fulton, D. A. *Polym. Chem.* **2013**, *4*, 368.
- (125) Mahon, C. S.; Fascione, M. A.; Sakonsinsiri, C.; McAllister, T. E.; Turnbull, W. B.; Fulton, D. A. *Org. Biomol. Chem.* **2015**, *13*, 2756.
- (126) Eby, R.; Schuerch, C. *Carbohydr. Res.* **1974**, *34*, 79.
- (127) Demchenko, A. V.; Rousson, E.; Boons, G. J. *Tetrahedron Lett.* **1999**, *40*, 6523.
- (128) Miljković, M.; Yeagley, D.; Deslongchamps, P.; Dory, Y. L. *J. Org. Chem.* **1997**, *62*, 7597.
- (129) Crich, D.; Hu, T.; Cai, F. *J. Org. Chem.* **2008**, *73*, 8942.

- (130) David, S.; Hanessian, S. *Tetrahedron* **1985**, *41*, 643.
- (131) Grindley, T. B. In *Synthetic Oligosaccharides*; American Chemical Society: 1994; Vol. 560, p 51.
- (132) Dong, H.; Zhou, Y.; Pan, X.; Cui, F.; Liu, W.; Liu, J.; Ramström, O. *J. Org. Chem.* **2012**, *77*, 1457.
- (133) Lichtenthaler, Frieder W.; Oberthür, M.; Peters, S. *Eur. J. Org. Chem.* **2001**, *2001*, 3849.
- (134) Kiessling, L. L.; Grim, J. C. *Chem. Soc. Rev.* **2013**, *42*, 4476.
- (135) Yilmaz, G.; Becer, C. R. *Front. Bioeng. Biotechnol.* **2014**, *2*, 39.
- (136) Bojarova, P.; Kren, V. *Biomater. Sci.* **2016**.
- (137) Lees, W. J.; Spaltenstein, A.; Kingery-Wood, J. E.; Whitesides, G. M. *J. Med. Chem.* **1994**, *37*, 3419.
- (138) Disney, M. D.; Zheng, J.; Swager, T. M.; Seeberger, P. H. *J. Am. Chem. Soc.* **2004**, *126*, 13343.
- (139) Richards, S.-J.; Jones, M. W.; Hunaban, M.; Haddleton, D. M.; Gibson, M. I. *Angew. Chem. Int. Ed. Engl.* **2012**, *51*, 7812.
- (140) Jackson, A. W.; Fulton, D. A. *Macromolecules* **2010**, *43*, 1069.
- (141) Chung, N. P. Y.; Breun, S. K. J.; Bashirova, A.; Baumann, J. G.; Martin, T. D.; Karamchandani, J. M.; Rausch, J. W.; Le Grice, S. F. J.; Wu, L.; Carrington, M.; KewalRamani, V. N. *J. Biol. Chem.* **2010**, *285*, 2100.
- (142) Sanchez-Navarro, M.; Rojo, J. *Drug News Perspect.* **2010**, *23*, 557.
- (143) Wang, S. K.; Liang, P. H.; Astronomo, R. D.; Hsu, T. L.; Hsieh, S. L.; Burton, D. R.; Wong, C. H. *Proc. Natl. Acad. Sci. USA* **2008**, *105*, 3690.
- (144) Martínez-Ávila, O.; Bedoya, L. M.; Marradi, M.; Clavel, C.; Alcamí, J.; Penadés, S. *ChemBioChem* **2009**, *10*, 1806.
- (145) Martinez-Avila, O.; Hijazi, K.; Marradi, M.; Clavel, C.; Campion, C.; Kelly, C.; Penades, S. *Chemistry* **2009**, *15*, 9874.
- (146) Ribeiro-Viana, R.; Sánchez-Navarro, M.; Luczkowiak, J.; Koeppe, J. R.; Delgado, R.; Rojo, J.; Davis, B. G. *Nat. Commun.* **2012**, *3*, 1303.
- (147) Luczkowiak, J.; Muñoz, A.; Sánchez-Navarro, M.; Ribeiro-Viana, R.; Ginieis, A.; Illescas, B. M.; Martín, N.; Delgado, R.; Rojo, J. *Biomacromolecules* **2013**, *14*, 431.
- (148) Arnáiz, B.; Martínez-Ávila, O.; Falcon-Perez, J. M.; Penadés, S. *Bioconjugate Chem.* **2012**, *23*, 814.
- (149) Robinson, A.; Fang, J.-M.; Chou, P.-T.; Liao, K.-W.; Chu, R.-M.; Lee, S.-J. *ChemBioChem* **2005**, *6*, 1899.

- (150) Benito-Alifonso, D.; Tremel, S.; Hou, B.; Lockyear, H.; Mantell, J.; Fermin, D. J.; Verkade, P.; Berry, M.; Galan, M. C. *Angew. Chem. Int. Ed. Engl.* **2014**, *53*, 810.
- (151) Babu, P.; Sinha, S.; Surolia, A. *Bioconjugate Chem.* **2007**, *18*, 146.
- (152) Kikkeri, R.; Lepenies, B.; Adibekian, A.; Laurino, P.; Seeberger, P. H. *J. Am. Chem. Soc.* **2009**, *131*, 2110.
- (153) Cambi, A.; Lidke, D. S.; Arndt-Jovin, D. J.; Figdor, C. G.; Jovin, T. M. *Nano Lett.* **2007**, *7*, 970.
- (154) Medintz, I. L.; Mattoussi, H. *Phys. Chem. Chem. Phys.* **2009**, *11*, 17.
- (155) Bock, K.; Pedersen, C. *J. Chem. Soc., Perkin Trans. 2* **1974**, 293.
- (156) Guo, Y.; Sakonsinsiri, C.; Nehlmeier, I.; Fascione, M. A.; Zhang, H.; Wang, W.; Pöhlmann, S.; Turnbull, W. B.; Zhou, D. *Angew. Chem. Int. Ed. Engl.* **2016**, *55*, 4738.
- (157) Saha, S. K.; Brewer, C. F. *Carbohydr. Res.* **1994**, *254*, 157.
- (158) Dahlmann, F.; Biedenkopf, N.; Babler, A.; Jahnen-Dechent, W.; Karsten, C. B.; Gnirß, K.; Schneider, H.; Wrensch, F.; O'Callaghan, C. A.; Bertram, S.; Herrler, G.; Becker, S.; Pöhlmann, S.; Hofmann-Winkler, H. *J. Infect. Dis.* **2015**, *212* (Suppl 2), S247.
- (159) Feinberg, H.; Castelli, R.; Drickamer, K.; Seeberger, P. H.; Weis, W. I. *J. Biol. Chem.* **2007**, *282*, 4202.
- (160) Hense, A.; V. Ley, S.; M. I. Osborn, H.; R. Owen, D.; Poisson, J. F.; L. Warriner, S.; E. Wesson, K. *J. Chem. Soc., Perkin Trans. 1.* **1997**, 2023.
- (161) Baeschlin, D. K.; Green, L. G.; Hahn, M. G.; Hinzen, B.; Ince, S. J.; Ley, S. V. *Tetrahedron: Asymmetry* **2000**, *11*, 173.
- (162) Deferrari, J. O.; Gros, E. G.; Mastronardi, I. O. *Carbohydr. Res.* **1967**, *4*, 432.
- (163) Ernst B. and Magnani J.L. *Nat.Rev. Drug Discov.* **2009**, *8*, 661.
- (164) Lima L.M.; Barreiro E.J. *Curr. Med. Chem.* **2005**, *12*, 23.
- (165) Rautio J.; Kumpulainen H.; Heimbach T.; Oliyai R.; Oh D.; Järvinen T.; Savolainen J. *Nat. Rev. Drug Discov.* **2008**, *7*, 255
- (166) Taylor N.R. and von Itzstein M. *J. Med. Chem.* **1994**, *37*, 616.
- (167) He G.; Massarella J.; Ward P. *Clin. Pharmacokinet.* **1999**, *37*, 471.
- (168) Prakash T.P.; Yu J.; Migawa M.T.; Kinberger G.A.; Wan W.B.; Østergaard M.E.; Carty R.L.; Vasquez G.; Low A.; Chappell A.; Schmidt K.; Aghajan M.; Crosby J.; Murray H.M.; Booten S.L.; Hsiao J.; Soriano A.; Machemer T.; Cauntay P.; Burel S.A.; Murray S.F.; Gaus H.; Graham M.J.; Swayze E.E.; Seth P.P. *J. Med. Chem.* **2016**, *59*, 2718.

- (169) Prakash T.P.; Graham M.J.; Yu J.; Carty R.; Low A.; Chappell A.; Schmidt K.; Zhao C.; Aghajan M.; Murray H.F.; Riney S.; Booten S.L.; Murray S.F.; Gaus H.; Crosby J.; Lima W.F.; Guo S.; Monia B.P.; Swayze E.E.; Seth P.P. *Nucleic Acids Res.* **2014**, *42*, 8796.
- (170) Tanaka T.; Ishitani H.; Miura Y.; Oishi K.; Takahashi T.; Suzuki T.; Shoda S.; Kimura Y. *ACS Macro Lett.* **2014**, *3*, 1074.
- (171) Trachtman H.; Cnaan A.; Christen E.; Gibbs K.; Zhao S.; Acheson D.W.; Weiss R.; Kaskel F.J.; Spitzer A.; Hirschman G.H.; Investigators of the HUS-SYNSORB Pk Multicenter Clinical Trial. *JAMA.* **2003**, *290*, 1337.
- (172) Karmali M.A.; *J. Infect. Dis.* **2004**, *189*, 355.
- (173) Haag R. and Kratz F. *Angew. Chem. Int. Ed. Engl.* **2006**, *45*, 1198.
- (174) Duncan R. and Vicent M.J. *Adv. Drug. Deliv. Rev.* **2013**, *65*, 60.
- (175) Giorgi M.E.; Agusti R.; de Lederkremer R.M. *Beilstein J. Org. Chem.* **2014**, *10*, 1433.
- (176) Lee H.; Lee M.Y.; Bhang S.H.; Kim B.S.; Kim Y.S.; Ju J.H.; Kim K.S.; Hahn S.K. *ACS Nano.* **2014**, *8*, 4790.
- (177) Kwon I. K.; Lee S.C.; Han B., Park K. *J. Control. Release.* **2012**, *164*, 108.
- (178) Deng, L.; Norberg, O.; Uppalapati, S.; Yan, M.; Ramstrom, O. *Org. Biomol. Chem.* **2011**, *9*, 3188.
- (179) Otman, O.; Boullanger, P.; Drockenmuller, E.; Hamaide, T. *Beilstein J. Org. Chem.* **2010**, *6*, 58.
- (180) Ross, A. J.; Sizova, O. V.; Nikolaev, A. V. *Carbohydr. Res.* **2006**, *341*, 1954.
- (181) Temeriusz, A.; Gubica, T.; Rogowska, P.; Paradowska, K.; Cyrański, M. K. *Carbohydr. Res.* **2005**, *340*, 1175.
- (182) Kuboki, A.; Sekiguchi, T.; Sugai, T.; Ohta, H. *Synlett* **1998**, *1998*, 479.
- (183) Gubica, T.; Temeriusz, A.; Paradowska, K.; Ostrowski, A.; Klimentowska, P.; Cyrański, M. K. *Carbohydr. Res.* **2009**, *344*, 1734.
- (184) Abbas, S. A.; Barlow, J. J.; Matta, K. L. *Carbohydr. Res.* **1982**, *106*, 59.
- (185) Uzawa, H.; Nishida, Y.; Sasaki, K.; Minoura, N.; Kobayashi, K. *ChemBioChem* **2003**, *4*, 640.
- (186) Goto, F.; Ogawa, T. *Tetrahedron Lett.* **1992**, *33*, 5099.
- (187) Sarkar, A. K.; Matta, K. L. *Carbohydr. Res.* **1992**, *233*, 245.
- (188) Agnihotri, G.; Tiwari, P.; Misra, A. K. *Carbohydr. Res.* **2005**, *340*, 1393.
- (189) Zhang, Z.; Magnusson, G. *Carbohydr. Res.* **1996**, *295*, 41.
- (190) Goebel, W. F.; Avery, O. T. *J. Exp. Med.* **1929**, *50*, 521.

- (191) Vic, G.; Hastings, J. J.; Howarth, O. W.; Crout, D. H. G. *Tetrahedron: Asymmetry* **1996**, *7*, 709.
- (192) Käsbeck, L.; Kessler, H. *Liebigs Ann.* **1997**, *1997*, 169.
- (193) Bochkov, A. F.; Obruchnikov, I. V.; Kochetkov, N. K. *Rus. Chem. Bull.* **1971**, *20*, 1186.
- (194) Lindberg, J.; Svensson, S. C. T.; Pålsson, P.; Konradsson, P. *Tetrahedron* **2002**, *58*, 5109.
- (195) Ellervik, U.; Magnusson, G. *J. Org. Chem.* **1998**, *63*, 9314.
- (196) Garegg, P. J.; Kvarnström, I.; Niklasson, A.; Niklasson, G.; Svensson, S. C. T. *J. Carbohydr. Chem.* **1993**, *12*, 933.
- (197) Liptak, A.; Jodal, I.; Harangi, J.; Nanasi, P. *Acta Chim. Hung.* **1983**, *113*, 415.
- (198) Sherman, A. A.; Mironov, Y. V.; Yudina, O. N.; Nifantiev, N. E. *Carbohydr. Res.* **2003**, *338*, 697.
- (199) Faltin, F.; Fehring, V.; Miethchen, R. *Synthesis* **2002**, *13*, 1851.
- (200) Li, Y.; Mo, H.; Lian, G.; Yu, B. *Carbohydr. Res.* **2012**, *363*, 14.
- (201) Lindhorst, T. K.; Kotter, S.; Krallmann-Wenzel, U.; Ehlers, S. *J. Chem. Soc., Perkin Trans. 1.* **2001**, 823.
- (202) Çarçabal, P.; Hünig, I.; Gamblin, D. P.; Liu, B.; Jockusch, R. A.; Kroemer, R. T.; Snoek, L. C.; Fairbanks, A. J.; Davis, B. G.; Simons, J. P. *J. Am. Chem. Soc.* **2006**, *128*, 1976.
- (203) Karunaratne, C. V.; Weldeghiorghis, T. K.; West, C. M.; Taylor, C. M. *J. Am. Chem. Soc.* **2014**, *136*, 15170.
- (204) Gachokidse *Russ. J. Gen. Chem.* **1952**, *22*, 247.
- (205) Upreti, M.; Ruhela, D.; Vishwakarma, R. A. *Tetrahedron* **2000**, *56*, 6577.
- (206) Jansson, A. M.; Meldal, M.; Bock, K. *J. Chem. Soc., Perkin Trans. 1.* **1992**, 1699.
- (207) Zhou, D.; Ying, L.; Hong, X.; Hall, E. A.; Abell, C.; Klenerman, D. *Langmuir* **2008**, *24*, 1659.
- (208) Zhang, H.; Feng, G.; Guo, Y.; Zhou, D. *Nanoscale* **2013**, *5*, 10307.
- (209) Zhan, N.; Palui, G.; Grise, H.; Tang, H.; Alabugin, I.; Mattoussi, H. *ACS Appl. Mater. Interfaces* **2013**, *5*, 2861.